Alma Mater Studiorum – Università di Bologna

DOTTORATO DI RICERCA IN

SCIENZE E TECNOLOGIE AGRARIE, AMBIENTALI E ALIMENTARI

Ciclo XXXII

Settore Concorsuale:07/E1

Settore Scientifico Disciplinare: AGR/07

DISSECTING THE HEAT-STRESS TOLERANCE QTLome IN DURUM WHEAT

Presentata da: Dott. EDER LICIERI GROLI

Coordinatore Dottorato

Chiar.mo Prof. Massimiliano Petracci

Supervisore

Chiar.mo Prof. Roberto Tuberosa

Co-supervisore

Dott. Karim Ammar
Dott. Marco Maccaferri

Esame finale anno 2020

Table of contents

ABSTRACT

Heat stress negatively affects wheat performance during its entire cycle, particularly during reproductive stage. In view of the clime change and the prediction of a continued increase in temperature in the new future, it is urgent to concentrate efforts to discovery new genetic sources able to improve the resilience of durum wheat to heat stress. In this direction, this study addressed two different experiments in durum wheat, in two different plant growth stages in order to identify novel QTLs suitable to be applied in marker assisted selection for heat tolerance. Chlorophyll fluorescence (ChlF) is a valuable indicator of plant response to environmental changes and allows for a detailed assessment of PSII activity in view of its non-invasive measurement and high-throughput phenotyping. In the first study (Chapter 2), the Light-Induced Fluorescence Transient (LIFT) method was used to access ChlF data under daylight condition in order to map QTLs for ChlF-related traits during vegetative growth stage in durum wheat under heat stress condition. Our results provide evidence that LIFT consistently measures ChlF under daylight condition at the level of high-throughput phenotyping combined with high accuracy which are required for Genome Wide Association Study (GWAS) aimed at identifying genomic regions affecting PSII activity. The 50 QTLs identified for ChlF-related traits under heat stress mostly clustered into five chromosomes hotspots unrelated to phenology, a feature that makes these QTLs a valuable asset for marker-assisted breeding programs across different latitudes. In the second study (Chapter 3), a set of 183 accessions suitable for GWAS, was exposed to optimal and high temperature during two crop seasons under field condition. Important agronomic traits were evaluated in order to identify valuable QTLs for GY and its components. The GWAS analysis identified several QTLs in the single years as well as in the joint analysis. From the total QTLs identified, 13 QTL clusters can be highlighted to be affecting heat tolerance across different years and/or different traits. Three different classes of adaptive QTLs for GY were identified in this study: Although *HS_QTL_Cluster_3B* and *HS_QTL_Cluster_4A* affect different traits across different years, they have a consistent effect only on GY. *HS_QTL_Cluster_1A* and *HS_QTL_Cluster_2A.2* have a concurrent effect on GY and plant height (PH), while two QTLs were identified affecting GY and number of spikes per linear meter (SPM - *HS_QTL_Cluster_5A.4*) and thousand kernels weight (TKW - *HS_QTL_Cluster_7A*).

1. Chapter 1: General introduction

1.1. Taxonomy, origin and evolution of wheat

The genus *Triticum* L. belongs to the *Poaceae* family, Triticeae tribe and *Triticinae* subtribe. Among a large variety of other species, this genus includes two major crops important for the human diet, namely, bread wheat (*Triticum aestivum* L.) and durum wheat (*Triticum turgidum* subsp. *durum* (Desf.) Husn.), which are cultivated in a large number of different environments worldwide. Although bread and durum wheat are very similar in many aspects, they differ from a genetic standpoint, because bread and durum wheat have a complex allotetraploid and allohexaploid genomes, respectively (Gupta *et al*., 1972; Ganal and Roder, 2007).

From a genetic standpoint, the genus *Triticum* is classified into three different categories based on the level of ploidy, with a basic set of chromosomes equal to seven (Bennici, 1986; Bálint *et al*., 2000):

1) Diploid genome: 2n = 2x = 14 chromosomes, with genome formula AA (*T. monococcum*, *T. urartu*, *T. speltoides*, *T. tauschii*);
2) Allotetraploid genome: 2n = 4x = 28 chromosomes, with genome formula AABB (*T. turgidum*) and AAGG (*T. timopheevi*);
3) Allohexaploid genome: 2n = 6x = 42 chromosome, with genome formula AABBDD (*T. aestivum*) and AAGGAA (*T. zhukovskyi*).

The allopolyploidization is the main process of the evolution of the polyploid *Triticum* species identified across time. Several natural interspecific hybridizations have occurred between the genus *Triticum* and *Aegilops* which have originated the species cultivated in nowadays (Kerby and Kuspira, 1987; Monneveux *et al*., 2000). The genome A, derived from the wild ancestor *T. urartu* (AA genome, 2n = 14), is the common genome to all wheat species (Dvořák, 2001). Although the origin of the A genome is well known, the origin of the B genome is more complex and still debated. Some studies suggest that the B genome is originated from the SS genome of an *Aegilops* species belonging to the *Sitopsis* section (van Slageren, 1994; Balint *et al*., 2000; Dvorak, 2001). However, Wang *et al*. (2000) suggested that the B genome derives from *A. speltoides*. Wild emmer wheat (*T. turgidum* ssp. *dicoccoides*) appears to be the most ancient species of the *turgidum* group (Bálint *et al*., 2000, Akhunov *et al*., 2010).

The hexaploid species, particularly *T. aestivum*, emerged from a second round of independent hybridization between the cultivated emmer *T. turgidum* ssp. *dicoccum* (AB genome), a descendent of *T. turgidum* ssp. *dicoccoides*, and *A. tauschii* (D genome). *T. aestivum* ssp. *spelta*

appears to be the ancient form of the modern hexaploid wheat currently cultivated, mostly known as common or bread wheat (McFadden and Sears, 1946; Slageren, 1994; Dubcovsky and Dvorak, 2007). Additional details about the phylogeny of wheat species is reported in Figure 1.1.

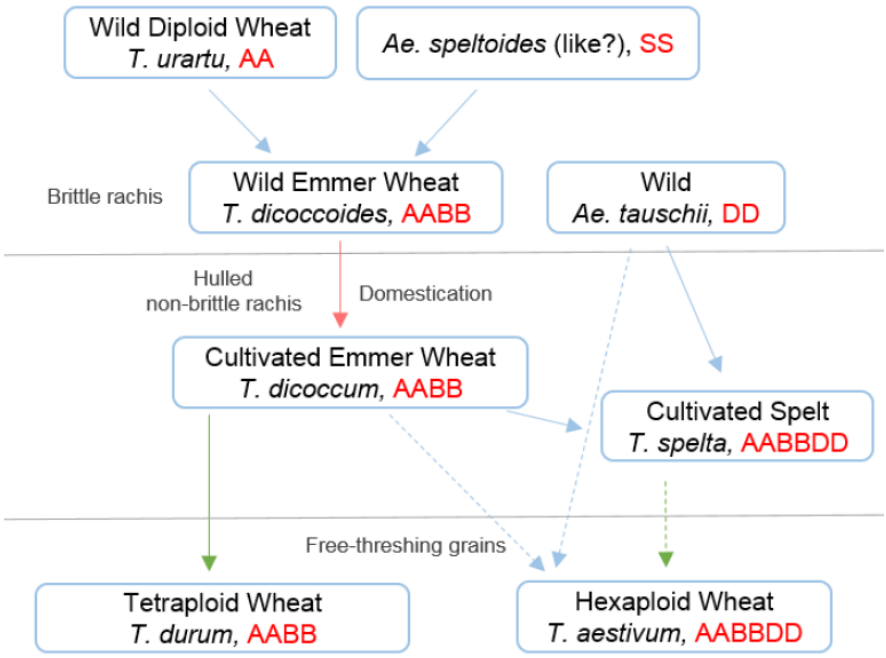

Figure 1.1. Phylogeny of the wheat species. The blue arrows indicate hybridization events, red arrows indicate domestication events and green arrows indicate selection events (adapted from Salamini *et al*., 2002; Kilian *et al*., 2010; Peng *et al*., 2011).

1.2. The importance of wheat in the world

Wheat (*Triticum* spp.) is one of the most import staple foods for the human diet in several countries (FAOSTAT, 2019) providing about 20% of the calories of the world's population as well as a similar proportion of daily protein for about 2.5 billion people, particularly, in less-developed countries (Braun *et al*., 2010; Reynolds *et al*., 2012). In 2017, wheat was cultivated in more than 218.5 million of hectares across the world, with a production of over 771.7 million tons across different countries as well as in different environmental conditions worldwide, mainly, in China, which is the principal wheat-producing country in the world (Figure 1.2) (FAOSTAT, 2019). In 2019, FAOSTAT estimates that the total production of wheat will be over than 766 million tons (FAOSTAT, 2019).

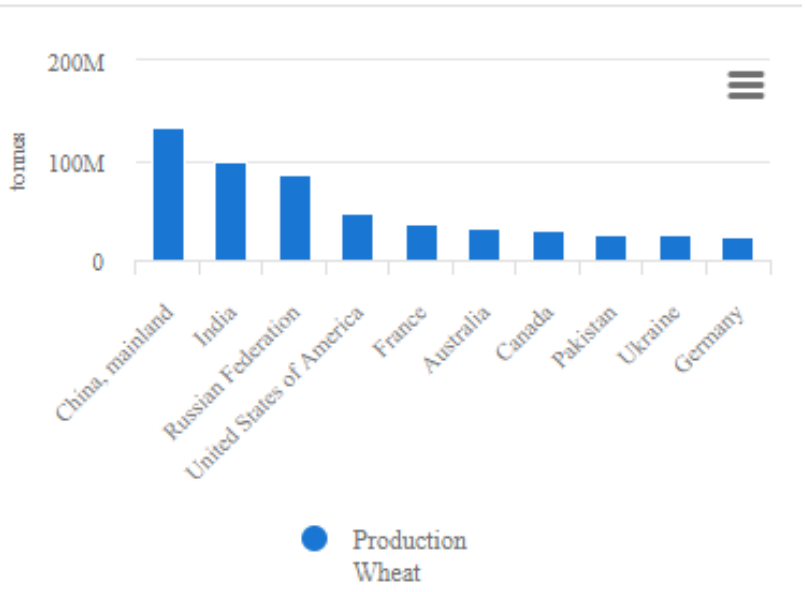

Figure 1.2. Main wheat-producing countries in 2017 (FAOSTAT, 2019).

Since the 1950s, global wheat production has increased over 300%, particularly, due to the constant yield increase and not due to the expansion of cultivated land. This fantastic increment in wheat yield has been possible due to genetic improvement (biotic and abiotic resistance, increase in yield potential) as well as improvement of agronomic practices (use of fertilizers, disease and weed control) (Reynolds and Borlaug, 2006; Reynolds *et al.*, 2012). At the same time, the perceptual of people living under hungry threshold dropped down from about 30 to 10%. Although, the proportion of people living under the hunger threshold has decreased, malnutrition is still one of the main causes of death in the world, with more than 820 million people going hungry each year, especially, in African and Asian countries (https://www.actionagainsthunger.org).

In view of that, the United Nations declared sustainable food safety as one of the most important goals to be achieved in the 21st century (https://sustainabledevelopment.un.org/). Various factors hamper the reaching this ambitious goal. Firstly, the world's population is expected to increase from 7.7 billion currently to 9.7 billion in 2050, reaching 11 billion people at the end of this century (ONU, 2019). Besides that, the new scenario of climate change will cause seasons with reductions in annual precipitation and more severe heat waves, affecting wheat production across the world (Lobell *et al.*, 2015; Asseng *et al.*, 2017; Zhao *et al.*, 2017). Therefore, it is

essential that wheat breeding programs around the world focus their attention on those genetic mechanisms that can provide better resilience of plants for extreme conditions.

1.3. The importance and use of durum wheat

Although wheat (*Triticum* spp.) is cultivated in over 218.5 million hectares across the world, durum wheat (*T. turgidum* subsp. *durum*) is cultivated only in about 5% of this area, especially in the Mediterranean Basin, Northern Plains between the USA and Canada, Southeastern USA and Northern Mexico. The remaining lands are used for bread wheat cultivation. In the crop season 2018/19, it was estimated that durum wheat production was 38.1 million tons, particularly in Canada (5.7), Italy (4.1), Turkey (3.6), Algeria (3.2) and Morocco (2.4 million tons), which are the top five durum wheat producers in the world (DG-Agri, 2019; USDA, 2019). These results clearly indicate the importance of durum wheat to the Mediterranean countries, which correspond to more than 50% of the total worldwide durum wheat production. Both bread and durum wheat are important crops with human consumption purposes.

Currently, durum wheat is the most cultivated tetraploid wheat species (AABB). However, the process of domestication of tetraploid wheat began from its wild progenitor *T. dicoccoides* about more than 10,000 years ago (Salamini *et al*., 2002). The geographical area of domestication of tetraploid wheat is suggested to be the Western part of the Fertile Crescent, Southeastern part of Turkey as well as the eastern regions of Iraq and Iran (Salamini *et al*., 2002; Zohary *et al*., 2012).

Although durum wheat corresponds to only 5% of the global wheat production, it is considered as a primary staple crop in the Mediterranean Basin, a region where durum wheat is grown under different environments prone to drought as well as heat stress conditions (Danzi *et al*., 2019; Kutiel, 2019). Durum wheat presents a vitreous very hard grain, which is composed of about 60.0-80.0% of carbohydrates (particularly starches), 8.0-16.0% of protein, 1.5-2.0% of fat, 1.5-2.0% of minerals, 2.0% of fibers, vitamins B and E (Peña et al., 2002). The main use of the durum wheat grain is to produce semolina (durum wheat flour), which is used in pasta production. Additionally, semolina is also used to make a traditional kind of bread in Morocco, as well as to make couscous and bulgur, typical dishes from North Africa countries (Charke *et al*., 2005).

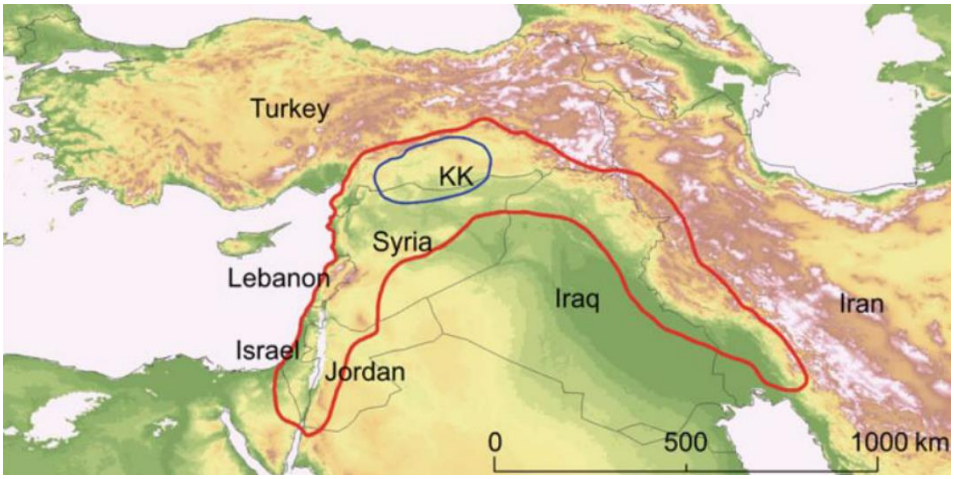

Figure 1.3. Region of the domestication of tetraploid wheat. The Fertile Crescent (red line) and core area (blue line) near the Karacadag Mountains in the southwest Turkey (Kilian *et al*., 2010).

1.4. Association mapping

The association mapping (AM) approach has received increasing attention for QTL mapping because it contributes to detecting the genetic basis of variation in physiological, developmental and morphological traits, as well as assembling core collections and developing genetic platforms for genotyping, phenotyping, analysis and interpretation of genetic data (Sukumaran and Yu, 2014).

Association mapping is a great tool to exploit genomic technologies and plant germplasm resources simultaneously, providing several advantages when compared with biparental linkage analysis, especially due to the high mapping resolution of casual traits and the identification of candidate genes. Association mapping populations are usually assembled from a large number of cultivars or elite breeding lines from different breeding program or sample accessions from specific germplasm collections. In this way, due to the fact that AM is based on the historic recombination present in the panel of accessions a high mapping resolution is expected and a higher number of alleles can be analyzed simultaneously (Zhu et al., 2008; Sukumaran and Yu, 2014).

Association mapping can be separated into two different approaches according to the goal of the research, (i) targeted candidate gene studies or (ii) large scale, genome-wide association studies (GWAS). In the candidate gene approach, genetic markers are genotyped at a specific locus putatively involved in a specific phenotype and then tested for the association between the genetic

markers and the phenotype. In plants, this approach has been very useful for candidate genes with extensive evidence of a role in the phenotype of interest. However, the choice of specific candidate genes as well as the genetic markers related to them involves some guesswork, limiting the use of this strategy to specific studies (Myles *et al*., 2009). On the other hand, in GWAS analysis the first step identifies a large number of reference genetic markers, typically Single Nucleotide Polymorphisms (SNP), covering the whole genome. In the next step, the high genome coverage of SNP markers will allow to identify genes and QTLs with unknown functions (Myles et al., 2009; Sukumaran and Yu, 2014).

According to Al-Maskri *et al*., (2012), association mapping involves six different steps (Figure 1.4): (i) selection of a diverse association panel of accessions from a natural population collection, which can include elite cultivars, elite breeding lines, landraces, wild or exotic accessions, (ii) a comprehensive and precise phenotyping for the traits of interest, (iii) genotyping of the population with a high number of genetic markers, usually SNPs markers, (iv) calculation of the population structure and kinship matrix in order to avoid declaring false positives in the analysis, (v) quantification of the linkage disequilibrium (LD) using an appropriate statistics method and finally (vi) the association between genotypic and phenotypic data are calculated using appropriate statistical software (for example Tassel), which allow for the tagging of the molecular marker closest to the causal gene for a specific trait.

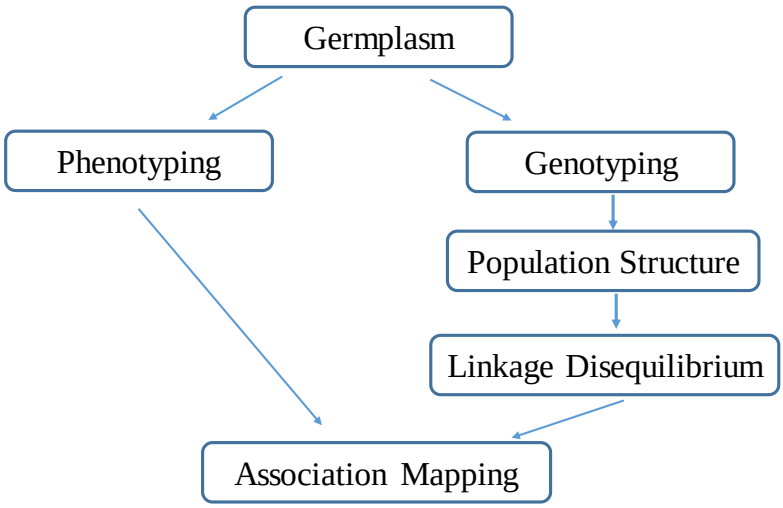

Figure 1.4. A simplified flowchart showing different stages of association mapping for tagging genes of interest using association mapping approach (adapted from Al-Maskri *et al*., 2012).

References

Al-Maskri AY, Sajjad M, Khan SH. 2012. Association mapping: a step forward to discovering new alleles for crop improvement. International Journal of Agriculture and Biology 14, 153–160.

Akhunov ED, Akhunov AR, Anderson OD, *et al*. 2010. Nucleotide diversity maps reveal variation in diversity among wheat genomes and chromosomes. BMC Genomics 11, 702.

Asseng S, Cammarano D, Basso B, et al. 2017. Hot spots of wheat yield decline with rising temperatures. Global Change Biology 23, 2464–2472.

Bálint AF, Kovács G, Sutka J. 2000. Origin and taxonomy of wheat in the light of recent research. Acta Agronomica. Hungarica 48, 301–313.

Bennici A. 1986. "Durum Wheat (*Triticum durum* Desf.), vol. 2. In: Bajaj YPS (Eds.), Biotechnology in agriculture and forestry 2. Berlin: Springer, 89–104.

Braun HJ, Atlin G, Payne T. 2010. Multi-location testing as a tool to identify plant response to global climate change. In Reynolds MP (Eds.), Climate Change and Crop Production. Surrey: CABI Climate Change Series, 115–138.

Clarke J, McCaig T, DePauw RM, *et al*. 2005. Commander Durum Wheat. Can. Journal of Plant Science, 901–904.

Danzi D, Briglia N, Petrozza A, Summerer S, Povero G, Stivaletta A, Cellini F, Pignone D, de Paola D, Janni M. 2019. Can high throughput phenotyping help food security in the Mediterranean area?. Frontiers in Plant Science 10, 737.

DG-Agri. European Commission – Agriculture and rural development. 2019. https://ec.europa.eu/agriculture/index_en.

Dubcovsky J, Dvorak J. 2007. Genome plasticity a key factor in the success of polyploid wheat under domestication. Science 316, 1862–1866.

Dvorak J, Akhunov ED, Akhunov AR, Deal KR, Luo MC. 2006. Molecular characterization of a diagnostic DNA marker for domesticated tetraploid wheat provides evidence for gene flow from wild tetraploid wheat to hexaploid wheat. Molecular Biology and Evolution 23, 1386-1396.

Dvořák, J. 2001. Triticum Species (Wheat). In: Brenner S, Miller JH (Eds.), Encyclopedia of genetics. New York: Academic, 2060–2068.

FAOSTAT. 2019. http://www.fao.org/faostat/en/#data.

Ganal MW, Roder MS. 2007. Microsatellite and SNP markers in wheat breeding, vol. 2. In: Varshney RK, Tuberosa R (Eds.), Genomic assisted crop improvement: genomics applications in crops. The Netherlands: Springer, 1-24.

Gupta PK. 1972. Cytogenetic evolution in the Triticinae: Homoeologous relationships. Genetica 43, 504–530.

Kerby K, Kuspira J. 1987. The phylogeny of the polyploid wheats *Triticum aestivum* (bread wheat) and *Triticum turgidum* (macaroni wheat). Genome 29, 722–737.

Kutiel H. 2019. Climatic uncertainty in the Mediterranean basin and its possible relevance to important economic sectors. Atmosphere 10, 10.

Lobell DB, Hammer GL, Chenu K, Zheng B, Mclean G, Chapman SC. 2015. The shifting influence of drought and heat stress for crops in northeast Australia. Global Change Biology 21, 4115–4127.

McFadden ES, Sears ER. 1946. The origin of *Triticum spelta* and its free-threshing hexaploid relatives. Journal of Heredity 37, 81–107.

Monneveux P, Zaharieva M, Rekika D. 2000. The utilization of *Triticum* and *Aegilops* species for the improvement of durum wheat. In: Royo C, Nachit MM, Di Fonzo N, Araus JL (Eds.), Durum Wheat Improvement in the Mediterranean Region: New Challenges. CIHEAM, Centre Udl-IRTA, ICARDA, CIMMYT, Zaragoza. Options Méditerranéennes, Series A, 40: 71–83.

Myles S, Peiffer J, Brown PJ, *et al*. 2009. Association mapping: critical considerations shift from genotyping to experimental design. Plant Cell 21, 2194–2202.

ONU. 2019. https://www.un.org/development/desa/en/news/population/world-population-prospects-2019.html.

Peña RJ. 2002. Wheat for bread and other foods. In: Curtis BC, Rajaram S, Macpherson HG (Eds.), Bread Wheat: Improvement and Production. FAO, Rome.

Reynolds MP, Foulkes J, Furbank R, Griffiths S, King J, Murchie EH, Parry M, Slafer G. 2012. Achieving yield gains in wheat. Plant, Cell and Environment 35, 1799–1823.

Reynolds MP, Borlaug N. 2006. Impacts of breeding on international collaborative wheat improvement. Journal of Agriculture Science 144, 3–17.

Salamini F, Özkan H, Brandolini A, Schäfer-Pregl R, Martin W. 2002. Genetics and geography of wild cereal domestication in the near east. Nature Reviews Genetics 3, 429–441.

Slageren M. 1994. Wild wheats: a monograph of *Aegilops* L. and *Amblyopyrum* (Jaub. & Spach) Eig (*Poaceae*). ICARDA / Wageningen Agricultural University Papers 94, 1–512.

Sukumaran S, Yu J. 2014. Association mapping of genetic resources: achievements and future perspectives. In: Tuberosa R, Graner A, Frison E (Eds.), Genomics of plants genetic resources. New York: Springer, 207–235.

USDA. United States Department of Agriculture. 2019. https://www.usda.gov/topics/data

Wang GZ, Matsuoka Y, Tsunewaki K. 2000. Evolutionary features of chondriome divergence in *Triticum* (wheat) and *Aegilop*s shown by RFLP analysis of mitochondrial DNAs. Theoretical and Applied Genetics 100, 221–231.

Zhao C, Liu B, Piao S, et al. 2017. Temperature increase reduces global yields of major crops in four independent estimates. Proceedings of the National Academy of Sciences of the USA 114, 9326–9331.

Zhu C, Core M, Buckler ES, Yu J. 2008. Status and prospects of association mapping in plants. Plant Genome 1, 5–20.

Zohary D, Hopf M, Weiss E. 2012. Domestication of plants in the Old World: the origin and spread of domesticated plants in Southwest Asia, Europe, and the Mediterranean Basin. Oxford University Press.

General Objectives

In view of the climate change and the prediction of a continued increase in temperature in the near future, it is urgent to discovery new genetic sources able to improve the resilience of the cultivated durum wheat to heat stress. In this direction, this study will focus on the dissection the heat stress tolerance QTLome of durum wheat in 183 durum cultivars and elite breeding lines suitable for Genome Wide Association Studies (GWAS) released in Mediterranean countries, Mexico and the USA, following the steps described bellow:

- Phenotyping for physiological traits in plants exposed to heat stress during the vegetative stage under a controlled environment;
- Phenotyping for grain yield and important agronomic traits in plants exposed to heat stress during the entire cycle under field conditions;
- Performing Genome Wide Association Study (GWAS), in order to identify chromosomic regions involved in the heat stress tolerance response in different growth stages.

2. Chapter 2: Chlorophyll fluorescence under daylight conditions as a proxy to dissect the QTLome for heat-stress tolerance in durum wheat

2.1. Introduction

Heat stress is a major factor limiting wheat yield and its stability, particularly in view of rising atmospheric temperature and the increased weather variability caused by climate change (Semenov and Shewry, 2011; Asseng *et al.*, 2017; Tuberosa *et al.*, 2019). Global warming models predict a substantial mean temperature increase (IPCC, 2014) coupled with more severe heat waves and reduction of annual precipitation (Lobell *et al.*, 2015; Liu *et al.*, 2016; Asseng *et al.*, 2017; Zhao *et al.*, 2017), especially in the Mediterranean basin (Danzi *et al*., 2019; Kutiel, 2019). It has been estimated that each degree-Celsius increase in the mean temperature can cause a global average loss of 6% of wheat yield, from 2.6% in China to 9.1% in India (Zhao *et al.*, 2017), clearly underlining the urgency to enhance wheat resilience to heat stress.

In wheat, heat stress (HS) reduces photosynthetic capacity (Ashraf and Harris, 2013; Feng *et al.*, 2014; Posch *et al.*, 2019), alters plant water relations (Wahid *et al.*, 2007; Hasanuzzaman *et al.*, 2013) and metabolic activities (Farooq *et al.*, 2011), increases the production of reactive oxygen species (Wang *et al.*, 2011; Chen and Yang, 2019; Sharma *et al.*, 2019) and, when occurring at flowering and grain filling reduces fertility and grain yield (Gautam *et al*., 2014; Akter and Islam, 2017; El Hassouni *et al*., 2019; Fabian *et al*., 2019).

Assessing directly heat tolerance in adult plants is not straightforward nor practical, particularly under field conditions. Typically, assessing heat tolerance under field conditions entails either (i) screening under delayed sowing date, in order to shift the wheat growing cycle when high temperatures occur, (ii) screening under artificial environment (e.g. plastic tunnel; El Hassouni *et al*., 2019) or (iii) screening in locations with constantly higher temperatures during vegetative growth flowering and/or grain filling stage.

Due to the medium-to-low heritability and relatively high G×E of heat tolerance, a reliable field evaluation also entails collecting data in multiple years and locations (El Hassounni *et al*., 2019; Sareen *et al*., 2019). All these options are not practical, especially when screening a large number of progenies/accessions as in the case of the large germplasm collections required in genome-wide association studies (GWAS) for QTLome dissection (Salvi and Tuberosa, 2015). Field screening targets either directly ear fertility, grain yield and grain quality parameters or, indirectly, single physiological component-traits related to HS tolerance (Tuberosa *et al.*, 2012) or a combination of both (Cossani and Reynolds, 2015; Reynolds *et al.*, 2017).

From a physiological standpoint, numerous biological mechanisms relevant to heat tolerance can be phenotyped such as growth maintenance and biomass accumulation under high temperatures (Reynolds *et al.*, 2017; El Hassouni *et al.*, 2019), fertility maintenance under HS at grain filling (El Hassouni *et al.*, 2019) and remobilization of water soluble carbohydrates during grain filling stage

(Reynolds *et al.*, 2015, 2017). Additional traits that have been considered as potential proxies relevant for thermotolerance include: (i) cell membrane stability under HS (Wahid *et al.*, 2007), (ii) total chlorophyll content, chlorophyll a/b ratio, photosynthetic capacity and chlorophyll fluorescence (Baker, 2008; Murchie and Lawson, 2013; Kalaji *et al.*, 2017; Posch *et al.*, 2019), (iii) capacity to avoid the overproduction of reactive oxygen species (ROS) (Wahid *et al.*, 2007; Cossani and Reynolds, 2012; Hossain *et al.*, 2015), (iv) antioxidant enzyme activity (Fahad *et al.*, 2017) and (v) increased synthesis of heat shock proteins (Wang *et al.*, 2004; Comastri *et al.*, 2018). Some of these adaptive traits are induced by HS while others are constitutively expressed. Once ascertained, proxy traits facilitate germplasm screening under controlled environments and, when correlated with yield and characterized by high heritability, can accelerate the selection of heat-resilient genotypes.

Among the main physiological traits, photosynthesis is particularly sensitive to HS, mainly due to damage to the photosynthetic machinery (e.g. Rubisco activity) and photosystem II (PSII) role in the electron transfer chain (Feng *et al.*, 2014; Mathur *et al.*, 2014; Posch *et al.*, 2019), decrease in leaf area expansion and premature leaf senescence (Akter and Islam, 2017). Photosynthesis is decreased by a reduced Rubisco activity even at moderate HS (Feller *et al.*, 1998; Wise *et al.*, 2004; Perdomo *et al.*, 2017) and more so at severe stress by the inhibition of PSII activity (Posch *et al.*, 2019). For this reason, photosynthesis has been considered as the most thermally-labile component of the photosynthetic electron transport chain (Wahid *et al.*, 2007; Feng *et al.*, 2014; Posch *et al.*, 2019).

Chlorophyll fluorescence (ChlF) is the trait most commonly used to investigate PSII, particularly due its non-invasive measurement coupled with fast and low-cost (Murchie and Lawson, 2013; Kalaji *et al.*, 2016, 2017). More in general, ChlF is considered a broader indicator of plant response to environmental changes (Murchie and Lawson, 2013).

The state of PSII can be monitored with ChlF measured on dark-adapted leaves or on leaves in ambient light. As ChlF measures light re-emitted from PSII, ambient light strongly interferes with its measure. For this reason, early experiments adopted the dark-adapted system which, due to its slow throughput, is unsuitable for the genetic dissection of the ChlF QTLome. This problem can be overcome by the adoption of the LIFT (Light-Induced Fluorescence Transient) method, a high-throughput approach which measures ChlF based on a modulating system where quick light flashes are used to induce fluorescence at a specific known frequency and the equipment is set to take measurements at the same frequency (Murchie and Lawson, 2013; Kalaji *et al.*, 2017; Keller *et al.*, 2018). In this way, the equipment will only measure fluorescence resulting from a specific known frequency and will avoid interference due to ambient light (Baker, 2008; Murchie and Lawson, 2013). As compared with the dark-adapted system, LIFT allows for the measurement of ChlF without

darkening the leaves, making it faster, less laborious and highly suitable for GWAS (Genome-wide Association Mapping Study), the approach most frequently used to dissect the genetic basis of quantitative traits.

Chlorophyll fluorescence has been used to elucidate plant responses of environmental cues and the fundamental mechanisms of photosynthesis (Fiorani and Schurr, 2013; Murchie and Lawson, 2013; Kalaji *et al.*, 2016; Posch *et al.,* 2019). Recently, the interest in ChlF focused on the possible application to crop improvement by linking physiological plant responses with genomic information has increased (Sharma *et al.*, 2012; Feng *et al.*, 2014; Azam *et al.*, 2015; Zhou *et al.,* 2015; Chen *et al.*, 2017). This notwithstanding, so far only a few studies have reported on the dissection of the ChlF QTLome in wheat under HS (Azam *et al*., 2015; Sharma *et al*., 2017; Bhusal *et al*., 2018) while no information is available for durum wheat, despite its cultivation mainly occurs in HS- prone regions.

This study reports the first results on mapping ChlF QTLs in durum wheat and presents a comparative analysis with QTL results obtained in bread wheat, hence contributing toward the identification of molecular markers suitable for the application of marker-assisted selection to mitigate the effects of HS in wheat.

2.2. Material and methods

2.2.1. Plant material

The panel (named hereafter as UNIBO-Durum Panel) used in this study included 183 elite durum cultivars and elite breeding lines from Italy, Morocco, Spain, Syria, Tunisia Mexico and USA that were chosen from a larger panel (336 accessions) based on their pedigree and heading date. Therefore, accessions with high identity-by-descent value based on pedigree and molecular maker data (Maccaferri *et al*. 2007 a, b) and/or with differences higher than 7 days in heading date in Mediterranean countries (Maccaferri *et al.*, 2011) were excluded in order to reduce possible bias of phenology on QTLome dissection (Tuberosa, 2012). Additional information about UNIBO-Durum Panel is reported in (Maccaferri *et al.*, 2006, 2011).

2.2.2. Phenotypic evaluation

The UNIBO-Durum Panel was evaluated under greenhouse conditions adopting a complete randomized design with three replicates and two treatments, control (no heat stress: NS) and heat stress (HS). Twenty seeds/accession were sown in 3-L pots (20x12x12 cm) filled with a mixed substrate of peat, vermiculite, sand and perlite (4:2:1.5:1) enriched with fertilizer. Pots were placed on benches (8x2 m) with a 1-cm deep water layer that maintained by capillarity a uniform soil moisture (80% soil-water capacity) in all pots. Seedlings were thinned to 12 plants/pot (the

experimental unit) and kept at 20±1 °C during the day and 14±1 °C at night, 50-70% relative humidity, 16-h photoperiod (700 µmol m^{-2} s^{-1} photosynthetic photon flux density at seedling level).

Plant phenology was recorded weekly according to the Zadoks *et al.* (1974) growth scale. The HS treatment was started when plants showed 4-5 unfolded leaves (Zadoks growth scale 14-15). For the HS treatment, pots were moved to an adjacent section in the same greenhouse where plants were acclimated (25±1 °C day and 18±1 °C at night; 16-h photoperiod) for 3 days, then daily temperature was gradually increased to 38±2 °C day and 25±2 °C at night. Chlorophyll fluorescence was measured at 5 and 7 days after starting the HS treatment. After that, plants were returned to control conditions and 3 days later a third ChlF measurement (recovery) was taken. Subsequently, plants were kept in control conditions for 21 days and two other traits were measured, namely, percentage of plants fully recovered after HS (HS survival rate, Rec_survival) and percentage of green leaf area (canopy) in the bulk of plants after HS (Rec_greenness).

2.2.3. Phenotyping for chlorophyll fluorescence

Chlorophyll fluorescence was measured using a Light-Induced Fluorescence Transient (LIFT – Version LIFT-REM, Soliense Inc., New York, USA) device (Figure 2.1).

The LIFT method provides valuable information about maximum fluorescence in the light (F_m'), steady-state fluorescence (F_s), and variable fluorescence (F_q') used to calculate the apparent quantum efficiency of PSII (F_q'/F_m'). Additionally, LIFT measures ChlF during PSII relaxation, providing information on the reoxidation efficiency of the primary quinone acceptor (Q_A) (Pieruschka *et al.*, 2010; Keller *et al.*, 2018).

This instrument is equipped with a blue LED (445 nm) excitation source used to manipulate the level of photosynthetic activity and ChlF. The LIFT device detects ChlF emission at 685±10 nm and monitors any background signal during inter-flashlet period subtracting this signal from the in-flashlet ChlF signal. Additionally, the ChlF yield is internally normalized against the excitation power of each flashlet to correct for smaller fluctuations, keeping the flashlet excitation power at a constant level along the entire fast repetition rate (FRR) excitation phase (Keller *et al.*, 2018). From a series of 300 sub-saturating measuring flashlets applied in FRR F_m', F_q' and F_s are retrieved in the excitation phase in 0.75 ms. From a further 127 flashlets with decreasing time intervals, the efficiency of reoxidation of the primary quinone electron acceptor (Q_A^-) was calculated at different times (0.65 ms (F_{r1}'/F_q') and 120 ms (F_{r2}'/F_q')) in 209 ms. Additional information is reported in Keller *et al.* (2018).

For ChlF phenotyping, the device was attached to a mobile custom-made positioning system and adjusted to a measuring distance of 60 cm from the soil surface (Figure 2.1). Control and HS plants

were measured continuously under ambient light conditions (seven flashes per experimental unit), and the F_q'/F_m' values derived from the LIFT measurements were averaged plant-wise.

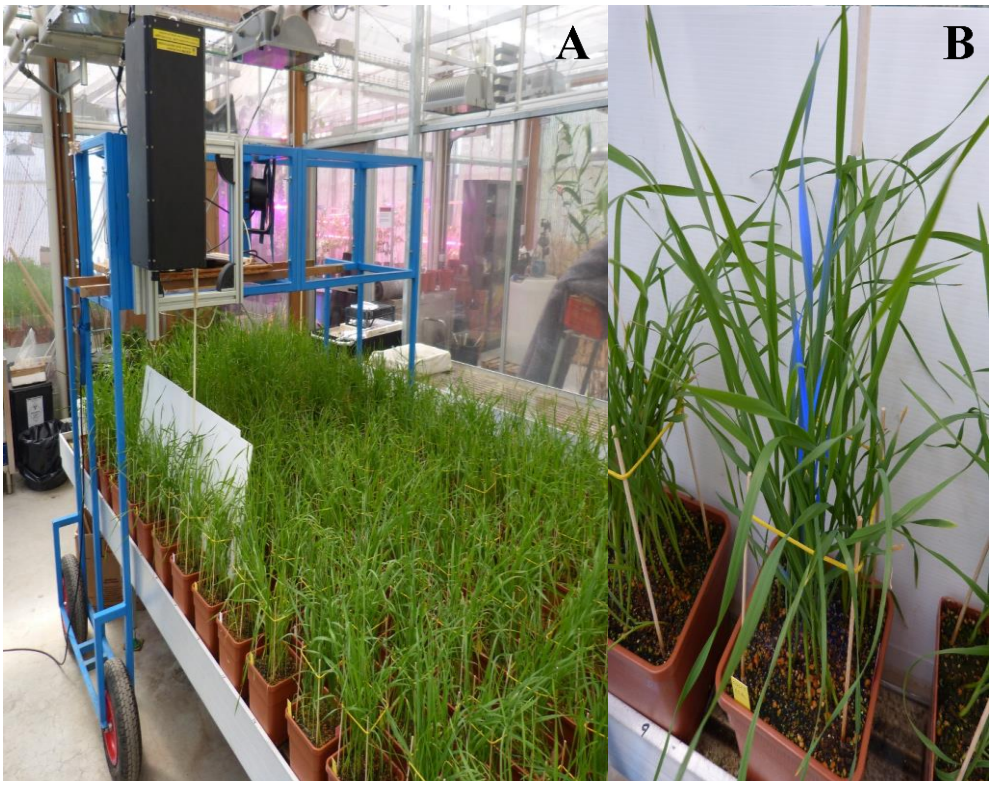

Figure 2.1. Light-Induced Fluorescence Transient (LIFT) equipment used to collect the data for chlorophyll fluorescence under greenhouse condition (A). Detail of the blue light flashes (B). The white panel between the row of pots were used only during the measurement time in order to avoid over position of the leaves from different pots (plots).

2.2.4. Cell membrane stability measurement

Cell membrane stability (CMS) was measured in a second experiment. Seeds were germinated in Petri dishes and then vernalized for two weeks at 6 °C. Four seedlings from each accession were transplanted in pots filled with the same substrate and and kept in greenhouse under the same environmental conditions previously described. Soil water capacity was maintained around 80% in order to avoid any water stress effect.

Cell membrane stability was measured in three different steps.

Firstly, when plants reached 14-15 Zadoks growth stage, 4-cm long leaf segments of the last fully expanded leaf were sampled from four plants. In a detached-leaf experiment, fully expanded leaves were cut in 2-cm long segments, divided in a “control-sample” and a “treated-sample”, washed in deionized water and placed in plastic vials containing 15 ml deionized water. The “treated-samples” were heat-treated in the incubator for 1 h at 45 °C. After the treatment, samples were kept at 4 °C for 24 h in order to allow for ion leakage in the water solution. In the following day, ion

leakage was measured using a conductivity meter. After measurements, all samples were autoclaved for 15 min at 121 °C and their ion leakage was measured again. This trait was named as "constitutive HS response" (CMS_Const) and CMS was calculated using the formula described by (Blum and Ebercon, 1981) CMS (%) = $((1 – (T_1/T_2))/(1 – (C_1/C_2)) \times 100$, where: T_1 and T_2 are the heat-stressed samples at first and second measurements (before and after autoclaving), respectively, and C_1 and C_2 are the control samples at first and second measurements (before and after autoclaving), respectively.

In the second step, control samples were collected and then plants were moved into a growth chamber at 37 °C for 24 h, followed by a 5 h exposure at 45 °C prior to the collection of the heat-stressed. Samples were kept at 4 °C for 24 h before measuring ion leakage. Subsequently, all samples were autoclaved for 15 min at 121 °C and their conductance measured again. The CMS has been calculated using the formula previously described. This trait was named acquired HS response (CMS_Acqui).

In the third step, samples collected from plants moved in growth chamber kept at 37 °C for 24 h (hardening), were kept in an incubator for 1 h at 45 °C. After the treatment all samples were kept at 4 °C for 24 h before measuring the conductance with a conductivity meter. After the measurements, all samples were autoclaved for 15 min at 121 °C and their conductance measured again. In this step of the experiment, CMS was calculated by using as control the value of the ions leakage measured on the samples used for the calculation of CMS_Acqui before the heat treatment. This trait was named constitutively-acquired HS response (CMS_Const_Acqui).

2.2.5. Reaction norm index

Reaction norm index (Δ) was calculated for each single genotype for all ChlF data (F_q'/F_m', F_{r1}'/F_q' and F_{r2}'/F_q'), using the following equation: $\Delta = ((Y_{HS} *100)/Y_{NS})$, where: Y_{HS} is the phenotypic mean for each accession under heat-stressed condition and, Y_{NS} is the phenotypic means for each accession under control condition. Values for Δ, control HS experiment were used for GWAS analysis.

2.2.6. SNP genotyping, population structure and GWAS analysis

Genomic DNA was extracted from each accession using NucleoSpin® 8/96 Plant II Core Kit from Macherey Nagel, after that, all samples of DNA were sent for SNP genotyping at TraitGenetics (http://www.traitgenetics.com/en/). Genotyping was processed using the Illumina iSelect 90K wheat SNP assay (Wang *et al*. 2014) and genotypes were called as described by Maccaferri *et al*. (2015a), while polymorphisms were mapped based on the tetraploid wheat-consensus- map-2015 (Maccaferri *et al*. 2015b).

Linkage disequilibrium (LD) among the markers was calculated in Haploview 4.2 software (Barrett *et al*. 2005) separately for each chromosome of the A and B genomes and only SNPs with known position and with a minor allele frequency (MAF) > 0.05 were taken into consideration. LD decay pattern as a function of consensus genetic distances was inspected considering squared allele frequency correlation (r^2) estimates obtained for all pairwise comparisons among intra-chromosomal SNPs. Curve fit and distance at which LD decays below r^2 0.3 were used to define the confidence intervals of QTLs detected in this study using a custom script in R (The R Core Team, 2016) as described in Maccaferri *et al*. (2015a).

Population structure was obtained in STRUCTURE 2.3.4 software (Pritchard *et al*. 2000) using a subset of 1,203 markers with $r^2 \geq 0.5$ which were obtained using tagger function in Haploview 4.2 (Barrett *et al.* 2005). STRUCTURE software was also used to perform the model-based quantitative assessment of subpopulation membership of the accessions and for this, only inferences based on molecular SNP data were used. STRUCTURE model included admixture and correlated allele frequencies among subpopulations. In order to identify the best number of subgroups for the population, numbers of hypothetical subpopulations ranging from k = 2 to 10 were performed using 50,000 burn-in interactions followed by 100,000 recorded Markov-Chain iterations and ten independent runs were carried out for each k in order to estimate the robustness of the population structure inference.

The rate of change in the logarithm of the probability of likelihood [LnP(D)] value between successive k-values (Δk statistics, Evanno *et al*. 2005) together with the inspection of the rate of variation (decline) in number of accessions clearly attributed to subpopulations (no. of accessions with Q membership's coefficient ≥ 0.5) and meaningful grouping based on pedigree and accessions passport data were used to predict the optimal number of subpopulations. Finally, the level of differentiation among subpopulations was determined using the Fixation Index (*Fst*) among all possible population pairwise combinations.

A maximum and optimal number of five subpopulations with accession memberships consistent with the known pedigree and passport data was chosen for subsequent analysis and GWAS results interpretation based upon the integrated analysis of (i) the derivation of the variance of the maximum likelihood estimation of the model plotted vs. increasing k (1k, Evanno *et al*., 2005) and (ii) analysis of pre-existing pedigree and passport information on the accessions included in the panel which provides an estimation of parentage among accessions. A kinship matrix of genetic relationships among individual accessions of the durum wheat panel was calculated with all non-redundant SNP markers (7,723) using Haploview 4.2 tagger function set to r^2 = 1.0. Kinship based

on Identity-by-State (IBS) among accessions was calculated in TASSEL (Trait Analysis by aSSociation, Evolution and Linkage) 5.2.37.

A total of 13,823 informative SNPs with minor allele frequency (MAF) > 0.05 were used for GWAS based on TASSEL 5.2.37 software using a Mixed Linear Model (MLM, Bradbury *et al.*, 2007), which included either kinship matrix (K) alone or with structure subpopulation membership estimates (Q) as random effects. MLM was performed according to Zhang *et al.* (2010) as follows: $y = X\beta + Z\mu + e$, where: y: phenotype value; β: fixed effect due to marker; μ: vector of random effects not accounted for by the markers; X and Z: incidence matrices that related y to β and μ; e: unobserved vector of random residual. According to GWAS Q-Q (quantile-quantile) plot results (Figure 2.2), MLM+K+Q showed the best results to control the P-value inflation associated to population structure.

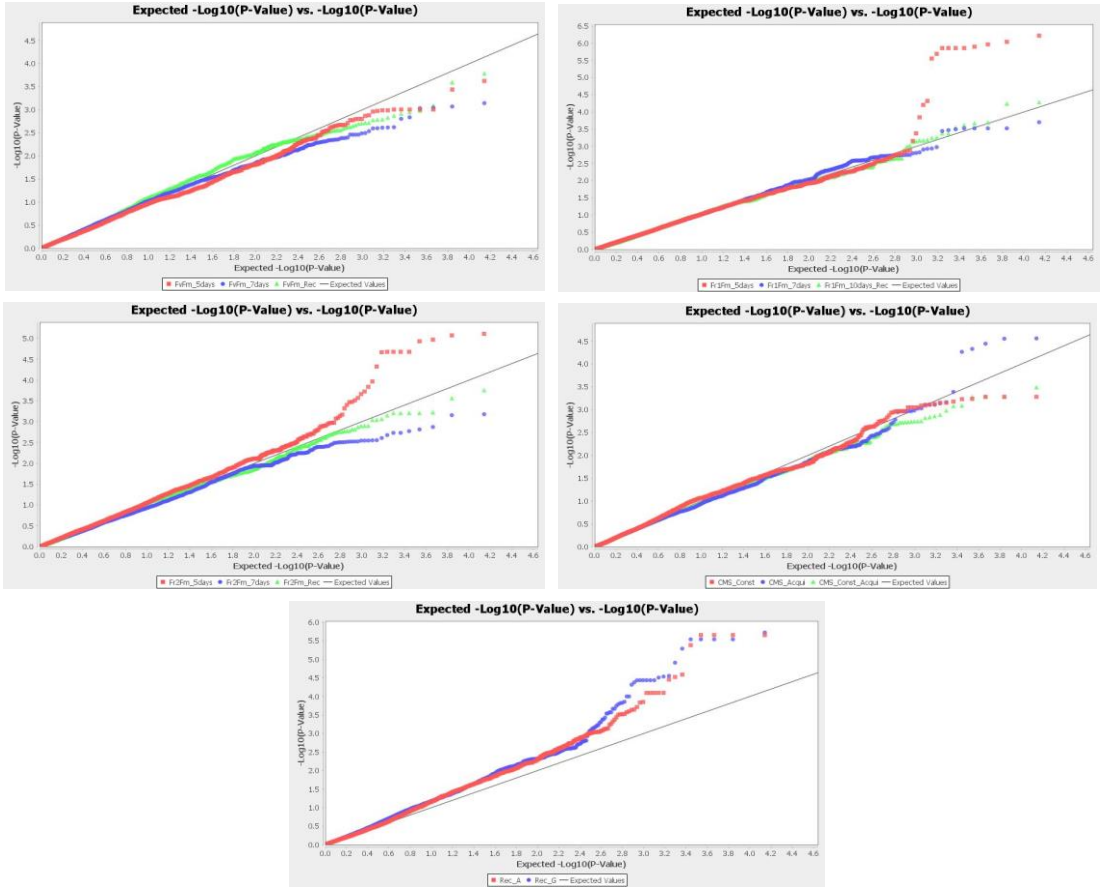

Figure 2.2. Q-Q (quantile-quantile) plot results of the GWAS analysis using the method Mixed Linear Model (MLM) + kinship matrix + population structure (Q) + phenology loci as covariate for maximum quantum efficiency of PSII (F_q'/F_m'), efficiency of reoxidation of the primary quinone electron acceptor at 0.65 ms (F_{r1}'/F_q') and 120 ms (F_{r2}'/F_q'), percentage of plants alive and fully recovered after heat stress (Rec_survival); percentage of green leaf area after heat stress (Rec_greenness); constitutive cell membrane stability (CMS_Const); acquired cell membrane stability (CMS_Acqui); constitutive-acquired cell membrane stability (CMS_Const_Acqui).

Thus, all GWAS analyses were performed based on MLM+K+Q model. Additionally, relevant loci for phenology (*PPD-A1, PPD-B1, FT-7A-indel, Rht-B1b,* and *VRN-A1*) were used as covariate, since these loci are strongly associated with the most important agronomic traits influenced by wheat growth, which may affect traits measured in this experiment.

The GWAS was carried out based on standard conditions of significance as follows: highly significant markers refer to $P < 0.0001$ while significant markers refer to $0.001 \geq P \geq 0.0001$. The average genetic distance at each LD decay under r^2 of 0.3, a threshold commonly adopted in GWAS studies (Maccaferri *et al.*, 2015a; Liu *et al.*, 2017; Condorelli *et al.*, 2018), was chosen to define QTL confidence intervals (cM). For this population, using SNP markers, the LD was 3.1 cM.

2.3. Results

2.3.1. Population structure of the UNIBO-Durum Panel

From a set of 13,823 polymorphic SNPs suitable for GWAS analysis (MAF ≥ 0.05), a reduced representative subset of 1,203 SNPs obtained after pruning for LD at $r = 0.50$ threshold were used to investigate the population structure of the 183 accessions of the UNIBO-Durum Panel.

Structure analysis presented a robust population genetic structure, as already reported in previous studies with a similar durum wheat germplasm, which have being analyzed using DArT®, SSR and/or SNP markers (Maccaferri *et al*. 2008, 2011; Letta *et al*. 2013; Liu *et al.* 2017; Condorelli *et al*. 2018). Structure analysis indicated the optimal number of *k* subpopulations for this group of genotypes was five. Considering $k = 5$ and Q membership coefficient ≥ 0.5, 142 accessions (77.6%) were clearly grouped into one of the five main gene pools identified in this study (Figure 2.3, Table A2.1), while 41 accessions (22.4%) did not show any correspondence with the five groups and for this reason they were considered as admixed accessions. The population structure division into five subgroups was strongly supported by pairwise comparison among and within subgroups based on Fixation Index (*Fst*), which reports about subpopulation diversity (Table A2.2) and by Neighbor Joining Tree (Figure 2.3).

Based on the structure results, the five subpopulations were as follows: (i) subpopulation 1 (S1) with 21 genotypes, mostly Italian genotypes developed for Mediterranean areas starting from North African and from Syrian landrace founders (e.g. Senatore Cappelli, Eiti, etc.), (ii) subpopulation 2 (S2) is the smallest subpopulation with 11 genotypes developed by ICARDA for dryland areas, mainly derived from crosses with the Syrian Haurani landrace, (iii) subpopulation 3 (S3) with 39 genotypes, mostly developed by ICARDA for temperate areas, (iv) subpopulation 4 (S4) is the largest subpopulation with 49 genotypes developed by CIMMYT and by several Mediterranean national research programs (Morocco, Tunisia, Italy, Spain) starting from the outstanding widely-

adapted Yavaros C79 germplasm (Yori/Anhinga//Flamingo pedigree) released in the '70s, and used as parents in different breeding programs around the world with the outstanding founder Karim in North Africa, Duilio and Latino in Italy, and Vitron in Spain as well as numerous ICARDA varieties and breeding lines for temperate areas (ICARDA-temperate), (v) subpopulation 5 (S5) with 22 genotypes from the CIMMYT wheat breeding program developed from the early 80's to early 90's starting from the outstanding Altar C84 germplasm.

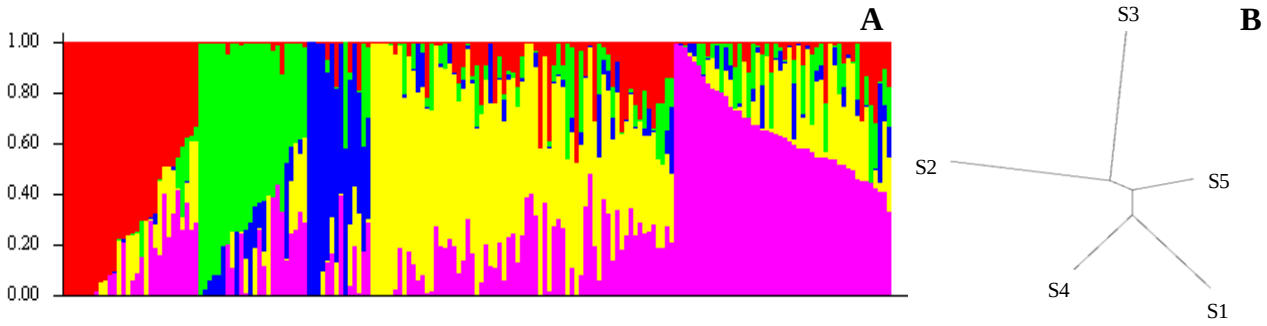

Figure 2.3. Bar plot (A) and neighbor joining tree (B) obtained with Structure 2.3.4 software for five durum wheat subpopulations sorted by Q and relative genetic distance.

2.3.2. Population structure effect on heat stress response distribution

The effect of population structure on phenotypic values was assessed by multiple regression analysis, using the best linear unbiased estimator (BLUE) values of the traits and the quantitative *Q* membership coefficients for each of the five main subpopulations and for each cultivar/breeding line obtained in TASSEL. Using BLUE, population structure moderately affected *Fq'/Fm'* at 7 days of heat stress (R^2 = 9.07%) and at recovery (R^2 = 11.48%), while showing stronger effects on *Fq'/Fm'* in control condition (R^2= 21.58%), Rec_survival (R^2 = 19.50%) and Rec_greenness (R^2= 21.06%) (Table 2.1).

The genetic structure of this population evidenced the presence of a highly structured diversity between subpopulations as shown by the analysis of the phenotypic values (Figures A2.1, A2.2). The subpopulations S1, S4 and S5 showed higher values of *Fq'/Fm'* than S2 and S3 under control condition (*Fq'/Fm'*_NS). Although S1, S4 and S5 showed higher values for *Fq'/Fm'*_NS, the difference between subpopulations was lower under heat stress (Figure A2.1). However, since *Fq'/Fm'* is highly related to PSII efficiency, any small reduction in *Fq'/Fm'* can affect considerably photosynthesis (Sharma *et al.* 2015). For the traits Rec_survival and Rec_greenness a considerable difference was evidenced between subpopulations, with S4 and S5 showing consistently higher values than S1, S2 and S3 (Figure A2.1), hence evidencing that different mechanisms of tolerance to heat stress affect *Fq'/Fm'* and Rec_survival and Rec_greenness.

2.3.3. Mean values, repeatability and correlation

Repeatability (h^2) values for F_q'/F_m' were 0.66 in NS, 0.50 at day 5 of stress, 0.71 on day 7 of stress and 0.63 at recovery (Table 2.1). Mean values for F_q'/F_m' decreased by 10% from NS (0.72) to 5 days of HS (0.64), and by 19% after 7 days of HS (0.58). Following the HS treatment, F_q'/F_m' of the recovered plants (0.67) was 6% lower as compared to NS (0.72) (Table 2.1, Figure 2.4).

Table 2.1. Descriptive statistics and repeatability (h2) estimates for heat stress response and chlorophyll fluorescence indexes in 183 elite cultivars and breeding lines from the UNIBO-Durum Panel grown under control and heat stress environment in controlled condition.

Trait	Stress treatment/period	Min.	Max.	Mean	St. dev.	h^2	C.V. (%)	R2 (%) [5]
F_q'/F_m' [1]	Control at 20°C	0.662	0.752	0.716	0.02	0.66	2.08	21.58
F_q'/F_m'	5 days of heat stress at 38°C	0.506	0.731	0.643	0.03	0.50	4.89	2.25
F_q'/F_m'	7 days of heat stress at 38°C	0.405	0.715	0.580	0.04	0.71	7.22	9.07
F_q'/F_m'	7 days of heat stress at 38°C + 3 days of recovery at 24°C	0.552	0.741	0.672	0.03	0.63	4.40	11.48
F_{r1}'/F_q'	Control at 20°C	0.143	0.294	0.221	0.02	0.57	10.04	4.50
F_{r1}'/F_q'	5 days of heat stress at 38°C	0.226	0.407	0.320	0.03	0.46	8.75	3.57
F_{r1}'/F_q'	7 days of heat stress at 38°C	0.205	0.329	0.266	0.02	0.55	8.17	1.68
F_{r1}'/F_q'	7 days of heat stress at 38°C + 3 days of recovery at 24°C	0.100	0.272	0.197	0.03	0.64	13.10	3.50
F_{r2}'/F_q'	Control at 20°C	0.475	0.670	0.591	0.03	0.56	5.26	3.74
F_{r2}'/F_q'	5 days of heat stress at 38°C	0.556	0.786	0.697	0.03	0.46	4.62	2.19
F_{r2}'/F_q'	7 days of heat stress at 38°C	0.565	0.727	0.650	0.03	0.44	4.52	1.39
F_{r2}'/F_q'	7 days of heat stress at 38°C + 3 days of recovery at 24°C	0.447	0.689	0.597	0.04	0.63	6.50	2.24
Rec_survival [2]	7 days heat stress at 38°C + 21 days of recovery at 24°C	11.20	100.00	55.45	26.80	0.80	18.34	19.50
Rec_greenness [3]	7 days heat stress at 38°C + 21 days of recovery at 24°C	6.20	93.70	42.62	19.04	0.83	14.68	21.06
CMS_Const [4]	1 h at 45°C	4.70	86.80	37.60	15.33	0.94	10.77	0.50
CMS_Acqui	5 h at 45°C	80.20	100.00	98.10	3.74	0.90	3.81	1.05
CMS_Const_Acqui	1 day at 37°C + 1 h at 45°C	22.60	100.00	71.01	12.19	0.96	17.16	1.05

[1] F_q'/F_m': maximum quantum efficiency of PSII; F_{r1}'/F_q': efficiency of reoxidation of the primary quinone electron acceptor at 0.65 ms; F_{r2}'/F_q': efficiency of reoxidation of the primary quinone electron acceptor at 120 ms. [2] Rec_survival: percentage of plants alive and fully recovered after 7 days of heat stress at 38°C + 21 days of recovery at 24°C. [3] Rec_greenness: percentage of green leaf area in the plants after 7 days of heat stress at 38°C + 21 days of recovery at 24°C. [4] CMS_Const: constitutive cell membrane stability after 1 h of heat stress at 45°C; CMS_Acqui: acquired cell membrane stability after 5 h of heat stress at 45°C; CMS_Const_Acqui: constitutive-acquired cell membrane stability after 1 day of heat stress at 37°C + 1 h at 45°C. [5] R^2 adjusted considering the five subgroups obtained by population structure analysis.

F_{r1}'/F_q' and F_{r2}'/F_q' showed similar effects on plants and were negatively correlated with F_q'/F_m' (Figure 2.5). Furthermore, both F_{r1}'/F_q' and F_{r2}'/F_q' parameters, conversely to F_q'/F_m', increased during the HS period. Mean values of F_{r1}'/F_q' increased by 45 and 20% at 5 and 7 days of

HS respectively, ranging from 0.20 at recovery to 0.32 at 5 days of HS. Similarly, F_{r2}'/F_q' increased by 18 and 10% at 5 and 7 days of HS, respectively, when compared with NS, while mean values increased from 0.59 at NS to 0.70 after 5 days of HS. The h^2 for F_{r1}'/F_q' ranged from 0.46 (5 days of HS) to 0.64 (recovery) while for F_{r2}'/F_q' ranged from 0.44 (7 days of HS) to 0.63 (recovery).

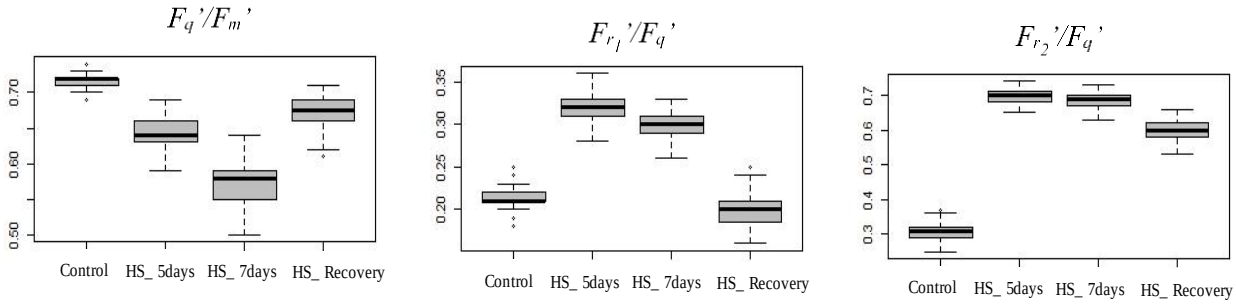

Figure 2.4. Boxplots of the best linear unbiased estimator (BLUE) of the traits for the UNIBO-Durum Wheat Panel measured under four different experimental conditions. (i) control, (ii) five days of heat stress, (iii) seven days of heat stress, and (iv) seven days of heat stress + three days of recovery. Maximum quantum efficiency of PSII (F_q'/F_m'), efficiency of reoxidation of the primary quinone electron acceptor at 0.65 ms (F_{r1}'/F_q') and 120 ms (F_{r2}'/F_q').

Correlations within F_q'/F_m' showed medium to high values (from 0.26 to 0.64 – values not shown) (Figure 2.5). Lower values were found for F_{r1}'/F_q' (from 0.26 to 0.30) and F_{r2}'/F_q' (from 0.25 to 0.34), except for the correlation between the data obtained at 5 days of HS as well as recovery. Comparing results between traits, very high values of correlation were found between F_{r1}'/F_q' and F_{r2}'/F_q' at 5 days (0.93), F_{r1}'/F_q' and F_{r2}'/F_q' at 7 days (0.97), and between F_{r1}'/F_q' and F_{r2}'/F_q' at recovery (0.97). F_q'/F_m' also showed significant but low correlation with Rec_survival and Rec_greenness, ranging from 0.29 to 0.42.

Rec_survival and Rec_greenness showed mean values of 55.5 and 42.6%, respectively, varying from 100 to 11.20% for Rec_survival and from 93.70 to 6.20% for Rec_greenness, respectively. Both Rec_survival and Rec_greenness showed high h^2 values (0.80 and 0.83, respectively) (Table 2.1), being correlated to F_q'/F_m' under NS and at an early stage of stress (F_q'/F_m' at day 5) though with low correlation values (0.35 and 0.36, respectively) (Figure 2.5). Rec_survival and Rec_greenness did not show any significant correlation with F_{r1}'/F_q' and F_{r2}'/F_q' at all stages as well as with CMS values.

Cell membrane stability (CMS) showed very high values of h^2, equal to 0.94 (CMS_Const), 0.90 (CMS_Acqui) and 0.96 (CMS_Const_Acqui). Notably, CMS was not significantly correlated with any of the other traits.

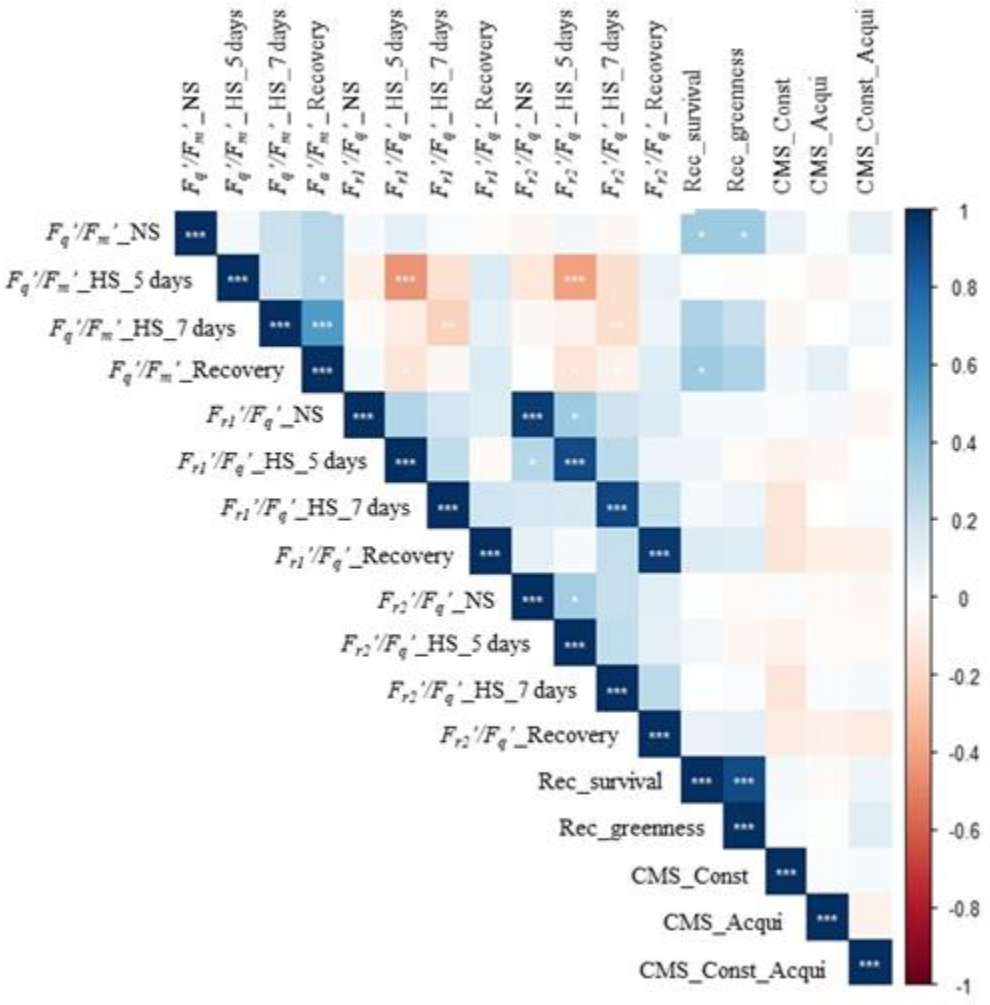

Figure 2.5. Pearson correlation coefficients between the traits maximum quantum efficiency of PSII (F_q'/F_m'), efficiency of reoxidation of the primary quinone electron acceptor at 0.65 ms (F_{r1}'/F_q') and 120 ms (F_{r2}'/F_q'), percentage of plants alive and fully recovered after heat stress (Rec_survival); percentage of green leaf area after heat stress (Rec_greenness); constitutive cell membrane stability (CMS_Const); acquired cell membrane stability (CMS_Acqui); constitutive-acquired cell membrane stability (CMS_Const_Acqui) under four different environmental condition (i) control (NS), and heat stress (HS) (ii) five days of heat stress, (iii) seven days of heat stress and (iv) seven days of heat stress + three days of recovery. Correlation significance: *** P < 0.001, ** P < 0.01, * P < 0.05.

2.3.4. GWAS results under control condition

A total of 13 QTLs for ChlF-related traits were identified under control condition (NS), seven for F_q'/F_m', two for F_{r1}'/F_q' and four for F_{r2}'/F_q' on chromosomes (chr) 1A (3 QTLs), 2B (1), 4B (1), 5B (1), 6B (4) and 7A (3) (Table A2.3). The phenotypic variation explained by each molecular marker (R^2) varied from 6.2% (*QF_{r1}'/F_q'_NS.ubo-1A.1*) to 8.7% (*QF_q'/F_m'_NS.ubo-5B.1*) with significance

(–$\log_{10}$ (P)) values ranging from 3.1 (*QF_{r1}'/F_q'_NS.ubo-1A.1*, *QF_{r1}'/F_q'_NS.ubo-7A.1* and *QF_{r2}'/F_q'_NS.ubo-1A.1*) to 4.1 (*QF_q'/F_m'_NS.ubo-6B.1*).

2.3.5. GWAS results under heat stress

Under HS conditions, 50 QTLs reached the significant threshold (–$\log_{10}$ (P) > 3.0) for the investigated traits (for details, see Table A2.4). Rec_survival showed the highest number of QTLs (8), followed by Rec_greenness, F_q'/F_m' at 7 days as well as F_q'/F_m' at recovery (each with 7 QTLs) and CMS_Const (6). For each one of the remaining traits, less than five QTLs were identified (Table A2.4). Among the 16 QTLs for F_q'/F_m', three of them located on chr 1A (132.1–147.6 cM), chr 3B (75.6–87.0 cM) and chr 7A (111.0–113.6 cM) showed concurrent effects at 7 days as well as at recovery time and between different traits as well.

Similar results were found for Rec_survival and Rec_greenness QTLs on chr 2A (186.1–189.8 cM), 2B (135.6–148.6 cM), 5A (106.0–115.8 cM), 5A (127.9–133.7 cM), 5A (137.2–142.6 cM), 6B (32.6–43.2 cM) and 7A (111.0–114.0 cM), practically all QTLs identified also for Rec_survival and Rec_greenness, except that on chr 6B (147.7–153.8 cM) for Rec_survival and on chr 3B (201.5–211.1 cM) for Rec_greenness (Table A2.4).

Under HS, the largest number of QTLs were mapped on chr 7A (8), 5A (6) and 6B (5) with –$\log_{10}$ (P) ranging from 3.00 (several markers) to 5.72 (*QRecG.ubo-5A.2*) and R^2 from 3.8% (*QRecG.ubo-3B*) to 13.4% (*QRecG.ubo-7A*).

Among the 50 QTLs reported under HS condition, 30 influenced more than one trait and 12 overlapped with one or more QTLs for Δ traits (Table A2.5). The three QTLs most consistently associated with multiple traits were located on chr 3B (76.0–82.2 cM: F_q'/F_m' at 7 days, F_q'/F_m' at recovery and F_{r2}'/F_q' at 5 days), chr 7A (100.6–108.5 cM: F_{r1}'/F_q' at 5 days, F_{r1}'/F_q' at 7 days and F_{r2}'/F_q' at 7 days) and chr 7A (110.0–116.3 cM affecting F_q'/F_m' at 7 days, F_q'/F_m' recovery, Rec_survival and Rec_greenness,) (Table A2.5).

2.3.6. GWAS for reaction norm index (Δ)

For Δ, GWAS was performed only for ChlF proxy (F_q'/F_m', F_{r1}'/F_q' and F_{r2}'/F_q') since the other traits had no corresponding NS (control). A total of 31 QTLs were identified for all Δ traits on Chr 1A, 1B, 2B, 3B, 6A, 6B, 7A and 7B (Table A2.6). The highest number of QTLs was identified for Fr_1'/F_q' recovery (7), F_q'/F_m' at 7 days (4), and F_{r2}'/F_q' recovery (4). Chromosomes 1A, 2B, 6A and 7A (6) presented the largest number of QTLs, with R^2 values from 5.7% (*QFr_2'/F_q'_Δ.ubo-7B.1* for F_{r2}'/F_q' at 5 days) to 11.4% (*QF_q'/F_m'_Δ.ubo-7A.2* for F_q'/F_m' recovery).

From the 31 QTLs identified for Δ, 19 influenced two or more traits. Among these, the two most important ones were mapped to chr 6A (60.0–66.9 cM) and chr 7A (107.0–114.0 cM) (Table A2.6). Thus, the most relevant ChlF stress-responsive QTL appears to be *QF_q'/F_m'_Δ.ubo-7A.2* which showed the strongest R^2 (11.4 and 13.4%) at 7 days of HS and at the end of the stress under recovery, respectively. The same QTL also affected F_{r1}'/F_q' at recovery.

2.3.7. QTL clusters: trait-specific or multi-traits, constitutive or adaptive

Considering both NS and HS experiments as well as Δ phenotypes, 15 QTL clusters affecting two or more traits across experimental conditions and/or across traits were identified (Table A2.5). In most cases, the QTL clusters showed similar direction of their effects on the single associated traits, hence supporting the hypothesis of prevailing pleiotropy rather than tight linkage as the cause of such concurrent effects (Tuberosa *et al.*, 2002). The identified QTL clusters can be categorized in two classes: (i) with specific effects on a unique trait and (ii) with effects observed in multiple traits and/or treatment conditions.

As to QTL clusters with trait-specific effects, it is worth mentioning *HS_QTL_cluster_1A.3* and *HS_QTL_cluster_7A.3* for F_q'/F_m', *HS_QTL_cluster_2B.1* and *HS_QTL_cluster_5A*, both for Rec_survival and Rec_greenness after recovery but not for ChlF (Table A2.5).

Among ChlF parameters, *HS_QTL_cluster_1A.2*, *HS_QTL_cluster_2B.2* and *HS_QTL_cluster_7A.1 s*howed specificity for F_{r1}'/F_q' and F_{r2}'/F_q' and not for F_q'/F_m' (Table A2.5). Notably, other QTLs showed multiple-trait effects including ChlF parameters on one side and either Rec or CMS traits on the other side as in the case of *HS_QTL_cluster_1A.1*, *HS_QTL_cluster_6A*, *HS_QTL_cluster_6B.1* and *HS_QTL_cluster_7A.2*.

As to QTL clusters for ChlF, three groups can be distinguished, i.e. those that showed effects under (i) NS only (*HS_QTL_cluster_6B.2*), (ii) both NS and HS conditions as well as considering reaction norms, and (iii) QTLs with mainly adaptive effects, identified only under HS and Δ, namely *HS_QTL_cluster_1A.1*, *HS_QTL_cluster_6A*, *HS_QTL_cluster_7A.3* and *HS_QTL_cluster_7B*. Thus, they can be highlighted as adaptive QTL clusters. The *HS_QTL_cluster_6A* affected F_{r1}'/F_q' and F_{r2}'/F_q' at 7 days of HS and recovery for both HS and Δ, while *HS_QTL_cluster_1A.1* affected F_{r1}'/F_q' and F_{r2}'/F_q' at 7 days of HS and recovery for Δ. The *HS_QTL_cluster_7A.2*, the most interesting one, affected F_q'/F_m' at 7 days of HS as well as at recovery for both HS and Δ, simultaneously, besides Rec_survival and Rec_greenness (Table A2.5).

Next, the allele frequency polymorphism and the allelic distribution among subpopulations for all QTL clusters were investigated.

Considering the 15 main QTL clusters, the cultivars/breeding lines harbored a number of beneficial alleles ranging from a minimum of four-six (as in the case of the Italian Ofanto, Claudio, Colosseo, ICARDA and North African Telset, Marzak, Belikh 2, Desert Durum Kronos) to a maximum of 10-12, including or not the beneficial haplotype at *HS_QTL_cluster_7A.2* (as in the case of Svevo, Iride, Ciccio, Pietrafitta Torrebianca, Duilio, Meridiano among the Italian cultivars and Karim, Razzak, Jawhar, Marjana, Omlahn, Altar84=Gallareta among those of CIMMYT/ICARDA origin) (data not shown). Cultivars/advanced lines belonging to subpopulations 1, 2 and 3 (those mainly directly related to original landrace selection founders of North African and Syrian origin) showed an average number of beneficial alleles equal to 8.0, 8.4 and 7.6, respectively, while the subpopulations later developed at CIMMYT and ICARDA appear enriched in beneficial alleles, up to 9.5 for subpopulation 4 (CIMMYT '70s and ICARDA temperate) and 9.9 for subpopulation 5 (CIMMYT'80) (data not shown).

The *HS_QTL_cluster_1A.3* is a *per se* QTL for F_q'/F_m' and showed specific effects at NS and HS conditions at 7 days. The beneficial allele for *HS_QTL_cluster_1A.3* was present in 84.6% of the accessions, while the negative allele was mostly identified in the S3 subpopulation.

The three main adaptive QTL clusters showed different patterns of beneficial allele distribution. At *HS_QTL_cluster_2B.2* the beneficial allele (*IWB9088-C*) is present in a ratio of 31/152 accessions in subpopulations 1, 2, 3 and admixed lines showing polymorphism while basically absent in subpopulations 4 and 5, mostly fixed for the negative allele. At *HS_QTL_cluster_6A* the beneficial allele (*IWB67403-C*) was present in the ratio of 126/50, with the alleles of the tag-marker *IWB67403* present in balanced frequencies in subpopulations 1, 3, 4 and mostly fixed for the beneficial allele in subpopulations 2 and 5. At *HS_QTL_cluster_7A.2*, the beneficial allele *IWB9105-G* showed a 75/99 ratio. *IWB9105* was polymorphic in subpopulations 2, 3, 4 and admixed accessions. However, subpopulations 1 and 3 were mostly fixed for the *IWB9105-A* unfavorable allele while subpopulations 4 and 5 were highly enriched or fixed for the *IWB9105-G* beneficial allele.

2.4. Discussion

The use of non-destructive high-throughput phenotyping (HTTP) is an important prerequisite for the accurate dissection of the QTLome and, eventually, the cloning of major QTLs governing the adaptive response of crops to climate change (Salvi and Tuberosa, 2015; Danzi *et al.*, 2019). Accordingly, the record temperatures in 2019 underline the urgency of identifying novel alleles able to mitigate the effects of HS in crops like wheat prevalently grown in heat-prone regions such as the Mediterranean Basin (Danzi *et al.*, 2019; Kutiel, 2019).

Along this line, this study reports the suitability and effectiveness of the LIFT method for the HTTP level required for the GWAS dissection of the QTLome for ChlF as a proxy to investigate the response to HS in wheat. ChlF measurements provide valuable information on the quantum efficiency of PSII and the efficiency of the reoxidation of PSII (Keller *et al.*, 2018). Any interference on PSII efficiency caused by HS condition potentially decreases photosynthesis and total carbon gain, hence decreasing plant growth and yield (Sharma *et al.*, 2015).

GWAS analysis is a powerful approach to dissect the QTLome of complex traits, such as HS (Zhang *et al.*, 2010; Korte and Farlow, 2013), provided that the effects due to population structure and other covariates, most importantly phenology, are duly accounted for in order to avoid declaring false positive QTLs (Yu *et al.*, 2006; Zhang *et al.*, 2010; Korte and Farlow, 2013). In this study, both population structure and phenology loci were used as covariates and the Q-Q plots for multiple models to select the best model to identify QTLs for HS tolerance. Accordingly, Q-Q plot analysis indicated the model MLM + K + Q + Phenology loci as the best one to avoid false positives (Figure 2.2).

Among the ChlF-related traits, the reduction in F_q'/F_m' (the equivalent of F_v/F_m in dark-adapted plants) ascertained with LIFT (-10 and -19% from NS to 5 and 7 days of HS, respectively) compares to the reduction (-9%) reported by Sharma *et al.* (2017) for bread wheat in the values of dark-adapted maximum quantum yield (F_v/F_m) working with RIL populations specifically segregating for this trait. Since the quantum yield tightly reflects PSII activity, even a small decrease in F_q'/F_m' strongly interferes with PSII activity and net photosynthesis rate during HS periods (Sharma *et al.*, 2017; Posch *et al.*, 2019). Genetic factors associated with stress-adaptive traits, such as those related to the photosynthetic process, have been conserved during plant evolution, since genotypes with reduced photosynthesis performance are naturally eliminated (Sharma *et al.*, 2017).

Chlorophyll fluorescence parameters, such as F_q'/F_m' have been largely used as important parameters to investigate genetic variability in tolerance to drought (Wang *et al.*, 2012; Jedmowski *et al.*, 2013; de Miguel *et al.*, 2014) and HS (Azam *et al.*, 2015; Sharma *et al.*, 2015; Zhou *et al.*, 2015; Chen *et al.*, 2017; Bhusal *et al.*, 2018; Makonya *et al.*, 2019) as well as to obtain information about QTLs for HS tolerance (Azam *et al.*, 2015; Sharma *et al.*, 2017; Bhusal *et al.*, 2018). The dissection of the QTLome affecting F_q'/F_m' and eventually cloning the major QTLs will be instrumental to (i) fully understand the effect of this trait on electron transport chain and CO_2 assimilation process (Baker, 2008; Sharma *et al.*, 2012; Posch *et al.*, 2019) and (ii) select novel genotypes more HS tolerant via marker-assisted selection and/or genome editing (Salvi and Tuberosa, 2015).

Based on the information obtained from the durum wheat consensus map (Maccaferri *et al.*, 2015b) it is possible to accurately compare the bread and durum wheat QTLomes in order to have a more comprehensive view on the genetic landscape of agronomic traits in these two crops closely related from a phylogenetic and functional standpoint.

Our study identified seven (NS), 16 (HS) and nine (Δ) QTLs affecting ChlF across different traits. For F_q'/F_m', five QTL clusters, namely *HS_QTL_cluster_1A.3* (chr arm 1AL), *HS_QTL_cluster_3B* (chr arm 3BL), *HS_QTL_cluster_7A.2* (chr arm 7AS), *HS_QTL_cluster_7A.3* (chr arm 7AL) and *HS_QTL_cluster_7B* (chr arm 7BL) (Table A2.5) were shown to (i) harbor allelic variants affecting F_q'/F_m' in different experimental conditions and (ii) tag chromosome regions previously reported to affect grain yield potential (Maccaferri *et al.*, 2011; Sukumaran *et al.*, 2018).

The significant allele for *HS_QTL_cluster_1A.3* showed a negative effect on plants under control condition while showing a positive effect when plants were exposed to seven days of HS. The UNIBO-Durum Panel appears already enriched with the beneficial allele at this QTL cluster, present in 92.9% of accessions (data not shown). Notably, the S3 accessions developed by ICARDA for temperate area did not carry the HS tolerant haplotype for this specific QTL cluster. The GWAS study of Maccaferri *et al.* (2011), conducted with a largely similar population evaluated across a broad range of Mediterranean environments and water regimes, detected significant QTL effects on thousand kernel weight (TKW), grain number per spike (GNO) and grain yield (GY) in the same chromosome region encompassed by the confidence interval (143.1–149.3 cM) of *HS_QTL_cluster_1A.3*.

The adaptive role of *HS_QTL_cluster_3B* for F_q'/F_m' was highlighted under 7 days of HS as well as under recovery condition, with 42.6% of the accessions sharing the HS-tolerant allele. In durum wheat, the chromosomic region where *HS_QTL_cluster_3B* is located has been shown to affect GNO (Maccaferri *et al.*, 2011; Sukumaran *et al.*, 2018), TKW (Maccaferri *et al.*, 2011; Graziani *et al.*, 2014) and GY (Sukumaran *et al.*, 2018).

HS_QTL_cluster_7A.2 is a remarkably adaptive QTL involved in the ChlF process, particularly in the maximum quantum efficiency of PSII (F_q'/F_m'). Moreover, *HS_QTL_cluster_7A.3* was shown to affect GNO in bread wheat (Shi *et al.*, 2017) while *HS_QTL_cluster_7B* overlapped with QTLs in durum wheat for TKW and GY reported in Maccaferri *et al.* (2011) and also for normalized difference vegetation index (NDVI) (Graziani *et al.*, 2014).

The *HS_QTL_cluster_6B.2* (chr arm 6BL) for F_q'/F_m' and Fr_2'/F_q' has been reported to affect also GNO and GY in a large panel of bread wheat evaluated across 29 different environments worldwide (Lozada *et al.*, 2018). Notably, the peak marker of this QTL (*IWA5504*) did not overlap with a major chr 6B QTL for phenology 50.0 cM away on the consensus map (Maccaferri *et al.*,

2015b). Therefore, it can be considered as a valuable QTL Cluster affecting ChlF during vegetative growth in wheat irrespectively of flowering time.

Recently, Keller *et al.* (2018) identified F_{r1}'/F_q' and F_{r2}'/F_q' as two new ChlF parameters able to report on the reoxidation efficiency of the primary quinone acceptor (QA) at different periods during the reoxidation process. While F_q'/F_m' is computed as the difference between ChlF signal emission when QA is in a partially oxidized and a fully reduced state in the PSII reaction centers, F_{r1}'/F_q' and F_{r2}'/F_q' are measured during the reoxidation phase of QA, hence reflecting the electron transport capacity from QA toward PSI. Therefore, both F_{r1}'/F_q' and F_{r2}'/F_q' provide additional information about electron transport otherwise not reported by F_q'/F_m' (Keller *et al.*, 2018). Notably, F_q'/F_m' was negatively correlated with both F_{r1}'/F_q' and F_{r2}'/F_q'. Higher values of Fr_1'/Fq' and F_{r2}'/Fq' indicate higher reoxidation efficiency of the primary quinone acceptor (QA).

According to the model established by Duysens and Sweers (1963), the fluorescence yield of PSII is controlled by the fraction of reduced QA within the sample. Consequently, fluorescence yield at any given time is determined by the reduction level of QA resulting from reduction via PSII and oxidation via PSI. Overall, PSII is regarded to be more heat labile than PSI (Berry and Björkman, 1980). Variable ChlF decreases under HS (Briantais *et al*. 1996) due to quenching of F_m. Additionally, an increase of F_0 occurs predominantly above a critical temperature, marking the onset of irreversible heat damage to PSII (Lazar and Ilik, 1997). Furthermore, PSII is structurally damaged under strong HS by the loss of manganese ions from the oxygen evolving complex (Enami *et al*. 1994).

The negative correlation of F_q'/F_m' and the reoxidation parameters F_{r1}'/F_q', F_{r2}'/F_q' indicates that the efficiency of QA reduction by PSII was reduced relative to the maintained efficiency of QA oxidation by PSI. Interestingly, F_q'/F_m' recovered efficiently after the end of the treatment, whereas the effect on F_{r2}'/F_q' was still persisting (Figure 2.4). This indicates a long-term impact of HS on electron transport processes beyond QA. In contrast, PSII efficiency is quickly restored following the observed acute inhibition during HS.

F_{r1}'/F_q' and F_{r2}'/F_q' were strongly correlated (Figure 2.5), indicating that chromosomic regions affect both traits simultaneously. This correlation is supported by the QTLs that concurrently affected both traits, since most QTLs for F_{r1}'/F_q' were also identified for F_{r2}'/F_q' (Table A2.4). Since F_{r1}'/F_q' and F_{r2}'/F_q' were only recently introduced as ChlF parameters to obtain information on the reoxidation of QA^- (Keller *et al.*, 2018), it is not possible to compare our results to those of other wheat studies. This notwithstanding, two QTL clusters (*HS_QTL_cluster_2B.2* and *HS_QTL_cluster_6A*) for F_{r1}'/F_q' and F_{r2}'/F_q' overlapped with those already reported to affect NDVI (Condorelli *et al.*, 2018), TKW (Wang *et al.*, 2009) and GNO (Maccaferri *et al.*, 2011; Shi *et al.*, 2017) in wheat. In summary, five cluster QTLs can be categorized as primary QTLs for ChlF traits,

namely, *HS_QTL_cluster_1A.1*, *HS_QTL_cluster_2B.2*, *HS_QTL_cluster_6A*, *HS_QTL_cluster_7A.1* and *HS_QTL_cluster_7A.2*.

Recently, Condorelli *et al.* (2018), evaluating a larger panel of durum wheat in which most of the accessions evaluated in this study were included, showed the effect of *HS_QTL_cluster_2B.2* on NDVI under drought stress condition. NDVI is related to chlorophyll content due to the absorption features of the molecule, and consequently to the photosynthetic capacity of the plant as well as F_{r1}'/F_q' and F_{r2}'/F_q', which suggests the involvement of *HS_QTL_cluster_2B.2* in the adaptive response of durum wheat to abiotic stresses. The *HS_QTL_cluster_6A* chromosome region has been shown to affect TKW (Wang *et al.*, 2009) and GNO in both bread (Shi *et al.*, 2017) and durum wheat (Maccaferri *et al.*, 2011). Although, *HS_QTL_cluster_1A.1* and *HS_QTL_cluster_7A.1* have not been previously reported in the literature, in our study showed consistent effect on F_{r1}'/F_q' and F_{r2}'/F_q'. Notably, *HS_QTL_cluster_1A.1*, beside affecting F_{r1}'/F_q' and F_{r2}'/F_q', also affected CMS_Const, a trait influenced by the production of reactive oxygen species (ROS) under HS (Wahid *et al.*, 2007).

QTL clusters with major effects were also identified for Rec_survival and Rec_greenness, as shown by *HS_QTL_cluster_2B.1* and *HS_QTL_cluster_5A*, hence highlighting that QTLs other than those governing ChlF traits are also major determinant of HS tolerance and that a successful survival under prolonged HS and a complete recovery of the green canopy can be achieved based on biochemical/physiological mechanisms other than those directly related to ChlF, such as heat-schock proteins (Comastri *et al.*, 2018). Furthermore, the *HS_QTL_cluster_5A* chromosome region has been reported to affect GNO (Quarrie *et al.*, 2005; Maccaferri *et al.*, 2011; Shi *et al.*, 2017), TKW (Quarrie *et al.*, 2005) and number of spikes per square meter (SPM) (Maccaferri *et al.*, 2011; Graziani *et al.*, 2014) in durum wheat.

2.5. Conclusions

Our results are first to report the use of the Light-Induced Fluorescence Transient (LIFT) technique to measure chlorophyll fluorescence (ChlF) at the level of high-throughput phenotyping and accuracy required by GWAS to identify the genomic regions affecting PSII activity under HS in daylight conditions, hence avoiding the time-consuming use of dark-adapted canopies. The majority of the QTLs detected for ChlF and other heat-stress related traits mostly clustered in five chromosome hotspots, unrelated to phenology, each one accounting for a substantial portion of the variability detected for the investigated traits, a feature that makes these QTLs particularly valuable for breeding programs spanning a broad range of latitudes. The different chromosomic regions influencing ChlF under HS as well the late recovery after stress, clearly indicate that specific loci control HS tolerance in different growth stages. Therefore, pyramiding of the beneficial haplotypes at the identified QTLs,

most likely an ongoing process due to the unconscious selection through decades of breeding for wide adaptation, appears a suitable strategy to increase HS tolerance in wheat. The genomics dissection of the major QTLs now greatly facilitated by the sequencing of wild emmer (Avni *et al.*, 2017) and durum wheat (Maccaferri *et al.*, 2019), together with future QTL metanalyses for HS tolerance across the Triticeae will provide unprecedented opportunities for genomics-assisted approaches able to select wheat cultivars more resilient to heat stress.

References

Akter N, Islam M. 2017. Heat stress effects and management in wheat. A review. Agronomy for Sustainable Development. 37, 37.

Allen M, Antwi-Agyei P, Aragon-Durand F, *et al*. 2019. Technical summary. In: Global warming of 1.5° C. An IPCC Special Report on the impacts of global warming of 1.5° C above pre-industrial levels and related global greenhouse gas emission pathways, in the context of strengthening the global response to the threat of climate change, sustainable development, and efforts to eradicate poverty. Masson-Delmotte V, Zhai P, Pörtner H-O, *et al*. (eds.). In Press.

Ashraf M, Harris P. 2013. Photosynthesis under stressful environments: An overview. Photosynthetica 51, 163–190.

Asseng S, Cammarano D, Basso B, *et al*. 2017. Hot spots of wheat yield decline with rising temperatures. Global Change Biology 23, 2464–2472.

Avni R, Nave M, Barad O, *et al*. 2017. Wild emmer genome architecture and diversity elucidate wheat evolution and domestication. Science 357, 93–97.

Azam F, Chang X, Jing R. 2015. Mapping QTL for chlorophyll fluorescence kinetics parameters at seedling stage as indicators of heat tolerance in wheat. Euphytica 202, 245–258.

Baker NR. 2008. Chlorophyll Fluorescence: A Probe of Photosynthesis In Vivo. Annual Review of Plant Biology 59, 89–113.

Barrett JC, Fry B, Maller J, Daly MJ. 2005. Haploview: analysis and visualization of LD and haplotype maps. Bioinformatics 21, 263–265.

Berry J, Björkman O. 1980. Photosynthetic response and adaption to temperature in higher plants. Annual Review of Plant Physiology 31, 491–543.

Bhusal N, Sharma P, Sareen S, Sarial A. 2018. Mapping QTLs for chlorophyll content and chlorophyll fluorescence in wheat under heat stress. Biologia Plantarum 62, 721–731.

Blum A, Ebercon A. 1981. Cell membrane stability as a measure of drought and heat tolerance in wheat. Crop Science 21, 43.

Bradbury PJ, Zhang Z, Kroon DE, Casstevens TM, Ramdoss Y, Buckler E. 2007. TASSEL: software for association mapping of complex traits in diverse samples. Bioinformatics 23, 2633–2635.

Briantais JM, Dacosta J, Goulas Y, Cucruet JM, Moya, I. 1996. Heat stress induces in leaves an increase of the minimum level of chlorophyll fluorescence, Fo: A time-resolved analysis. Photosynthesis Research 48, 189–196.

Canè MA, Maccaferri M, Nazemi G, Salvi S, Francia R, Colalongo C, Tuberosa R. 2014. Association mapping for root architectural traits in durum wheat seedlings as related to agronomic performance. Molecular Breeding 34, 1629–1645.

Chen YE, Zhang CM, Su YQ, Ma J, Zhang ZW, Yuan M, Zhang HY, Yuan S. 2017. Responses of photosystem II and antioxidative systems to high light and high temperature co-stress in wheat. Environmental and Experimental Botany 135, 45–55.

Chen Q, Yang G. 2019. Signal function studies of ROS, especially RBOH-dependent ROS, in plant growth, development and environmental stress. Journal of Plant Growth Regulation 1–15.

Comastri A, Janni M, Simmonds J, Uauy C, Pignone D, Nguyen HT, Marmiroli N. 2018. Heat in wheat: exploit reverse genetic techniques to discover new alleles within the Triticum durum sHsp26 family. Frontiers in Plant Science 9, 1337.

Condorelli GE, Maccaferri M, Newcomb M, Andrade-Sanchez P, White JW, French A, Sciara G, Ward R, Tuberosa T. 2018. Comparative aerial and ground based high throughput phenotyping for the genetic dissection of NDVI as a proxy for drought adaptive traits in durum wheat. Frontiers in Plant Science 9, 893.

Cossani CM, Reynolds MP. 2012. Physiological traits for improving heat tolerance in wheat. Plant Physiology 160, 1710–1718.

Cossani CM, Reynolds MP. 2015. Heat stress adaptation in elite lines derived from synthetic hexaploid wheat. Crop Science 55, 2719–2735.

Danzi D, Briglia N, Petrozza A, Summerer S, Povero G, Stivaletta A, Cellini F, Pignone D, de Paola D, Janni M. 2019. Can high throughput phenotyping help food security in the Mediterranean area?. Frontiers in Plant Science 10, 737.

Duysens LNM, Sweers HE. 1963. Mechanisms of two photochemical reactions in algae as studied by means of fluorescence, In: Japanese Society of Plant Physiologists (ed) Studies on microalgae and photosynthetic bacteria, Special Issue of Plant and Cell Physiology. University of Tokyo Press, Tokyo, pp 353–372.

El Hassouni K, Belkadi B, Filali-Maltouf A, Tidiane-Sall A, Al-Abdallat A, Nachit M, Bassi FM. 2019. Loci controlling adaptation to heat stress occurring at the reproductive stage in durum wheat. Agronomy 9, 414.

Enami I, Kitamura M, Tomo T, Isokawa Y, Ohta H, Katoh S. 1994. Is the primary cause of thermal inactivation of oxygen evolution in spinach PSII membranes release of the extrinsic 33 kDa protein or of Mn?. BBA Bioenergetics 1186, 52-58.

Evanno G, Regnaut S, Goudet J. 2005. Detecting the number of clusters of individuals using the software STRUCTURE: A simulation study. Molecular Ecology 14, 2611–2620.

Fábián A, Sáfrán E, Szabó-Eitel G, Barnabás B, Jäger K. 2019. Stigma functionality and fertility are reduced by heat and drought co-stress in wheat. Frontiers in Plant Science 10, 244.

Fahad S, Bajwa AA, Nazir U, *et al*. 2017. Crop production under drought and heat stress: plant responses and management options. Frontiers in Plant Science 8, 1147.

Farooq M, Bramley H, Palta JA, Siddique KHM. 2011. Heat stress in wheat during reproductive and grain-filling phases. Critical Reviews in Plant Sciences 30, 491–507.

Feller U, Crafts-Brandner SJ, Salvucci ME. 1998. Moderately high temperatures inhibit ribulose-1,5-bisphosphate carboxylase/oxygenase (Rubisco) activase-mediated activation of Rubisco. Plant Physiology 116, 539–546.

Feng B, Liu P, Li G, Dong ST, Wang FH, Kong LA, Zhang JW. 2014. Effect of heat stress on the photosynthetic characteristics in flag leaves at the grain-filling stage of different heat-resistant winter wheat varieties. Journal of Agronomy and Crop Science 200, 143–155.

Fiorani F, Schurr U. 2013. Future scenarios for plant phenotyping. Annual Review of Plant Biology 64, 267–291.

Gautam A, Agrawal D, SaiPrasad SV, Jajoo A. 2014. A quick method to screen high and low yielding wheat cultivars exposed to high temperature. Physiology and Molecular Biology of Plants 20, 533–537.

Graziani M, Maccaferri M, Royo C, Salvatorelli F, Tuberosa R. 2014. QTL dissection of yield components and morpho-physiological traits in a durum wheat elite population tested in contrasting thermo-pluviometric conditions. Crop Pasture Science 65, 80–95.

Hasanuzzaman M, Nahar K, Alam MM, Roychowdhury R, Fujita M. 2013. Physiological, biochemical, and molecular mechanisms of heat stress tolerance in plants. International Journal of Molecular Sciences 14, 9643–9684.

Hossain MA, Bhattacharjee S, Armin S-M, Qian P, Xin W, Li H-Y, Burritt DJ, Fujita M, Tran L-SP. 2015. Hydrogen peroxide priming modulates abiotic oxidative stress tolerance: insights from ROS detoxification and scavenging. Frontiers in Plant Science 6, 420.

IPCC, 2014 Climate Change 2014: Synthesis Report. Contribute of Working Groups I, II, III to the Fifth Assessment Report of the Intergovernmental Panel on Climate Change [Core Writing Team, Pachauri RK, Meyer LA (eds.)]. IPCC, Geneva, Switzerland, 151pp.

Jedmowski C, Ashoub A, Brüggemann W. 2013. Reactions of egyptian landraces of Hordeum vulgare and Sorghum bicolor to drought stress, evaluated by the OJIP fluorescence transient analysis. Acta Physiologiae Plantarum 35, 345–354.

Kalaji HM, Jajoo A, Oukarroum A, Brestic M, Zivcak M, Samborska IA, Cetner MD, Lukasik I, Goltsev V, Ladle LJ. 2016. Chlorophyll a fluorescence as a tool to monitor physiological status of plants under abiotic stress conditions. Acta Physiologiae Plantarum 38, 102.

Kalaji HM, Schansker G, Brestic M, *et al*. 2017. Frequently asked questions about chlorophyll fluorescence, the sequel. Photosynthesis Research 132, 13–66.

Keller B, Vass I, Matsubara S, Paul K, Jedmowski C, Pieruschka R, Nedbal L, Rascher U, Muller O. 2018. Maximum fluorescence and electron transport kinetics determined by light-induced fluorescence transients (LIFT) for photosynthesis phenotyping. Photosynthesis Research 1–13.

Korte A, Farlow A. 2013. The advantages and limitations of trait analysis with GWAS: a review. Plant Methods 9, 29.

Kutiel H. 2019. Climatic uncertainty in the Mediterranean basin and its possible relevance to important economic sectors. Atmosphere 10, 10.

Lazar D, Ilik P. 1997. High-temperature induced chlorophyll fluorescence changes in barley leaves. Comparison of the critical temperatures determined from fluorescence induction and from fluorescence temperature curve. Plant Science 124, 159-164.

Letta T, Maccaferri M, Badebo M, Ammar K, A. Ricci, Crossa J, Tuberosa R. 2013. Searching for novel sources of field resistance to Ug99 and Ethiopian stem rust races in durum wheat via association mapping. Theoretical and Applied Genetics 126, 1237–1256.

Liu B, Liu L, Asseng S, Zou X, Li J, Cao W, Zhu Y. 2016. Modelling the effects of heat stress on post-heading durations in wheat: A comparison of temperature response routines. Agricultural and Forest Meteorology 222, 45–58.

Liu W, Maccaferri M, Bulli P, Rynearson S, Tuberosa R, Chen X, PumphreyM. 2017. Genome-wide association mapping for seedling and field resistance to Puccinia striiformis f. sp. tritici in elite durum wheat. Theoretical and Applied Genetics 130, 649–667.

Lobell DB, Hammer GL, Chenu K, Zheng B, Mclean G, Chapman S. 2015. The shifting influence of drought and heat stress for crops in northeast Australia. Global Change Biology 21, 4115–4127.

Lozada DN, Mason RE, Sukumaran S, Dreisigacker S. 2018. Validation of grain yield QTLs from soft winter wheat using a CIMMYT spring wheat panel. Crop Science 58, 1964–1971.

Maccaferri M, Sanguineti MC, Natoli V, *et al*. 2006. A panel of elite accessions of durum wheat (Triticum durum Desf.) suitable for association mapping studies. Plant Genetic Resources 4, 79–85.

Maccaferri M, Stefanelli S, Rotondo F, Tuberosa R, Sanguineti MC. 2007a. Relationships among durum wheat accessions. I. Comparative analysis of SSR, AFLP, and phenotypic data. Genome 50, 373–384.

Maccaferri M, Sanguineti MC, Xie C, Smith JSC, Tuberosa R. 2007b. Relationships among durum wheat accessions. II. A comparison of molecular and pedigree information. Genome, 50, 385–399.

Maccaferri M, Sanguineti MC, Corneti S, *et al*. 2008. Quantitative trait loci for grain yield and adaptation of durum wheat (Triticum durum Desf.) across a wide range of water availability. Genetics 178, 489–511.

Maccaferri M, Sanguineti MC, Demontis A, *et al*. 2011. Association mapping in durum wheat grown across a broad range of water regimes. Journal of Experimental Botany 62, 409–438.

Maccaferri M, Zhang J, Bulli P, Abate Z, Chao S, Cantu D, Bossolini E, Chen X, Pumphrey M, Dubcovsky J. 2015a. A genome-wide association study of resistance to stripe rust (Puccinia striiformis f. sp. tritici) in a worldwide collection of hexaploid spring wheat (Triticum aestivum L.). G3 5, 449–465.

Maccaferri M, Ricci A, Salvi S, *et al*. 2015b. A high-density, SNP-based consensus map of tetraploid wheat as a bridge to integrate durum and bread wheat genomics and breeding. Plant Biotechnology Journal 13, 648–663.

Maccaferri M, Harris NS, Twardziok SO, *et al*. 2019. Durum wheat genome highlights past domestication signatures and future improvement targets. Nature Genetics 51, 885–895.

Makonya GM, Ogola JBO, Muasya AM, Crespo O, Maseko S, Valentine AJ, Ottosen C-O, Rosenqvist E, Chimphango SBM, 2019. Chlorophyll fluorescence and carbohydrate concentration as field selection traits for heat tolerant chickpea genotypes. Plant Physiology and Biochemistry 141, 172–182.

Mathur S, Agrawal D, Jajoo A. 2014. Photosynthesis: Response to high temperature stress. Journal of Photochemistry and Photobiology B: Biology 137, 116–126.

de Miguel M, Cabezas J-A, de María N, *et al*. 2014. Genetic control of functional traits related to photosynthesis and water use efficiency in Pinus pinaster Ait. drought response: integration of genome annotation, allele association and QTL detection for candidate gene identification. BMC Genomics 15, 464.

Murchie EH, Lawson T. 2013. Chlorophyll fluorescence analysis: A guide to good practice and understanding some new applications. Journal of Experimental Botany 64, 3983–3998.

Perdomo JA, Capó-Bauçà S, Carmo-Silva E, Galmés J. 2017. Rubisco and rubisco activase play an important role in the biochemical limitations of photosynthesis in rice, wheat, and maize under high temperature and water deficit. Frontiers in Plant Science 8, 490.

Pieruschka R, Klimov D, Kolber ZS, Berry JA. 2010. Monitoring of cold and light stress impact on photosynthesis by using the laser induced fluorescence transient (LIFT) approach. Functional Plant Biology 37, 395–402.

Posch BC, Kariyawasam BC, Bramley H, Coast O, Richards RA, Reynolds MP, Trethowan R, Atkin O. 2019. Exploring high temperature responses of photosynthesis and respiration to improve heat tolerance in wheat. Journal of Experimental Botany. https://doi.org/10.1093/jxb/erz257

Pritchard JK, Stephens M, Donnelly P. 2000. Inference of population structure using multilocus genotype data. Genetics 155, 945–959.

Quarrie SA, Steed A, Calestani C, *et al*. 2005. A high-density genetic map of hexaploid wheat (Triticum aestivum L.) from the cross Chinese Spring × SQ1 and its use to compare QTLs for grain yield across a range of environments. Theoretical and Applied Genetics 110, 865–880.

Reynolds MP, Tattaris M, Cossani CM, Ellis M, Yamaguchi-Shinozaki K, Pierre CS. 2015. Exploring genetic resources to increase adaptation of wheat to climate change. Advances in Wheat Genetics: From Genome to Field. pp 355–368 Springer Japan, Tokyo.

Reynolds MP, Pask AJD, Hoppitt WJE, *et al*. 2017. Strategic crossing of biomass and harvest index—source and sink-achieves genetic gains in wheat. Euphytica 213, 257.

Salvi S, Tuberosa R. 2015. The crop QTLome comes of age. Current Opinion in Biotechnology 32, 179–185.

Sareen S, Bhusal N, Kumar M, Bhati PK, Munjal R, Kumari J, Kumar S, Sarial AK. 2019. Molecular genetic diversity analysis for heat tolerance of indigenous and exotic wheat genotypes. Journal of Plant Biochemistry and Biotechnology 1, 9.

Semenov MA, Shewry PR. 2011. Modelling predicts that heat stress, not drought, will increase vulnerability of wheat in Europe. Scientific Reports 1, 66.

Sharma DK, Andersen SB, Ottosen CO, Rosenqvist E. 2012. Phenotyping of wheat cultivars for heat tolerance using chlorophyll a fluorescence. Functional Plant Biology 39, 936–947.

Sharma DK, Andersen SB, Ottosen CO, Rosenqvist E. 2015. Wheat cultivars selected for high Fv/Fm under heat stress maintain high photosynthesis, total chlorophyll, stomatal conductance, transpiration and dry matter. Physiologia Plantarum 153, 284–298.

Sharma DK, Torp AM, Rosenqvist E, Ottosen CO, Andersen SB. 2017. QTLs and potential candidate genes for heat stress tolerance identified from the mapping populations specifically segregating for Fv/Fm in wheat. Frontiers in Plant Science 8, 1668.

Sharma A, Shahzad B, Kumar V, *et al*. 2019. Phytohormones regulate accumulation of osmolytes under abiotic stress. Biomolecules 9, 285.

Shi W, Hao C, Zhang Y, *et al*. 2017. A combined association mapping and linkage analysis of kernel number per spike in common wheat (*Triticum aestivum* L.). Frontiers in Plant Science 8, 1412.

Sukumaran S, Lopes M, Dreisigacker S, Reynolds MP. 2018. Genetic analysis of multi-environmental spring wheat trials identifies genomic regions for locus-specific trade-offs for grain weight and grain number. Theoretical and Applied Genetics 131, 985–998.

The R Core Team (2016). R: A Language and Environment for Statistical Computing.

Tuberosa R, Salvi S, Sanguineti MC, Landi P, Maccaferri M, Conti S. 2002. Mapping QTLs regulating morpho-physiological traits and yield: case studies, shortcomings and perspectives in drought-stressed maize. Annals of Botany 89, 941–963.

Tuberosa R. 2012. Phenotyping for drought tolerance of crops in the genomics era. Frontiers in Physiology 3, 347.

Tuberosa R, Maccaferri M, Salvi S. 2019. Leveraging the QTLome to enhance climate change resilience in cereals, p. 612 in Advanced in breeding techiniques for cereal crops, edited by Ordon F., Friedt W. Burleigh Dodds, Cambridge.

Wahid A, Gelani S, Ashraf M, Foolad MR. 2007. Heat tolerance in plants: an overview. Environmental and Experimental Botany 61, 199–223.

Wang W, Vinocur B, Shoseyov O, Altman A. 2004. Role of plant heat-shock proteins and molecular chaperones in the abiotic stress response. Trends in Plant Science 9, 244–252.

Wang RX, Hai L, Zhang XY, You GX, Yan CS, Xiao SH. 2009. QTL mapping for grain filling rate and yield-related traits in RILs of the Chinese winter wheat population Heshangmai × Yu8679. Theoretical and Applied Genetics 118, 313–325.

Wang X, Cai J, Jiang D, Liu F, Dai T, Cao W. 2011. Pre-anthesis high-temperature acclimation alleviates damage to the flag leaf caused by post-anthesis heat stress in wheat. Journal of Plant Physiology 168, 585–593.

Wang ZX, Chen L, Ai J, Qin HY, Liu YX, Xu PL, Jiao ZQ, Zhao Y, Zhang T. 2012. Photosynthesis and activity of photosystem II in response to drought stress in Amur Grape (Vitis amurensis Rupr.). Photosynthetica 50, 189–196.

Wang S, Wong D, Forrest K, *et al*. 2014. Characterization of polyploid wheat genomic diversity using a high-density 90 000 single nucleotide polymorphism array. Plant Biotechnology Journal 12, 787–796.

Wang S, Xu S, Chao S, Sun Q, Liu S, Xia G. 2019. A genome-wide association study of highly heritable agronomic traits in durum wheat. Frontiers in Plant Science 10, 919.

Wise RR, Olson AJ, Schrader SM, Sharkey TD. 2004. Electron transport is the functional limitation of photosynthesis in field-grown Pima cotton plants at high temperature. Plant, Cell and Environment 27, 717–724.

Yu J, Pressoir G, Briggs WH, *et al*. 2006. A unified mixed-model method for association mapping that accounts for multiple levels of relatedness. Nature Genetics 38, 203–208.

Zadoks JC, Chang TT, Konzak CF. 1974. A decimal code for the growth stages of cereals. Weed Research 14, 415–421.

Zhang Z, Ersoz E, Lai CQ, *et al*. 2010. Mixed linear model approach adapted for genome-wide association studies. Nature Genetics 42, 355–360.

Zhao C, Liu B, Piao S, *et al*. 2017. Temperature increase reduces global yields of major crops in four independent estimates. Proceedings of the National Academy of Sciences of the USA 114, 9326–9331.

Zhou R, Yu X, Kjær KH, Rosenqvist E, Ottosen CO, Wu Z. 2015. Screening and validation of tomato genotypes under heat stress using Fv/Fm to reveal the physiological mechanism of heat tolerance. Environmental and Experimental Botany 118, 1-11.

3. Chapter 3: Genome Wide Association Studies reveals novel QTLs for grain yield and grain yield components under heat stress condition

3.1. Introduction

Bread (*Triticum aestivum* L.) and durum wheat (*T. turgidum* subsp. *durum* (Desf.) Husn.) are cultivated in a large number of different environments across the world, and they provide over 20% of the calories and protein consumption of the human diet (FAOSTAT, 2017). Importantly, the environments where both crops as well as other important ones are cultivated have undergone notable changes due to effects of global warming (Asseng *et al*., 2017; Zhao *et al*., 2017; Tuberosa *et al*., 2019).

Heat stress is one of the most important factors affecting grain yield and its stability in wheat as well as other crops in the new climate scenario (Semenov and Shewry, 2011; Tuberosa *et al*., 2019). Recent studies based on global warming models have predicted a consistent increase of the mean temperature in the near future (IPCC, 2014). The new scenario of climate change will provide seasons with reduction of annual precipitation and more severe heat waves (Lobell *et al*., 2015; Asseng *et al*., 2017; Zhao *et al*., 2017), especially in the Mediterranean Basin, a very important region for durum wheat production (Danzi *et al*., 2019; Kutiel, 2019). According to Zhao *et al*. (2017), on average, wheat grain yield can be reduced by 6% for each °C increased in the mean temperature. This result highlights the urgency to select new wheat varieties more tolerant to heat stress environments.

Grain yield (GY) has always been one of the most important objectives in cultivated crops. However, improving GY performance has always been challenging due the fact that it is a quantitative trait, controlled by a plethora of genes with small effect and is highly influenced by environmental conditions and crop management, which results in low heritability (Mangini *et al*., 2018; Sukumaran *et al*., 2018; El Hassouni *et al*., 2019; Li *et al*., 2019; Sareen *et al*., 2019; Wang *et al*., 2019). Additionally, the genetic gain of wheat is stagnating in the last years. Several studies have reported that the genetic gain of wheat from 1994 to 2010 fluctuated from 0.6 to 1.0%, values clearly insufficient to meeting the demand predicted by 2050 (for more details see Reynolds *et al*., 2012).

Although the evaluation of GY is difficult due its complexity, it is a trait significantly associated with number of spikes per area (SPM), grain numbers per spike (GNO) and thousand kernel weight (TKW). Additionally, plant height (PH), grain shape, flag leaf angle and spike architecture can eventually affect GY through effects on photosynthetic intensity, dry matter translocation, and grain filling process (Lloveras *et al*., 2004; Zhou *et al*., 2007; Xiao *et al*., 2012;

Gao *et al*., 2017; Liu *et al*., 2019). These traits have higher heritability (h^2) than GY and consequently they are more effectively selected in a breeding programs (Li *et al*., 2019).

The genetic gain in GY achieved in modern breeding has been related to the negative effect of the *rht* genes on the height of the released cultivars since 1960s (Zhou *et al*., 2007; Tian *et al*., 2017, 2019), increase in harvest index (Gao *et al*., 2017), increase in the number of spikes per area (SPM), grain number per spike (GNO) and grain weight per spike (Mangini *et al*., 2018). However, due the fixation of the *rht* genes, further improvement in grain yield potential will be achieved only by a detailed genetic understanding of the components of grain yield combined with marker-assisted selection applied to breeding programs around the world (Li *et al*., 2019).

During the entire growth cycle, heat stress can affect plant performance by (i) reducing photosynthetic capacity (Murchie and Lawson, 2013; Posch *et al*., 2019), (ii) reducing cell membrane stability (Wahid *et al*., 2007) and (iii) enhancing the production of reactive oxygen species (ROS) (Cossani and Reynolds, 2012; Hossain *et al*., 2015). Notably, wheat plants are more sensitive to heat stress during reproductive stages (Farooq *et al*., 2011) due the fact that seed set is strongly dependent on the functionality of male and female gametes, both highly affected by heat stress (Prasad and Djanaguiraman, 2014). According to Prasad and Djanaguiraman (2014), the two most sensitive periods for heat stress in wheat are at about seven days before anthesis as well as one day before anthesis. Additionally, floret fertility starts decreasing above 24 °C, reaching about 0% of fertile floret with temperature of 35 °C. The direct effect of heat stress on floret fertility is caused by the reduction of pollen fertility as well as abnormalities in pollen, stigma and style (Prasad and Djanaguiraman, 2014; Fábián *et al*., 2019). Fábián *et al*. (2019), working simultaneously with heat and drought stress, identify significant differences in the number of fertile florets comparing tolerant and sensitive genotypes. The sensitive genotype showed a reduction of about 47.5% in the floret fertility, leading to a reduction of 55% in the grain production and affect consistently the GY components. According to the authors, the damage to the female reproductive organs is responsible for 34% of the gross fertility loss, while the damage on male reproductive organs account to 66% of the gross fertility loss.

On the view of the strong negative effect of heat stress on GY, this study aims to perform a GWAS analysis in a durum wheat panel suitable for GWAS, in different crop seasons in order to identify major QTLs affecting GY and its components for the identification of molecular

markers suitable for marker assisted selection in order to reduces the effect of heat stress on durum wheat.

3.2. Material and methods

3.2.1. Plant material

The accessions used in this study are part of the UNIBO-Durum Panel, a set of 183 elite durum cultivars and elite breeding lines from Mediterranean countries (Italy, Morocco, Spain, Syria, Tunisia), Mexico and USA which were chosen from a larger panel (336 accessions) based on their pedigree and heading date. Accordingly, accessions with high identity-by-descent value based on pedigree and molecular maker data (Maccaferri *et al*., 2007 a, b) and/or with differences higher than 7 days in heading date in Mediterranean countries (Maccaferri *et al.*, 2011) were excluded in order to reduce possible bias of phenology on QTLome dissection (Tuberosa, 2012). Additional information about UNIBO-Durum Panel is reported in Maccaferri *et al.* (2006, 2011).

3.2.2. Environment characterization

The field experiment was conducted at the Campo Experimental Norman E. Borlaug (CENEB) in Ciudad Obregon, Sonora, Mexico. The CENEB is the research center of International Maize and Wheat Improvement Center (CIMMYT) in the northwest of Mexico (27º 20’ N; 109º 54’ W; 38 m above sea level) (Liu *et al*., 2019). According to the classification system developed by CIMMYT, the CENEB location is characterized into the mega environment (ME), as ME1 during the normal wheat season (sowing in the last week of November) and as ME5 during late wheat season (sowing in the last week of February) (Rajaram *et al*., 1994; Mondal *et al*., 2013). ME classification defines ME1 as an optimally irrigated and highly productive environment where wheat grows in cool temperatures but may suffer from terminal heat stress, while ME5 is defined as a warm humid, tropical or subtropical region, where continuous high temperatures are a major constraint to wheat production (Mondal *et al*., 2013).

3.2.3. Phenotypic evaluation

The UNIBO-Durum Panel was phenotyped during 2017-2018 (referred as 2018 hereafter) and 2018-2019 (referred as 2019 hereafter) crop season at CENEB under two different environmental conditions, namely (i) control (NS – optimal sowing date, last week of November/first week of December) and (ii) heat stress (HS – late sowing date, last week of

February/first week of March) in order to expose plants to higher than normal temperature during their entire cycle. The experiment was carried out in a complete randomized block design with two replicates, and the experimental unit (plots) consisted of 1.68 m^2 (2 rows x 2.1 m x 0.8 m). In order to avoid any drought stress confounding, plants were kept well-watered by artificial irrigation. Fertilization, weed, pest and disease control were made following the specifics protocols of CIMMYT. Information about the evolution of temperature increase during the different crop season is reported in the Figure 3.1.

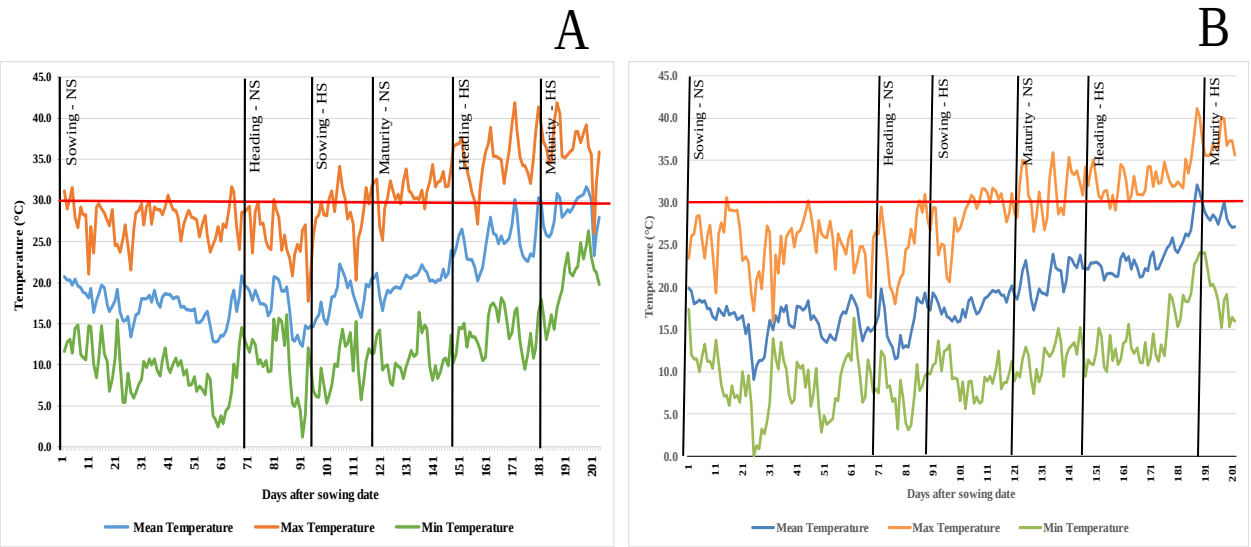

Figure 3.1. Maximum, minimum and mean temperature in Ciudad Obregon (Mexico) from the sowing date of control experiment to the maturity date of heat stress experiment during the wheat growing seasons 2017-2018 (A) and 2018-2019 (B).

During the entire growth cycle, the following traits were evaluated: (i) phenological traits: days to heading (HD), estimated as the number of days from the date of sowing until 50% of the spikes had completed emerged from the flag leaf (growth stage 59 – Zadoks *et al*., 1974); days to maturity (DTM), estimated as the number of days from the date of sowing until 50% of the plants had the apices of the culm colored as straw yellow (approximately growth stage 87 – Zadoks *et al*., 1974) and plant height (PH), measured as the length from the soil surface until the spike basis, in cm; (ii) number of spikes per linear meter (SPM), estimated by counting the number of spikes in 0.5 m in two different sections of each experimental unit; (iii) number of spikelets per spike (SKT), estimated by counting the number of spikelets in five single spikes; (iv) grain number per

spike (GNO), estimated by counting the grain number of five spikes in each experimental unit using a seed counter (Pfeuffer GmbH Seed Counter); (v) grain weight per spike (SGW), estimated by weighing the number of grains produced by five spikes, in grams; (vi) thousand kernel weight (TKW), estimated by weighing 1,000 whole grains, in grams; (vii) test weight (TWT), estimated by weighing a volume of 500 mL of whole grains and later converted to kilograms per hectoliter (kg hl^{-1}); (viii) grain length (GLE); (ix) grain width (GWI) and (x) grain yield (GY), estimated by weighing the mass of grains harvested in the experimental unit in grams and later converted to kilograms per hectares (kg ha^{-1}). The traits TKW, TWT, GLE and GWI were estimated by using the Digital Image Analysis System for Grain version 2.5.1 (SeedCount™ – Next Instruments Pty Ltd).

3.2.4. Statistical analysis

All statistical analyses were performed using the software R (The R Core Team, 2016). Before performing the genetic analysis and correlation between traits the Best Linear Unbiased Estimators (BLUEs) values of each single accession were obtained separately for the different treatments (NS, HS), different crop seasons (2018, 2019) as well as for the joint analysis considering both crop seasons (2018, 2019). BLUEs were calculated using the *lmer4* package (Bates *et al*., 2015), considering "Genotype" as fixed variable, while replicate, column and row were considered as random variables. For the joint analysis, "Genotype" was considered as fixed variable, while Year, "Replicate:Year", "Genotype:Year" were considered as random variables. Broad sense heritability (h^2) was estimated by using "*repeatability*" function of the package "*repeatability*" (Wolak *et al*., 2012). The correlation analysis was performed with BLUEs values previously obtained and was calculated using the "*corrplot*" package (Wei and Simko, 2017).

3.2.5. Reaction norm index

In order to identify the difference between NS and HS plants, the reaction norm index (Δ) was calculated for both crop seasons (2018, 2019) as well as for the joint analysis using the following equation: $\Delta = ((Y_{HS} * 100)/Y_{NS})$, where: Y_{HS} is the phenotypic mean for each accession under heat-stressed condition and, Y_{NS} is the corresponding phenotypic mean under control condition.

3.2.6. SNP genotyping, population structure and GWAS analysis

A total of 13,823 informative SNPs with minor allele frequency (MAF) > 0.05 were used for GWAS based on TASSEL 5.2.37 software using a Mixed Linear Model (MLM, Bradbury *et al*., 2007), which included either kinship matrix (K) alone or with structure subpopulation membership estimates (Q) as random effects. MLM was performed according to Zhang *et al*. (2010). Figures 3.3, 3.4 and 3.5 reports the Q-Q (quantile-quantile) plot results.

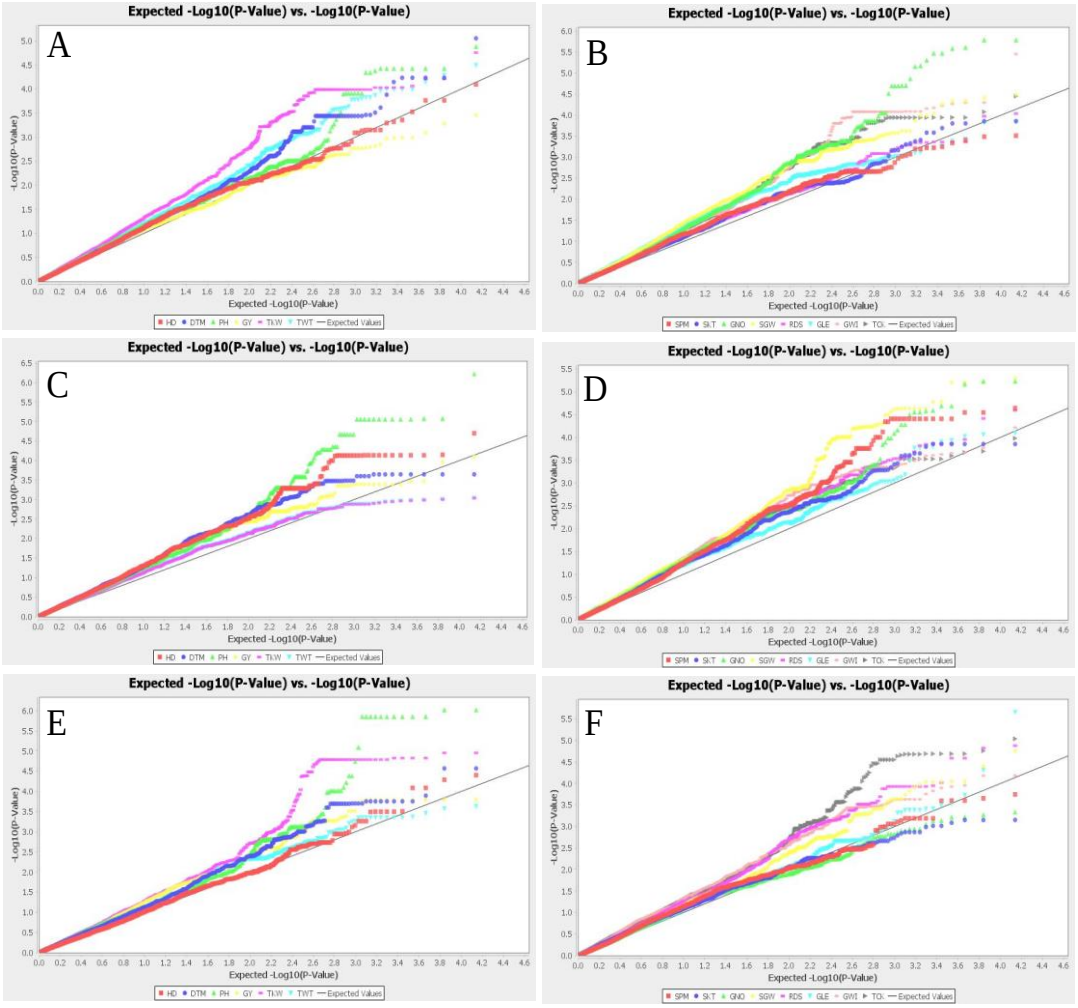

Figure 3.3. Q-Q (quantile-quantile) plot results of the GWAS analysis using the method Mixed Linear Model (MLM) + Kinship matrix + population structure (Q) + phenology loci for days to heading (HD), days to maturity (DTM), plant height (PH), grain yield (GY), thousand kernel weight (TKW), test weight (TWT), number of spikes per linear meter (SPM), number of spikelets per spike (SKT), grain number per spike (GNO), grain weight per spike (SGW), grain length (GLE), grain width (GWI) in the crop season of 2019. A-B) control experiment. C-D) heat stress experiment. E-F) reaction norm index.

According to GWAS Q-Q (quantile-quantile) plot results, MLM+K+Q showed the best results to control the P-value inflation associated to population structure for the three different data sets (2018, 2019 and joint analysis). Thus, all GWAS analyses were performed based on MLM+K+Q model. Additionally, relevant loci for phenology (*PPD-A1*, *PPD-B1*, *FT-7A-indel*, *Rht-B1b* and *VRN-A1*) were used as covariate, since these loci are strongly associated with the most important agronomic traits influenced by wheat growth and, as such, may affect traits measured in this experiment.

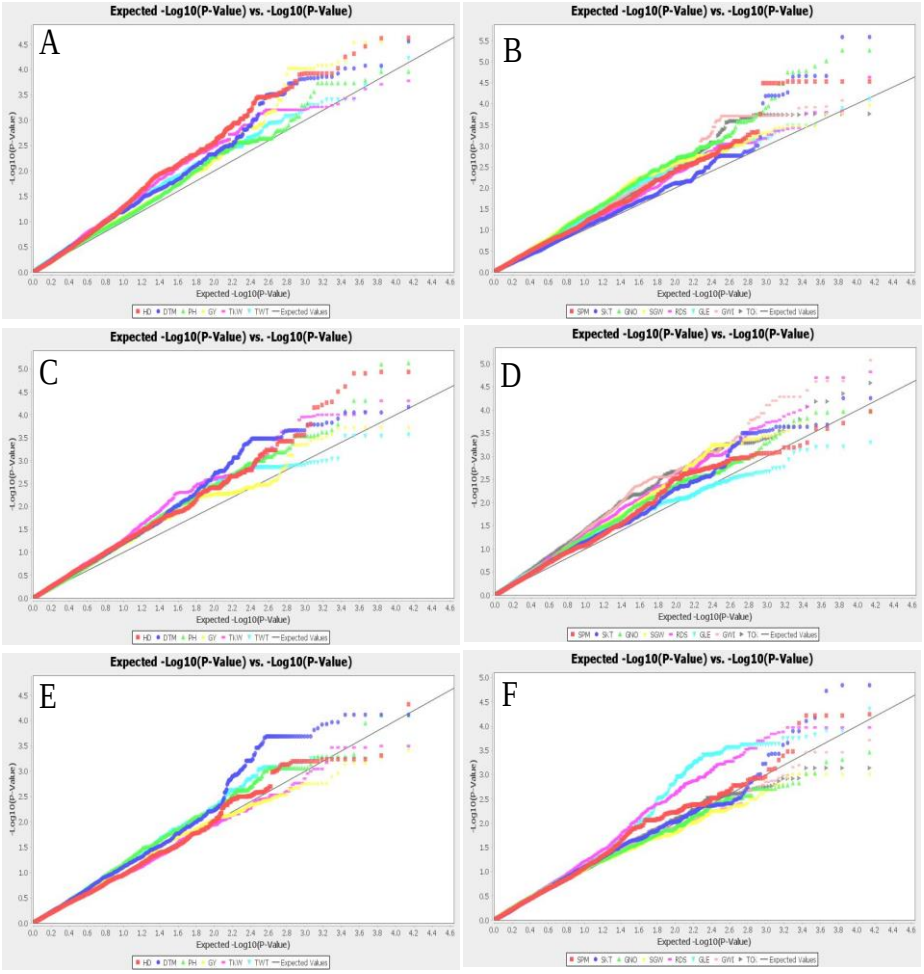

Figure 3.4. Q-Q (quantile-quantile) plot results of the GWAS analysis using the method Mixed Linear Model (MLM) + Kinship matrix + population structure (Q) + phenology loci for days to heading (HD), days to maturity (DTM), plant height (PH), grain yield (GY), thousand kernel weight (TKW), test weight (TWT), number of spikes per linear meter (SPM), number of spikelets per spike (SKT), grain number per spike (GNO), grain weight per spike (SGW), grain length (GLE), grain width (GWI) in the crop season of 2018. A-B) control experiment. C-D) heat stress experiment. E-F) reaction norm index.

The GWAS was carried out based on standard conditions of significance as follows: highly significant markers refer to $P < 0.0001$ while significant markers refer to $0.001 \geq P \geq 0.0001$. The average genetic distance at each LD decay with $r^2 < 0.3$, a threshold commonly adopted in GWAS studies (Maccaferri *et al*., 2015a; Liu *et al*., 2017; Condorelli *et al*., 2018; Mangini *et al*., 2018; Garcia *et al*., 2019), was chosen to define QTL confidence intervals (cM), which was identified as 3.1 cM for this population. GWAS analysis was performed for NS, HS and Δ under both crop seasons singularly, as well as considering both crop seasons together (joint analysis). Additional information about DNA extraction, genotyping process, linkage disequilibrium (LD), population structure and GWAS analysis is reported in Chapter 2.

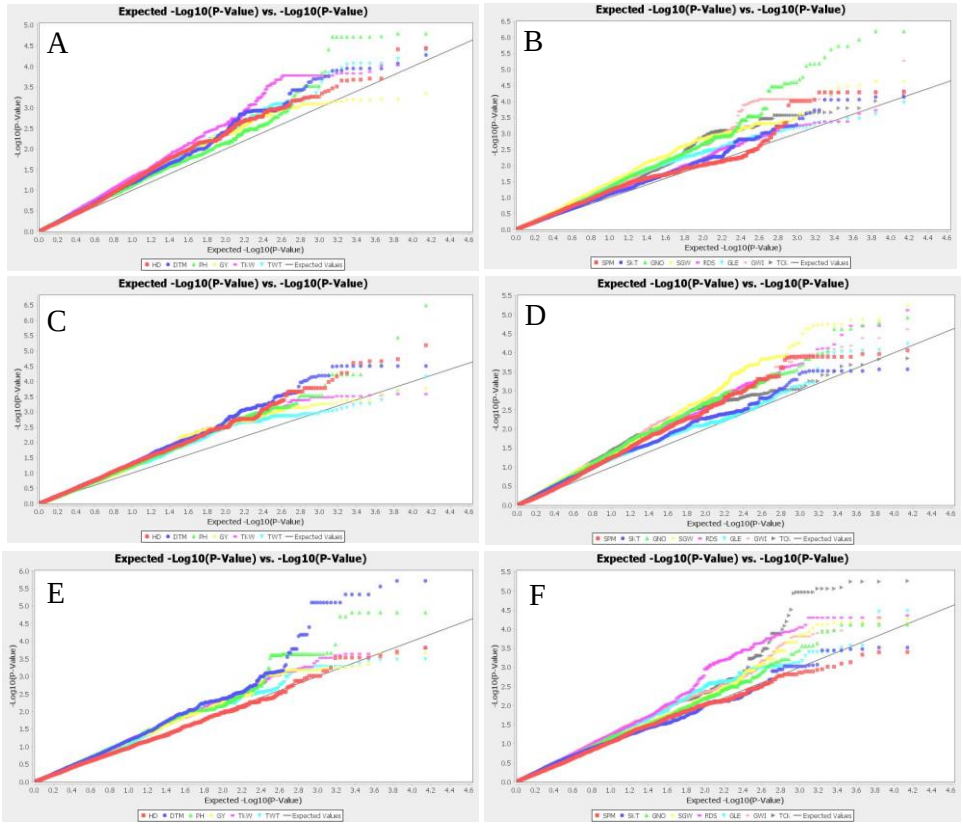

Figure 3.5. Q-Q (quantile-quantile) plot results of the GWAS analysis using the method Mixed Linear Model (MLM) + Kinship matrix + population structure (Q) + phenology loci for days to heading (HD), days to maturity (DTM), plant height (PH), grain yield (GY), thousand kernel weight (TKW), test weight (TWT), number of spikes per linear meter (SPM), number of spikelets per spike (SKT), grain number per spike (GNO), grain weight per spike (SGW), grain length (GLE), grain width (GWI) for the joint analysis obtained with data from both 2018 and 2019 crop season. A-B) control experiment. C-D) heat stress experiment. E-F) reaction norm index.

3.3. Results

3.3.1. Agronomic performance of the UNIBO-Durum Panel

The agronomic performance of the accessions in the two crop seasons are reported in Table 3.1 (crop season 2019), Table 3.2 (crop season 2018) and Table 3.3 (joint analysis considering both crop season), which present the descriptive statistics and the repeatability in broad sense (h^2) for all traits. Details on the agronomic performance of the accessions is also presented in Figure 3.6, which reports the boxplots for the different treatments (NS, HS) in the two crop seasons (2018, 2019). On average, plants showed higher values for all traits in 2019 (Table 3.1) than 2018 (Table 3.2) in both treatments (NS, HS) (Figure 3.6). All traits showed medium to high h^2 and medium to low coefficient of variation (CV) in both seasons and treatments, except GY under NS for the joint analysis (h^2 = 0.34) (Table 3.3). Because no significant genotype x crop season interaction was detected for the investigated traits, the results reported and commented hereafter are based on the mean values of the two seasons and not those obtained separately in the different crop seasons (2018, 2019).

Table 3.1. Descriptive statistics and repeatability (h^2) estimate for heat stress response in 183 elite cultivars and breeding lines from the UNIBO-Durum Panel grown under control and heat stress environment under field condition during the crop season 2019.

Year 2019										
Trait[1]	Control					Heat Stress				
	Mean	Range	Std [2]	CV [3] (%)	h^2 [4]	Mean	Range	Std	CV (%)	h^2
HD	80.9	69.0-106.0	6.9	1.42	0.99	59.1	52.0-84.0	2.6	1.37	0.97
DTM	130.8	121.0-147.0	5.1	1.12	0.96	89.7	82.0-102.0	3.7	1.96	0.85
PH	86.5	70.0-150.0	10.8	4.04	0.94	60.3	40.0-105.0	7.5	6.12	0.81
GY	7.0	4.1-10.3	1.1	11.76	0.62	3.1	0.7-5.4	0.9	17.26	0.76
TKW	58.0	37.1-71.6	5.8	2.98	0.95	51.7	35.2-65.7	5.1	3.61	0.93
TWT	80.3	74.0-83.7	1.7	0.73	0.94	78.5	72.1-82.3	1.8	0.91	0.92
SPM	118.0	82.0-178.0	17.6	11.57	0.57	90.9	50.0-138.0	16.1	12.22	0.43
SKT	19.3	15.3-28.0	2.3	5.63	0.85	15.9	12.3-20.0	1.4	4.66	0.83
GNO	57.9	36.0-84.5	9.3	7.46	0.87	39.7	15.2-65.2	7.1	7.92	0.88
SGW	3.4	2.0-4.8	0.5	8.02	0.81	2.1	0.9-3.3	0.4	8.47	0.85
GLE	7.7	6.6-8.5	0.3	0.79	0.97	7.3	6.4-8.2	0.3	1.55	0.91
GWI	3.6	3.1-3.9	0.1	1.23	0.95	3.3	2.7-3.8	0.2	1.95	0.91

[1] HD: days to heading; DTM: days to maturity; PH: plant height; GY: grain yield; TKW: thousand kernel weight; TWT: test weight; SPM: number of spikes per linear meter; SKT: number of spikelets per spike; GNO: grain number per spike; SGW: grain weight per spike; GLE: grain length; GWI: grain width. [2] std: standard deviation. [3] CV: coefficient of variation. [4] h^2: broad sense heritability.

Traits related to phenology as HD and DTM, as well as PH were strongly affected by HS. On average, HD reduced by 25.8% from NS (80.3 days) to HS (59.6 days). In the same way, DTM reduced by 30.1% (NS = 126.9 days, HS = 88.1 days) and PH reduced by 31.2% from 83.6 cm under NS to 57.5 cm under HS (Table 3.3). As expected, HD, DTM and PH showed very high values of h^2, always above 0.74 in all crop seasons and treatments. These traits were highly correlated between them under NS treatment HD x DTM (0.91, values not shown), HD x PH (0.37), DTM x PH (0.38) while under HS only HD x DTM (0.83) showed significant correlation (Figure 3.7). Additionally, HD and DTM were positively correlated with SKT (0.72, NS; 0.32, HS), and negatively correlated with GY (-0.26, HS), TKW (-0.45, NS), TWT (-0.46, NS; -0.31, HS), GLE (-0.13, NS; -0.11, HS) and GWI (-0.41, NS) while PH correlated positively with SPM (0.51, NS), and SKT (0.32, NS), as well as negatively with TKW (-0.30, NS; -0.17, HS), SGW (-0.22, NS), GLE (-0.27, NS; -0.32, HS), and GWI (-0.19, NS) (Figure 3.7).

Table 3.2. Descriptive statistics and repeatability (h^2) estimate for heat stress response in 183 elite cultivars and breeding lines from the UNIBO-Durum Panel grown under control and heat stress environment under field condition during the crop season 2018.

	Year 2018									
Trait[1]	Control					Heat Stress				
	Mean	Range	Std [2]	CV [3] (%)	h^2 [4]	Mean	Range	Std	CV (%)	h^2
HD	79.6	67.0-108.0	6.2	2.52	0.94	60.0	53.0-84.0	3.5	1.76	0.97
DTM	123.1	116.0-144.0	5.4	1.99	0.89	86.5	80.0-104.0	4.0	1.87	0.92
PH	80.8	60.0-145.0	10.8	4.53	0.94	54.8	30.0-85.0	7.7	8.15	0.78
GY	5.5	2.9-7.9	0.9	12.03	0.63	2.3	0.2-4.1	0.8	23.84	0.68
TKW	54.2	39.0-68.0	5.4	2.76	0.96	44.0	30.7-57.6	4.4	4.07	0.91
TWT	80.5	70.2-83.9	1.8	0.74	0.94	77.7	70.7-81.6	1.7	0.88	0.92
SPM	126.1	86.0-190.0	18.6	9.78	0.63	94.8	48.0-134.0	14.4	12.79	0.40
SKT	17.6	14.2-23.2	1.6	6.29	0.69	15.8	12.2-20.0	1.2	4.57	0.78
GNO	49.4	31.2-79.0	7.5	8.25	0.82	36.3	14.7-54.7	6.0	11.76	0.68
SGW	2.7	1.6-4.5	0.4	9.66	0.76	1.6	0.5-2.2	0.3	13.47	0.63
GLE	7.5	6.6-8.3	0.3	0.94	0.97	7.5	6.6-8.1	0.3	1.23	0.93
GWI	3.5	3.1-3.8	0.1	1.27	0.94	3.2	2.8-3.6	0.1	1.54	0.92

[1] HD: days to heading; DTM: days to maturity; PH: plant height; GY: grain yield; TKW: thousand kernel weight; TWT: test weight; SPM: number of spikes per linear meter; SKT: number of spikelets per spike; GNO: grain number per spike; SGW: grain weight per spike; GLE: grain length; GWI: grain width. [2]std: standard deviation. [3] CV: coefficient of variation. [4] h^2: broad sense heritability.

The h^2 for GY ranged from 0.34 under NS for the joint analysis (Table 3.3) to 0.76 under HS in the crop season 2019 (Table 3.1). GY under NS was 21.4% higher in the crop season 2019

(7.0 t ha^{-1}) (Table 3.1) when compared with crop season 2018 (5.5 t ha^{-1}), the same result can be observed under HS (-25.8%) from 3.1 t ha^{-1} (2019) to 2.3 t ha^{-1} (2018) (Table 3.1, 3.2). Heat stress affected consistently and similarly GY in both crop seasons -58.2% (2.3 t ha^{-1}) in 2018 (Table 3.2) and -56.0% (3.1 t ha^{-1}) in 2019 (Table 3.1). In the joint analysis, GY was 6.2 and 2.7 t ha^{-1} (-56.5%) in NS and HS conditions, respectively (Table 3.3). Taking into consideration the data of the joint analysis, GY under NS was positively correlated with TWT (0.41, values not shown) and SGW (0.39), as well as with GY (0.49), TWT (0.41), SPM (0.29), GNO (0.36) and SGW (0.46) under HS (Figure 3.7). On the other hand, GY under HS was positively correlated with TWT (0.28, NS; 0.60, HS), SPM (0.58, HS), GNO (0.45, HS), SGW (0.60, HS), PH (0.48, HS), as well as negatively correlated with HD (-0.26, NS; -0.21, HS), DTM (-0.29, NS) and SKT (-0.22, NS) (Figure 3.7).

Table 3.3. Descriptive statistics and repeatability (h^2) estimate for heat stress response in 183 elite cultivars and breeding lines from the UNIBO-Durum Panel grown under control and heat stress environment under field condition considering both 2019 and 2018 crop season.

Joint Analysis										
Trait[1]	Control					Heat Stress				
	Mean	Range	Std [2]	CV [3] (%)	h^2 [4]	Mean	Range	Std	CV (%)	h^2
HD	80.3	67.0-108.0	6.6	2.71	0.97	59.6	52.0-84.0	3.8	2.54	0.95
DTM	126.9	116.0-147.0	6.5	1.80	0.74	88.1	80.0-104.0	4.2	2.13	0.86
PH	83.6	60.0-150.0	11.2	5.23	0.93	57.5	30.0-105.0	8.4	7.68	0.82
GY	6.2	2.9-10.3	1.3	13.13	0.34	2.7	0.2-5.4	0.9	21.90	0.72
TKW	56.1	37.1-71.6	5.9	3.74	0.92	47.8	30.7-65.7	6.2	4.56	0.70
TWT	80.4	70.2-83.9	1.8	0.84	0.96	78.1	70.7-82.3	1.8	1.13	0.91
SPM	122.0	82.0-190.0	18.6	11.66	0.65	92.8	48.0-138.0	15.5	13.44	0.53
SKT	18.4	14.2-28.0	2.1	7.08	0.74	15.9	12.2-20.0	1.3	5.55	0.82
GNO	53.7	31.2-84.5	9.5	9.16	0.77	38.0	14.7-65.2	6.8	10.88	0.83
SGW	3.1	1.6-4.8	0.6	9.40	0.55	1.8	0.5-3.3	0.4	11.76	0.50
GLE	7.6	6.6-8.5	0.3	1.14	0.95	7.4	6.4-8.2	0.3	1.51	0.91
GWI	3.5	3.1-3.9	0.1	1.59	0.91	3.2	2.7-3.8	0.2	2.02	0.89

[1] HD: days to heading; DTM: days to maturity; PH: plant height; GY: grain yield; TKW: thousand kernel weight; TWT: test weight; SPM: number of spikes per linear meter; SKT: number of spikelets per spike; GNO: grain number per spike; SGW: grain weight per spike; GLE: grain length; GWI: grain width. [2] std: standard deviation. [3] CV: coefficient of variation. [4] h^2: broad sense heritability.

Yield components (SPM, SKT, GNO, SGW) showed medium to high values of h^2, ranging from 0.50 (SGW, HS) to 0.83 (GNO, HS) (Table 3.3). All four traits were negatively affected by HS as follows: SGW from 3.1 to 1.8 g spike^{-1} (-41.9%), GNO from 53.7 to 38.0 grains spike^{-1}

(-29.2%), SPM from 122 to 92.8 spikes m^{-1} (-23.9%) and SKT from 18.4 to 15.9 spikelets $spike^{-1}$ (-13.6%) (Table 3.3). SGW under NS positively correlated with GY (0.38, NS; 0.22, HS), GNO (0.71, NS; 0.58, HS), as well as negatively correlated with PH (-0.22, NS) and SPM (-0.56, NS). GNO correlated with SKT (0.39, NS; 0.41, HS), HD (0.31, HS), DTM (0.31, HS), TKW (-0.47, NS; -0.31, HS), GLE (-0.31, NS; -0.24, HS), and GWI (-0.44, NS; -0.31, HS). SKT was correlated with HD (0.72 - NS, 0.46 - HS), DTM (0.75, NS; 0.38, HS), GY (-0.22, HS), TKW (-0.47, NS; -0.18, HS), TWT (-0.42, NS, -0.24, HS), GLE (-0.24, NS; -0.24, HS), GWI (-0.22, NS), and SPM (-0.16, HS).

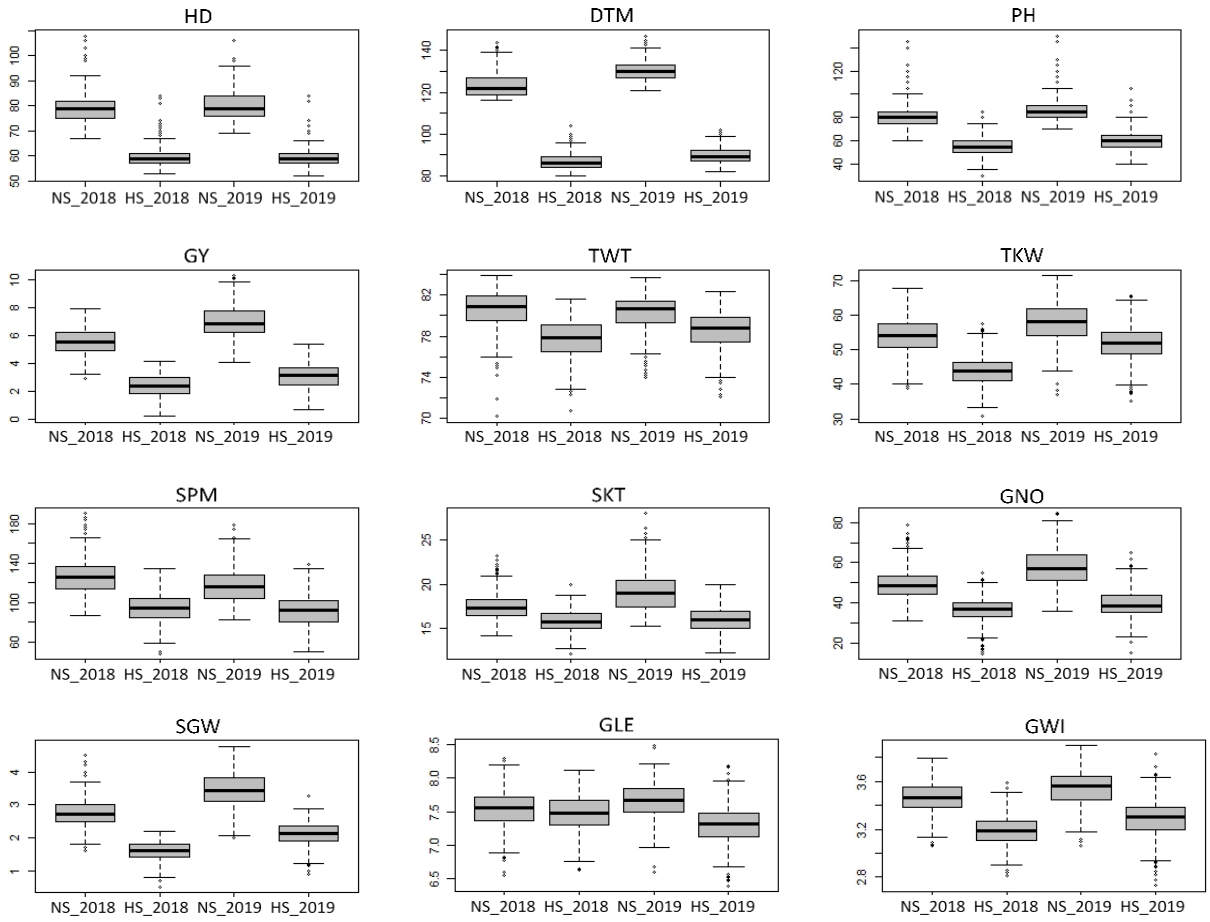

Figure 3.6. Boxplots of the best linear unbiased predictor (BLUE) of the traits of the UNIBO-Durum Panel measured under two different environments, control (NS) and heat stress (HS) during two crop seasons (2018, 2019) for the traits days to heading (HD), days to maturity (DTM), plant height (PH), grain yield (GY), thousand kernel weight (TKW), test weight (TWT), number of spikes per linear meter (SPM), number of spikelets per spike (SKT), grain number per spike (GNO), grain weight per spike (SGW), grain length (GLE), and grain width (GWI).

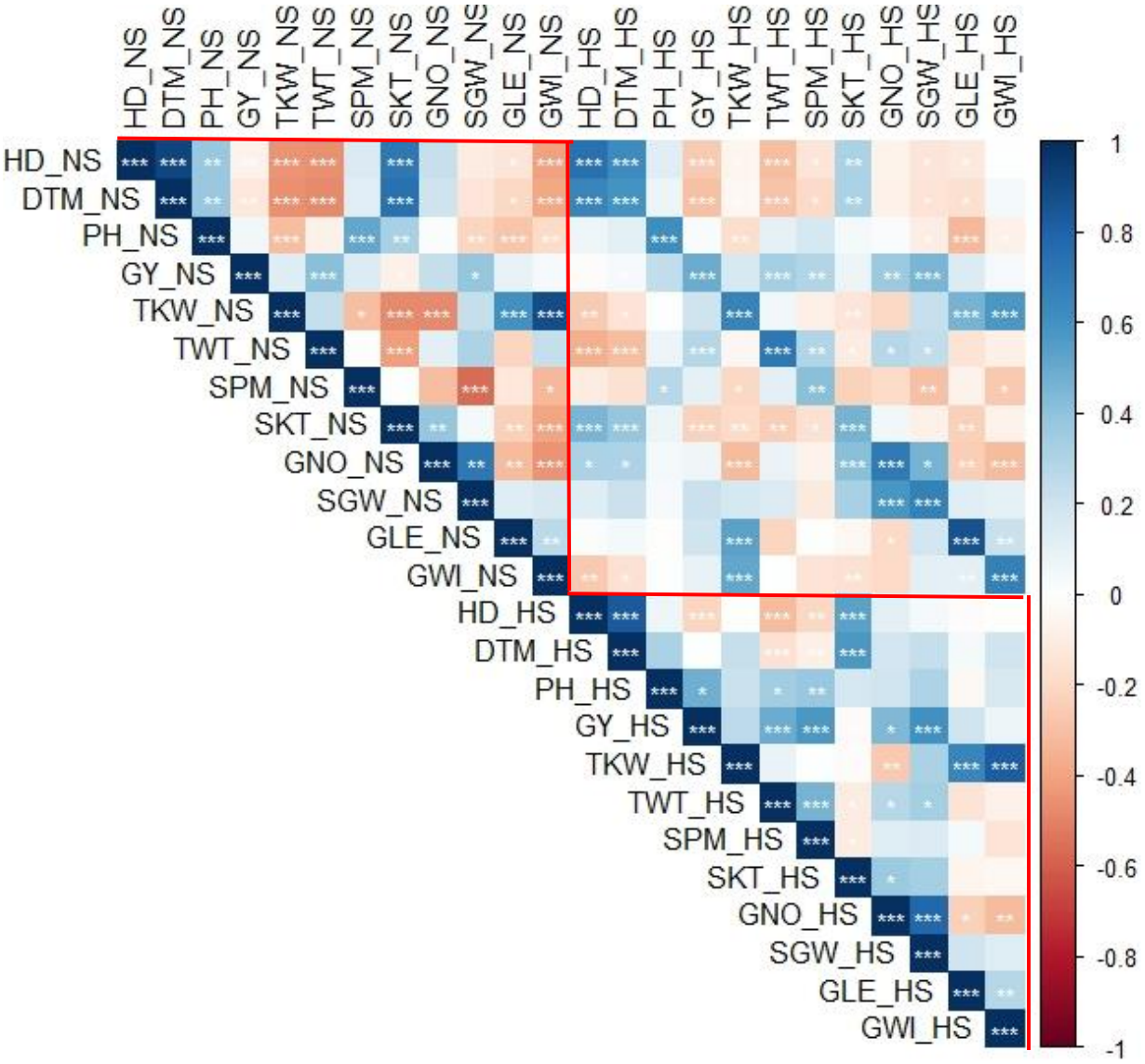

Figure 3.7. Pearson correlation of the best linear unbiased predictor (BLUE) considering both crop seasons (2018, 2019 and joint analysis) for the traits: days to heading (HD), days to maturity (DTM), plant height (PH), grain yield (GY), thousand kernel weight (TKW), test weight (TWT), number of spikes per linear meter (SPM), number of spikelets per spike (SKT), grain number per spike (GNO), grain weight per spike (SGW), grain length (GLE), and grain width (GWI) measured under two different environments, control (NS) and heat stress (HS). *** P < 0.001, ** P < 0.01, * P < 0.05.

Traits related to grain filling and kernel morphology, namely, TKW, TWT, GLE and GWI showed high values of h^2 (above 0.70, Table 3.3), and were the traits least affected by HS. From this set of traits TKW had the highest reduction from NS (56.1 g) to HS (47.8 g), a reduction of 14.8% (Table 3.3). GWI (3.5 mm, NS; 3.2 mm, HS), TWT (80.4 kg hl^{-1}, NS; 78.1 kg hl^{-1}, HS),

and GLE (7.6 mm, NS; 7.4 mm, HS) presented a reduction of 8.6, 2.9 and 2.6% due the effect of HS, respectively. Regarding the correlation values, TKW was positively correlated with GLE (0.61, NS; 0.46, HS), GWI (0.88, NS; 0.58, HS) as well as negatively correlated with HD, DTM, PH under both treatments, and SPM, GNO, SGW under NS (Figure 3.7). TWT was positively correlated with GY (NS, HS), SPM, GNO, and SGW (HS), on the other way, it was negatively correlated with HD, DTM, and SKT (HS). GLE and GWI were positively correlated between them in both treatments (0.27, NS; 0.22, HS), while they correlated negatively with HD, DTM, and SKT (NS, HS) (Figure 3.7).

3.3.2. Population structure of the UNIBO-Durum Panel

According to the Structure analysis, the UNIBO-Durum Panel includes five distinct subpopulations identified as follows: (i) subpopulation 1 (S1) with 21 genotypes, mostly Italian genotypes developed for Mediterranean areas starting from North African and from Syrian landrace founders (e.g. Senatore Cappelli, Eiti, etc.), (ii) subpopulation 2 (S2) is the smallest subpopulation with 11 genotypes developed by ICARDA for dryland areas, mainly derived from crosses with the Syrian Haurani landrace, (iii) subpopulation 3 (S3) with 39 genotypes, mostly developed by ICARDA for temperate areas, (iv) subpopulation 4 (S4) is the largest subpopulation with 49 genotypes developed by CIMMYT and by several Mediterranean national research programs (Morocco, Tunisia, Italy, Spain) starting from the outstanding widely-adapted Yavaros C79 germplasm (Yori/Anhinga//Flamingo pedigree) released in the ‘70s, and used as parents in different breeding programs around the world with the outstanding founder Karim in North Africa, Duilio and Latino in Italy, and Vitron in Spain as well as numerous ICARDA varieties and breeding lines for temperate areas (ICARDA-temperate), (v) subpopulation 5 (S5) with 22 genotypes from the CIMMYT wheat breeding program developed from the early ‘80s to early ‘90s starting from the outstanding Altar C84 germplasm. Additional details about population structure are reported in Chapter 2.

3.3.3. GWAS results under control condition

The main results under control condition (NS) are reported in Table 3.4. Additional information about the single QTLs with their respective confidence interval, peak marker position,

allele frequency, significance ($-\log_{10}$ (P)) and percentage of phenotypic variation explained by the peak marker (R^2) are reported in the appendices (Tables A3.1, A3.4 and A3.7).

Table 3.4. List of *per se* QTLs identified in the three different analysis (2018, 2019, joint analysis) under control condition (NS).

Peak marker	Chr	Marker position (cM) [1]	Confidence interval (cM) [2]	Alleles [3]	Effect	Allele Frequency	-log(p-value)	R^2 (%)	Traits [4]
IWB57868	1A	1.7	0.1-4.8	**A**/G	+	67/116	4.0-4.8	3.4-4.6	PH
IWA1562	2A	7.8	4.7-10.9	**C**/T	-	22/161	3.1-3.3	5.9-6.2	GNO
IWB8665	2A	114.5	111.4-117.6	**C**/T	+	14/169	5.0-6.2	10.4-13.6	GNO
IWB72263	2A	197.6	194.5-200.7	**A**/G	-	39/138	3.5-4.8	6.2-8.5	TKW, GWI
wPt-8404	2B	31.4	28.3-34.5	**A**/T	-	47/136	3.1-3.3	3.4-4.0	HD
IWB33109	2B	76.6	73.5-79.7	**C**/T	-	80/100	4.6-5.6	9.3-12.3	GNO
wPt-1140	2B	121.9	118.8-125.0	**A**/T	-	80/102	3.6-3.7	6.9-7.8	SGW
IWB71865	4A	36.2	33.1-39.3	**C**/T	+	14/167	3.1-3.7	3.1-4.6	HD, DTM
wPt-8443	4A	91.6	88.5-94.7	**A**/T	-	164/19	3.5-4.1	4.0-4.4	DTM
IWB44783	4A	113.9	110.8-117.0	**A**/G	+	161/22	3.1-3.8	5.1-6.4	TWT
IWB25162	4B	15.6	12.5-18.7	**C**/T	-	97/84	3.6-4.1	7.0-8.3	GLE
IWB10692	5A	150.3	147.2-153.4	**C**/T	-	164/16	4.1-4.5	4.2-6.4	HD, PH
IWB5705	5B	48.9	45.8-52.0	**C**/T	+	169/14	4.0-5.1	4.5-5.5	DTM
IWB30932	6A	11.2	8.1-14.3	**A**/G	-	169/14	3.3-4.2	5.1-7.1	TWT
IWB64047	6A	120.5	117.4-123.6	**A**/G	+	138/43	3.2-3.3	5.1-5.6	TKW
IWB29457	6B	20.4	17.3-23.5	**C**/T	-	69/114	3.2-3.8	5.0-6.6	TWT
IWB25855	7B	0.1	0.1-3.2	**A**/G	+	130/53	3.6-4.2	7.3-8.1	GWI
IWB60292	7B	120.4	117.3-123.5	**C**/T	-	16/167	3.6-5.1	6.1-8.7	TWT

[1] marker position of the peak marker based on the tetraploid wheat consensus map (Maccaferri *et al*., 2015a).
[2] confidence intervals based on LD of the UNIBO-Durum Panel.
[3] the allelic effect refers to the allele highlighted in bold.
[4] plant height (PH), grain number per spike (GNO), thousand kernel weight (TKW), grain width (GWI), days to heading (HD), grain weight per spike (SGW), days to maturity (DTM), test weight (TWT), grain length (GLE).

A total of 77 (2018), 96 (2019) and 113 QTLs (joint analysis) were identified with $-\log_{10}$ (P) ≥ 3.0 (equal to $p \leq 10^{-3}$), respectively. The significance of the QTLs ($-\log_{10}$ (P)) ranged from 3.0 to 6.2 (*QGNO_NSJA.ubo-2A.4*; Table A3.7), in the same way, the phenotypic variation explained by each single QTL (R^2) ranged from 2.5% (*QPH_NS18.ubo-4A.2*; Table A3.4) to 13.6% (*QGNO_NSJA.ubo-2A.4*) (Table A3.7).

Considering the LD of the UNIBO-Durum Panel (3.1 cM), and comparing the QTLs identified under NS in the three different analysis (2018, 2019 and joint analysis) 22 *per se* QTLs (identified in the three different analysis) were found to affect the same trait, mainly, in chromosomes (chr) 2A and 4A (four QTLs) (Table 3.4).

A *per se* QTL with $-\log_{10}$ (P) higher than 4.0 was identified for PH on chr 1A (1.7 cM). Three QTLs were identified on chr 2A, two of which peaked for GNO at 7.8 and 114.5 cM, the latter accounting for at least 10.4% of the phenotypic variation for this trait (Table 3.4). Additionally, a QTL for TKW and GWI peaked at 197.6 cM on chr 2A. A second *per se* QTL for GWI was identified on chr 7B (0.1 cM). On chr 2B three *per se* QTLs were identified at 31.4 (HD), 76.6 (GNO), and 121.9 cM (SGW). Three other QTLs were identified on chr 4A for HD and DTM (36.2 cM), DTM (91.6 cM), and TWT (113.9 cM). Three other *per se* QTLs were identified for TWT on chr 6A (11.2 cM), 6B (20.4 cM) and 7B (120.4 cM). On chr 5A the *per se* QTL at 150.3 cM was identified for HD and PH, while a QTL for DTM (48.9 cM) was identified on chr 5B (Table 3.4).

3.3.4. GWAS results under heat stress condition

Under heat stress (HS) condition, the number of significant QTLs was 105 in 2018, 110 in 2019 and 128 in the joint analysis with $-\log_{10}$ (P) from 3.0 to 6.5 (*QPH_HSJA.ubo-4B* – Table A3.8) and R^2 values ranging from 4.1% (*QHD_HS18.ubo-3B.3* – Table A3.5) to 13.6% (*QPH_HSJA.ubo-4B* – Table A3.8). Additional details about the single QTLs identified under HS condition are reported in appendices (Tables A3.2, A3.5 and A3.8).

According to the comparison between the analysis performed in the three different conditions (2018, 2019, joint analysis) it was possible to identify 17 *per se* QTLs expressed for the same trait in the three different conditions, mainly, on chr 2B and 5B (both with three QTLs) (Table 3.5).

Four QTLs were identified for GWI on chr 5A (136.3 cM), 5B (165.2 cM), 7B (0.1 cM) and 7B (15.8 cM), all of them showing a negative effect on phenotype (Table 3.5). Two additional QTLs were identified on chr 5B for SGW (117.1 cM) and PH (145.9 cM). An additional QTL was identified for PH on chr 2A (118.4 cM). Two QTLs were pointed out for HD on chr 1B (43.6 cM) and 6A (72.4 cM), both with a negative effect on phenotype. Three QTLs were identified on chr 2B for GNO (76.6 cM), TKW (90.8 cM) and TWT (183.6 cM). A second QTL for TWT was identified on chr 7A (82.4 cM) and for GNO on chr 3B (51.9 cM). A single QTL was for GLE on chr 4B (15.6 cM), DTM on chr 4B (69.3 cM) and GY on chr 3B (5.0 cM) (Table 3.5).

Table 3.5. List of *per se* QTLs identified in the three different analysis (2018, 2019, joint analysis) under heat stress condition (HS).

Peak marker	Chr	Marker position (cM) [1]	Confidence interval (cM) [2]	Alleles [3]	Effect	Allele Frequency	-log(p-value)	R^2 (%)	Traits
IWB69041	1B	43.6	40.5-46.7	**A**/G	-	160/12	3.0-3.8	5.3-5.6	HD
IWB66088	2A	118.4	115.3-121.5	**A**/G	+	11/170	3.2-4.2	6.0-8.7	PH
IWB33109	2B	76.6	73.5-79.7	**C**/T	-	80/98	4.6-4.9	8.6-9.1	GNO
IWB27823	2B	90.8	87.7-93.9	**C**/T	+	24/148	3.5-3.6	6.5-6.7	TKW
IWB65020	2B	183.6	180.5-186.7	**A**/G	-	163/20	3.1-3.7	5.3-7.1	TWT
wPt-9012	3B	5,0	1.9-8.1	**A**/T	-	156/19	3.0-3.6	5.9-7.3	GY
IWB10783	3B	51.9	48.8-55.0	**C**/T	+	94/87	3.2-4.1	5.5-7.2	GNO
IWB25162	4B	15.6	12.5-18.7	**C**/T	-	95/84	3.2-4.2	6.3-8.8	GLE
IWB4211	4B	69.3	66.2-72.4	**A**/G	-	38/139	3.5-4.5	6.0-8.4	DTM
IWB73200	5A	136.3	133.2-139.4	**A**/G	-	100/73	3.3-3.6	6.8-7.7	GWI
IWB68333	5B	117.1	114.0-120.2	**C**/T	+	163/16	4.2-5.3	8.3-10.4	SGW
IWB56221	5B	145.9	142.8-149.0	**A**/G	-	167/12	3.1-3.6	5.8-7.2	PH
IWA8031	5B	165.2	162.1-168.3	**C**/T	-	148/29	3.6-5.1	7.4-10.8	GWI
IWB50963	6A	72.4	69.3-75.5	**A**/G	-	161/18	3.1-4.1	4.2-7.3	HD
IWB27700	7A	82.4	79.3-85.5	**C**/T	+	14/169	3.0-3.4	5.6-6.0	TWT
IWB60028	7B	0.1	0.1-3.2	**C**/T	-	59/122	3.1-4.2	5.8-8.7	GWI
IWB74056	7B	15.8	12.7-18.9	**C**/T	-	92/89	3.3-3.9	6.2-8.1	GWI

[1] marker position of the peak marker based on the tetraploid wheat consensus map (Maccaferri *et al*., 2015a). [2] confidence intervals based on LD of the UNIBO-Durum Panel. [3] the allele effect is referred to the allele highlighted in bold. [4] plant height (PH), grain number per spike (GNO), thousand kernel weight (TKW), grain width (GWI), days to heading (HD), grain weight per spike (SGW), days to maturity (DTM), test weight (TWT), grain length (GLE).

3.3.5. GWAS results for reaction norm index (Δ)

A total of 72 (2018), 70 (2019) and 80 QTLs (joint analysis) were identified for reaction norm index (Δ). The significance of the QTL ($-\log_{10}$ (P)) ranged from 3.0 to 5.9 (*QPH_Δ19.ubo-1A* – Table A3.3), while the phenotypic variation explained by the QTL (R^2) ranged from 3.2% (*QHD_Δ19.ubo-3A* – Table A3.3) to 12.4% (*QPH_Δ19.ubo-1A* – Table A3.3). More information about the singles QTLs identified for reaction norm index are reported in the appendices material (Table A3.3, A3.6, A3.9).

As for NS and HS, the comparison between the three different analysis (2018, 2019, joint analysis) was made also for reaction norm index (Δ). Through the comparison analysis, nine *per se* QTLs were identified for five different traits, mainly on chr 5B (3 QTLs – Table 3.6).

PH was pointed out in three different chromosomic regions, namely, chr 2A (118.4 cM), 5B (2.7 cM), and 5B (10.3 cM). As well as for PH, TWT was also identified in three chromosomic regions, on chr 2B (185.8 cM), 4B (97.5 cM), and 7A (82.4 cM). Additionally, single QTLs was identified for DTM on chr 5A (140.6 cM), HD on chr 5A (150.3 cM), and SGW on chr 5B (117.1 cM) (Table 3.6).

Table 3.6. List of *per se* QTLs identified in the three different analysis (2018, 2019, joint analysis) for reaction norm index (Δ).

Peak marker	Chr	Marker position (cM) [1]	Confidence interval (cM) [2]	Alleles [3]	Effect	Allele Frequency	-log(p-value)	R^2 (%)	Traits [4]
IWB66088	2A	118.4	115.3-121.5	**A**/G	8.02	11/170	3.1-4.1	5.7-7.6	PH
IWB758	2B	185.8	182.7-188.9	**A**/G	1.46	34/146	3.1-3.6	6.8-8.1	TWT
IWB7100	4B	97.5	94.4-100.6	**A**/C	0.21	99/75	3.1-3.5	6.0-7.7	TWT
IWB38719	5A	140.6	137.5-143.7	**C**/T	1.83	87/84	4.5-5.7	8.7-12.1	DTM
IWB10692	5A	150.3	147.2-153.4	**C**/T	4.11	157/15	3.8-4.4	4.9-5.0	HD
IWB5398	5B	2.7	0.1-5.8	**C**/T	0.50	111/70	3.3-4.7	6.3-9.1	PH
IWA3607	5B	10.3	7.2-13.4	**A**/G	-9.32	170/11	3.2-4.8	5.9-9.4	PH
IWB68333	5B	117.1	114.1-120.2	**C**/T	8.71	159/15	3.9-4.3	8.7-10.2	SGW
IWB27700	7A	82.4	79.3-85.5	**C**/T	2.02	14/167	3.7-3.8	7.5-8.4	TWT

[1] marker position of the peak marker based on the tetraploid wheat consensus map (Maccaferri *et al*., 2015a). [2] confidence intervals based on LD of the UNIBO-Durum Panel. [3] the allele effect is referred to the allele highlighted in bold. [4] plant height (PH), test weight (TWT), days to maturity (DTM), days to heading (HD), grain weight per spike (SGW).

From the total of *per se* QTLs identified for Δ, four of them were also identified under HS, indicating that these QTLs are strong adaptive QTLs expressed in both analysis (HS, Δ), as well as, in the three different analysis (2018, 2019, joint analysis). The four QTLs identified were as follow: one on chr 2A (118.4 cM) for PH, one on chr 5B (117.1 cM) for SGW, as well as two for TWT on chr 2B (185.8 cM), and 7A (82.4 cM), respectively (Table 3.5, 3.6).

3.3.6. QTL clusters across traits into single years

The results of the QTL cluster analysis across traits into single years (2018, 2019, joint analysis) with their respective peak marker, chromosome position, allele frequency and confidence interval are reported in the Table 3.7 (year 2018), Table 3.8 (year 2019), and Table 3.9 (joint analysis).

In the year 2018 was identified six QTL clusters (also known as hotspot QTL) expressed five or more time across the different analysis (NS, HS, Δ) (Table 3.7). Unfortunately, no QTL clusters were identified for GY in the year 2018, nevertheless, the identified QTL clusters affected mainly phenological traits (HD, DTM, and PH) as well as traits related to grain filling and format. The *HS_QTL_Cluster_2A.1* on chr 2A (117.6 cM) mainly affects phenological traits (HD_NS, DTM_NS, PH_HS, and PH_ Δ) as well as GNO_NS (Table 3.7). This QTL appears to be an adaptive QTL for PH, since it was also identified at the same confidence interval in both *per se* analysis (HS, Δ) (Table 3.5, 3.6). On chr 2B was identified *HS_QTL_Cluster_2B.1* QTL cluster which has a pronounced effect on traits characterized as components of the GY (SPM_NS, GNO_NS, GNO_HS, SGW_HS). The *HS_QTL_Cluster_4B.1* (chr 4B, 13.7 cM) was identified affecting phenological traits (HD_NS, HD_HS, DTM_HS, and PH_HS) as well as traits related to grain filling and format (GLE_NS, GLE_HS, and TKW_NS). Three QTL clusters were identified on chr 5A, namely, on position 106.6, 136.3, and 150.3 cM also for traits related to grain filling and format, as well as phenological traits ((Table 3.7).

Ten QTL clusters were identified in the year 2019 (Table 3.8). From the total number of QTL clusters, four of them showed an adaptive effect on GY, since they were expressed in both HS and Δ. Some of them, like *HS_QTL_Cluster_1A* (chr 1A, 67.8 cM), and *HS_QTL_Cluster_2A.2* (chr 2A, 117.6 cM) showed a concurrent effect on GY and PH (Table 3.8). Additionally, the cluster QTL *HS_QTL_Cluster_4A* (chr 4A, 172.0 cM), although affects other traits, has a consistent effect solely in GY. In the same way, the *HS_QTL_Cluster_5A.4* (chr 5A – 146.5 cM) was identified to be negatively affecting GY and SPM. Two more adaptive QTLs were identified on chr 2B and 5B, respectively. The *HS_QTL_Cluster_2B.3* cluster (chr 2B, 126.9 cM) has a concurrent effect on DTM and TKW, while the *HS_QTL_Cluster_5B* (chr 5B, 142.6 cM) affects SGW.

The four main adaptive QTL clusters identified in 2019, which were involved in the GY response, showed different patterns of beneficial allele distribution (data not shown). At *HS_QTL_Cluster_1A*, the beneficial allele (IWB40833 – C) is identified in a ratio of 163/18 in the UNIBO-Durum Panel accessions, basically, fixed in the subpopulations S4, S5 and admixed accessions, while showing no polymorphism in subpopulations S1, S2 and S3 (for additional information about subpopulations, see Chapter 2). At *HS_QTL_Cluster_2A.2* the beneficial allele (IWB65286 – T) was present in a ratio of 148/34, mostly fixed in S2 and S5, present in balanced

frequency in S1 and S3, while in S4 and admixed accessions the unfavorable allele (IWB65286 – C) was mostly fixed. At *HS_QTL_Cluster_4A*, the beneficial allele (wPt-5172 – T) was present in a ratio of 15/166, present in balance frequency in S1 and S2, in low frequency in S3 and admixed accessions, as well as absent in S4 and S5. At *HS_QTL_Cluster_5A.4* the beneficial allele (IWA7255 – G) was present in a ratio of 18/162, present in high frequency in S2, mostly absent in S1, S3 and S4, present in low frequency in admixed accessions, on the other hand, the unfavorable allele (IWA7255 – A) was fixed in S5.

Considering the joint analysis, eight QTL clusters were identified (Table 3.9), and six of them are adaptive QTLs identified under HS, as well as for Δ. Two of them are adaptive QTLs for PH, which were identified on chr 2A (117.6 cM, *HS_QTL_Cluster_2A.2*) and chr 2B (74.5 cM, *HS_QTL_Cluster_2B.1*) (Table 3.9). The *HS_QTL_Cluster_2A.2* appears to be a strong adaptive QTL for PH, since it affected PH in the same confidence interval also in 2018 and 2019. Three QTL clusters were identified for GY, namely, *HS_QTL_Cluster_3B* (chr 3B, 5.0 cM), *HS_QTL_Cluster_4A* (chr 4A, 172.0 cM), and *HS_QTL_Cluster_7A* (chr 7A, 103.8 cM) which has a concurrent effect with TKW (Table 3.9). The *HS_QTL_Cluster_4A* was also identified at the exactly same chromosomic position in 2019, indicating the importance of this QTL in the response of GY under heat stress in durum wheat. Finally, *HS_QTL_Cluster_4B.3* (4B, 92.9 cM) QTL cluster showed concurrent effect on GNO and SGW, two important components of GY.

The frequency of the beneficial allele as well as their ratio for the four main QTLs are reported below. At *HS_QTL_Cluster_3B*, the unfavorable allele (wPt-9012 – A) was present in a higher frequency (156/19), fixed in the subpopulation S5, present in high frequency in S2, S3, S4 and admixed accessions, while the beneficial allele (wPt-9012 – T) was present basically in S2 subpopulation (data not shown). At *HS_QTL_Cluster_4A*, the beneficial allele (wPt-5172 – T) was present in a lower frequency (16/167), present in a balanced frequency in S1 and S2, while almost absent in S3, S4, S5 and admixed accessions. At *HS_QTL_Cluster_4B.3*, the UNIBO-Durum Panel is enriched with the beneficial allele (IWB71883 – T), which was identified in a ratio of 164/11, fixed in S2, S3, S4 and S5, while being balanced in S1. At *HS_QTL_Cluster_7A*, the beneficial allele (IWB9633 – G) was identified in high frequency (164/11), which was fixed in S2 and S5, as well as mostly frequent in S1, S3, S4 and admixed accessions.

Table 3.7. List of GWAS-QTL clusters identified at the UNIBO-Durum Panel with their respective effect on days to heading (HD), days to maturity (DTM), grain number per spike (GNO), plant height (PH), number of spikes per linear meter (SPM), grain weight per spike (SGW), thousand kernel weight (TKW), grain length (GLE), test weight (TWT), number of spikelets per spike (SKT), and grain width (GWI) under two environmental conditions: control (NS) and heat stress (HS) as well as for reaction norm index (Δ) in the crop season 2018.

QTL Cluster	Peak marker	Chr.	Marker position (cM) [1]	Allele [2]	Allele frequency	Confidence interval (cM)	Traits [3]	QTLs from literature [4]
HS_QTL_Cluster_2A.1	IWB13965	2A	117.6	**C**/T	32/146	114.5-120.7	HD_NS (+), DTM_NS (+), GNO_NS (-), PH_HS (-), PH_Δ (-)	
HS_QTL_Cluster_2B.1	IWB22852	2B	74.5	**C**/T	14/166	71.4-77.6	SPM_NS (+), GNO_NS (-), SGW_NS (+), GNO_HS (+), PH_Δ (+)	PH[a], GY[a], TWT[a]
HS_QTL_Cluster_4B.1	IWB63893	4B	13.7	**A**/G	40/139	10.6-16.8	HD_NS (-), TKW_NS (-), GLE_NS (-), HD_HS (-), DTM_HS (-), PH_HS (-), GLE_HS (-)	
HS_QTL_Cluster_5A.1	IWB9126	5A	106.6	**A**/C	165/13	103.5-110.7	SPM_NS (+), HD_HS (-), TKW_Δ (+), TWT_Δ (+), SKT_Δ (+)	
HS_QTL_Cluster_5A.2	IWB55564	5A	136.3	**A**/G	79/97	133.2-139.4	TKW_NS (-), TKW_HS (-), GWI_HS (+), DTM_Δ (-), PH_Δ (-)	
HS_QTL_Cluster_5A.3	IWB10692	5A	150.3	**C**/T	164/14	147.2-153.4	HD_NS (-), PH_NS (-), TWT_NS (+), DTM_HS (-), PH_HS (-), TKW_Δ (-), TWT_Δ (-)	

[1] marker position of the peak marker based on the tetraploid wheat consensus map (Maccaferri *et al*., 2015a). [2] the allele effect is referred to the allele highlighted in bold. [3] (-) and (+) the signal in parenthesis indicated the allele effect on the trait. [4] [a] Maccaferri *et al*., 2011.

Table 3.8. List of GWAS-QTL clusters identified at the UNIBO-Durum Panel with their respective effect on plant height (PH), grain yield (GY), days to maturity (DTM), grain weight per spike (SGW), grain width (GWI), thousand kernel weight (TKW) test weight (TWT), grain number per spike (GNO), number of spikes per linear meter (SPM), number of spikelets per spike (SKT), and grain length (GLE) under two environmental conditions: control (NS) and heat stress (HS) as well as for reaction norm index (Δ) in the crop season 2019.

QTL Cluster	Peak marker	Chr.	Marker position (cM) [1]	Allele [2]	Allele frequency	Confidence interval (cM)	Traits [3]	QTLs from literature [4]
HS_QTL_Cluster_1A	IWB40833	1A	67.8	**C**/T	163/18	64.7-70.9	PH_HS (+), GY_HS (+), DTM_Δ (+), PH_Δ (+), GY_Δ (+), SGW_Δ (+), GWI_Δ (+)	
HS_QTL_Cluster_2A.2	IWB65286	2A	117.6	**C**/T	34/148	114.5-120.7	TKW_NS (+), TWT_NS (-), GNO_NS (+), PH_HS (-), GY_HS (-), PH_Δ (-), GY_Δ (-)	SGW[a], GNO[a], TKW[a]
HS_QTL_Cluster_2A.3	IWB72263	2A	197.6	**A**/G	39/138	193.1-200.2	TKW_NS (-), GNO_NS (+), GWI_NS (-), SGW_HS (-), GWI_Δ (+)	
HS_QTL_Cluster_2B.2	IWB33109	2B	76.6	**C**/T	80/98	73.5-79.7	TKW_NS (+), GNO_NS (-), SGW_NS (-), PH_HS (-), GNO_HS (-), SGW_HS (-), DTM_Δ (-)	
HS_QTL_Cluster_2B.3	IWB47474	2B	126.9	**A**/G	49/130	123.8-130.0	TWT_NS (+), DTM_HS (-), TKW_HS (-), DTM_Δ (-), TKW_Δ (-), GWI_Δ (-)	
HS_QTL_Cluster_4A	wPt-5172	4A	172.0	**A**/T	166/15	168.9-175.1	TWT_NS (-), GY_HS (-), SPM_HS (-), SKT_HS (+), GY_Δ (-)	SGW[a], GNO[a], TKW[a]
HS_QTL_Cluster_4B.2	IWB25162	4B	15.6	**C**/T	95/84	12.5-18.7	GLE_NS (-), HD_HS (+), TKW_HS (-), GNO_HS (+), GLE_HS (-)	
HS_QTL_Cluster_5A.4	IWA7255	5A	146.5	**A**/G	162/18	143.4-149.6	HD_NS (-), PH_NS (-), PH_HS (-), GY_HS (-), SPM_HS (-), SKT_HS (+), GY_Δ (-), SPM_Δ (-)	
HS_QTL_Cluster_5B	IWB8035	5B	142.6	**C**/T	35/144	139.5-145.7	PH_HS (-), GY_HS (-), SPM_HS (-), SGW_HS (-), GWI_HS (-), GNO_Δ (-), SGW_Δ (-)	
HS_QTL_Cluster_6B	IWB4259	6B	94.8	**A**/G	156/24	90.3-96.5	PH_NS (-), SPM_NS (-), SGW_NS (+), GWI_NS (+), TKW_Δ (-), SKT_Δ (+), GWI_Δ (-)	

[1] marker position of the peak marker based on the tetraploid wheat consensus map (Maccaferri *et al*., 2015a). [2] the allele effect is referred to the allele highlighted in bold. [3] (-) and (+) the signal in parenthesis indicated the allele effect on the trait. [4] [a] Mangini *et al*., 2018.

Table 3.9. List of GWAS-QTL clusters identified at the UNIBO-Durum Panel with their respective effect on days to heading (HD), days to maturity (DTM), test weight (TWT), grain number per spike (GNO), plant height (PH), thousand kernel weight (TKW), grain weight per spike (SGW), grain width (GWI), grain yield (GY), and number of spikes per linear meter (SPM) under two environmental conditions: control (NS) and heat stress (HS) as well as for reaction norm index (Δ) considering the joint analysis.

QTL Cluster	Peak marker	Chr.	Marker position (cM) [1]	Allele [2]	Allele frequency	Confidence interval (cM)	Traits [3]	QTLs from literature [4]
HS_QTL_Cluster_2A.2	IWB65286	2A	117.6	**C**/T	34/148	114.5-120.7	HD_NS (+), DTM_NS (+), TWT_NS (-), GNO_NS (+), PH_HS (-), PH_Δ (-)	SGW[d], GNO[d], TKW[d]
HS_QTL_Cluster_2B.3	IWB62322	2B	7.9	**C**/T	160/22	4.8-11.0	TKW_NS (-), SGW_NS (-), GWI_NS (-), HD_HS (+), TKW_HS (-), GNO_HS (+), GWI_HS (-)	
HS_QTL_Cluster_2B.1	IWB22852	2B	74.5	**C**/T	15/160	71.4-77.6	TWT_NS (+), GNO_NS (+), SGW_NS (+), PH_HS (+), GNO_HS (+), SGW_HS (+), PH_Δ (+)	PH[a], GY[a], TWT[a]
HS_QTL_Cluster_2B.4	IWB40126	2B	130.1	**C**/T	173/10	127.0-133.2	GY_NS (-), TWT_NS (-), PH_HS (-), TKW_HS (-), SPM_HS (-), SGW_HS (-)	
HS_QTL_Cluster_3B	wPt-9012	3B	5.0	**A**/T	156/19	1.9-8.1	GNO_NS (+), GY_HS (-), TKW_HS (-), SPM_HS (-), GY_Δ (-)	NDVI[b,c], TKW[b], TWT[b], SPAD[b]
HS_QTL_Cluster_4A	wPt-5172	4A	172.0	**A**/T	167/16	168.9-175.1	PH_NS (-), TWT_NS (-), SPM_NS (-), PH_HS (-), GY_HS (-), SPM_HS (-), GY_Δ (-)	SGW[d], GNO[d], TKW[d]
HS_QTL_Cluster_4B.3	IWB71883	4B	92.9	**C**/T	11/164	89.8-96.0	GNO_HS (-), SGW_HS (-), HD_Δ (-), GNO_Δ (-), SGW_Δ (-)	
HS_QTL_Cluster_7A	IWB9633	7A	103.8	**A**/G	11/164	100.7-106.9	GY_HS (-), TKW_HS (-), GY_Δ (-), TKW_Δ (-), GNO_Δ (-), SGW_Δ (-), GLE_Δ (-)	

[1] marker position of the peak marker based on the tetraploid wheat consensus map (Maccaferri *et al*., 2015a). [2] the allele effect is referred to the allele highlighted in bold. [3] (-) and (+) the signal in parenthesis indicated the allele effect on the trait. [4] [a] Maccaferri *et al*., 2011; [b] Graziani *et al*., 2014; [c] Condorelli *et al*., 2018; [d] Mangini *et al*., 2018.

3.4. Discussion

The frequency and severity of high temperature stress are increasing consistently and are expected to reach worrying levels in the near future (Asseng *et al*., 2017; Zhao *et al*., 2017, ICCS 2019), which underlines the urgency of identifying novel alleles able to mitigate the effects of heat stress in crops like durum wheat prevalently grown in heat-prone regions such as the Mediterranean Basin (Danzi *et al.*, 2019; Kutiel, 2019).

In the last years, several studies have been developed aiming to map QTLs related to GY in biparental populations under heat stress (Tricker *et al*., 2018), as well as in order to mapping GY loci using Genome Wide Association Studies (GWAS) (Maccaferri *et al*., 2011; Sukumaran *et al*., 2015, 2018; Lozada *et al*., 2017; Garcia *et al*., 2019). However, domestication and selection processes have created a genetic bottleneck over time, particularly for self-pollinating species like wheat, due the removal of low frequency alleles, hence decreasing genetic variability, increasing linkage disequilibrium (LD) and creating linkage drag (Hamblin *et al*., 2011). GWAS studies based on large number of accessions, offer an opportunity to identify the effects of novel alleles while allowing for the dissection of the QTLome of complex traits, such as HS (Zhang *et al.*, 2010; Korte and Farlow, 2013). Importantly, the use of population structure and other covariates, most importantly phenology, allows to avoid declaring false positive QTLs (Yu *et al.*, 2006; Zhang *et al.*, 2010; Korte and Farlow, 2013). In this study, both population structure and phenology loci were used as covariates as well as the Q-Q plots for multiple models were used to select the best model to identify QTLs for heat stress tolerance. According to Q-Q plot analysis, the model MLM + K + Q + Phenology loci was identified as the best model to avoid false positives in all analysis (2018, 2019, joint analysis) (Figures 3.3, 3.4, 3.5) respectively.

In this study, a panel (UNIBO-Durum Panel) of 183 elite durum wheat cultivars and elite breeding lines from Mediterranean countries, USA and Mexico was evaluated in two different crop seasons (2018, 2019 and jointly), in order to dissect the QTLome of durum wheat under heat stress condition.

The best performance of the plants in the crop season of 2019, in comparison with the crop season of 2018, particularly for GY, can be explained by the lower temperature faced by plants during the grain filling growth stage in the crop season of 2019 (Figure 3.1), since several studies have demonstrated that plants are very sensitive to heat stress during flowering and grain filling stages, which affects several reproductive (Cossani and Reynolds, 2012; Fábián *et al*., 2019),

metabolic (Wahid *et al*., 2007; Farooq *et al*., 2011) and/or physiological (Gautam *et al*., 2014, Sharma *et al*., 2017; Posch *et al*., 2019) processes.

On average, heat stress reduced GY by 56.5% (Table 3.3). Sukumaran *et al.* (2018), working in the same environment and location identified a higher reduction of GY (71.7%) due HS in durum wheat. GY was negatively correlated with the phenological traits HD and DTM under NS as well as HS condition (Figure 3.7), indicating that the advantage for GY is given by earlier genotypes. On the other hand, GY was positively correlated with TWT in both NS and HS conditions.

In order to obtain a more comprehensive view on the genetic profile of agronomic traits we compare the QTLomes of durum and bread wheat using the information of the durum wheat consensus map (Maccaferri *et al*., 2015a). Importantly, such comparison is greatly facilitated by the availability in both durum and bread wheat of consensus maps assembled with SNP data produced by the same Illumina 90K SNP platform (Wang et al., 2014; Maccaferri et al., 2019).

Our study identified 22 (NS), 17 (HS), and nine (Δ) *per se* QTLs affecting the same trait across the different analysis (2018, 2019, joint analysis). Additionally, we identified six (2018), ten (2019), eight (joint analysis) QTL clusters in the three different analysis. From the total of *per se* and QTLs clusters, 13 QTLs can be highlighted with effect across different years and/or different traits (Table 3.7, 3.8, 3.9).

The *HS_QTL_Cluster_2B.1* is an adaptive QTLs for PH, while *HS_QTL_Cluster_1A* and *HS_QTL_Cluster_2A.2* besides the effect on PH, affect also GY. The UNIBO-Durum Panel appears to be enriched with the beneficial allele for *HS_QTL_Cluster_1A* (IWB40833 – T, 90.1%), and *HS_QTL_Cluster_2A.2* (IWB65286 – T, 81.3%), while *HS_QTL_Cluster_2B.1* is enriched with the unfavorable allele (IWB22852 – T, 91.4%) (data not shown). In this study, we identified several chromosomic regions for GY that co-localized with PH with concurrent additive effects. The same situation was also identified in other studies, in wheat (Sukumaran *et al*., 2016, 2018; Sehgal *et al*., 2017) and barley (Tondelli *et al*. 2014). However, the most important QTL clusters identified in your study, did not overlap with those for phenological traits (HD, DTM), a finding common to other studies where accessions with large difference in phenology were considered (Sukumaran *et al*., 2018; Garcia *et al*., 2019), differently from this study where accessions were pre-selected to narrow the range in flowering date (in Mediterranean countries). Furthermore, the use of phenological genes as covariate was able to remove the co-localization of GY with HD and

DTM in our analysis. According to Shavrukov *et al*. (2017), phenological traits and PH are associated with plant adaptation and can be associated with abiotic stress escape. Among the three main QTL clusters affecting PH, *HS_QTL_Cluster_2B.1* was identified in the same chromosomic region of a QTL identified by Maccaferri *et al*. (2011). In that study, developed in several field trials across the Mediterranean Basin and under different water regimes, the authors identified a QTL affecting PH, GY and TWT. Additionally, a QTL at the same location of *HS_QTL_Cluster_2A.2* was identified by Mangini *et al*. (2018) affecting SGW, GNO and TKW.

On chr 3B (5.0 cM) and 4A (172.0 cM) two QTL clusters affected mainly GY, namely, *HS_QTL_Cluster_3B* and *HS_QTL_Cluster_4A*, respectively. For both adaptive QTL clusters the UNIBO-Durum Panel shows a small number of accessions with the beneficial allele. Notably, for *HS_QTL_Cluster_3B* only, 10.6% of the accessions have the beneficial allele (wPt-9012 – T), which was identified mainly in accessions developed in Italy and Mediterranean countries, as well as by ICARDA for dryland areas. The *HS_QTL_Cluster_3B* has been reported to affect TKW, TWT, NDVI and SPAD (Graziani *et al*., 2014) and NDVI (Condorelli *et al*., 2018). Additionally, *HS_QTL_Cluster_3B* was identified very close to a QTL affecting HD, PH, PdL, TWT and GY (Maccaferri *et al*., 2011). In the same way, *HS_QTL_Cluster_4A* showed even fewer accessions with the beneficial allele (wPt-5172 – T, 8.7%), which were basically identified only in Italian and Mediterranean accessions (data not shown). This QTL has been reported to affect SGW, GNO and TKW (Mangini *et al*., 2018), i.e. the components of GY. Although, some of the accessions of the UNIBO-Durum Panel were specifically developed by ICARDA for temperate areas, they did not show the beneficial allele for these QTL clusters.

Two adaptive QTL clusters *HS_QTL_Cluster_5A.4* and *HS_QTL_Cluster_7A* identified in 2019 and in the joint analysis, respectively affect, besides GY, SPM and TKW, respectively. While the UNIBO-Durum Panel is enriched with the beneficial allele (IWB9633 – G, 93.7%) for *HS_QTL_Cluster_7A*, shows low frequency of the beneficial allele (IWA7255 – G, 10.0%) for *HS_QTL_Cluster_5A.4*, which is present mainly in accessions developed by ICARDA for dryland areas.

Increasing GY in plants has always been a difficult process due the fact that this is a quantitative trait controlled by several loci, presents a low heritability and is strongly influenced by environmental conditions (Mangini *et al*., 2018). A strategy that can be used to overcame this problem is to divide total GY into GY components (Kuzay *et al*., 2019), in this sense,

HS_QTL_Cluster_5A.4 and *HS_QTL_Cluster_7A* are promising since they were identified affecting GY and also two GY components (SPM, TKW). According to Mangini *et al*, (2018), SPM and TKW are characterized as two of the primary components of the GY. Besides that, TKW is also important due the fact that it is strictly related to milling quality.

The adaptive effect of the QTL clusters *HS_QTL_Cluster_4B.3* and *HS_QTL_Cluster_5B* was highlighted in the joint analysis and in 2019, respectively. Although both QTLs do not affect GY directly, they affect traits strictly related to GY, namely SGW (*HS_QTL_Cluster_4B.3* and *HS_QTL_Cluster_5B*) and GNO (only *HS_QTL_Cluster_4B.3*). These QTLs are already enriched with the HS-tolerant allele at the peak marker position, since the beneficial allele (IWB71883 – T) is identified in 93.7% of the accessions of the UNIBO-Durum Panel for *HS_QTL_Cluster_4B.3*, while the beneficial allele (IWB8035 – T) for *HS_QTL_Cluster_5B* is identified in 80.4% of the accessions.

Similar to the results of this study (Figure 3.7), other studies have reported a negative correlation between GNO and TKW (Borrás *et al*., 2004; Zhang *et al*., 2017, Sukumaran *et al*., 2018), this situation has avoided a faster genetic gain in wheat breeding (Foulkes *et al*., 2011; Sukumaran *et al*., 2018). On the other hand, SGW and GNO (Figure 3.7) are frequently correlated positively (Mangini *et al*., 2018). Phenotypic correlation between traits usually are due to genetic linkage and pleiotropy, in this sense, using markers developed for the QTLs *HS_QTL_Cluster_4B.3* and *HS_QTL_Cluster_7A* may be a valuable alternative to pyramiding the beneficial alleles for GNO, SGW (*HS_QTL_Cluster_4B.3*) and TKW (*HS_QTL_Cluster_7A*) in order to improve, indirectly, GY performance.

3.5. Conclusions

This study reports three different classes of QTLs potentially involved in the GY response under heat stress. The *HS_QTL_Cluster_3B* and *HS_QTL_Cluster_4A*, although affect other traits in specific situation is constantly expressed only for grain yield, while other QTLs affect grain yield and its components or grain yield and plant height. The different chromosomic regions affecting GY and its components under HS, clearly indicate that specific loci affect directly or indirectly final GY performance. In this way, pyramiding of the beneficial allele at the chromosomic regions identified to affect GY and its components appears as a valuable strategy to increase heat stress tolerance in durum wheat. Besides that, the recent genome sequencing of wild

emmer (Avni *et al*., 2017) and durum wheat (Maccaferri *et al*., 2019) provides novel opportunities for a finer and more effective dissection of the major QTLs identified in this study in order to develop user-friendly molecular markers suitable to select durum wheat cultivar more tolerant to heat stress.

References

Asseng S, Cammarano D, Basso B, *et al*. 2017. Hot spots of wheat yield decline with rising temperatures. Global Change Biology 23, 2464–2472.

Avni R, Nave M, Barad O, *et al*. 2017. Wild emmer genome architecture and diversity elucidate wheat evolution and domestication. Science 357, 93–97.

Bates D, Mächler M, Bolker B, Walker S. 2015. Fitting Linear Mixed-Effects Models Using lme4. Journal of Statistical Software 67, 1–48.

Borrás L, Slafer GA, Otegui ME. 2004. Seed dry weight response to source-sink manipulations in wheat, maize and soybean: A quantitative reappraisal. Field Crops Research 86, 131–146.

Bradbury PJ, Zhang Z, Kroon DE, Casstevens TM, Ramdoss Y, Buckler E. 2007. TASSEL: software for association mapping of complex traits in diverse samples. Bioinformatics 23, 2633–2635.

Condorelli GE, Maccaferri M, Newcomb M, Andrade-Sanchez P, White JW, French A, Sciara G, Ward R, Tuberosa T. 2018. Comparative aerial and ground based high throughput phenotyping for the genetic dissection of NDVI as a proxy for drought adaptive traits in durum wheat. Frontiers in Plant Science 9, 893.

Cossani CM, Reynolds MP. 2012. Physiological traits for improving heat tolerance in wheat. Plant Physiology 160, 1710–1718.

Danzi D, Briglia N, Petrozza A, Summerer S, Povero G, Stivaletta A, Cellini F, Pignone D, de Paola D, Janni M. 2019. Can high throughput phenotyping help food security in the Mediterranean area?. Frontiers in Plant Science 10, 737.

El Hassouni K, Belkadi B, Filali-Maltouf A, Tidiane-Sall A, Al-Abdallat A, Nachit M, Bassi FM. 2019. Loci controlling adaptation to heat stress occurring at the reproductive stage in durum wheat. Agronomy 9, 414.

Fábián A, Sáfrán E, Szabó-Eitel G, Barnabás B, Jäger K. 2019. Stigma functionality and fertility are reduced by heat and drought co-stress in wheat. Frontiers in Plant Science 10, 244.

FAOSTAT .2017. FAOSTAT https://www.fao.org/faostat/en/#data. Food and Agriculture Organization (FAO) of the United Nations.

Farooq M, Bramley H, Palta JA, Siddique KHM. 2011. Heat stress in wheat during reproductive and grain-filling phases. Critical Reviews in Plant Sciences 30, 491–507.

Foulkes MJ, Slafer GA, Davies WJ, Berry PM, Sylvester-Bradley R, Martre P, Calderini DF, Griffiths S, Reynolds MP. 2011. Raising yield potential of wheat. III. Optimizing partitioning to grain while maintaining lodging resistance. Journal of Experimental Botany 62, 469–486.

Garcia M, Eckermann P, Haefele S, Satija S, Sznajder B, Timmins A, Baumann U, Wolters P, Mather DE, Fleury D. 2019. Genome-wide association mapping of grain yield in a diverse collection of spring wheat (*Triticum aestivum* L.) evaluated in southern Australia. Plos One 14.

Gao F, Ma D, Yin G, Rasheed A, Dong Y, Xiao Y, Xia X, Wu X, He Z. 2017. Genetic progress in grain yield and physiological traits in Chinese wheat cultivars of southern Yellow and Huai valley since 1950. Crop Science 57, 760–773.

Graziani M, Maccaferri M, Royo C, Salvatorelli F, Tuberosa R. 2014. QTL dissection of yield components and morpho-physiological traits in a durum wheat elite population tested in contrasting thermo-pluviometric conditions. Crop Pasture Science 65, 80–95.

Gautam A, Agrawal D, SaiPrasad SV, Jajoo A. 2014. A quick method to screen high and low yielding wheat cultivars exposed to high temperature. Physiology and Molecular Biology of Plants 20, 533–537.

Hamblin MT, Buckler ES, Jannink JL. 2011. Population genetics of genomics-based crop improvement methods. Trends in Genetics. 27, 98–106.

Hossain MA, Bhattacharjee S, Armin SM, Qian P, Xin W, Li HY, Burritt D, Fujita M, Tran LSP. 2015. Hydrogen peroxide priming modulates abiotic oxidative stress tolerance: insights from ROS detoxification and scavenging. Frontiers in Plant Science 6, 420.

IPCC, 2014 Climate Change 2014: Synthesis Report. Contribute of Working Groups I, II, III to the Fifth Assessment Report of the Intergovernmental Panel on Climate Change [Core Writing Team, Pachauri RK, Meyer LA (eds.)]. IPCC, Geneva, Switzerland, 151pp.

Korte A, Farlow A. 2013. The advantages and limitations of trait analysis with GWAS: a review. Plant Methods 9, 29.

Kutiel H. 2019. Climatic uncertainty in the Mediterranean basin and its possible relevance to important economic sectors. Atmosphere 10, 10.

Kuzay S, Xu Y, Zhang J, *et al*. 2019. Identification of a candidate gene for a QTL for spikelet number per spike on wheat chromosome arm 7AL by high-resolution genetic mapping. Theoretical and Applied Genetics 132, 2689-2705.

Li L, Mao X, Wang J, Chang X, Reynolds MP, Jing R. 2019. Genetic dissection of drought and heat-responsive agronomic traits in wheat. Plant, Cell and Environment 42, 2540-2553.

Liu C, Sukumaran S, Claverie E, Sansaloni C, Dreisigacker S, Reynolds MP. 2019. Genetic dissection of heat and drought stress QTLs in phenology-controlled synthetic-derived recombinant inbred lines in spring wheat. Molecular Breeding, 39, 34.

Liu W, Maccaferri M, Bulli P, Rynearson S, Tuberosa R, Chen X, PumphreyM. 2017. Genome-wide association mapping for seedling and field resistance to *Puccinia striiformis* f. sp. *tritici* in elite durum wheat. Theoretical and Applied Genetics 130, 649–667.

Lobell DB, Hammer GL, Chenu K, Zheng B, Mclean G, Chapman SC. 2015. The shifting influence of drought and heat stress for crops in northeast Australia. Global Change Biology 21, 4115–4127.

Lloveras J, Manent J, Viudas J, López A, Santiveri P. (2004. Seeding rate influence on yield and yield components of irrigated winter wheat in a Mediterranean climate. Agronomy Journal 96, 1258–1265.

Lozada DN, Mason RE, Babar MA, *et al*. 2017. Association mapping reveals loci associated with multiple traits that affect grain yield and adaptation in soft winter wheat. Euphytica 213, 222.

Maccaferri M, Sanguineti MC, Natoli V, *et al*. 2006. A panel of elite accessions of durum wheat (*Triticum durum* Desf.) suitable for association mapping studies. Plant Genetic Resources 4, 79–85.

Maccaferri M, Stefanelli S, Rotondo F, Tuberosa R, Sanguineti MC. 2007a. Relationships among durum wheat accessions. I. Comparative analysis of SSR, AFLP, and phenotypic data. Genome 50, 373–384.

Maccaferri M, Sanguineti MC, Xie C, Smith JSC, Tuberosa R. 2007b. Relationships among durum wheat accessions. II. A comparison of molecular and pedigree information. Genome, 50, 385–399.

Maccaferri M, Sanguineti MC, Demontis A, *et al*. 2011. Association mapping in durum wheat grown across a broad range of water regimes. Journal of Experimental Botany 62, 409–438.

Maccaferri M, Ricci A, Salvi S, *et al*. 2015a. A high-density, SNP-based consensus map of tetraploid wheat as a bridge to integrate durum and bread wheat genomics and breeding. Plant Biotechnology Journal 13, 648–663.

Maccaferri M, Harris NS, Twardziok SO, *et al*. 2019. Durum wheat genome highlights past domestication signatures and future improvement targets. Nature Genetics 51, 885–895.

Mangini G, Gadaleta A, Colasuonno P, *et al*. 2018. Genetic dissection of the relationships between grain yield components by genome-wide association mapping in a collection of tetraploid wheats. Plos One 13, e0190162.

Mondal S, Singh RP, Crossa J, *et al*. 2013. Earliness in wheat: A key to adaptation under terminal and continual high temperature stress in South Asia. Field Crops Research 151, 19–26.

Murchie EH, Lawson T. 2013. Chlorophyll fluorescence analysis: A guide to good practice and understanding some new applications. Journal of Experimental Botany 64, 3983–3998.

Prasad PVV, Djanaguiraman M. 2014. Response of floret fertility and individual grain weight of wheat to high temperature stress: Sensitive stages and thresholds for temperature and duration. Functional Plant Biology 41, 1261–1269.

Posch BC, Kariyawasam BC, Bramley H, Coast O, Richards RA, Reynolds MP, Trethowan R, Atkin O. 2019. Exploring high temperature responses of photosynthesis and respiration to improve heat tolerance in wheat. Journal of Experimental Botany. https://doi.org/10.1093/jxb/erz257

Rajaram S, Van Ginkel M, Fischer RA. 1994. CIMMYT's wheat breeding mega-environments

Reynolds MP, Foulkes J, Furbank R, Griffiths S, King J, Murchie EH, Parry M, Slafer G. 2012. Achieving yield gains in wheat. Plant, Cell and Environment 35, 1799–1823.

Salvi S, Tuberosa R. 2015. The crop QTLome comes of age. Current Opinion in Biotechnology 32, 179–185.

Sareen S, Bhusal N, Kumar M, Bhati PK, Munjal R, Kumari J, Kumar S, Sarial AK. 2019. Molecular genetic diversity analysis for heat tolerance of indigenous and exotic wheat genotypes. Journal of Plant Biochemistry and Biotechnology 1, 9.

Sehgal D, Autrique E, Singh R, Ellis M, Singh S, Dreisigacker S. 2017. Identification of genomic regions for grain yield and yield stability and their epistatic interactions. Scientific Reports 7, 41578.

Semenov MA, Shewry PR. 2011. Modelling predicts that heat stress, not drought, will increase vulnerability of wheat in Europe. Scientific Reports 1, 66.

Sharma DK, Torp AM, Rosenqvist E, Ottosen CO, Andersen SB. 2017. QTLs and potential candidate genes for heat stress tolerance identified from the mapping populations specifically segregating for Fv/Fm in wheat. Frontiers in Plant Science 8, 1668.

Shavrukov Y, Kurishbayev A, Jatayev S, Shvidchenko V, Zotova L, Koekemoer F, De Groot S, Soole K, Langridge P. 2017. Early flowering as a drought escape mechanism in plants: How can it aid wheat production? Frontiers in Plant Science 8, 1950.

Sukumaran S, Lopes M, Dreisigacker S, Reynolds MP. 2018. Genetic analysis of multi-environmental spring wheat trials identifies genomic regions for locus-specific trade-offs for grain weight and grain number. Theoretical and Applied Genetics 131, 985–998.

Sukumaran S, Lopes MS, Dreisigacker S, Dixon LE, Zikhali M, Griffiths S, Zheng B, Chapman S, Reynolds MP. 2016. Identification of earliness per se flowering time locus in spring wheat through a genome-wide association study. Crop Science 56, 2962–2972.

Sukumaran S, Dreisigacker S, Lopes M, Chavez P, Reynolds MP. 2015. Genome-wide association study for grain yield and related traits in an elite spring wheat population grown in temperate irrigated environments. Theoretical and Applied Genetics 128, 353–363.

The R Core Team (2016). R: A Language and Environment for Statistical Computing.

Tian X, Zhu Z, Xie L, *et al*. 2019. Preliminary exploration of the source, spread, and distribution of *Rht*24 reducing height in bread wheat. Crop Science 59, 19–24.

Tian X, Wen W, Xie L, *et al*. 2017. Molecular mapping of reduced plant height gene *Rht*24 in bread wheat. Frontiers in Plant Science 8, 1379.

Tondelli A, Francia E, Visioni A, *et al*. 2014. QTLs for barley yield adaptation to Mediterranean environments in the "Nure" × "Tremois" biparental population. Euphytica, 197, 73–86.

Tricker PJ, Elhabti A, Schmidt J, Fleury D. 2018. The physiological and genetic basis of combined drought and heat tolerance in wheat. Journal of Experimental Botany 69, 3195–3210.

Tuberosa R. 2012. Phenotyping for drought tolerance of crops in the genomics era. Frontiers in Physiology 3, 347.

Tuberosa R, Maccaferri M, Salvi S. 2019. Leveraging the QTLome to enhance climate change resilience in cereals, p. 612 in Advanced in breeding techniques for cereal crops, edited by Ordon F., Friedt W. Burleigh Dodds, Cambridge.

Wahid A, Gelani S, Ashraf M, Foolad MR. 2007. Heat tolerance in plants: an overview. Environmental and Experimental Botany 61, 199–223.

Wang S, Xu S, Chao S, Sun Q, Liu S, Xia G. 2019. A genome-wide association study of highly heritable agronomic traits in durum wheat. Frontiers in Plant Science 10, 919.

Wei T, Simko V. 2017. R package "corrplot": Visualization of a Correlation Matrix (Version 0.84).

Wolak ME, Fairbairn DJ, Paulsen YR. 2012. Guidelines for Estimating Repeatability. Methods in Ecology and Evolution 3, 129-137.

Xiao YG, Qian ZG, Wu K, Liu JJ, Xia XC, Ji WQ, He ZH. 2012. Genetic gains in grain yield and physiological traits of winter wheat in Shandong province, China, from 1969 to 2006. Crop Science 52, 44–56.

Yu J, Pressoir G, Briggs WH, *et al*. 2006. A unified mixed-model method for association mapping that accounts for multiple levels of relatedness. Nature Genetics 38, 203–208.

Zadoks JC, Chang TT, Konzak CF. 1974. A decimal code for the growth stages of cereals. Weed Research 14, 415–421.

Zhang H, Zhang F, Li G, Zhang S, Zhang Z, Ma L. 2017. Genetic diversity and association mapping of agronomic yield traits in eighty-six synthetic hexaploid wheat. Euphytica 213, 111.

Zhang Z, Ersoz E, Lai CQ, *et al*. 2010. Mixed linear model approach adapted for genome-wide association studies. Nature Genetics 42, 355–360.

Zhao C, Liu B, Piao S, *et al*. 2017. Temperature increase reduces global yields of major crops in four independent estimates. Proceedings of the National Academy of Sciences of the USA 114, 9326–9331.

Zhou Y, He ZH, Sui XX, Xia XC, Zhang XK, Zhang GS. 2007. Genetic improvement of grain yield and associated traits in the Northern China Winter Wheat Region from 1960 to 2000. Crop Science 47, 245–253.

Appendices

Table 2A.1 Genetic structure of the UNIBO-Durum Panel accessions determined through model- based clustering in STRUCTURE 2.3.4 software. Subpopulation 1 (S1) included twenty accessions from Italy and early 1970s CIMMYT germplasm; Subpopulation 2 (S2) included eleven accessions from ICARDA breeding programs for dryland areas; Subpopulation 3 (S3) included thirty-nine accessions from ICARDA breeding programs for temperate areas; Subpopulation 4 (S4) included forty-nine accessions characterized as late 1970s CIMMYT germplasm, widely adapted to Mediterranean conditions, and Subpopulation 5 (S5) included twenty-two accessions from late 1980s to early 1990s CIMMYT accessions, with high yield potential.

Accession Code	Accession Name	S1	S2	S3	S4	S5
		Italy - Mediterranean	ICARDA-Dryland	ICARDA-Temperate	CIMMYT'70 - ICARDA	CIMMYT'80
DP114	VALNOVA*	0.999	0.000	0.000	0.000	0.001
DP095	GARGANO	0.971	0.026	0.001	0.001	0.001
DP002	CANNIZZO	0.937	0.061	0.000	0.000	0.001
DP006	MONGIBELLO	0.917	0.078	0.001	0.001	0.003
DP105	OFANTO	0.916	0.082	0.001	0.001	0.001
DP094	FORTORE	0.795	0.195	0.002	0.003	0.005
DP076	ANTON	0.751	0.000	0.204	0.001	0.045
DP107	PLINIO	0.747	0.001	0.112	0.138	0.002
DP085	CICCIO	0.745	0.253	0.000	0.001	0.001
DP099	IXOS	0.739	0.002	0.244	0.006	0.009
DP004	LESINA	0.737	0.118	0.009	0.135	0.001
DP106	PLATANI	0.709	0.284	0.002	0.001	0.003
DP079	ARCANGELO	0.644	0.165	0.006	0.183	0.002
DP140	GEZIRA 17	0.629	0.102	0.260	0.005	0.004
DP084	CAPPELLI*	0.619	0.201	0.121	0.057	0.003
DP008	PIETRAFITTA	0.598	0.000	0.001	0.396	0.004
DP096	GRAZIA	0.579	0.002	0.387	0.002	0.030
DP010	TORREBIANCA	0.551	0.001	0.439	0.001	0.008
DP003	CLAUDIO	0.541	0.002	0.332	0.002	0.124
DP087	COLOSSEO	0.501	0.048	0.28	0.164	0.007
DP089	CRESO*	0.501	0.002	0.201	0.293	0.003
DP060	AWALBIT	0.000	0.999	0.000	0.000	0.000
DP071	OMRABI 5	0.000	0.999	0.000	0.000	0.000
DP160	MASSARA 1	0.000	0.998	0.000	0.000	0.001
DP187	YOUNES 1	0.000	0.899	0.001	0.095	0.004
DP182	TELSET 5	0.047	0.747	0.133	0.004	0.068
DP148	ICARDA125	0.001	0.688	0.171	0.139	0.001
DP167	OMLAHN 3	0.005	0.688	0.001	0.131	0.175

DP055	MARZAK	0.001	0.591	0.398	0.008	0.002
DP083	CAPEITI 8*	0.417	0.582	0.000	0.000	0.000
DP166	OMGENIL 3	0.024	0.572	0.036	0.248	0.120
DP169	OMSNIMA 1	0.001	0.562	0.197	0.238	0.002
DP029	ARIESOL	0.001	0.001	0.995	0.002	0.001
DP147	SEBOU	0.001	0.002	0.988		0.005
DP149	ICARDA78	0.001	0.001	0.983	0.001	0.014
DP110	ROQUENO	0.001	0.040	0.944	0.014	0.001
DP030	ARTENA	0.001	0.051	0.922	0.024	0.001
DP081	BRAVADUR	0.083	0.001	0.911	0.003	0.003
DP116	WESTBRED 881	0.127	0.001	0.870	0.001	0.001
DP136	CHAM 1	0.007	0.002	0.840	0.095	0.056
DP109	REVA	0.055	0.002	0.820	0.116	0.006
DP049	1808 INRA	0.006	0.094	0.811	0.082	0.007
DP189	KOFA	0.192	0.001	0.805	0.002	0.001
DP102	MESSAPIA	0.010	0.092	0.790	0.101	0.007
DP028	ALDEANO	0.082	0.063	0.747	0.104	0.004
DP077	APPIO	0.166	0.001	0.733	0.004	0.095
DP086	COLORADO	0.239	0.012	0.731	0.017	0.002
DP137	DERAA*	0.002	0.001	0.703	0.220	0.075
DP044	SENADUR	0.179	0.001	0.702	0.001	0.116
DP033	BOLENGA	0.172	0.055	0.676	0.090	0.007
DP145	HEIDER	0.003	0.021	0.676	0.288	0.013
DP181	SHABHA	0.126	0.169	0.656	0.003	0.045
DP108	PRODURA	0.047	0.004	0.652	0.292	0.004
DP120	ANGRE	0.220	0.001	0.646	0.015	0.119
DP034	BOLIDO	0.058	0.008	0.640	0.292	0.002
DP012	CIMMYT 36	0.012	0.081	0.629	0.260	0.018
DP013	CIMMYT 41	0.007	0.004	0.627	0.291	0.071
DP032	BOABDIL	0.001	0.008	0.614	0.365	0.012
DP098	ITALO	0.093	0.221	0.597	0.020	0.069
DP039	DURCAL	0.001	0.003	0.586	0.407	0.004
DP074	STOJOCRI	0.188	0.020	0.584	0.117	0.092
DP111	SVEVO	0.006	0.008	0.582	0.396	0.008
DP100	KRONOS	0.279	0.001	0.571	0.101	0.048
DP073	SEBAH	0.096	0.039	0.549	0.298	0.018
DP048	1807 INRA	0.083	0.061	0.547	0.304	0.004
DP154	KORIFLA	0.191	0.001	0.543	0.025	0.240
DP133	BLK2	0.001	0.001	0.541	0.454	0.004
DP066	KRS/HAUCAN	0.001	0.074	0.537	0.375	0.014
DP104	MOHAWK	0.202	0.002	0.520	0.275	0.001
DP176	QUADALETE	0.095	0.077	0.520	0.225	0.083
DP040	DUROI	0.002	0.013	0.500	0.440	0.044
DP056	OURGH	0.000	0.000	0.000	0.999	0.001
DP064	KARIM	0.000	0.000	0.000	0.999	0.001

DP091	DUILIO	0.000	0.000	0.000	0.999	0.001
DP266		0.000	0.000	0.000	0.999	0.001
DP130	BICRE*	0.008	0.001	0.001	0.990	0.001
DP119	AINZEN 1	0.001	0.000	0.024	0.931	0.044
DP121	AMEDAKUL 1	0.008	0.002	0.189	0.799	0.002
DP082	BRONTE	0.204	0.014	0.004	0.776	0.002
DP118	AGHRASS 1	0.001	0.001	0.173	0.770	0.055
DP183	TENSIFT 1	0.100	0.009	0.124	0.767	0.002
DP047	1805 INRA	0.001	0.189	0.062	0.744	0.004
DP159	MARSYR 1	0.036	0.139	0.085	0.740	0.002
DP168	OMRUF 2	0.039	0.007	0.009	0.729	0.216
DP171	OTB 6	0.260	0.002	0.015	0.717	0.006
DP186	WADALMEZ 1	0.001	0.001	0.275	0.716	0.008
DP123	ARISLAHN	0.066	0.015	0.195	0.710	0.014
DP254	SAMAYOA C2004	0.099	0.003	0.192	0.702	0.004
DP177	RAZZAK	0.001	0.079	0.223	0.692	0.005
DP142	GUEROU 1	0.001	0.001	0.193	0.685	0.120
DP134	BRACHOUA	0.070	0.001	0.091	0.677	0.161
DP175	QUABRACH 1	0.049	0.037	0.141	0.675	0.098
DP132	BIGOST 1	0.004	0.015	0.304	0.671	0.006
DP135	CHAHBA88	0.015	0.013	0.167	0.671	0.134
DP005	MERIDIANO	0.242	0.004	0.001	0.663	0.090
DP156	LAHN*	0.036	0.001	0.053	0.661	0.248
DP153	KHABUR 1	0.060	0.002	0.201	0.651	0.086
DP072		0.001	0.229	0.115	0.649	0.006
DP157	LOUKOS 1	0.001	0.002	0.111	0.648	0.237
DP068	MOULSABIL 2	0.087	0.003	0.208	0.647	0.055
DP184	TERBOL 97	0.020	0.085	0.064	0.629	0.203
DP124	ATLAST 1	0.013	0.022	0.232	0.622	0.111
DP158	MAAMOURI 1	0.015	0.002	0.249	0.613	0.121
DP155	LAGONIL 2	0.076	0.003	0.131	0.612	0.178
DP125	AUS 1	0.085	0.013	0.240	0.609	0.054
DP164	NILE	0.001	0.002	0.393	0.603	0.002
DP061	BCR/3/CHAM 1//GTA/STR	0.002	0.001	0.403	0.591	0.003
DP161	MIKI 1	0.009	0.055	0.320	0.588	0.029
DP037	BORLI	0.001	0.001	0.001	0.581	0.416
DP062	CHABA/DERAA	0.001	0.001	0.367	0.576	0.055
DP053	JAWHAR	0.027	0.004	0.015	0.568	0.386
DP090	DON PEDRO	0.065	0.006	0.273	0.566	0.090
DP117	WESTBRED TURBO	0.124	0.008	0.302	0.564	0.002
DP188	YOUSEF 1	0.061	0.025	0.269	0.556	0.089
DP093	FLAMINIO	0.461	0.001	0.001	0.536	0.002
DP151	KABIR 1	0.276	0.059	0.112	0.534	0.019
DP054	MARJANA	0.000	0.000	0.000	0.521	0.478

DP173	OUASLAHN 1	0.323	0.053	0.085	0.510	0.029
DP122	AMMAR 1	0.003	0.007	0.355	0.506	0.129
DP038	CANYON	0.001	0.003	0.483	0.503	0.011
DP015	CIMMYT 52	0.000	0.000	0.000	0.000	0.999
DP041	GALLARETA	0.000	0.000	0.000	0.000	0.999
DP036	BOMBASI	0.000	0.000	0.000	0.002	0.997
DP258		0.001	0.000	0.001	0.001	0.997
DP016	CIMMYT 67	0.000	0.000	0.000	0.003	0.996
DP045	SULA	0.000	0.000	0.000	0.003	0.996
DP021	CIMMYT 136	0.000	0.000	0.000	0.004	0.995
DP024	CIMMYT 22	0.001	0.000	0.017	0.001	0.981
DP017	CIMMYT 73	0.001	0.000	0.000	0.054	0.945
DP080	ARCOBALENO	0.001	0.000	0.000	0.059	0.939
DP011	CIMMYT 23	0.001	0.001	0.079	0.001	0.918
DP025	CIMMYT 24	0.002	0.006	0.088	0.003	0.901
DP020	CIMMYT 108	0.001	0.001	0.001	0.219	0.778
DP023	CIMMYT 19	0.001	0.010	0.213	0.001	0.775
DP097	IRIDE	0.000	0.000	0.000	0.240	0.758
DP255		0.004	0.001	0.058	0.181	0.756
DP253	JUPARE C2003	0.006	0.002	0.090	0.154	0.748
DP042	ILLORA	0.137	0.002	0.153	0.001	0.707
DP018	CIMMYT 78	0.001	0.001	0.001	0.296	0.701
DP257		0.005	0.003	0.295	0.011	0.687
DP262		0.001	0.042	0.191	0.092	0.674
DP256		0.006	0.005	0.163	0.288	0.538
Admixed accessions (Q membership's coefficient < 0.5)						
DP007	NORBA	0.167	0.007	0.369	0.079	0.377
DP027	CIMMYT 266	0.001	0.002	0.234	0.274	0.489
DP031	ASTIGI	0.001	0.001	0.407	0.101	0.490
DP035	BOLO	0.275	0.002	0.264	0.049	0.411
DP050	1809 INRA	0.140	0.065	0.408	0.284	0.103
DP057	TAREK	0.001	0.120	0.342	0.462	0.075
DP063	CHACAN	0.092	0.003	0.237	0.425	0.243
DP065		0.061	0.080	0.328	0.484	0.047
DP067	LAGOST 3	0.153	0.027	0.249	0.384	0.187
DP069	OMBAR	0.009	0.473	0.011	0.318	0.190
DP075	ZEINA 1	0.246	0.001	0.188	0.326	0.238
DP088	CORTEZ	0.215	0.066	0.460	0.252	0.007
DP103	MEXICALI 75	0.310	0.000	0.444	0.001	0.244
DP112	TRINAKRIA	0.450	0.406	0.140	0.003	0.001
DP113	VALBELICE	0.410	0.414	0.172	0.003	0.001
DP126	AWALI 1	0.119	0.006	0.451	0.293	0.131
DP127	RADIOSO	0.412	0.135	0.246	0.206	0.001
DP128	AZEGHAR 2	0.112	0.265	0.211	0.271	0.141

DP131	BICREDERAA 1	0.054	0.057	0.385	0.488	0.016
DP139	GEROMTEL	0.120	0.087	0.141	0.475	0.177
DP141	GIDARA 2	0.007	0.393	0.410	0.036	0.154
DP144	HAURANI	0.278	0.401	0.291	0.010	0.020
DP146	ICARDA121	0.202	0.095	0.273	0.289	0.142
DP150	JORDAN	0.357	0.002	0.289	0.333	0.019
DP163	LAGOST 1	0.007	0.004	0.496	0.422	0.072
DP170	ORT 1	0.122	0.002	0.422	0.004	0.451
DP172	OUASERL 1	0.203	0.244	0.060	0.490	0.004
DP178	SAADA3/DDS//MTL 1	0.157	0.116	0.332	0.217	0.178
DP179	SAJUR	0.181	0.001	0.427	0.072	0.319
DP185	TUNSYR 1	0.221	0.002	0.189	0.350	0.239
DP251		0.003	0.003	0.179	0.458	0.357
DP252	ATIL C2000	0.002	0.010	0.323	0.176	0.489
DP259		0.011	0.002	0.281	0.368	0.338
DP260		0.001	0.004	0.286	0.401	0.307
DP261		0.002	0.001	0.237	0.455	0.305
DP263		0.003	0.110	0.253	0.376	0.258
DP264		0.002	0.001	0.197	0.491	0.309
DP265		0.025	0.002	0.266	0.344	0.365
DP267		0.002	0.002	0.453	0.235	0.308
DP268		0.015	0.009	0.346	0.449	0.181
DP269		0.057	0.001	0.292	0.320	0.330

* founders accessions

Table A2.2. Fixation Index (Fst) of population differentiation due to genetic structure (STRUCTURE 2.3.4). Subpopulation 1 (S1) included twenty accessions from Italy and early 1970s CIMMYT germplasm; Subpopulation 2 (S2) included eleven accessions from ICARDA breeding programs for dryland areas; Subpopulation 3 (S3) included thirty-nine accessions from ICARDA breeding programs for temperate areas; Subpopulation 4 (S4) included fourty-nine accessions characterized as late 1970s CIMMYT germplasm, widely adapted to Mediterranean conditions, and Subpopulation 5 (S5) included twenty-two accessions from late 1980s to early 1990s CIMMYT accessions, with high yield potential.

Subpopulation	Fixation Index (*Fst*)
S1 (ITALY)	0.553
S2 (ICARDA dryland - West Asia)	0.742
S3 (ICARDA temperate)	0.269
S4 (CIMMYT '70)	0.604
S5 (CIMMYT '80)	0.739

Table A2.3. List of GWAS-QTLs significantly associated with maximum quantum efficiency of PSII (F_q'/F_m'); efficiency of reoxidation of the primary quinone electron acceptor at 0.65 ms (F_{r1}'/F_q') and 120 ms (F_{r2}'/F_q') under control condition (NS).

Trait	Treat.	QTL ID	Peak marker	Chr	Marker position (cM) [1]	Flanking Markers	Confidence interval (cM) [2]	Allele [3]	Allele frequency	Allele effect	-log10(P) [4]	R^2 (%)
F_q'/F_m'	NS	*QFq'/Fm'_NS.ubo-1A.1*	IWB9176	1A	146.2	IWB45411-wPt-6853	143.7-167.4	**A**/G	28/154	-0.006	3.9	8.4
		QFq'/Fm'_NS.ubo- 4B.1	IWA1768	4B	7.4	IWB12274-IWB72973	3.9-20.8	**C**/T	27/147	0.005	3.2	6.7
		QFq'/Fm'_NS.ubo- 5B.1	IWB3651	5B	2.0	wPt-1302-IWB10074	0.1-6.5	**C**/T	148/29	0.004	3.9	8.7
		QFq'/Fm'_NS.ubo- 6B.1	IWA1851	6B	33.6	wPt-1830-wPt-7540	31.7-41.3	**A**/G	140/38	0.004	4.1	8.6
		QFq'/Fm'_NS.ubo- 6B.2	IWA5504	6B	73.8	IWB11021-IWB59862	69.3-81.8	**C**/T	133/45	0.005	3.6	7.5
		QFq'/Fm'_NS.ubo- 6B.3	IWB26622	6B	91.8	IWB47030-IWA723	87.5-95.1	**A**/G	153/27	0.005	3.8	7.7
		QFq'/Fm'_NS.ubo- 7A.1	IWB9105	7A	113.2	IWB10205-IWB71999	111-113.6	**A**/G	99/75	-0.015	3.0	6.4
F_{r1}'/F_q'	NS	*QFr1'/Fq'_NS.ubo- 1A.1*	IWA3419	1A	80.9	IWB35039-IWB38369	75.1-85.1	**A**/G	13/161	-0.015	3.1	6.2
		QFr1'/Fq'_NS.ubo- 7A.1	IWB72952	7A	89.8	IWB53918-IWB11003	89.2-102.3	**A**/G	108/58	-0.013	3.1	6.6
F_{r2}'/F_q'	NS	*QFr2'/Fq'_NS.ubo- 1A.1*	IWA3419	1A	80.9	IWB35039-IWB38369	75.1-85.1	**A**/G	13/161	-0.027	3.1	6.2
		QFr2'/Fq'_NS.ubo- 2B.1	IWB9088	2B	170.9	IWB27775-IWB5439	148.6-172.3	**C**/T	29/146	0.019	3.2	6.3
		QFr2'/Fq'_NS.ubo- 6B.1	IWB36146	6B	77.5	IWB6960-IWB33737	76.5-85.9	**A**/G	97/70	0.022	3.3	6.9
		QFr2'/Fq'_NS.ubo-7A.1	IWB72165	7A	100.6	IWB4104-IWB11003	89.6-102.3	**G**/T	50/114	0.025	3.8	8.3

[1] marker position of the peak marker based on the tetraploid wheat consensus map (Maccaferri et al., 2015a). [2] the confidence interval was chosen according to SNP markers with p-value < 0.001. [3] the allele effect is referred to the allele highlighted in bold. [4] -log 10 (P) refers to p-value < 0.001.

Table A2.4. List of GWAS-QTLs significantly associated with maximum quantum efficiency of PSII (F_q'/F_m') at 5, 7 days and recovery; efficiency of reoxidation of the primary quinone electron acceptor at 0.65 ms (F_{r1}'/F_q') and 120 ms (F_{r2}'/F_q') at 5, 7 days and recovery; percentage of plants alive and fully recovered after heat stress (Rec_survival); percentage of green leaf area in the plants after heat stress (Rec_greenness); constitutive cell membrane stability (CMS_Const); acquired cell membrane stability (CMS_Acqui); constitutive-acquired cell membrane stability (CMS_Const_Acqui) under heat stress condition (HS).

Trait	Treat.	QTL ID	Peak marker	Chr	Marker position (cM) [1]	Flanking Markers	Confidence interval (cM) [2]	Alleles [3]	Allele Frequency	Effect	-log10(P) [4]	R^2 (%)
Fq'/Fm'	5 days	*QFq'/Fm'_HS.ubo-1A.1*	IWB66889	1A	31.9	wPt-3698 - IWB43982	28.3 - 38.0	**C**/T	36/144	-0.010	3.00	5.6
		QFq'/Fm'_HS.ubo-3A.1	IWB20567	3A	110.2	IWB72993 - IWB36101	100.2 - 112.3	**A**/G	118/52	0.009	3.00	6.1
F_q'/F_m'	7 days	*QFq'/Fm'_HS.ubo-1A.2*	IWB2767	1A	145.0	wPt-0769 - IWB34872	132.1 - 147.6	**C**/T	17/163	-0.002	3.20	7.0
		QFq'/Fm'_HS.ubo-3A.2	IWB67124	3A	122.3	IWB10607 - IWB71615	114.9 - 122.7	**A**/G	37/145	-0.015	3.10	6.5
		QFq'/Fm'_HS.ubo-3B.1	IWB72057	3B	79.1	IWB11716 - IWB70414	75.6 - 87	**C**/T	108/74	-0.008	3.00	6.2
		QFq'/Fm'_HS.ubo-6B.1	IWB57839	6B	37.8	wPt-0554 - wPt-2479	33.6 - 43.2	**C**/T	49/134	-0.026	3.90	8.4
		QFq'/Fm'_HS.ubo-6B.2	IWB55082	6B	66.4	IWB65137 - IWB57964	64.1 - 67.8	**C**/T	112/66	0.021	3.10	6.5
		QFq'/Fm'_HS.ubo-7A.1	IWB9105	7A	113.2	IWB10205 - IWB71999	111 - 113.6	**A**/G	99/75	-0.013	3.00	6.4
		QFq'/Fm'_HS.ubo-7B.1	IWB30547	7B	97.4	IWB63652 - IWB22830	91.1 - 98.0	**A**/G	16/147	-0.027	3.00	6.6
F_q'/F_m'	Recovery	*QFq'/Fm'_HS.ubo-1A.3*	IWB9176	1A	146.2	wPt-0769 - IWB34872	132.1 - 147.6	**C**/T	22/154	-0.002	3.00	5.6
		QFq'/Fm'_HS.ubo-3B.2	IWB72057	3B	79.1	IWB11716 - IWB70414	75.6 - 87	**C**/T	108/74	-0.008	3.29	7.2
		QFq'/Fm'_HS.ubo-4A.1	wPt-8443	4A	91.6	IWA7058 - IWB72783	88.5 - 94.3	**A**/T	161/18	-0.012	3.06	6.4
		QFq'/Fm'_HS.ubo-6A.1	IWB5563	6A	0.1	IWB21876 - IWB66600	0.1 - 12.8	**C**/T	24/156	0.012	3.41	7.4
		QFq'/Fm'_HS.ubo-7A.2	IWB9105	7A	113.2	IWB10205 - IWB71999	111 - 113.6	**A**/G	99/75	-0.015	3.00	6.6
		QFq'/Fm'_HS.ubo-7A.3	IWB12402	7A	137.5	IWA2058 - IWB73857	135.1 - 138.7	**A**/G	29/150	0.022	3.1	6.7
		QFq'/Fm'_HS.ubo-7B.2	IWB6712	7B	32.4	IWB73049 - IWB35358	31.7 - 43.6	**A**/G	145/33	0.009	3.27	6.6
F_{r1}'/F_q'	5 days	*QFr1'/Fq'_HS.ubo-7A.1*	IWB72739	7A	102.4	IWB38504 - IWB8555	96.2 - 106.4	**C**/T	24/147	0.011	3.25	7.1
		QFr1'/Fq'_HS.ubo-7A.1	IWB1525	7B	151.6	IWB73751 - IWB59225	146.2 - 158.7	**C**/T	65/101	-0.011	3.80	9.4
F_{r1}'/F_q'	7 days	*QFr1'/Fq'_HS.ubo-7A.2*	IWB12099	7A	107.6	IWB8555 - IWB71999	106.4 - 113.6	**A**/G	8/165	-0.013	3.00	5.5
F_{r1}'/F_q'	Recovery	*QFr1'/Fq'_HS.ubo-1A.1*	IWB444	1A	97.3	IWA3859 - IWB31771	94.9 - 99.9	**C**/T	29/139	-0.024	3.01	5.9
		QFr1'/Fq'_HS.ubo-7B.2	IWB30547	7B	97.4	IWB63652 - IWB22830	91.1 - 98.0	**A**/G	15/143	-0.016	3.00	6.2
F_{r2}'/F_q'	5 days	*QFr2'/Fq'_HS.ubo-3B.1*	IWB72456	3B	79.1	IWB73440 - IWB8047	75.2 - 87.1	**C**/T	97/62	0.022	3.55	8.6

		QFr2'/Fq'_HS.ubo-7A.1	IWB72567	7A	102.3	IWB38504 - IWB8555	96.2 - 106.4	**C**/T	22/146	0.030	4.10	9.5
F_{r2}'/F_q'	7 days	*QFr2'/Fq'_HS.ubo-7A.2*	IWB53562	7A	142.8	IWA2009 - IWB56095	142.6 - 147.4	**A**/G	120/44	-0.017	3.40	7.8
F_{r2}'/F_q'	Recovery	*QFr2'/Fq'_HS.ubo-1A.1*	IWB444	1A	97.3	IWA3859 - IWB31771	94.9 - 99.9	**C**/T	29/139	-0.023	3.01	5.8
		QFr2'/Fq'_HS.ubo-1B.1	IWB5678	1B	150.9	IWB18553 - IWB34487	149.7 - 155.3	**C**/T	64/107	0.017	3.00	6.6
Rec_survival	HS	*QRecA.ubo- 2A.1*	IWB7065	2A	186.2	IWB71948 - IWB9798	186.1 - 189.8	**G**/T	38/129	3.27	3.01	6.0
		QRecA.ubo- 2B.1	IWB67250	2B	146.8	IWA7996 - wPt-5242	144.8 - 148.6	**C**/T	69/96	2.72	3.56	4.6
		QRecA.ubo-5A.1	IWA2429	5A	113.3	IWB360 - IWB70054	106.6 - 115.8	**C**/T	67/100	-3.25	3.35	6.3
		QRecA.ubo-5A.2	IWB28952	5A	133.7	IWB71984 - IWB72737	127.9 - 133.7	**G**/T	65/104	3.27	3.90	6.2
		QRecA.ubo-5A.3	IWA1829	5A	142.5	IWB20688 - IWB36340	137.2 - 142.6	**C**/T	80/92	4.23	5.65	12.0
		QRecA.ubo-6B.1	wPt-3309	6B	36.0	wPt-0554 - wPt-7540	33.6 - 41.3	**A**/T	124/46	3.67	3.83	7.9
		QRecA.ubo-6B.2	IWA3947	6B	152.2	IWB71379 - wPt-9589	147.7 - 153.8	**A**/G	36/135	-3.27	3.14	6.0
		QRecA.ubo-7A.1	IWB51612	7A	112.6	IWB10205 -IWB71893	111.0 - 114.0	**C**/T	103/63	-2.24	4.67	11.4
Rec_greenness	HS	*QRecG.ubo-2A.1*	IWB7065	2A	186.2	IWB71948-IWB9798	186.1-189.8	**G**/T	38/129	2.35	3.82	8.1
		QRecG.ubo.2B	IWB67250	2B	146.8	IWA7996-wPt-5242	144.8-148.6	**C**/T	69/96	1.89	3.60	5.8
		QRecG.ubo.3B	IWB35514	3B	209.1	IWB26651-wPt-6961	201.5-211.1	**A**/C	96/74	1.31	3.76	3.8
		QRecG.ubo.5A.1	IWB28952	5A	133.7	IWB71984-IWB72737	127.9-133.7	**G**/T	65/104	2.20	4.53	9.8
		QRecG.ubo.5A.2	IWB73408	5A	141.0	IWB20688-IWB36340	137.2-142.6	**A**/G	79/91	-2.60	5.72	12.4
		QRecG.ubo.5B	IWB68150	5B	6.5	IWA868-IWB30458	2.7-7.7	**A**/G	84/87	-2.06	3.22	6.3
		QRecG.ubo.7A	IWB66046	7A	113.3	IWB10205-IWB71893	111.0-114.0	**G**/T	103/66	-1.82	5.43	13.4
CMS_Const	HS	*QCMS_Const.ubo-1A.1*	IWA3419	1A	80.9	IWB56354-IWB3489	80.9-84.7	**A**/G	13/152	-3.13	3.16	7.2
		QCMS_Const.ubo-2A.1	IWB67664	2A	117.6	IWB32024-IWB46634	114.5-121.0	**A**/G	133/26	-3.01	3.94	8.4
		QCMS_Const.ubo-3A.1	IWB41338	3A	135.1	wPt-3816-IWB39922	130.2-135.8	**G**/T	12/151	-3.22	3.24	6.8
		QCMS_Const.ubo-5B.1	IWA1585	5B	53.8	IWB71672-IWB24135	50.2-57.8	**A**/G	21/131	-3.16	3.21	8.0
		QCMS_Const.ubo-6A.1	IWB71083	6A	46.9	IWB66507-IWA5257	45.2-51.2	**A**/G	33/129	-2.24	3.62	7.2
		QCMS_Const.ubo-6B.1	IWB71650	6B	129.1	IWB8068-IWB8282	125.9-129.1	**A**/G	74/86	-1.94	3.27	7.8
CMS_Acqui	HS	*QCMS_Acqui.ubo-4A.1*	IWB46973	4A	42.7	IWA4321-IWA5236	37.8-46.5	**A**/G	115/47	49.69	4.48	12.3
		QCMS_Acqui.ubo-6A.1	IWB71426	6A	60.0	IWB73438-IWB73434	56.8-63.1	**A**/G	78/84	-44.10	3.58	7.7
CMS_Const_Acqui	HS	*QCMS_Const_Acqui.ubo-5A.1*	IWB60157	5A	106.6	IWB65371-IWA3827	102.2-110.5	**G**/T	144/16	-75.50	3.10	7.1

[1] marker position of the peak marker based on the tetraploid wheat consensus map (Maccaferri et al., 2015a). [2] tthe confidence interval was chosen according to SNP markers with p-value < 0.001. [3] the allele effect is referred to the allele highlighted in bold. [4] -log $_{10}$ (P)) refers to p-value < 0.001.

Table A2.5. List of GWAS-QTL clusters identified at the UNIBO-Durum Panel and significantly associated with quantum efficiency of PSII (F_q'/F_m'), efficiency of reoxidation of the primary quinone electron acceptor at 0.65 ms (F_{r1}'/F_v') and 120 ms (F_{r2}'/F_v'), percentage of plants alive and fully recovered after heat stress (Rec_survival), percentage of green leaf area in the plants after heat stress (Rec_greenness), constitutive cell membrane stability (CMS_Const), acquired cell membrane stability (CMS_Acqui), and constitutive-acquired cell membrane stability (CMS_Const_Acqui).

QTL cluster	Peak marker	Chr	Marker position (*cM*) [1]	Allele [2]	Allele frequency	Confidence interval (*cM*)	Trait [3]	QTLs from literature [4]
HS_QTL_cluster_1A.1	IWA3419	1A	80.9	**A**/G	13/161	77.0 - 84.0	*Fr₁'/Fv'*_NS (-), *Fr₁'/Fv'*_HSI_7days (+), *Fr₁'/Fv'*_HSI_Rec (+), *Fr₂'/Fv'*_NS (-), Fr₂'/Fv'_HSI_5days (+), *Fr₂'/Fv'*_HSI_7days (+), *Fr₂'/Fv'*_HSI_Rec (+), CMS_Const (-),	
HS_QTL_cluster_1A.2	IWB444	1A	97.3	**C**/T	29/139	94.2 - 100.4	*Fr₁'/Fv'*_HS_Rec (-), *Fr₁'/Fv'*_HSI_Rec (-), *Fr₂'/Fv'*_HS_Rec (-)	
HS_QTL_cluster_1A.3	IWB9176	1A	146.2	**A**/G	28/154	143.1 - 149.3	*Fq'/Fm'*_NS (-), *Fq'/Fm'*_HS_7days (-)	TKW[c], GNO[c], GY[c]
HS_QTL_cluster_2B.1	IWB67250	2B	146.8	**C**/T	69/96	143.7 - 149.9	Rec_survival (+), Rec_greenness (+)	
HS_QTL_cluster_2B.2	IWB9088	2B	170.9	**C**/T	31/152	166.3 - 174.3	*Fr₁'/Fv'*_HSI_7days (-), *Fr₁'/Fv'*_HSI_Rec (-), *Fr₂'/Fv'*_NS (+), *Fr₂'/Fv'*_HSI_7days (-), *Fr₂'/Fv'*_HSI_Rec (-)	NDVI[f]
HS_QTL_cluster_3B	IWB72057	3B	79.1	**C**/T	108/74	76.0 - 82.2	*Fq'/Fm'*_HS_7days (-), *Fq'/Fm'*_HSI_Rec (-), *Fr₂'/Fv'*_HS_5days (+)	GNO[c,h], TKW[c,d], GY[h]
HS_QTL_cluster_5A	IWB28952	5A	133.7	**G**/T	65/104	130.6 - 136.8	Rec_survival (+), Rec_greenness (+)	GNO[a,c,e], TKW[a], SPM[c,d]
HS_QTL_cluster_5B	IWB3651	5B	2.0	**C**/T	148/29	0.1 - 6.9	Rec_greenness (-), Fq'/Fm'_NS (+)	
HS_QTL_cluster_6A	IWB67403	6A	62.1	**A**/C	50/126	59.0 - 65.2	*Fr₁'/Fv'*_HSI_7days (+), *Fr₁'/Fv'*_HSI_Rec (+), *Fr₂'/Fv'*_HSI_5days (+), *Fr₂'/Fv'*_HSI_7days (+), *Fr₂'/Fv'*_HSI_Rec (+), CMS_Acqui (-),	TKW[b], GNO[c,e]

HS_QTL_cluster_6B.1	IWA1851	6B	33.6	**A**/G	140/38	30.5 - 36.7	Fq'/Fm'_NS (+), Fq'/Fm'_HSI_7days (+), Rec_survival (+)	
HS_QTL_cluster_6B.2	IWA5504	6B	73.8	**C**/T	133/45	70.5 - 77.8	*Fq'/Fm'*_NS (+), *Fr_2'/Fv'*_NS (-)	GNO[g], GY[g]
HS_QTL_cluster_7A.1	IWB40423	7A	108.3	**C**/T	15/164	100.6 - 108.5	*Fr_1'/Fv'*_HS_5days (+), *Fr_1'/Fv'*_HS_7days (+), *Fr_1'/Fv'*_HSI_Rec(+), *Fr_2'/Fv'*_NS (+), Fr_2'/Fv'_HS_5days (+), *Fr_2'/Fv'*_HSI_Rec (+)	
HS_QTL_cluster_7A.2	IWB9105	7A	113.2	**A**/G	99/75	110.1 - 116.3	*Fq'/Fm*'_NS (-), *Fq'/Fm*'_HS_7days (-), *Fq'/Fm*'_HS_Rec (-), *Fq'/Fm*'_HSI_7days (-), *Fq'/Fm*'_HSI_Rec (-), Rec_survival (-), Rec_greenness (-)	
HS_QTL_cluster_7A.3	IWB12402	7A	137.5	**A**/G	29/150	134.0 - 140.6	*Fq'/Fm'*_HS_Rec (+), *Fq'/Fm'*_HSI_Rec (+)	GNO[e], GC[i]
HS_QTL_cluster_7B	IWB30547	7B	97.4	**A**/G	16/147	94.3 - 100.5	*Fq'/Fm'*_HS_7days (-), *Fq'/Fm'*_HSI_7days (-), *Fr_1'/Fv'*_HS_Rec (-)	TKW[c], GY[c], NDVI[d]

[1] marker position of the peak marker based on the tetraploid wheat consensus map (Maccaferri *et al*., 2015a). [2] the allele effect is referred to the allele highlighted in bold. [3] Control experiment (NS); heat stress experiment (HS); reaction norm index (Δ); five days of heat stress at 38°C (5 days); seven days of heat stress at 38°C (7 days); recovery after seven days of 38°C of heat stress + 3 days of recovery at 24°C (Rec); (-) and (+) the signal in parenthesis indicated the allele effect on the trait. [4] Thousand kernel weight (TKW); grain number (GNO); grain yield (GY); normalized difference vegetation index (NDVI); spike number per linear meter (SPM); glume color (GC). [4] [a] Quarrie *et al*., 2005, [b] Wang *et al*., 2009, [c] Maccaferri *et al*., 2011, [d] Graziani *et al*., 2014, [e] Shi *et al*., 2017, [f] Condorelli *et a*l., 2018, [g] Lozada *et al*., 2018, [h] Sukumaran *et al*., 2018, [i] Wang *et al*., 2019.

Table A2.6. List of GWAS-QTLs for reaction norm index (Δ) significantly associated with maximum quantum efficiency of PSII (F_q'/F_m'); efficiency of reoxidation of the primary quinone electron acceptor at 0.65 ms (F_{r1}'/F_q') and 120 ms (F_{r2}'/F_q').

Trait	Treat.	QTL ID	Peak marker	Chr	Marker position (cM) [1]	Flanking Markers	Confidence interval (cM)[2]	Alleles [3]	Allele frequency	Effect	-log10(P) [4]	R^2 (%)
F_q'/F_m'	5 days	Q*Fq'/Fm'_HSI.ubo*-2B.1	IWB48376	2B	108.9	IWA2253-IWB26325	108.2-110.6	**A**/G	15/165	-4.4	4.5	10.5
		Q*Fq'/Fm'_HSI.ubo*-6A.1	IWB8323	6A	126.5	IWB71409-IWB68609	124.6-127.1	**A**/G	50/124	-2.3	3.4	7.9
F_q'/F_m'	7 days	*QFq'/Fm'_Δ.ubo-6B.1*	IWA1851	6B	33.6	wPt-8153-IWB36095	29.6-37.4	**A**/G	140/38	2.7	3.1	6.2
		QFq'/Fm'_Δ.ubo-6B.2	IWB25986	6B	55.5	wPt-7540-IWB69518	41.3-55.8	**A**/G	166/16	4.6	3.6	7.5
		QFq'/Fm'_Δ.ubo-7A.1	IWB5607	7A	113.1	IWB10205-IWB73246	111-113.9	**A**/G	86/88	-2.4	3.2	6.1
		QFq'/Fm'_Δ.ubo-7B.1	IWB30547	7B	97.4	IWB73341-IWB8766	92.9-97.4	**A**/G	16/147	-4.7	3.0	6.7
F_q'/F_m'	Recovery	*QFq'/Fm'_Δ.ubo-3B.1*	IWB72057	3B	79.1	IWB25473-IWB73053	67.2-79.6	**C**/T	108/74	-2.1	4.0	9.2
		QFq'/Fm'_Δ.ubo-7A.2	IWB51612	7A	112.6	IWB10205-IWB71893	111.0-114.0	**C**/T	109/65	-2.2	4.7	11.4
		QFq'/Fm'_Δ.ubo-7A.3	IWB12402	7A	137.5	IWA2058-IWB73857	135.1-138.7	**A**/G	29/150	2.8	3.4	7.3
F_{r1}'/F_q'	5 days	*QFr1'/Fq'_Δ.ubo-2B.1*	IWB50352	2B	136.6	IWB31368-wPt-8693	135.6-137.9	**C**/T	25/155	9.9	3.0	6.2
		QFr1'/Fq'_Δ.ubo-7A.1	IWB8251	7A	78.0	IWA3760-IWB48426	70.7-79.9	**C**/T	127/44	-9.5	4.0	9.3
F_{r1}'/Fq'	7 days	*QFr1'/Fq'_Δ.ubo-1A.1*	IWA3419	1A	80.9	IWB11628-IWB65398	76.9-84.7	**A**/G	13/169	11.2	3.4	6.9
		QFr1'/Fq'_Δ.ubo-2B.2	IWB9088	2B	170.9	IWB59226-IWB30420	167.1-174.3	**C**/T	31/152	-6.4	3.0	6.1
		QFr1'/Fq'_Δ.ubo-6A.1	IWB73434	6A	64.9	IWB69886-IWB9318	62-67.3	**A**/G	16/161	9.6	3.1	6.1
F_{r1}'/F_q'	Recovery	*QFr1'/Fq'_Δ.ubo-1A.2*	IWA3419	1A	80.9	IWA6708-IWB3489	77.7-84.5	**A**/G	13/169	9.4	3.0	6.9
		QFr1'/Fq'_Δ.ubo-1A.3	IWB72588	1A	97.3	IWA7570-IWB6984	95.5-98.2	**C**/T	31/146	-1.1	3.7	8.4
		QFr1'/Fq'_Δ.ubo-1B.1	IWB10690	1B	150.9	IWA4022-IWB965	150.9-152.5	**C**/T	69/107	7.3	3.3	7.5
		QFr1'/Fq'_Δ.ubo-2B.3	IWB9088	2B	170.9	IWB59226-IWB30420	167.1-174.3	**C**/T	31/152	-6.0	3.0	6.7
		QFr1'/Fq'_Δ.ubo-6A.2	IWB67403	6A	62.1	IWB45770-IWA5778	60-66.9	**A**/C	50/126	7.0	3.4	6.7
		QFr1'/Fq'_Δ.ubo-7A.2	IWB40423	7A	108.3	IWB2862-IWB31570	107-112.2	**C**/T	15/164	14.6	3.1	6.7
		QFr1'/Fq'_Δ.ubo-7B.1	IWB40237	7B	129.9	IWA1345-IWB44493	127-130.7	**A**/G	40/132	7.2	3.1	6.9
F_{r2}'/F_q'	5 days	*QFr2'/Fq'_Δ.ubo-1A.1*	IWB67072	1A	77.1	IWB70352-IWB65398	76.2-84.7	**A**/G	23/155	16.7	3.5	6.9
		QFr2'/Fq'_Δ.ubo-6A.1	IWB67403	6A	62.1	IWB45770-IWA5778	60-66.9	**A**/C	50/126	14.2	3.4	6.7
		QFr2'/Fq'_Δ.ubo-7B.1	IWB72574	7B	0.1	IWB25854-IWB55570	0.1-5.2	**C**/T	56/124	-1.2	3.0	5.7

F_{r2}'/F_q'	7 days	*QFr2'/Fq'_Δ.ubo-1A.2*	IWA4283	1A	77.1	IWB35039-IWB38369	75.1-85.1	**C**/T	171/10	-2.3	3.4	6.5
		QFr2'/Fq'_Δ.ubo-2B.1	IWB9088	2B	170.9	IWB1091-IWB30420	166.3-174.3	**C**/T	31/152	-1.4	3.2	6.1
		QFr2'/Fq'_Δ.ubo-6A.2	IWB67403	6A	62.1	IWB45770-IWA5778	60-66.9	**A**/C	50/126	13.5	3.2	6.4
F_{r2}'/F_q'	Recovery	*QFr2'/Fq'_Δ.ubo-1A.3*	IWA5174	1A	77.5	IWB70352-IWB38369	76.2-85.1	**A**/C	169/11	-2.2	3.5	7.2
		QFr2'/Fq'_Δ.ubo-2B.2	IWB9088	2B	170.9	IWB54597-IWB30420	170-174.3	**C**/T	31/152	-1.5	3.5	7.1
		QFr2'/Fq'_Δ.ubo-6A.3	IWB67403	6A	62.1	IWB45770-IWA5778	60-66.9	**A**/C	50/126	13.8	3.3	6.8
		QFr2'/Fq'_Δ.ubo-7A.1	IWB40423	7A	108.3	IWB2862-IWB31570	107-112.2	**C**/T	15/164	3.1	4.2	9.3

[1] marker position of the peak marker based on the tetraploid wheat consensus map (Maccaferri *et al*., 2015a). [2] tthe confidence interval was chosen according to SNP markers with p-value < 0.001. [3] the allele effect is referred to the allele highlighted in bold. [4] $-\log_{10}$ (P) refers to p-value < 0.001.

Figure A2.1. Boxplots of the best linear unbiased estimator (BLUE) based on five subgroups separeted by population structure for the UNIBO-Durum Panel measured under four different experimental conditions. (i) control, (ii) 5 days of heat stress, (iii) 7 days of heat stress and (iv) 7 days of heat stress + 3 days of recovery. Maximum quantum efficiency of PSII (F_q'/F_m'), efficiency of reoxidation of the primary quinone electron acceptor at 0.65 ms (F_{r1}'/F_q') and 120 ms (F_{r2}'/F_q'), percentage of plants alive and fully recovered after heat stress (Rec_survival); percentage of green leaf area after heat stress (Rec_greenness); constitutive cell membrane stability (CMS_Const); acquired cell membrane stability (CMS_Acqui); constitutive-acquired cell membrane stability (CMS_Const_Acqui).

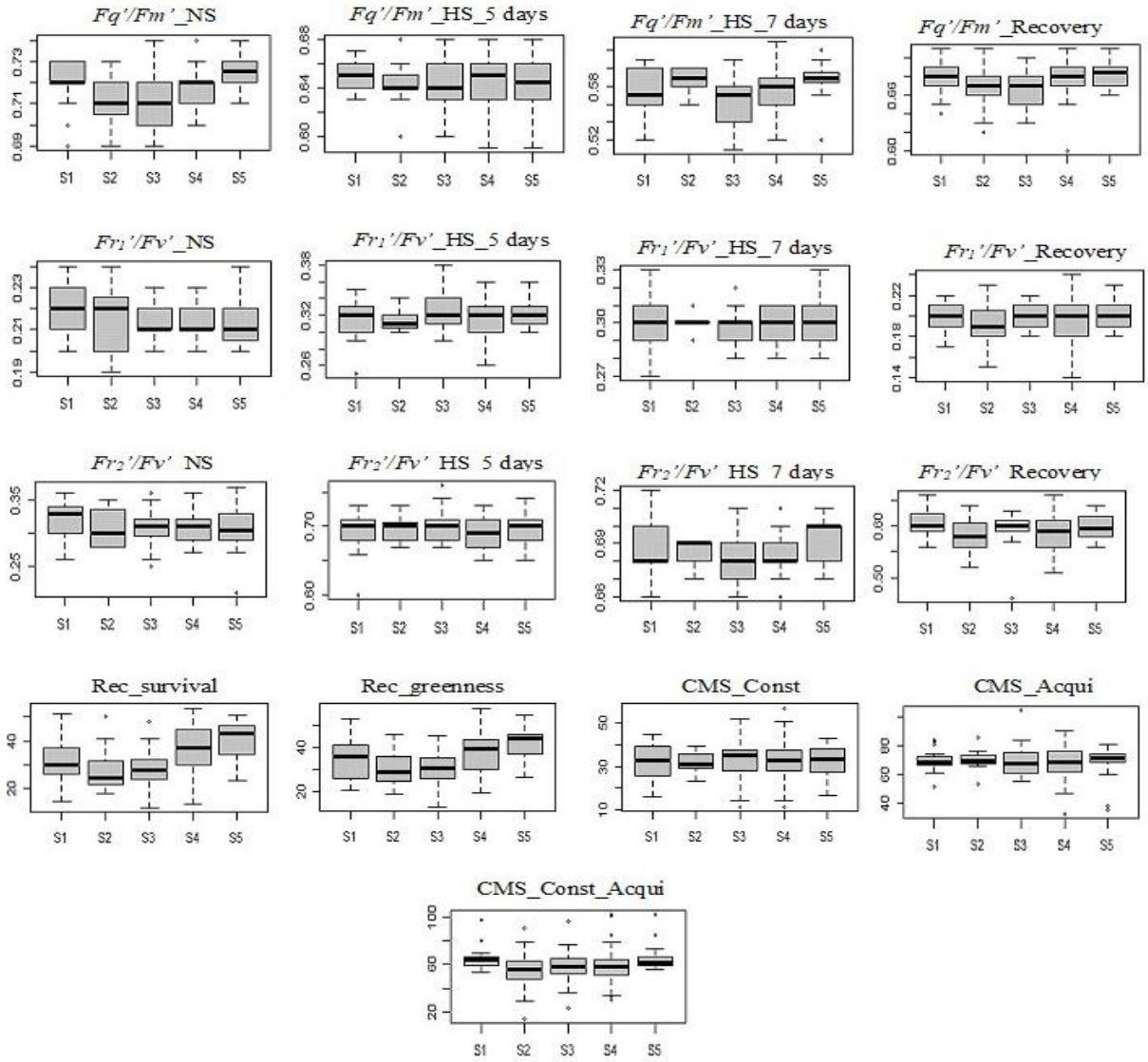

Figure A2.2. Boxplots for reaction norm index of the best linear unbiased estimator (BLUE) based on five subgroups separated by population structure for the UNIBO-Durum Panel measured under four different experimental conditions (i) control, (ii) five days of heat stress, (iii) seven days of heat stress and (iv) seven days of heat stress + three days of recovery. Maximum quantum efficiency of PSII (F_q'/F_m'), efficiency of reoxidation of the primary quinone electron acceptor at 0.65 ms (F_{r1}'/F_q') and 120 ms (F_{r2}'/F_q').

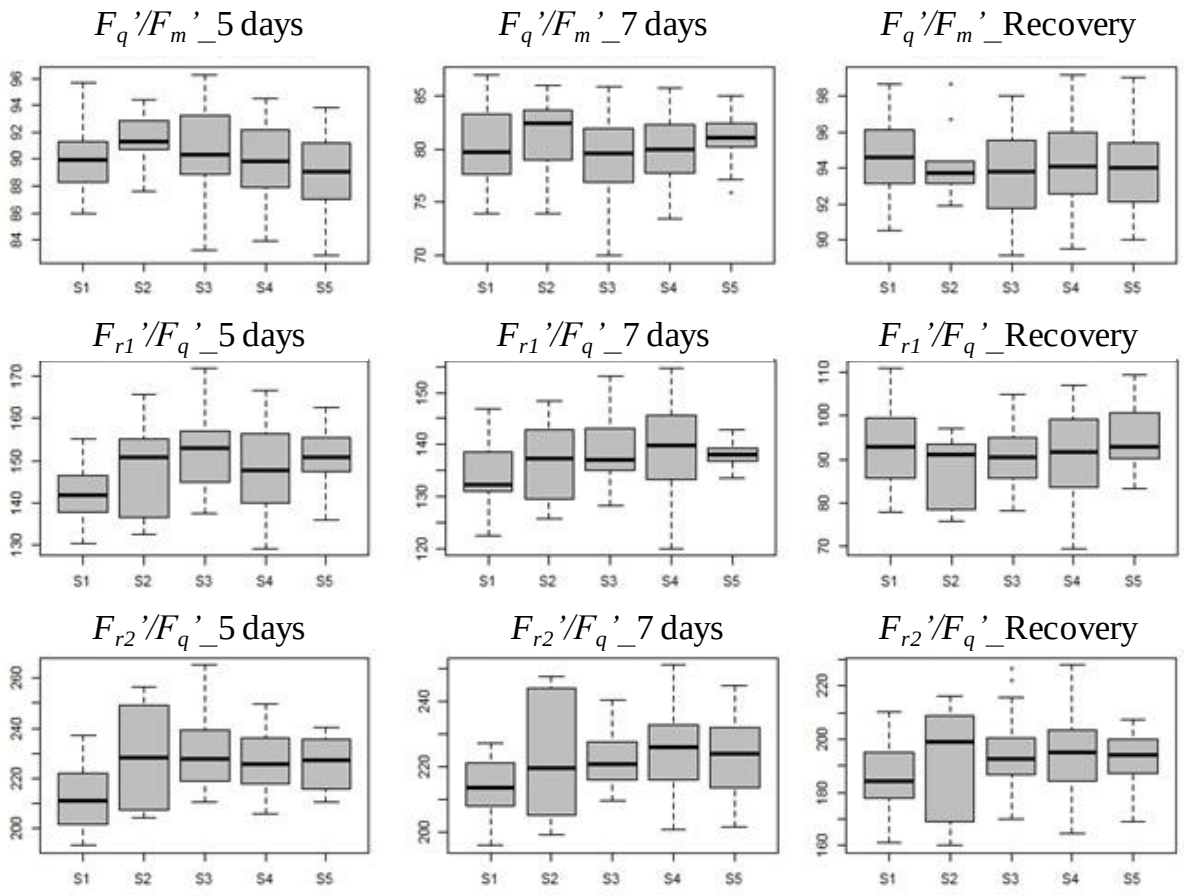

Table A3.1. List of GWAS-QTLs significantly associated with the traits days to heading (HD), days to maturity (DTM), plant height (PH), grain yield (GY), thousand kernel weight (TKW), test weight (TWT), number of spikes per linear meter (SPM), number of spikelets per spike (SKT), grain number per spike (GNO), grain weight per spike (SGW), grain length (GLE), and grain width (GWI) under control condition in the crop season of 2019.

Trait	Treat. [1]	QTL ID	Peak marker	Chr	Marker position (cM) [2]	Flanking Markers	Confidence Interval (cM) [3]	Alleles [4]	Effect	Allele Frequency	-LOG(p-value) [5]	R^2 (%)
HD	NS	*QHD_NS19.ubo-1B*	IWB69550	1B	50.2	IWA107-IWA1109	47.1-53.9	**A**/C	-5.33	170/12	3.5	3.7
HD	NS	*QHD_NS19.ubo-2A*	IWB67306	2A	46.6	IWB1280-IWB146	36.8-50.5	**C**/T	-7.25	99/81	3.1	3.2
HD	NS	*QHD_NS19.ubo-2B*	wPt-8404	2B	31.4	IWB8893-IWB73192	27.7-37.2	**A**/T	-3.19	47/136	3.3	3.4
HD	NS	*QHD_NS19.ubo-4A*	IWB71863	4A	36.1	IWA1137-IWB32882	25.8-41.3	**C**/T	-4.60	169/14	3.1	3.1
HD	NS	*QHD_NS19.ubo-4B*	IWB52318	4B	53.0	IWB35114-IWB72279	48.3-53.0	**A**/G	4.05	22/161	3.4	3.4
HD	NS	*QHD_NS19.ubo-5A*	IWB10692	5A	150.3	IWB71757-IWB72381	147.1-155.0	**C**/T	-8.16	164/16	4.1	4.4
DTM	NS	*QDTM_NS19.ubo-2B*	wPt-8404	2B	31.4	IWB8893-IWB73192	27.7-37.2	**A**/T	-2.16	47/136	3.0	3.0
DTM	NS	*QDTM_NS19.ubo-3B*	IWB65493	3B	158.5	IWB9158-IWA1094	152.6-163.2	**C**/T	-2.80	50/132	3.5	3.6
DTM	NS	*QDTM_NS19.ubo-4A.1*	IWB71865	4A	36.2	IWA1137-IWB32882	25.8-41.3	**C**/T	3.53	14/169	3.5	3.5
DTM	NS	*QDTM_NS19.ubo-4A.2*	wPt-8443	4A	91.6	IWA7058-IWA4425	88.5-97.7	**A**/T	-3.22	164/19	3.9	4.0
DTM	NS	*QDTM_NS19.ubo-5A*	IWB29625	5A	43.8	IWB66553-IWB47433	40.6-47.3	**A**/C	-4.16	12/171	3.4	3.5
DTM	NS	*QDTM_NS19.ubo-5B*	IWB41039	5B	48.9	IWB7509-IWA6526	45.0-52.2	**C**/T	-7.19	11/172	5.1	5.5
DTM	NS	*QDTM_NS19.ubo-6A*	IWB56339	6A	72.4	IWA6724-IWB9445	68.3-83.7	**A**/G	-3.27	163/18	3.2	3.2
DTM	NS	*QDTM_NS19.ubo-7B*	IWB60292	7B	120.4	IWB74053-IWA1345	114.9-127.0	**C**/T	3.43	16/167	3.1	3.1
PH	NS	*QPH_NS19.ubo-1A*	IWB57868	1A	1.7	wPt-4676-wPt-0196	0.1-5.2	**A**/G	5.48	67/116	4.4	4.6
PH	NS	*QPH_NS19.ubo-3B*	IWB1757	3B	32.0	IWB39127-wPt-1349	27.1-36.6	**A**/C	-6.30	164/19	3.1	3.0
PH	NS	*QPH_NS19.ubo-4B*	IWA103	4B	27.6	IWB72527-IWB12150	21.3-30.8	**C**/T	14.68	18/164	4.9	5.2
PH	NS	*QPH_NS19.ubo-5A*	IWB10692	5A	150.3	IWB71757-IWB72381	147.1-155.0	**C**/T	-12.42	164/16	3.9	4.0
PH	NS	*QPH_NS19.ubo-6A*	IWB113	6A	125.9	IWB16528-IWA1866	122.8-129.4	**A**/C	-6.23	32/150	3.4	3.3
PH	NS	*QPH_NS19.ubo-6B*	IWB38810	6B	91.5	IWB73860-IWB4259	87.8-94.8	**C**/T	4.90	142/41	3.3	3.2
GY	NS	*QGY_NS19.ubo-3B*	IWB29048	3B	44.6	IWB48996-IWA3725	41.3-48.9	**A**/G	-0.56	47/133	3.5	6.8
TKW	NS	*QTKW_NS19.ubo-2A.1*	IWB49366	2A	100.1	IWB43447-IWB66497	96.9-106.5	**A**/G	4.45	149/34	3.5	5.7
TKW	NS	*QTKW_NS19.ubo-2A.2*	IWB7897	2A	109.0	IWB69369-IWB62891	102.0-112.4	**G**/T	-4.31	17/166	3.2	5.1

TKW	NS	*QTKW_NS19.ubo-2A.3*	IWB8076	2A	114.7	IWB40575-IWB50642	110.1-118.4	**C**/T	-4.95	13/170	3.3	5.3
TKW	NS	*QTKW_NS19.ubo-2A.4*	IWB72263	2A	197.6	IWB12196-IWB72975	193.4-201.1	**A**/G	-4.41	39/138	4.8	8.5
TKW	NS	*QTKW_NS19.ubo-3A*	IWB72223	3A	82.6	IWA1019-IWB72035	79.5-86.9	**A**/G	3.21	113/69	3.4	5.6
TKW	NS	*QTKW_NS19.ubo-6A*	IWA8438	6A	120.5	IWB70454-IWB45558	117.1-123.6	**A**/G	-3.51	43/138	3.5	5.6
TKW	NS	*QTKW_NS19.ubo-6B*	IWB46958	6B	36.0	IWB7468-wPt-4742	32.6-40.0	**A**/G	2.83	105/78	3.1	4.8
TKW	NS	*QTKW_NS19.ubo-7A.1*	wPt-7767	7A	0.1	IWB11946-wPt-0002	0.1-3.8	**A**/T	4.51	21/162	3.5	5.7
TKW	NS	*QTKW_NS19.ubo-7A.2*	IWB73135	7A	7.2	wPt-4625-IWB62296	3.8-10.6	**C**/T	-4.41	161/22	3.5	5.7
TKW	NS	*QTKW_NS19.ubo-7B*	wPt-4843	7B	0.1	IWB22624-wPt-7975	0.1-3.7	**A**/T	3.46	138/45	3.3	5.4
TWT	NS	*QTWT_NS19.ubo-1A*	IWB59083	1A	115.9	IWB74445-IWB51933	112.4-119.8	**A**/G	1.05	23/160	3.3	5.5
TWT	NS	*QTWT_NS19.ubo-1B.1*	IWB2667	1B	109.0	IWA3341-IWB35712	106.0-113.4	**A**/G	-1.55	11/172	3.6	6.1
TWT	NS	*QTWT_NS19.ubo-1B.2*	IWB11265	1B	162.5	IWB71657-wPt-6142	158.0-165.6	**A**/G	0.75	131/48	3.1	5.1
TWT	NS	*QTWT_NS19.ubo-2A*	IWB65286	2A	117.6	IWB32024-IWB46634	114.5-121.0	**C**/T	-1.19	34/148	3.8	6.5
TWT	NS	*QTWT_NS19.ubo-2B.1*	IWB34613	2B	73.7	IWB56915-IWB39220	70.1-76.8	**A**/G	-2.07	167/15	4.3	7.6
TWT	NS	*QTWT_NS19.ubo-2B.2*	IWA2261	2B	129.8	IWA3973-IWA2318	126.6-133.0	**A**/G	-1.15	138/41	4.5	8.1
TWT	NS	*QTWT_NS19.ubo-3B*	IWB32274	3B	127.5	IWB9408-IWB20294	122.5-131.4	**A**/G	-1.09	21/162	3.6	6.0
TWT	NS	*QTWT_NS19.ubo-4A.1*	IWA4321	4A	37.8	IWA1137-IWB32882	25.8-41.3	**C**/T	-1.41	15/168	3.9	6.7
TWT	NS	*QTWT_NS19.ubo-4A.2*	IWB44783	4A	113.9	IWB28717-IWB48435	110.7-118.3	**A**/G	1.00	161/22	3.1	5.1
TWT	NS	*QTWT_NS19.ubo-4A.3*	IWB53393	4A	171.2	IWB71811-IWB18740	167.6-175.8	**A**/G	-1.22	164/19	3.0	4.9
TWT	NS	*QTWT_NS19.ubo-4B*	IWB72399	4B	55.6	IWB72287-IWB72211	51.8-58.7	**A**/G	-0.71	88/93	3.0	5.0
TWT	NS	*QTWT_NS19.ubo-5A.1*	IWB71078	5A	26.5	IWB72697-IWB14353	19.9-29.8	**C**/T	-0.75	116/67	3.0	5.0
TWT	NS	*QTWT_NS19.ubo-5A.2*	IWA8588	5A	111.0	IWB9509-tPt-0353	106.6-114.15	**G**/T	-1.27	13/170	3.1	5.0
TWT	NS	*QTWT_NS19.ubo-6A.1*	IWB30932	6A	11.2	IWB36803-IWB71874	6.8-14.3	**A**/G	-1.41	169/14	3.8	6.5
TWT	NS	*QTWT_NS19.ubo-6A.2*	IWB62858	6A	66.9	IWB74244-IWA1194	62.8-71.8	**C**/T	1.45	174/9	3.2	5.2
TWT	NS	*QTWT_NS19.ubo-6B.1*	IWB10612	6B	4.6	wPt-0351-IWA6759	2.2-8.0	**A**/G	-1.33	15/168	3.5	5.9
TWT	NS	*QTWT_NS19.ubo-6B.2*	IWB29457	6B	20.4	IWB72988-IWB60219	15.2-23.9	**C**/T	-0.82	69/114	3.8	6.6
TWT	NS	*QTWT_NS19.ubo-7B*	IWB60292	7B	120.4	IWB74053-IWA1345	114.9-127.0	**C**/T	-1.38	16/167	3.6	6.1
SPM	NS	*QSPM_NS19.ubo-3B*	IWB46567	3B	209.6	wPt-0665-wPt-6961	206.1-211.1	**A**/C	10.40	50/131	3.2	6.0
SPM	NS	*QSPM_NS19.ubo-4B.1*	IWA4662	4B	21.7	IWB73227-IWB73001	18.4-26.4	**G**/T	-11.88	42/138	3.5	6.7
SPM	NS	*QSPM_NS19.ubo-4B.2*	IWB73473	4B	77.8	IWB27260-IWA2823	74.7-81.3	**G**/T	-10.77	151/32	3.3	6.4
SPM	NS	*QSPM_NS19.ubo-6A*	IWB39866	6A	127.1	IWB29924-IWB73095	124.0-131.2	**A**/G	9.20	63/117	3.1	5.8
SPM	NS	*QSPM_NS19.ubo-6B*	IWB71917	6B	95.9	IWB72356-IWA670	92.6-100.2	**A**/G	-15.58	170/11	3.5	6.8
SPM	NS	*QSPM_NS19.ubo-7A*	IWB13779	7A	130.0	IWB8935-IWB45289	126.0-134.6	**C**/T	-8.86	61/121	3.0	5.6
SKT	NS	*QSKT_NS19.ubo-2B*	IWB25860	2B	115.5	IWB73809-IWA6559	112.3-118.7	**A**/G	1.60	23/160	3.4	4.7

SKT	NS	*QSKT_NS19.ubo-3B*	IWB34730	3B	126.2	IWB9408-IWB20294	122.5-131.4	**A**/G	1.47	19/164	3.2	4.3
SKT	NS	*QSKT_NS19.ubo-6B*	IWB44252	6B	147.7	IWB10649-IWB46643	140.9-152.2	**A**/G	2.11	19/163	3.8	5.4
GNO	NS	*QGNO_NS19.ubo-2A.1*	IWB23116	2A	9.4	IWB64569-IWB44526	6.0-13.2	**A**/G	4.90	109/74	3.2	6.2
GNO	NS	*QGNO_NS19.ubo-2A.1*	IWB68412	2A	16.7	IWB73487-IWB69599	13.2-20.5	**A**/G	-5.08	73/109	3.5	7.0
GNO	NS	*QGNO_NS19.ubo-2A.2*	IWB49366	2A	100.1	IWB26960-IWB66497	95.0-106.5	**A**/G	-9.10	149/34	4.9	10.3
GNO	NS	*QGNO_NS19.ubo-2A.3*	IWB8665	2A	114.5	IWB7897-IWB3177	109.0-117.7	**C**/T	11.22	14/169	5.8	12.7
GNO	NS	*QGNO_NS19.ubo-2A.4*	IWA4870	2A	197.6	IWB12196-IWB72976	193.4-200.7	**C**/T	-5.72	134/46	3.2	6.7
GNO	NS	*QGNO_NS19.ubo-2B*	IWB33109	2B	76.6	IWB62870-IWA50	73.2-80.6	**C**/T	-6.87	80/100	5.6	12.3
GNO	NS	*QGNO_NS19.ubo-3A*	IWB25665	3A	171.7	IWB8509-wPt-0549	167.4-176.5	**A**/G	7.82	170/13	3.0	5.9
GNO	NS	*QGNO_NS19.ubo-4B*	IWA1861	4B	101.3	IWB29648-IWA2031	98.2-105.5	**C**/T	-5.82	95/88	4.0	8.1
GNO	NS	*QGNO_NS19.ubo-5A*	IWB7817	5A	14.3	IWB9216-IWB72697	10.5-19.9	**A**/G	-6.82	28/154	3.3	6.6
GNO	NS	*QGNO_NS19.ubo-7A.1*	IWB58414	7A	7.0	IWB1110-IWB62296	2.4-10.6	**C**/T	7.76	163/20	3.4	6.7
GNO	NS	*QGNO_NS19.ubo-7A.2*	IWB57104	7A	15.2	IWB9788-IWB73940	11.5-21.9	**C**/T	7.65	165/18	3.1	6.0
SGW	NS	*QSGW_NS19.ubo-1B.1*	IWB9781	1B	93.4	IWB73156-IWB69337	89.1-96.8	**A**/G	0.31	140/42	4.0	8.0
SGW	NS	*QSGW_NS19.ubo-1B.2*	IWB64092	1B	109.0	IWB3634-IWB35712	103.0-113.4	**A**/G	-0.47	11/172	3.2	6.1
SGW	NS	*QSGW_NS19.ubo-2A.1*	IWA1562	2A	7.8	IWB7398-IWB6542	2.3-11.2	**C**/T	-0.33	22/161	3.4	6.4
SGW	NS	*QSGW_NS19.ubo-2A.2*	IWB58322	2A	17.5	IWB66737-IWB35771	13.7-21.9	**A**/G	-0.33	26/157	3.5	6.8
SGW	NS	*QSGW_NS19.ubo-2B.1*	IWB50438	2B	67.2	IWB8126-IWA1114	64.0-71.0	**C**/T	-0.26	113/66	3.3	6.3
SGW	NS	*QSGW_NS19.ubo-2B.2*	IWB33109	2B	76.6	IWB62870-IWA50	73.2-80.6	**C**/T	-0.29	80/100	4.5	9.1
SGW	NS	*QSGW_NS19.ubo-2B.3*	wPt-1140	2B	121.9	IWB69270-IWB32410	114.4-124.4	**A**/T	-0.28	80/102	3.6	6.9
SGW	NS	*QSGW_NS19.ubo-3A.1*	IWB20642	3A	66.3	IWB72751-IWB71028	59.1-72.2	**A**/G	0.32	126/56	3.5	6.7
SGW	NS	*QSGW_NS19.ubo-3A.2*	IWA7970	3A	83.5	IWB9725-IWB72035	79.5-86.9	**G**/T	-0.31	38/143	3.0	5.7
SGW	NS	*QSGW_NS19.ubo-3A.3*	IWB11134	3A	140.5	IWA2518-IWB72058	136.5-147.1	**C**/T	-0.47	12/171	3.5	6.7
SGW	NS	*QSGW_NS19.ubo-3B*	IWB62088	3B	1.3	IWB64431-IWB8755	0.1-4.7	**A**/G	0.24	85/91	3.2	6.3
SGW	NS	*QSGW_NS19.ubo-4B*	IWB71725	4B	4.8	IWB73506-IWB28293	0.3-10.0	**G**/T	0.29	49/130	3.2	6.0
SGW	NS	*QSGW_NS19.ubo-5A.1*	IWB71918	5A	113.2	IWB9509-IWB49311	106.6-116.3	**C**/T	0.25	88/94	3.1	5.9
SGW	NS	*QSGW_NS19.ubo-5A.2*	IWB67291	5A	178.3	IWB72903-IWB2075	174.2-183.0	**C**/T	0.22	106/75	3.1	5.8
SGW	NS	*QSGW_NS19.ubo-6B*	IWB1948	6B	90.3	wPt-6889-IWB74068	86.7-93.4	**A**/G	0.31	149/32	3.4	6.5
SGW	NS	*QSGW_NS19.ubo-7A*	IWB59995	7A	32.6	IWB73683-IWB3124	28.6-39.8	**C**/T	-0.31	28/155	3.2	6.0
GLE	NS	*QGLE_NS19.ubo-3A.1*	IWB14646	3A	33.1	IWB8715-IWB24651	26.9-36.7	**A**/G	-0.23	14/169	3.0	5.6
GLE	NS	*QGLE_NS19.ubo-3A.2*	IWB72751	3A	59.1	IWB71974-IWB67595	55.3-64.2	**G**/T	-0.18	135/47	3.4	6.5
GLE	NS	*QGLE_NS19.ubo-3A.3*	IWB72223	3A	82.6	IWA1019-IWB72035	79.5-86.9	**A**/G	0.15	113/69	3.0	5.6
GLE	NS	*QGLE_NS19.ubo-4B.1*	IWB25162	4B	15.6	IWB4336-IWB73117	12.1-18.7	**C**/T	-0.16	97/84	3.8	7.4

GLE	NS	*QGLE_NS19.ubo-4B.2*	IWB52318	4B	53.0	IWB35114-IWB72279	48.3-56.1	**A**/G	0.23	22/161	3.8	7.5
GLE	NS	*QGLE_NS19.ubo-4B.3*	IWB27735	4B	110.4	IWB7266-IWB37064	106.0-113.8	**G**/T	0.16	135/46	3.3	6.3
GWI	NS	*QGWI_NS19.ubo-2A*	IWB72263	2A	197.6	IWB12196-IWB72975	193.4-201.1	**A**/G	-0.13	39/138	5.5	11.4
GWI	NS	*QGWI_NS19.ubo-6B.1*	IWB46958	6B	36.0	IWB7468-wPt-4742	32.6-40.0	**A**/G	0.08	105/78	3.4	6.3
GWI	NS	*QGWI_NS19.ubo-6B.2*	IWB4259	6B	94.8	IWB70007-IWB46951	91.5-98.4	**A**/G	0.11	158/24	3.3	6.0
GWI	NS	*QGWI_NS19.ubo-7A*	IWB624	7A	7.2	wPt-7767-IWB62296	0.1-10.6	**C**/T	-0.11	161/22	3.2	5.8
GWI	NS	*QGWI_NS19.ubo-7B*	wPt-4843	7B	0.1	IWB22624-wPt-7975	0.1-3.7	**A**/T	0.11	138/45	4.2	8.1

[1] Treat.: treatment. [2] marker position of the peak marker based on the tetraploid wheat consensus map (Maccaferri et al., 2015a). [3] confidence intervals based on LD of the UNIBO-Durum Panel. [4] the allele effect is referred to the allele highlighted in bold. [5] -log (p-value) refers to p-value < 0.001.

Table A3.2. List of GWAS-QTLs significantly associated with the traits days to heading (HD), days to maturity (DTM), plant height (PH), grain yield (GY), thousand kernel weight (TKW), test weight (TWT), number of spikes per linear meter (SPM), number of spikelets per spike (SKT), grain number per spike (GNO), grain weight per spike (SGW), grain length (GLE), and grain width (GWI) under heat stress condition in the crop season of 2019.

Trait	Treat. [1]	QTL ID	Peak marker	Chr	Marker position (cM) [2]	Flanking Markers	Confidence Interval (cM) [3]	Alleles [4]	Effect	Allele Frequency	-LOG(p-value) [5]	R^2 (%)
HD	HS	*QHD_HS19.ubo-1B.1*	IWB57547	1B	44.0	IWB67970-IWB73176	40.8-47.1	**A**/C	-1.38	70/105	3.0	5.3
HD	HS	*QHD_HS19.ubo-1B.2*	IWB42110	1B	90.1	wPt-3579-IWA4488	87.0-93.3	**A**/G	-2.14	165/15	3.1	5.2
HD	HS	*QHD_HS19.ubo-2B*	IWB9088	2B	170.9	IWB59226-IWB30420	167.1-174.3	**C**/T	1.67	31/150	3.2	5.3
HD	HS	*QHD_HS19.ubo-4B.1*	IWB12274	4B	3.9	IWB73506-IWB73905	0.3-7.4	**A**/C	-1.89	31/148	3.4	5.8
HD	HS	*QHD_HS19.ubo-4B.2*	IWB49194	4B	16.0	IWB8084-IWA3290	12.8-19.3	**A**/G	-1.50	115/66	4.1	7.2
HD	HS	*QHD_HS19.ubo-4B.3*	IWB12150	4B	30.8	IWA103-IWB73919	27.6-33.9	**A**/G	-4.73	164/16	3.2	5.2
HD	HS	*QHD_HS19.ubo-6A*	IWB50963	6A	72.4	IWA6724-IWB9445	68.3-83.7	**A**/G	-2.61	161/18	4.1	7.3
HD	HS	*QHD_HS19.ubo-6B*	IWB2097	6B	152.2	IWB44252-IWB10420	147.7-155.9	**A**/G	-3.26	161/19	4.7	8.4
HD	HS	*QHD_HS19.ubo-7B.1*	IWB73349	7B	142.6	IWB71474-IWB41479	139.2-146.2	**A**/G	-1.31	77/103	3.4	5.7
HD	HS	*QHD_HS19.ubo-7B.2*	IWA4306	7B	154.7	IWB1121-IWB57792	151.6-157.8	**C**/T	2.20	160/21	3.2	5.2
DTM	HS	*QDTM_HS19.ubo-1B*	IWB30247	1B	98.8	IWB73608-IWB60525	95.1-102.3	**A**/C	-3.01	163/17	3.6	6.4
DTM	HS	*QDTM_HS19.ubo-2B.1*	IWB217	2B	0.1	IWB12069-IWB22939	0.1-3.5	**G**/T	3.32	163/16	3.3	5.8
DTM	HS	*QDTM_HS19.ubo-2B.2*	IWB12239	2B	128.3	IWB73040-IWA1389	124.9-131.6	**A**/G	-2.40	30/147	3.4	5.9
DTM	HS	*QDTM_HS19.ubo-4B*	IWB4211	4B	69.3	IWB44068-IWB72018	65.5-72.4	**A**/G	-2.21	38/139	3.5	6.0
DTM	HS	*QDTM_HS19.ubo-5B.1*	IWB49617	5B	155.7	IWB7593-IWB75132	152.5-159.8	**C**/T	1.93	55/125	3.0	5.2
DTM	HS	*QDTM_HS19.ubo-5B.2*	IWB36006	5B	166.1	IWB8583-IWB9424	160.6-171.2	**C**/T	2.31	24/154	3.1	5.1
DTM	HS	*QDTM_HS19.ubo-5B.3*	IWB39017	5B	190.9	IWB8500-IWB73352	187.5-194.7	**C**/T	-1.86	79/102	3.2	5.5
DTM	HS	*QDTM_HS19.ubo-6A*	IWA911	6A	67.5	IWB74244-IWB73605	62.8-72.6	**A**/G	3.62	9/172	3.3	5.6
DTM	HS	*QDTM_HS19.ubo-7A.1*	IWB61471	7A	82.6	IWB36370-IWA3673	78.9-87.7	**A**/G	-2.91	37/143	3.1	5.2
DTM	HS	*QDTM_HS19.ubo-7A.2*	IWB73706	7A	150.9	IWB56095-IWB70696	147.4-154.4	**C**/T	1.95	89/92	3.6	6.3
PH	HS	*QPH_HS19.ubo-1A*	IWA4292	1A	67.8	IWB51724-IWA3934	61.2-71.6	**C**/T	-8.41	18/162	5.1	10.7
PH	HS	*QPH_HS19.ubo-2A*	IWB66088	2A	118.4	IWB7707-IWB71282	114.8-123.9	**A**/G	9.54	11/170	4.2	8.6
PH	HS	*QPH_HS19.ubo-2B.1*	IWB22852	2B	74.5	IWB6607-IWA3924	71.0-77.9	**C**/T	10.05	15/166	3.2	6.2
PH	HS	*QPH_HS19.ubo-2B.2*	IWA7909	2B	149.0	IWB2073-IWB46631	145.8-153.0	**A**/G	-7.80	15/165	4.1	8.3

PH	HS	*QPH_HS19.ubo-4B*	IWB19555	4B	30.8	IWA103-IWB73919	27.6-33.9	**A**/G	-22.89	167/22	6.2	13.6
PH	HS	*QPH_HS19.ubo-5A*	IWB64235	5A	147.4	IWB73503-IWB66619	142.8-151.4	**A**/G	10.56	17/161	4.3	8.9
PH	HS	*QPH_HS19.ubo-5B.1*	IWA3607	5B	10.3	IWB5398-IWA5176	2.7-13.5	**A**/G	-10.16	170/11	4.7	9.7
PH	HS	*QPH_HS19.ubo-5B.2*	IWB30577	5B	142.6	IWB53460-wPt-3329	138.5-146.1	**C**/T	-5.58	34/144	3.6	7.2
PH	HS	*QPH_HS19.ubo-6B*	IWB8960	6B	10.3	IWA1494-IWA8314	7.2-15.2	**A**/G	7.96	12/169	3.3	6.3
GY	HS	*QGY_HS19.ubo-1A*	IWB40833	1A	67.8	IWB51724-IWA1594	61.2-71.3	**C**/T	0.82	163/18	3.5	7.0
GY	HS	*QGY_HS19.ubo-2A*	IWB66088	2A	118.4	IWB7707-IWB71282	114.8-123.9	**A**/G	1.03	11/170	3.2	6.3
GY	HS	*QGY_HS19.ubo-3B*	wPt-9012	3B	5.0	IWB71522-IWB4344	1.6-8.2	**A**/T	-0.87	158/23	3.0	5.9
GY	HS	*QGY_HS19.ubo-4A*	wPt-5172	4A	172.0	IWB72285-IWB18740	168.6-175.8	**A**/T	-1.02	166/15	4.0	8.2
GY	HS	*QGY_HS19.ubo-5A.1*	IWB28279	5A	50.5	IWA3349-IWB10273	47.4-54.6	**C**/T	-0.82	162/19	3.1	6.1
GY	HS	*QGY_HS19.ubo-5A.2*	IWA7255	5A	146.5	IWB73503-IWB27060	142.8-149.7	**A**/G	-1.02	162/18	3.1	6.1
GY	HS	*QGY_HS19.ubo-5B.1*	IWA3607	5B	10.3	IWA2915-wPt-8157	7.2-13.5	**A**/G	-1.05	170/11	3.4	6.7
GY	HS	*QGY_HS19.ubo-5B.2*	IWB56221	5B	145.9	IWB8035-IWB6823	142.6-149.0	**A**/G	-0.97	171/10	3.1	6.0
GY	HS	*QGY_HS19.ubo-7A*	IWB20735	7A	75.2	IWB9080-IWB74061	70.7-78.6	**C**/T	-0.68	133/46	4.1	8.6
TKW	HS	*QTKW_HS19.ubo-1B*	IWB2690	1B	162.1	IWB71657-wPt-2968	158.0-165.4	**C**/T	4.19	161/22	3.1	5.26
TKW	HS	*QTKW_HS19.ubo-2A*	wPt-9277	2A	198.7	IWB72339-IWB72975	194.8-201.1	**A**/T	-3.10	45/137	3.2	5.47
TKW	HS	*QTKW_HS19.ubo-2B.1*	IWA3407	2B	8.3	IWB22939-IWB71518	3.5-12.4	**A**/G	4.08	26/157	3.5	6.2
TKW	HS	*QTKW_HS19.ubo-2B.2*	IWB72239	2B	90.8	IWA4605-wPt-2664	87.7-93.2	**A**/C	-4.51	154/26	3.6	6.6
TKW	HS	*QTKW_HS19.ubo-2B.3*	IWB41234	2B	128.4	IWB73040-wPt-8569	124.9-131.9	**A**/G	-3.72	31/148	3.6	6.5
TKW	HS	*QTKW_HS19.ubo-4B*	IWB49194	4B	16.0	IWB8084-IWA3290	12.8-19.3	**A**/G	2.73	115/68	3.4	6.0
TKW	HS	*QTKW_HS19.ubo-5B*	IWB71438	5B	157.5	wPt-8125-IWB11985	154.5-160.6	**A**/G	2.80	63/118	3.1	5.4
TKW	HS	*QTKW_HS19.ubo-6A*	IWB9898	6A	5.9	IWB35466-IWB49468	3.0-9.0	**C**/T	-2.50	101/79	3.1	5.5
TKW	HS	*QTKW_HS19.ubo-7A*	IWB74033	7A	106.4	IWB73952-IWB10205	102.4-111.0	**A**/C	-2.96	118/59	3.2	5.9
TWT	HS	*QTWT_HS19.ubo-1A*	IWB12579	1A	99.8	wPt-8882-IWB23855	96.4-102.9	**G**/T	-1.40	153/29	3.2	5.7
TWT	HS	*QTWT_HS19.ubo-1B*	IWB8612	1B	43.6	IWB7810-IWA44	39.9-46.9	**G**/T	-1.66	14/165	3.8	7.0
TWT	HS	*QTWT_HS19.ubo-2B.1*	IWB6017	2B	88.4	IWB4384-wPt-2664	84.0-93.2	**A**/G	2.03	11/172	3.0	5.2
TWT	HS	*QTWT_HS19.ubo-2B.2*	IWB65020	2B	183.6	IWB8157-IWB22415	180.1-187.1	**A**/G	-1.73	163/20	3.1	5.3
TWT	HS	*QTWT_HS19.ubo-3B*	IWB71664	3B	158.5	IWB32656-IWA1094	155.5-163.2	**C**/T	-1.06	127/56	3.1	5.5
TWT	HS	*QTWT_HS19.ubo-4A.1*	IWB19834	4A	157.4	IWB9122-wPt-3506	154.0-161.2	**C**/T	-1.64	157/26	3.5	6.2
TWT	HS	*QTWT_HS19.ubo-4A.2*	IWA3422	4A	172.9	IWB72285-IWB46967	168.6-175.8	**A**/G	1.86	13/170	3.2	5.6
TWT	HS	*QTWT_HS19.ubo-7A*	IWB27700	7A	82.4	IWB36370-IWA3673	78.9-87.7	**C**/T	2.08	14/169	3.4	6.0
TWT	HS	*QTWT_HS19.ubo-7B*	IWB3581	7B	177.2	wPt-2356-IWB10793	173.7-181.1	**C**/T	1.87	164/19	3.4	6.1

SPM	HS	*QSPM_HS19.ubo-1B*	IWB38151	1B	83.9	IWB71349-wPt-3579	79.6-87.0	**A**/G	7.85	97/81	3.3	7.0
SPM	HS	*QSPM_HS19.ubo-2B.1*	IWB45933	2B	132.3	IWB70548-IWB22281	128.7-135.6	**C**/T	-19.11	170/11	3.8	8.2
SPM	HS	*QSPM_HS19.ubo-2B.2*	IWB10623	2B	181.6	wPt-4892-IWB6614	177.5-185.7	**A**/G	-13.11	154/24	3.6	7.9
SPM	HS	*QSPM_HS19.ubo-4A.1*	wPt-3766	4A	144.6	IWB66212-IWB67551	140.7-147.9	**A**/T	-17.77	168/13	4.3	9.7
SPM	HS	*QSPM_HS19.ubo-4A.2*	IWB19834	4A	157.4	IWB9122-wPt-3506	154.0-161.2	**C**/T	-14.72	155/26	3.8	8.4
SPM	HS	*QSPM_HS19.ubo-4A.3*	IWB42675	4A	173.8	wPt-8657-IWB46967	170.0-175.8	**A**/G	-14.13	151/30	4.5	10.3
SPM	HS	*QSPM_HS19.ubo-5A*	IWA2350	5A	146.5	IWB56489-IWB27060	142.8-149.7	**G**/T	-18.80	163/18	4.1	9.1
SPM	HS	*QSPM_HS19.ubo-5B*	IWB56221	5B	145.9	IWB8035-IWB6823	142.6-149.0	**A**/G	-15.29	171/10	3.1	6.5
SKT	HS	*QSKT_HS19.ubo-1A.1*	IWB59699	1A	143.7	tPt-7724-IWB9191	140.0-146.8	**C**/T	-0.88	148/32	3.2	6.2
SKT	HS	*QSKT_HS19.ubo-1A.2*	wPt-1011	1A	167.4	IWB7910-wPt-6853	150.2-167.4	**A**/T	-0.90	149/32	3.3	6.5
SKT	HS	*QSKT_HS19.ubo-2A*	wPt-2293	2A	154.6	IWB70002-IWB47578	151.2-157.7	**A**/T	-0.93	137/44	3.6	7.0
SKT	HS	*QSKT_HS19.ubo-2B*	IWB318	2B	137.9	IWB3603-IWB35839	134.8-141.0	**A**/G	-0.86	109/72	3.1	5.8
SKT	HS	*QSKT_HS19.ubo-5A.1*	IWB25138	5A	146.5	IWB73503-IWB27060	142.8-149.7	**A**/G	-1.61	167/14	3.3	6.3
SKT	HS	*QSKT_HS19.ubo-5A.2*	IWB66511	5A	199.3	IWB23336-IWA7880	196.2-206.0	**C**/T	1.01	40/140	3.1	5.9
SKT	HS	*QSKT_HS19.ubo-5B*	IWB66356	5B	112.7	wPt-0498-IWB66975	109.0-116.1	**C**/T	1.36	162/15	3.9	7.9
SKT	HS	*QSKT_HS19.ubo-6B*	IWB65313	6B	69.0	IWA2975-IWA7818	65.9-73.5	**G**/T	-1.05	21/159	3.0	5.7
SKT	HS	*QSKT_HS19.ubo-7B*	IWB49994	7B	176.7	IWB73580-IWB10793	173.5-181.1	**A**/C	-1.13	144/36	3.8	7.7
GNO	HS	*QGNO_HS19.ubo-2A*	IWA3368	2A	109.5	IWB66497-IWB65481	106.5-116.5	**A**/C	-7.22	161/19	5.2	10.1
GNO	HS	*QGNO_HS19.ubo-2B*	IWB33109	2B	76.6	IWB12041-IWA50	73.2-80.6	**C**/T	-4.45	80/98	4.6	8.8
GNO	HS	*QGNO_HS19.ubo-3B*	IWB10783	3B	51.9	IWB6460-wPt-1159	48.8-55.0	**C**/T	3.72	94/87	3.4	6.1
GNO	HS	*QGNO_HS19.ubo-4B.1*	IWB65475	4B	16.0	IWB28293-IWA3290	10.0-19.3	**C**/T	-3.61	114/67	3.4	6.1
GNO	HS	*QGNO_HS19.ubo-4B.2*	IWB71806	4B	99.9	IWB75109-IWA3654	96.7-103.3	**G**/T	-4.70	81/99	4.6	8.7
GNO	HS	*QGNO_HS19.ubo-5A*	IWB14134	5A	128.5	IWB26707-IWA6706	125.0-132.3	**C**/T	5.28	163/18	3.1	5.5
GNO	HS	*QGNO_HS19.ubo-5B*	IWA5742	5B	59.2	IWB8032-IWB8536	55.0-63.2	**A**/G	-3.57	96/83	3.0	5.3
GNO	HS	*QGNO_HS19.ubo-6A*	IWA3909	6A	127.1	IWB29924-IWB73095	124.0-131.2	**A**/G	7.49	10/171	3.4	6.1
GNO	HS	*QGNO_HS19.ubo-7B*	IWB41483	7B	146.2	IWB73350-wPt-5892	142.5-150.0	**A**/G	4.01	54/127	3.3	5.9
SGW	HS	*QSGW_HS19.ubo-2A.1*	IWA3368	2A	109.5	IWB66497-IWB11039	106.5-113.0	**A**/C	-0.31	161/19	3.9	7.2
SGW	HS	*QSGW_HS19.ubo-2A.2*	IWA2938	2A	176.5	IWB7563-IWB72723	171.0-179.6	**A**/C	-0.17	84/97	3.2	5.7
SGW	HS	*QSGW_HS19.ubo-2A.3*	IWB9045	2A	193.1	IWB9798-IWB55230	189.8-196.5	**C**/T	-0.20	48/131	3.0	5.3
SGW	HS	*QSGW_HS19.ubo-2B*	IWB33109	2B	76.6	IWB12041-IWB8031	73.2-80.6	**C**/T	-0.17	80/98	3.0	5.2
SGW	HS	*QSGW_HS19.ubo-3A*	IWB70107	3A	59.1	IWB71974-IWB67595	55.3-64.2	**A**/C	-0.20	72/107	3.6	6.4
SGW	HS	*QSGW_HS19.ubo-3B*	IWB26270	3B	41.3	wPt-8686-IWB29048	36.8-44.6	**A**/G	0.20	105/76	3.9	7.0

SGW	HS	*QSGW_HS19.ubo-4B.1*	IWB67166	4B	68.3	IWB73007-IWA3287	64.4-71.8	**A**/G	0.21	122/57	3.6	6.5
SGW	HS	*QSGW_HS19.ubo-4B.2*	IWB71806	4B	99.9	IWB75109-IWA3654	96.7-103.3	**G**/T	-0.20	81/90	3.5	6.3
SGW	HS	*QSGW_HS19.ubo-5B.1*	IWB68333	5B	117.1	IWB72093-IWB11813	112.1-121.7	**C**/T	0.42	163/16	5.3	10.4
SGW	HS	*QSGW_HS19.ubo-5B.2*	rPt-7889	5B	144.5	IWB68186-IWA4182	141.2-148.6	**A**/T	0.23	148/33	3.2	5.6
SGW	HS	*QSGW_HS19.ubo-6A*	IWB6825	6A	109.3	IWB70344-IWB12203	105.7-112.9	**A**/G	-0.31	168/13	3.1	5.4
SGW	HS	*QSGW_HS19.ubo-7B*	wPt-3533	7B	142.7	IWB71474-IWB41479	139.2-146.2	**A**/T	-0.20	54/127	3.5	6.3
GLE	HS	*QGLE_HS19.ubo-1A*	wPt-4676	1A	0.1	-IWB65373	-4.6	**A**/T	0.15	62/119	3.1	5.8
GLE	HS	*QGLE_HS19.ubo-1B*	IWB71657	1B	158.0	tPt-6091-IWB62169	154.6-161.5	**C**/T	-0.26	14/167	3.9	7.6
GLE	HS	*QGLE_HS19.ubo-4A*	IWB22357	4A	104.2	IWB12388-IWA3774	98.9-108.9	**C**/T	0.27	170/11	3.1	5.8
GLE	HS	*QGLE_HS19.ubo-4B.1*	IWB25162	4B	15.6	IWB4336-IWB73117	12.1-18.7	**C**/T	-0.16	95/84	4.1	8.1
GLE	HS	*QGLE_HS19.ubo-4B.2*	IWB32544	4B	103.3	IWB73910-IWB4448	99.9-109.1	**C**/T	-0.22	23/157	4.1	8.0
GLE	HS	*QGLE_HS19.ubo-5A*	IWB10273	5A	54.6	IWB70873-IWB66579	50.5-58.1	**C**/T	-0.16	59/116	3.2	6.1
GLE	HS	*QGLE_HS19.ubo-7B*	IWA4888	7B	189.7	IWB858-IWA7003	186.0-193.0	**A**/G	-0.18	133/47	3.0	5.7
GWI	HS	*QGWI_HS19.ubo-2B*	IWA3407	2B	8.3	IWB22939-IWB11421	3.5-11.6	**A**/G	0.14	25/156	4.2	8.8
GWI	HS	*QGWI_HS19.ubo-4B*	IWB17754	4B	68.3	IWB73007-IWA3287	64.4-71.8	**A**/G	-0.10	51/127	3.7	7.5
GWI	HS	*QGWI_HS19.ubo-5A*	IWB55564	5A	136.3	IWB8003-IWB58257	132.3-141.4	**A**/G	-0.09	83/97	3.3	6.8
GWI	HS	*QGWI_HS19.ubo-5B.1*	IWB8035	5B	142.6	IWB53460-IWB28555	138.5-145.9	**C**/T	-0.11	35/144	3.2	6.3
GWI	HS	*QGWI_HS19.ubo-5B.2*	IWB71438	5B	157.5	wPt-8125-IWB11985	154.5-160.6	**A**/G	0.09	61/118	3.3	6.7
GWI	HS	*QGWI_HS19.ubo-5B.3*	IWA8031	5B	165.2	IWB8583-IWB9424	160.6-171.2	**C**/T	-0.11	148/29	3.6	7.4
GWI	HS	*QGWI_HS19.ubo-7A*	IWB10884	7A	95.5	wPt-3373-IWB34298	92.0-99.5	**C**/T	-0.11	44/133	3.6	7.5
GWI	HS	*QGWI_HS19.ubo-7B.1*	IWB60028	7B	0.1	IWB22624-IWB67086	0.1-3.3	**C**/T	-0.09	59/122	3.4	6.8
GWI	HS	*QGWI_HS19.ubo-7B.2*	IWB74056	7B	15.8	IWB6455-wPt-7318	10.2-19.2	**C**/T	-0.08	92/89	3.4	6.8

[1] Treat.: treatment. [2] marker position of the peak marker based on the tetraploid wheat consensus map (Maccaferri et al., 2015a). [3] confidence intervals based on LD of the UNIBO-Durum Panel. [4] the allele effect is referred to the allele highlighted in bold. [5] -log (p-value) refers to p-value < 0.001.

Table A3.3. List of GWAS-QTLs for reaction norm index (Δ) significantly associated with the traits days to heading (HD), days to maturity (DTM), plant height (PH), grain yield (GY), thousand kernel weight (TKW), test weight (TWT), number of spikes per linear meter (SPM), number of spikelets per spike (SKT), grain number per spike (GNO), grain weight per spike (SGW), grain length (GLE), and grain width (GWI) in the crop season of 2019.

Trait	Treat. [1]	QTL ID	Peak marker	Chr	Marker position (cM) [2]	Flanking Markers	Confidence Interval (cM) [3]	Alleles [4]	Effect	Allele Frequency	-LOG(p-value) [5]	R^2 (%)
HD	Δ	*QHD_Δ19.ubo-2A*	IWB67306	2A	46.6	IWB1280-IWB146	36.8-50.5	**C**/T	4.59	99/79	3.5	3.7
HD	Δ	*QHD_Δ19.ubo-3A*	wPt-6956	3A	123.1	IWB65658-IWB72172	119.5-127.7	**A**/T	1.78	116/63	3.1	3.2
HD	Δ	*QHD_Δ19.ubo-5A*	IWB10692	5A	150.3	IWA2350-IWB72381	146.5-155.0	**C**/T	5.17	163/15	4.4	4.9
DTM	Δ	*QDTM_Δ19.ubo-1A*	IWA6835	1A	68.9	IWB51724-IWB6733	61.2-72.2	**C**/T	-1.86	22/158	3.3	5.7
DTM	Δ	*QDTM_Δ19.ubo-2B.1*	wPt-7158	2B	40.9	IWB73192-IWA7916	37.2-44.2	**A**/T	1.47	61/120	3.2	5.6
DTM	Δ	*QDTM_Δ19.ubo-2B.2*	IWB41646	2B	73.2	IWA2556-IWB22630	70.1-76.6	**A**/G	2.25	21/159	3.8	6.7
DTM	Δ	*QDTM_Δ19.ubo-2B.3*	IWA2131	2B	127.7	IWB22798-IWB41461	124.5-130.9	**A**/C	1.50	148/30	3.2	5.4
DTM	Δ	*QDTM_Δ19.ubo-5A*	IWB38719	5A	140.6	IWB71521-IWB73503	137.2-142.8	**C**/T	1.66	89/88	4.6	8.7
DTM	Δ	*QDTM_Δ19.ubo-7A*	IWB46130	7A	91.2	IWB8142-IWB11840	87.7-94.7	**A**/G	1.87	157/22	3.0	5.2
PH	Δ	*QPH_Δ19.ubo-1A*	IWA4292	1A	67.8	IWB51724-IWA3934	61.2-71.6	**C**/T	-9.04	18/162	5.9	12.4
PH	Δ	*QPH_Δ19.ubo-2A*	IWB66088	2A	118.4	IWB7707-IWB71282	114.8-123.9	**A**/G	8.02	11/170	3.1	5.7
PH	Δ	*QPH_Δ19.ubo-2B.1*	IWB73971	2B	50.0	IWB70191-IWA4554	46.3-53.4	**C**/T	6.59	157/22	3.2	6.2
PH	Δ	*QPH_Δ19.ubo-2B.2*	IWA7909	2B	149.0	IWB2073-IWB46631	145.8-153.0	**A**/G	-6.68	15/165	3.1	5.8
PH	Δ	*QPH_Δ19.ubo-5B.1*	IWB5398	5B	2.7	wPt-1302-IWA4790	0.1-6.5	**C**/T	0.50	111/70	3.3	6.3
PH	Δ	*QPH_Δ19.ubo-5B.2*	IWA3607	5B	10.3	IWA4313-IWA5176	6.8-13.5	**A**/G	-9.32	170/11	4.0	7.8
GY	Δ	*QGY_Δ19.ubo-1A*	IWB40833	1A	67.8	IWB51724-IWA1594	61.2-71.3	**C**/T	11.76	163/18	3.4	6.9
GY	Δ	*QGY_Δ19.ubo-2A*	IWB66088	2A	118.4	IWB7707-IWB71282	114.8-123.9	**A**/G	16.56	11/170	3.7	7.8
GY	Δ	*QGY_Δ19.ubo-2B*	IWB29874	2B	48.2	IWA3868-IWB3418	45.1-53.0	**C**/T	13.44	157/21	3.8	8.2
GY	Δ	*QGY_Δ19.ubo-3B*	wPt-9012	3B	5.0	IWB71522-IWB4344	1.6-8.2	**A**/T	-13.70	158/23	3.4	7.0
GY	Δ	*QGY_Δ19.ubo-4A*	wPt-5172	4A	172.0	IWB72285-IWB18740	168.6-175.8	**A**/T	-13.10	166/15	3.2	6.6
GY	Δ	*QGY_Δ19.ubo-5A*	IWA7255	5A	146.5	IWB73503-IWB27060	142.8-149.7	**A**/G	-14.70	162/18	3.0	6.1
GY	Δ	*QGY_Δ19.ubo-5B*	IWA3607	5B	10.3	IWA2915-IWA5176	7.2-13.5	**A**/G	-15.20	170/11	3.3	6.7
TKW	Δ	*QTKW_Δ19.ubo-1B*	IWB12819	1B	63.3	IWA4557-IWB47790	59.1-67.2	**A**/G	1.49	15/168	3.1	5.719

TKW	Δ	*QTKW_Δ19.ubo-2A*	IWB75255	2A	186.1	IWB7444-IWA5840	182.3-189.8	**C**/T	-0.90	29/154	4.6	9.026
TKW	Δ	*QTKW_Δ19.ubo-3B.1*	IWB31170	3B	3.4	IWB64431-IWB9061	0.1-6.5	**A**/G	0.66	84/91	4.1	8.296
TKW	Δ	*QTKW_Δ19.ubo-3B.2*	IWB45372	3B	100.9	IWB49370-IWA6221	97.2-104.62	**A**/G	-0.95	38/142	3.1	5.649
TKW	Δ	*QTKW_Δ19.ubo-6B.1*	IWB26174	6B	95.6	IWB72452-IWA670	92.3-100.2	**C**/T	-0.43	158/22	4.6	9.331
TKW	Δ	*QTKW_Δ19.ubo-6B.2*	IWB73470	6B	153.1	IWB65683-IWB73036	148.9-155.9	**A**/G	1.68	171/12	3.2	5.793
TKW	Δ	*QTKW_Δ19.ubo-7A.1*	IWB27700	7A	82.4	IWB36370-IWA3673	78.9-87.7	**C**/T	2.49	14/169	3.7	7.072
TKW	Δ	*QTKW_Δ19.ubo-7A.2*	IWB72273	7A	116.0	IWB21992-IWB11124	112.9-123.1	**A**/G	-0.68	30/153	3.2	5.836
TKW	Δ	*QTKW_Δ19.ubo-7B.1*	wPt-4843	7B	0.1	IWB22624-wPt-7975	0.1-3.7	**A**/T	-0.69	138/45	3.3	5.975
TKW	Δ	*QTKW_Δ19.ubo-7B.2*	IWB74657	7B	112.5	IWB13236-IWB74053	108.6-114.9	**A**/C	-0.68	127/52	3.3	6.154
TKW	Δ	*QTKW_Δ19.ubo-7B.3*	IWB65673	7B	122.1	IWA1971-IWA1345	120.4-127.0	**C**/T	-0.83	135/46	3.0	5.503
TWT	Δ	*QTWT_Δ19.ubo-2B.1*	IWB47474	2B	126.9	IWB13303-IWB25766	123.8-130.1	**A**/G	-1.22	49/130	3.4	7.5
TWT	Δ	*QTWT_Δ19.ubo-2B.2*	IWB9088	2B	170.9	IWB59226-wPt-6643	167.1-176.0	**C**/T	-1.29	31/150	3.4	7.4
TWT	Δ	*QTWT_Δ19.ubo-2B.3*	IWB758	2B	185.8	IWA3773-IWB63909	181.6-189.1	**A**/G	1.46	34/146	3.6	8.1
TWT	Δ	*QTWT_Δ19.ubo-4B*	IWB7100	4B	97.5	IWB57170-IWA1861	94.0-101.3	**A**/C	0.21	99/75	3.2	7.0
TWT	Δ	*QTWT_Δ19.ubo-5A*	IWB66619	5A	151.4	IWB71757-IWB72381	147.1-155.0	**A**/G	2.12	15/164	3.2	7.08
TWT	Δ	*QTWT_Δ19.ubo-7A*	IWB27700	7A	82.4	IWB36370-IWA3673	78.9-87.7	**C**/T	2.02	14/167	3.8	8.423
SPM	Δ	*QSPM_Δ19.ubo-1B*	IWB36872	1B	83.9	IWB71349-wPt-3579	79.6-87.0	**C**/T	-12.80	163/18	3.7	6.8
SPM	Δ	*QSPM_Δ19.ubo-4A*	wPt-0105	4A	144.6	IWB66212-IWB67551	140.7-147.85	**A**/T	-15.00	168/13	3.6	6.5
SPM	Δ	*QSPM_Δ19.ubo-5A*	IWA4805	5A	147.4	IWB73503-IWB73541	142.8-151.2	**G**/T	21.25	14/167	3.7	6.6
SKT	Δ	*QSKT_Δ19.ubo-5B*	IWB59928	5B	191.7	IWB134-IWB73351	188.6-194.9	**G**/T	4.06	113/67	3.2	4.7
SKT	Δ	*QSKT_Δ19.ubo-6B.1*	IWB72972	6B	94.2	IWB73501-IWB46951	90.4-98.4	**C**/T	-4.53	140/33	3.0	4.9
SKT	Δ	*QSKT_Δ19.ubo-6B.2*	IWB36435	6B	147.5	IWB71117-IWB28557	140.1-151.0	**C**/T	5.34	151/29	3.1	4.6
GNO	Δ	*QGNO_Δ19.ubo-1B*	IWB280	1B	162.3	IWB71657-wPt-2968	158.0-165.4	**C**/T	5.78	133/47	3.1	5.6
GNO	Δ	*QGNO_Δ19.ubo-5A*	IWB40699	5A	208.8	IWB48691-IWB35997	201.1-213.8	**C**/T	-10.30	24/156	3.2	5.8
GNO	Δ	*QGNO_Δ19.ubo-5B.1*	wPt-5604	5B	117.9	IWB10362-IWB11813	113.9-121.7	**A**/T	-8.74	18/162	3.3	6.1
GNO	Δ	*QGNO_Δ19.ubo-5B.2*	IWB52826	5B	140.3	IWB51456-IWA584	135.8-143.7	**C**/T	5.18	77/103	3.3	6.0
SGW	Δ	*QSGW_Δ19.ubo-1A*	IWA6835	1A	68.9	IWB51724-IWB6733	61.2-72.2	**C**/T	-8.06	22/158	3.4	7.4
SGW	Δ	*QSGW_Δ19.ubo-3B*	IWB41105	3B	25.4	IWB64404-IWB64361	22.3-29.3	**C**/T	8.11	164/17	3.4	7.3
SGW	Δ	*QSGW_Δ19.ubo-4B*	IWB72259	4B	115.2	IWB32863-IWB67498	110.4-118.8	**G**/T	-5.10	117/64	3.3	7.1
SGW	Δ	*QSGW_Δ19.ubo-5B.1*	IWB25678	5B	54.6	IWB71672-IWB24135	50.2-57.8	**A**/G	-8.18	22/159	3.2	6.9
SGW	Δ	*QSGW_Δ19.ubo-5B.2*	IWB68333	5B	117.1	IWB10362-IWB11813	113.9-121.7	**C**/T	9.59	163/16	3.9	8.7
SGW	Δ	*QSGW_Δ19.ubo-5B.3*	IWB22567	5B	140.3	IWB51456-rPt-7889	135.8-144.5	**C**/T	5.84	81/100	4.4	10.0

SGW	Δ	*QSGW_Δ19.ubo-6B*	IWB72406	6B	31.3	IWB62494-IWB2600	27.8-34.7	**A**/G	9.43	170/11	3.2	6.7
GLE	Δ	*QGLE_Δ19.ubo-1A*	IWB6234	1A	1.7	wPt-4676-wPt-0196	0.1-5.2	**C**/T	-2.07	21/160	3.5	7.0
GLE	Δ	*QGLE_Δ19.ubo-1B*	IWB58817	1B	43.5	IWB7810-IWA44	39.9-46.9	**A**/G	1.64	28/146	3.0	5.9
GLE	Δ	*QGLE_Δ19.ubo-5A*	IWB40699	5A	208.8	IWA7880-IWB35997	206.0-213.8	**C**/T	2.61	24/156	4.3	8.9
GLE	Δ	*QGLE_Δ19.ubo-7A.1*	IWB11124	7A	123.1	IWA3941-IWB46770	118.0-128.1	**G**/T	1.24	67/114	3.1	6.0
GLE	Δ	*QGLE_Δ19.ubo-7A.2*	IWB9749	7A	130.7	IWB8935-IWB45289	126.0-134.6	**A**/G	-1.77	67/113	5.7	12.3
GWI	Δ	*QGWI_Δ19.ubo-1A*	IWB56058	1A	70.7	IWA2995-IWB35039	67.7-75.1	**C**/T	3.49	164/13	3.0	5.6
GWI	Δ	*QGWI_Δ19.ubo-1B.1*	IWB72106	1B	14.3	IWB12258-wPt-0655	8.7-17.8	**A**/G	2.54	111/69	3.4	6.4
GWI	Δ	*QGWI_Δ19.ubo-1B.2*	IWA139	1B	43.5	IWB7810-IWA44	39.9-46.9	**C**/T	-2.97	147/29	3.4	6.5
GWI	Δ	*QGWI_Δ19.ubo-2A*	IWB12196	2A	193.4	IWB75255-IWB74253	186.1-197.6	**C**/T	-2.53	53/126	3.9	7.7
GWI	Δ	*QGWI_Δ19.ubo-2B*	IWB73198	2B	126.7	IWB48071-IWA2261	123.4-129.8	**A**/G	-2.47	49/130	3.4	6.5
GWI	Δ	*QGWI_Δ19.ubo-4B*	IWB17754	4B	68.3	IWB73007-IWA3287	64.4-71.8	**A**/G	-2.36	51/127	3.5	6.7
GWI	Δ	*QGWI_Δ19.ubo-6B.1*	IWB33858	6B	60.6	IWB56050-IWB1248	57.1-64.1	**A**/G	2.30	43/137	3.6	7.0
GWI	Δ	*QGWI_Δ19.ubo-6B.2*	IWB26174	6B	95.6	IWB72452-IWB73225	92.3-98.4	**C**/T	-3.35	156/22	4.2	8.4
GWI	Δ	*QGWI_Δ19.ubo-7A*	IWB20735	7A	75.2	IWB9080-IWB74061	70.7-78.6	**C**/T	-2.38	133/46	3.1	5.8

[1] Treat.: treatment. [2] marker position of the peak marker based on the tetraploid wheat consensus map (Maccaferri et al., 2015a). [3] confidence intervals based on LD of the UNIBO-Durum Panel. [4] the allele effect is referred to the allele highlighted in bold. [5] -log (p-value) refers to p-value < 0.001.

Table A3.4. List of GWAS-QTLs significantly associated with the traits days to heading (HD), days to maturity (DTM), plant height (PH), grain yield (GY), thousand kernel weight (TKW), test weight (TWT), number of spikes per linear meter (SPM), number of spikelets per spike (SKT), grain number per spike (GNO), grain weight per spike (SGW), grain length (GLE), and grain width (GWI) under control condition in the crop season of 2018.

Trait	Treat. [1]	QTL ID	Peak marker	Chr	Marker position (cM) [2]	Flanking Markers	Confidence Interval (cM) [3]	Alleles [4]	Effect	Allele Frequency	-log(p-value) [5]	R^2 (%)
HD	NS	*QHD_NS18.ubo-1B*	IWB68893	1B	43.6	IWB67970-IWA44	40.8-46.9	**A**/G	-5.81	166/13	4.4	6.4
HD	NS	*QHD_NS18.ubo-2A*	IWB13965	2A	117.6	IWB32024-IWB46634	114.5-121.0	**C**/T	4.19	32/146	3.0	4.0
HD	NS	*QHD_NS18.ubo-2B*	wPt-8404	2B	31.4	IWB8893-IWB73192	27.7-37.2	**A**/T	-3.20	46/134	3.1	4.0
HD	NS	*QHD_NS18.ubo-4A*	IWB71865	4A	36.2	IWA1137-IWB32882	25.8-41.3	**C**/T	5.11	14/167	3.4	4.6
HD	NS	*QHD_NS18.ubo-4B.1*	IWB32911	4B	12.0	IWB73905-IWA2125	7.4-15.5	**C**/T	-4.26	33/144	3.8	5.2
HD	NS	*QHD_NS18.ubo-4B.2*	IWB34794	4B	69.3	IWB44068-IWA2218	65.5-72.4	**A**/G	3.57	138/37	3.6	5.0
HD	NS	*QHD_NS18.ubo-5A*	IWB10692	5A	150.3	IWB71757-IWB72381	147.1-155.0	**C**/T	-8.90	164/14	4.5	6.4
HD	NS	*QHD_NS18.ubo-7A.1*	IWB22516	7A	76.0	IWB9080-IWB36304	70.7-79.9	**A**/G	4.96	24/158	3.3	4.4
HD	NS	*QHD_NS18.ubo-7A.2*	IWB60067	7A	89.6	IWB66777-IWB65337	84.6-92.9	**C**/T	4.03	44/131	3.6	5.1
HD	NS	*QHD_NS18.ubo-7A.3*	IWB71893	7A	114.0	IWB10205-IWA3941	111.0-118.0	**C**/T	3.14	111/61	3.4	4.8
DTM	NS	*QDTM_NS18.ubo-1B*	IWB69041	1B	43.6	IWB7810-IWA44	39.9-46.9	**A**/G	-4.05	167/13	3.9	4.8
DTM	NS	*QDTM_NS18.ubo-2A.1*	IWB26617	2A	24.5	IWB69599-IWB71223	20.5-32.3	**A**/G	2.65	119/58	3.3	4.0
DTM	NS	*QDTM_NS18.ubo-2A.2*	IWB13965	2A	117.6	IWB8665-IWB46634	114.5-121.0	**C**/T	3.60	32/146	3.8	4.7
DTM	NS	*QDTM_NS18.ubo-2B*	IWB67650	2B	171.7	IWB59226-IWB68812	167.1-174.8	**A**/G	2.70	40/128	3.4	4.3
DTM	NS	*QDTM_NS18.ubo-4A.1*	IWB71865	4A	36.2	IWA1137-IWB32882	25.8-41.3	**C**/T	4.73	14/167	4.9	6.3
DTM	NS	*QDTM_NS18.ubo-4A.2*	wPt-8443	4A	91.6	wPt-2221-IWA4425	88.5-97.7	**A**/T	-3.39	161/18	3.5	4.4
DTM	NS	*QDTM_NS18.ubo-5A*	IWB25201	5A	199.1	IWB5178-IWA7880	195.1-206.0	**A**/G	3.85	12/167	3.1	3.6
DTM	NS	*QDTM_NS18.ubo-5B*	IWB5705	5B	48.9	IWB7509-IWA6526	45.0-52.2	**C**/T	5.43	167/13	4.0	5.0
DTM	NS	*QDTM_NS18.ubo-6A*	IWB50963	6A	72.4	IWA6724-IWB9445	68.3-83.7	**A**/G	-3.64	161/17	3.3	3.9
DTM	NS	*QDTM_NS18.ubo-7A.1*	IWB60067	7A	89.6	IWB66777-IWB65337	84.6-92.9	**C**/T	3.54	44/131	4.7	6.2
DTM	NS	*QDTM_NS18.ubo-7A.2*	IWB68176	7A	153.7	IWA719-IWB10044	150.9-157.3	**A**/G	2.29	67/114	3.3	3.9
PH	NS	*QPH_NS18.ubo-1A*	IWB61980	1A	1.5	wPt-4676-IWB65373	0.1-4.6	**C**/T	-4.76	110/67	4.0	3.4
PH	NS	*QPH_NS18.ubo-4A.1*	IWB43361	4A	71.2	IWB69766-IWB29840	66.8-77.1	**A**/C	5.84	18/161	3.2	2.5
PH	NS	*QPH_NS18.ubo-4A.2*	wPt-5172	4A	172.0	IWB72285-IWB46967	168.6-175.8	**A**/T	-7.37	159/15	3.0	2.5

PH	NS	*QPH_NS18.ubo-5A*	IWB27060	5A	149.7	IWB63075-IWB72381	146.5-155.0	**A**/G	-12.85	167/12	3.1	2.5
PH	NS	*QPH_NS18.ubo-5B*	IWB22567	5B	140.3	IWB51456-IWA584	135.8-143.7	**C**/T	3.68	83/98	3.1	2.5
GY	NS	*QGY_NS18.ubo-5A*	IWB10985	5A	56.5	IWB70406-IWB28350	48.8-63.4	**G**/T	-0.63	36/145	3.1	6.2
GY	NS	*QGY_NS18.ubo-5B*	wPt-5928	5B	117.9	IWB72038-IWB68691	53.0-60.8	**A**/T	-0.76	18/160	3.9	8.2
GY	NS	*QGY_NS18.ubo-7A.1*	IWB62310	7A	187.1	IWB29819-IWB20258	182.9-190.5	**A**/G	-0.47	106/73	3.6	7.2
GY	NS	*QGY_NS18.ubo-7A.2*	IWB34223	7A	197.6	IWB73864-IWA501	193.9-200.8	**C**/T	0.52	124/52	3.8	7.8
GY	NS	*QGY_NS18.ubo-7B*	IWB73917	7B	13.8	IWB6455-IWB3369	10.2-17.3	**A**/C	0.54	71/99	4.3	9.5
TKW	NS	*QTKW_NS18.ubo-2A*	IWB72263	2A	197.6	IWB12196-IWB41523	193.4-200.7	**A**/G	-3.55	38/138	3.5	6.2
TKW	NS	*QTKW_NS18.ubo-2B*	IWB62322	2B	7.9	IWB22939-wPt-9958	3.5-11.3	**C**/T	-4.21	154/22	3.4	5.9
TKW	NS	*QTKW_NS18.ubo-4B*	IWB25162	4B	15.6	IWB4336-IWB70256	12.1-18.7	**C**/T	-2.85	97/82	3.5	5.9
TKW	NS	*QTKW_NS18.ubo-5A*	IWA1486	5A	136.3	IWA6706-IWB3132	133.2-140.1	**A**/G	3.27	73/105	3.2	5.3
TKW	NS	*QTKW_NS18.ubo-6A.1*	IWB71109	6A	5.9	wPt-9075-IWB49468	0.9-9.0	**A**/G	2.46	89/86	3.0	5.1
TKW	NS	*QTKW_NS18.ubo-6A.2*	IWB35245	6A	122.4	IWB50956-IWB11419	119.0-125.6	**C**/T	3.07	62/112	3.3	5.6
TKW	NS	*QTKW_NS18.ubo-7B*	IWB55430	7B	0.1	IWB22624-wPt-7975	0.1-3.7	**C**/T	-3.14	55/116	3.3	5.6
TWT	NS	*QTWT_NS18.ubo-2B*	IWB61082	2B	121.5	IWB69796-IWB29225	115.5-124.9	**A**/G	0.78	111/68	3.1	4.9
TWT	NS	*QTWT_NS18.ubo-3B*	IWB68475	3B	159.5	IWB32656-IWA1094	155.5-163.2	**A**/C	-0.76	86/88	3.1	5.0
TWT	NS	*QTWT_NS18.ubo-4A*	IWB44783	4A	113.9	IWB28717-IWB48435	110.7-118.3	**A**/G	1.04	158/20	3.1	5.3
TWT	NS	*QTWT_NS18.ubo-5A.1*	IWB10054	5A	70.8	IWB72382-IWB35865	67.7-74.8	**C**/T	-1.05	137/42	3.3	5.3
TWT	NS	*QTWT_NS18.ubo-5A.2*	IWB72363	5A	151.8	IWB73150-IWB72381	147.4-155.0	**A**/G	-1.68	18/163	3.2	5.0
TWT	NS	*QTWT_NS18.ubo-5B*	IWB61577	5B	72.9	IWB47848-IWB70679	69.3-75.2	**A**/G	-1.44	158/22	3.5	5.7
TWT	NS	*QTWT_NS18.ubo-6A.1*	IWB30932	6A	11.2	IWB36803-IWB71873	6.8-14.3	**A**/G	-1.29	169/14	3.3	5.1
TWT	NS	*QTWT_NS18.ubo-6A.2*	IWB66012	6A	62.1	IWB61420-IWA6033	58.9-66.8	**A**/G	0.95	140/41	3.0	4.6
TWT	NS	*QTWT_NS18.ubo-6B*	IWB29457	6B	20.4	IWB72988-IWB60219	15.2-23.9	**C**/T	-0.74	68/109	3.2	5.0
TWT	NS	*QTWT_NS18.ubo-7A*	IWB71382	7A	154.6	IWB9770-wPt-5949	150.9-158.2	**C**/T	0.81	116/65	3.3	5.2
TWT	NS	*QTWT_NS18.ubo-7B.1*	IWB3274	7B	89.8	IWB68015-IWB13066	86.6-92.9	**C**/T	0.25	64/112	3.2	5.2
TWT	NS	*QTWT_NS18.ubo-7B.2*	IWB60292	7B	120.4	IWB74053-IWA1345	114.9-127.0	**C**/T	-1.72	16/164	5.1	8.7
SPM	NS	*QSPM_NS18.ubo-2A*	IWB72639	2A	107.7	IWB69369-IWB10949	102.0-112.0	**G**/T	-10.43	122/55	3.1	5.5
SPM	NS	*QSPM_NS18.ubo-2B.1*	IWB29827	2B	75.4	IWB62221-IWA10	72.2-78.5	**A**/C	-10.42	43/131	3.2	5.6
SPM	NS	*QSPM_NS18.ubo-2B.2*	IWA7113	2B	161.5	IWB8338-wPt-7004	158.3-164.8	**C**/T	-17.06	168/12	3.1	5.6
SPM	NS	*QSPM_NS18.ubo-4B*	IWB19555	4B	30.8	IWA103-IWB73919	27.6-33.9	**A**/G	-32.19	169/14	3.4	6.0
SPM	NS	*QSPM_NS18.ubo-5A*	IWB33240	5A	9.7	IWB55024-IWB10603	3.0-12.9	**G**/T	23.25	170/11	4.7	9.0
SPM	NS	*QSPM_NS18.ubo-6B*	IWB31754	6B	52.6	wPt-8783-IWA3410	45.4-55.9	**C**/T	-18.82	173/10	3.7	6.7

SKT	NS	*QSKT_NS18.ubo-2B*	IWA1130	2B	88.4	IWB4384-wPt-2664	84-93.2	**C**/T	1.93	171/10	3.7	5.6
SKT	NS	*QSKT_NS18.ubo-5A.1*	IWB69498	5A	80.9	IWB71455-IWB10427	77.5-84.2	**A**/G	-1.55	12/170	3.5	5.4
SKT	NS	*QSKT_NS18.ubo-5A.2*	IWB9777	5A	110.5	IWB9509-IWB72977	106.6-113.7	**A**/G	-2.16	174/9	5.4	8.9
GNO	NS	*QGNO_NS18.ubo-1B*	IWB6730	1B	83.2	IWB71349-IWB67259	79.6-87.1	**A**/G	-4.07	129/46	3.4	6.8
GNO	NS	*QGNO_NS18.ubo-2A.1*	IWA1562	2A	7.8	IWB7398-IWB17231	2.3-11.2	**C**/T	-4.93	21/158	3.3	6.2
GNO	NS	*QGNO_NS18.ubo-2A.2*	IWB8665	2A	114.5	IWB7897-IWA812	109.0-117.6	**C**/T	7.70	13/166	5.0	10.4
GNO	NS	*QGNO_NS18.ubo-2B.1*	IWB69462	2B	60.1	IWB72352-IWB60422	56.4-65.0	**A**/G	-3.83	82/91	3.4	6.5
GNO	NS	*QGNO_NS18.ubo-2B.2*	IWB22630	2B	76.6	IWB62870-IWA50	73.2-80.6	**C**/T	4.33	99/77	4.6	9.3
GNO	NS	*QGNO_NS18.ubo-2B.3*	IWB56173	2B	115.0	IWB26325-IWA6559	110.6-118.7	**C**/T	3.64	102/73	3.3	6.7
GNO	NS	*QGNO_NS18.ubo-2B.4*	IWB12654	2B	132.6	IWB28591-IWB102	129.5-135.8	**C**/T	-4.05	52/126	3.1	5.9
SGW	NS	*QSGW_NS18.ubo-2B.1*	IWB32007	2B	72.1	IWB24241-IWA3924	68.7-77.9	**G**/T	-0.24	79/95	3.8	7.5
SGW	NS	*QSGW_NS18.ubo-2B.2*	IWB52361	2B	122.2	IWA6559-IWA3973	118.7-126.6	**C**/T	0.22	108/68	3.7	7.8
SGW	NS	*QSGW_NS18.ubo-2B.3*	IWB12654	2B	132.6	IWB28591-IWB102	129.5-135.8	**C**/T	-0.23	52/126	3.4	6.8
SGW	NS	*QSGW_NS18.ubo-3A*	wPt-1888	3A	174.4	IWB8784-IWA1457	170.6-181.4	**A**/T	-0.22	122/58	4.1	8.3
SGW	NS	*QSGW_NS18.ubo-6B*	IWA7725	6B	25.2	IWB7778-IWB73576	22.1-28.3	**C**/T	0.19	113/67	3.2	6.2
GLE	NS	*QGLE_NS18.ubo-4B.1*	IWB25162	4B	15.6	IWB4336-IWB73117	12.1-18.7	**C**/T	-0.16	93/84	4.1	8.3
GLE	NS	*QGLE_NS18.ubo-4B.2*	IWB56642	4B	114.0	IWB32863-IWB67498	110.4-118.8	**A**/G	-0.15	52/125	3.5	7.1
GLE	NS	*QGLE_NS18.ubo-5B*	IWB39735	5B	54.0	IWB71672-IWB24135	50.2-57.8	**A**/G	0.15	88/88	3.2	6.4
GWI	NS	*QGWI_NS18.ubo-2A*	IWB72262	2A	197.6	IWB12196-IWB72976	193.4-200.7	**A**/C	0.11	134/41	5.0	10.7
GWI	NS	*QGWI_NS18.ubo-6A*	IWB74235	6A	122.1	IWA7572-IWB6085	119-125.3	**A**/G	-0.08	116/62	3.2	6.2
GWI	NS	*QGWI_NS18.ubo-7B*	IWB55430	7B	0.1	IWB22624-wPt-7975	0.1-3.7	**C**/T	-0.08	58/121	3.6	7.3

[1] Treat.: treatment. [2] marker position of the peak marker based on the tetraploid wheat consensus map (Maccaferri et al., 2015a). [3] confidence intervals based on LD of the UNIBO-Durum Panel. [4] the allele effect is referred to the allele highlighted in bold. [5] -log (p-value) refers to p-value < 0.001.

Table A3.5. List of GWAS-QTLs significantly associated with the traits days to heading (HD), days to maturity (DTM), plant height (PH), grain yield (GY), thousand kernel weight (TKW), test weight (TWT), number of spikes per linear meter (SPM), number of spikelets per spike (SKT), grain number per spike (GNO), grain weight per spike (SGW), grain length (GLE), and grain width (GWI) under heat stress condition in the crop season of 2018.

Trait	Treat. [1]	QTL ID	Peak marker	Chr	Marker position (cM) [2]	Flanking Markers	Confidence interval (cM) [3]	Alleles [4]	Effect	Allele Frequency	-log(p-value) [5]	R^2 (%)
HD	HS	*QHD_HS18.ubo-1B*	IWB68893	1B	43.6	IWB7810-IWA44	39.9-46.9	**A**/G	-3.8	166/13	3.8	5.4
HD	HS	*QHD_HS18.ubo-2B.1*	IWB58948	2B	0.1	IWB12069-IWB22939	0.1-3.5	**A**/G	3.0	148/31	3.2	4.5
HD	HS	*QHD_HS18.ubo-2B.2*	IWB59983	2B	165.9	IWB64535-IWB21324	161.8-169.5	**C**/T	-2.7	145/34	3.4	4.6
HD	HS	*QHD_HS18.ubo-3B.1*	IWB43450	3B	41.3	wPt-8686-IWB29048	36.8-44.6	**C**/T	-2.6	142/35	3.4	4.8
HD	HS	*QHD_HS18.ubo-3B.2*	wPt-9432	3B	74.3	IWB8392-IWB41807	70.1-79.1	**A**/T	-2.6	34/139	3.2	4.4
HD	HS	*QHD_HS18.ubo-3B.3*	IWB65493	3B	158.5	IWB9158-IWA1094	152.6-163.2	**C**/T	-2.6	50/128	3	4.1
HD	HS	*QHD_HS18.ubo-4B*	IWB32911	4B	12	IWB73905-IWA2125	7.4-15.5	**C**/T	-3.1	33/144	3.9	5.7
HD	HS	*QHD_HS18.ubo-5A*	IWB9126	5A	106.6	IWB65371-IWB9777	102.2-110.5	**A**/C	-4.1	166/14	3.8	5.3
HD	HS	*QHD_HS18.ubo-6A*	IWB38780	6A	72.4	IWA6724-IWB9445	68.3-83.7	**G**/T	-3.5	164/16	3.1	4.2
HD	HS	*QHD_HS18.ubo-7A*	IWB49879	7A	113.1	IWB65077-IWA3941	109.1-118	**C**/T	-3.9	21/159	4.2	5.9
HD	HS	*QHD_HS18.ubo-7B*	wPt-7219	7B	210.7	IWB69563-wPt-0126	206.9-214.3	**A**/T	-2.5	74/97	4.0	5.8
DTM	HS	*QDTM_HS18.ubo-1A*	IWA6649	1A	10.6	wPt-3870-IWB63712	6.7-15.3	**A**/G	-4.2	149/32	3.3	5.1
DTM	HS	*QDTM_HS18.ubo-3A*	wPt-7992	3A	9.6	IWB65712-IWA851	5.9-16.5	**A**/T	-2.8	37/139	3.8	6.3
DTM	HS	*QDTM_HS18.ubo-4A*	IWB50371	4A	41.3	IWA4321-IWB32978	37.8-44.6	**C**/T	4.1	10/171	3.1	4.7
DTM	HS	*QDTM_HS18.ubo-4B.1*	IWB12274	4B	3.9	IWB73506-IWA1768	0.3-7.4	**A**/C	-3.0	25/145	3.2	5.3
DTM	HS	*QDTM_HS18.ubo-4B.2*	IWB32911	4B	12	IWB73905-IWA2125	7.4-15.5	**C**/T	-3.1	33/143	4.2	6.9
DTM	HS	*QDTM_HS18.ubo-4B.3*	IWB45064	4B	16	IWB8084-IWA3290	12.8-19.3	**C**/T	2.8	147/29	3.0	4.7
DTM	HS	*QDTM_HS18.ubo-4B.4*	IWB34794	4B	69.3	IWB44068-IWB72018	65.5-72.4	**A**/G	2.8	137/38	4.5	7.6
DTM	HS	*QDTM_HS18.ubo-5A.1*	IWB34418	5A	142.5	IWB72992-IWA2350	138.6-146.5	**A**/G	2.6	84/95	4.4	7.5
DTM	HS	*QDTM_HS18.ubo-5A.2*	IWB10692	5A	150.3	IWB72051-IWB72381	147.1-155.0	**C**/T	-5.0	163/14	3.1	4.7
DTM	HS	*QDTM_HS18.ubo-5A.3*	IWB7730	5A	199.1	IWB68625-IWA7880	196.2-206.0	**C**/T	-3.7	166/11	3.1	5.0
DTM	HS	*QDTM_HS18.ubo-6A.1*	IWB73616	6A	40.9	IWB3978-IWB24955	37.3-44.1	**C**/T	-2.8	143/33	3.2	5.0
DTM	HS	*QDTM_HS18.ubo-6A.2*	IWB50963	6A	72.4	IWA6724-IWB9445	68.3-83.7	**A**/G	-3.2	160/17	3.1	4.7
DTM	HS	*QDTM_HS18.ubo-7A.1*	IWB64582	7A	30.9	IWB26552-IWB7431	24.6-34.0	**A**/G	3.2	16/163	3.2	5.0

DTM	HS	*QDTM_HS18.ubo-7A.2*	IWB25236	7A	43.2	IWB3124-IWB28409	39.8-48.5	**A**/G	3.7	16/165	3.7	6.0
DTM	HS	*QDTM_HS18.ubo-7A.3*	IWB60068	7A	89.6	IWB66777-IWB65337	84.6-92.9	**A**/G	2.8	44/132	3.6	5.9
DTM	HS	*QDTM_HS18.ubo-7B*	wPt-7219	7B	210.7	IWB69563-wPt-0126	206.9-214.3	**A**/T	-2.3	74/96	3.5	6.1
PH	HS	*QPH_HS18.ubo-1A*	IWB68798	1A	1.7	wPt-4676-wPt-0196	0.1-5.2	**C**/T	4.8	71/111	4.0	7.7
PH	HS	*QPH_HS18.ubo-1B*	IWB47684	1B	33	IWB3666-IWA284	29.9-36.9	**C**/T	7.9	172/10	3.2	5.8
PH	HS	*QPH_HS18.ubo-2A.1*	IWB66088	2A	118.4	IWB7707-IWB71282	114.8-123.9	**A**/G	8.4	11/170	3.2	6.0
PH	HS	*QPH_HS18.ubo-2A.2*	IWB36028	2A	181.2	IWB74851-IWB71948	176.5-186.1	**A**/G	-8.6	165/14	3.9	7.6
PH	HS	*QPH_HS18.ubo-2B*	IWB68283	2B	140.3	IWA8195-IWA7652	137.2-143.9	**C**/T	6.6	26/149	3.4	6.6
PH	HS	*QPH_HS18.ubo-4A.1*	IWB71180	4A	57.1	IWB53508-IWA402	51.3-63.8	**A**/G	-5.9	157/20	3.1	5.8
PH	HS	*QPH_HS18.ubo-4A.2*	IWB61552	4A	171.4	IWB71811-IWB18740	167.6-175.8	**G**/T	8.2	17/158	4.0	7.9
PH	HS	*QPH_HS18.ubo-4B*	IWB63893	4B	13.7	IWB69930-IWB45994	10.2-17.6	**A**/G	-5.6	40/139	3.5	6.5
PH	HS	*QPH_HS18.ubo-5A.1*	IWB54064	5A	43.8	IWB66553-IWB47433	40.6-47.3	**A**/G	8.9	10/169	3.3	6.5
PH	HS	*QPH_HS18.ubo-5A.2*	IWB10692	5A	150.3	IWB72051-IWB72381	147.1-155.0	**C**/T	-10.1	164/14	3.1	5.9
PH	HS	*QPH_HS18.ubo-5B.1*	IWB30992	5B	2.7	wPt-1302-IWA4790	0.1-6.5	**C**/T	9.2	11/172	3.8	7.1
PH	HS	*QPH_HS18.ubo-5B.2*	IWB56221	5B	145.9	IWB8035-IWB6823	142.6-149.0	**A**/G	-7.8	167/12	3.1	5.8
PH	HS	*QPH_HS18.ubo-6B.1*	wPt-2689	6B	2.7	wPt-0351-IWB1461	2.2-6.1	**A**/T	-9.3	167/13	3.9	7.5
PH	HS	*QPH_HS18.ubo-6B.2*	IWB6478	6B	8	wPt-3774-wPt-2714	4.8-11.5	**C**/T	-9.9	167/13	4.4	8.6
PH	HS	*QPH_HS18.ubo-6B.3*	IWB73427	6B	69.9	IWB5662-IWA7818	66.5-73.5	**A**/C	-5.3	43/131	3.3	6.6
GY	HS	*QGY_HS18.ubo-2A*	IWA2731	2A	67.3	IWB35896-IWA3193	63.4-74.6	**C**/T	0.8	166/11	4.5	8.8
GY	HS	*QGY_HS18.ubo-3B*	IWB64968	3B	8	IWB11523-IWB14117	4.9-12.3	**A**/G	-0.5	135/40	3.4	6.2
GY	HS	*QGY_HS18.ubo-5B*	rPt-7889	5B	144.5	IWB68186-IWA4182	141.2-148.6	**A**/T	0.5	142/29	3.6	6.8
GY	HS	*QGY_HS18.ubo-7A*	IWB71609	7A	45.9	IWB9603-IWB24920	41.5-49.9	**A**/C	0.5	144/29	4.0	7.7
TKW	HS	*QTKW_HS18.ubo-1B*	IWB73390	1B	153.7	IWB18553-wPt-5915	149.7-157.8	**A**/G	-2.3	91/87	3.4	5.8
TKW	HS	*QTKW_HS18.ubo-2A*	IWB75252	2A	208.4	IWB4717-wPt-2696	204.7-211.5	**A**/G	-2.8	43/131	3.5	6.6
TKW	HS	*QTKW_HS18.ubo-2B*	IWB59746	2B	90.8	IWA4605-IWA326	87.7-100.7	**C**/T	3.8	24/147	3.5	6.5
TKW	HS	*QTKW_HS18.ubo-3B.1*	IWB66970	3B	4.2	IWB13576-IWB35536	1.1-7.4	**A**/G	3.1	38/136	3.1	5.5
TKW	HS	*QTKW_HS18.ubo-3B.2*	IWB73014	3B	19.4	IWB1925-IWB72015	15.4-22.8	**C**/T	2.8	60/116	3.5	6.3
TKW	HS	*QTKW_HS18.ubo-5A*	IWB73200	5A	136.3	IWB8003-IWB3132	132.3-140.1	**A**/G	-3.1	103/74	3.9	7.2
TKW	HS	*QTKW_HS18.ubo-5B*	IWB6532	5B	165.7	IWB8583-IWB9424	160.6-171.2	**C**/T	3.2	30/145	4.1	7.7
TKW	HS	*QTKW_HS18.ubo-6B*	IWB24238	6B	85.9	IWB58026-IWB71758	82.5-89.1	**G**/T	-2.3	61/116	3.0	5.2
TKW	HS	*QTKW_HS18.ubo-7B*	IWB44493	7B	130.7	IWA6618-IWB3095	127.6-135.6	**C**/T	2.5	45/131	3.1	5.4
TWT	HS	*QTWT_HS18.ubo-2A*	IWB49411	2A	8.4	IWB7398-IWB71860	2.3-12.2	**C**/T	1.1	148/29	3.0	5.6

TWT	HS	*QTWT_HS18.ubo-2B.1*	IWB6017	2B	88.4	IWB4384-wPt-2664	84.0-93.2	**A**/G	2.2	10/162	3.0	5.6
TWT	HS	*QTWT_HS18.ubo-2B.2*	IWB53581	2B	181.6	wPt-4892-IWB15331	177.5-185.8	**A**/G	-1.4	140/38	3.7	7.1
TWT	HS	*QTWT_HS18.ubo-2B.3*	wPt-0891	2B	191.5	wPt-8284-IWB31342	188.2-191.9	**A**/T	1.1	46/127	3.0	5.5
TWT	HS	*QTWT_HS18.ubo-3A*	IWB22148	3A	129.2	IWB58868-IWB12566	125.5-135.1	**A**/G	1.8	9/171	3.2	5.8
TWT	HS	*QTWT_HS18.ubo-3B*	IWB63250	3B	76.5	wPt-5939-IWB73053	72.9-79.6	**A**/G	-0.9	94/78	3.1	6.0
TWT	HS	*QTWT_HS18.ubo-5A*	IWB34418	5A	142.5	IWB72992-IWA2350	138.6-146.5	**A**/G	-0.9	85/93	3.2	5.8
TWT	HS	*QTWT_HS18.ubo-5B.1*	IWB25204	5B	34.2	IWB72021-IWB72886	30.3-38.1	**A**/G	1.0	87/86	4.1	7.9
TWT	HS	*QTWT_HS18.ubo-5B.2*	IWB40999	5B	40.3	IWB54368-IWB66993	35.0-43.8	**A**/C	-1.0	84/85	3.8	7.7
TWT	HS	*QTWT_HS18.ubo-7A*	IWB27700	7A	82.4	IWB36370-IWA3673	78.9-87.7	**C**/T	1.9	14/165	3.0	5.6
SPM	HS	*QSPM_HS18.ubo-4B*	IWB19555	4B	30.8	IWA103-IWB73919	27.6-33.9	**A**/G	-20.4	169/14	3.1	5.5
SPM	HS	*QSPM_HS18.ubo-5A*	IWB6716	5A	208.8	IWB48691-IWB35997	201.1-213.8	**A**/C	-12.0	154/24	3.5	6.7
SPM	HS	*QSPM_HS18.ubo-6A*	IWB72784	6A	4.8	wPt-9075-IWB7466	0.9-8.5	**A**/G	-5.1	81/96	3.2	5.8
SKT	HS	*QSKT_HS18.ubo-1A*	IWB72019	1A	59.7	IWB69155-IWA2995	55.3-67.7	**A**/G	0.7	60/114	3.7	7.7
SKT	HS	*QSKT_HS18.ubo-2A.1*	IWA2938	2A	176.5	IWB7563-IWB72723	171.0-179.6	**A**/C	-0.6	83/94	3.8	7.9
SKT	HS	*QSKT_HS18.ubo-2A.2*	IWB22672	2A	208.7	IWB4717-wPt-0623	204.7-212.1	**A**/G	-0.7	124/59	3.1	5.7
SKT	HS	*QSKT_HS18.ubo-7A.1*	IWB11337	7A	10.3	IWB624-IWA1735	7.2-14.1	**C**/T	-0.7	76/97	3.4	6.7
SKT	HS	*QSKT_HS18.ubo-7A.2*	IWB52737	7A	148	IWB4764-IWB418	144.8-152.8	**A**/G	0.6	64/105	3.0	6.1
GNO	HS	*QGNO_HS18.ubo-1B*	IWB72607	1B	116.7	IWB60038-IWA3497	113.4-120.8	**A**/G	4.9	37/137	4.1	7.3
GNO	HS	*QGNO_HS18.ubo-2A.1*	IWB69005	2A	199.5	IWB72339-IWA5978	194.8-204.3	**C**/T	-3.9	37/143	3.3	5.4
GNO	HS	*QGNO_HS18.ubo-2A.2*	IWB60386	2A	206.8	IWB72975-IWB10090	201.1-210.6	**A**/G	3.7	148/34	3.0	4.9
GNO	HS	*QGNO_HS18.ubo-2B*	IWB33109	2B	76.6	IWB62870-IWB8031	73.2-80.6	**C**/T	-3.6	80/99	4.7	8.6
GNO	HS	*QGNO_HS18.ubo-3B*	IWB23630	3B	51.9	IWB6460-wPt-1159	48.8-55.0	**A**/C	2.9	91/81	3.2	5.5
GNO	HS	*QGNO_HS18.ubo-4A*	rPt-7285	4A	134.1	IWB66725-IWB53635	130.8-139.2	**A**/T	2.8	95/74	3.2	5.8
GNO	HS	*QGNO_HS18.ubo-4B*	IWB70794	4B	3	IWB33242-IWA1768	0.1-7.4	**A**/G	-5.8	11/171	3.2	5.3
GNO	HS	*QGNO_HS18.ubo-7A.1*	IWB72301	7A	44.9	IWB9603-IWB74166	41.5-49.7	**C**/T	3.2	111/62	3.3	5.9
GNO	HS	*QGNO_HS18.ubo-7A.2*	IWB7484	7A	68.7	wPt-7785-IWB70642	64.4-74.4	**C**/T	-0.9	98/79	3.9	6.7
SGW	HS	*QSGW_HS18.ubo-1B.1*	IWB69351	1B	96.2	IWB5761-IWB48950	92.8-99.7	**A**/G	0.2	47/127	3.1	6.5
SGW	HS	*QSGW_HS18.ubo-1B.2*	IWB72607	1B	116.7	IWB60038-IWA3497	113.4-120.8	**A**/G	0.3	37/137	4.6	9.3
SGW	HS	*QSGW_HS18.ubo-3A.1*	IWB47601	3A	65.9	IWB72751-IWB71028	59.1-72.2	**C**/T	0.3	165/14	4.0	7.5
SGW	HS	*QSGW_HS18.ubo-3A.2*	IWB71564	3A	122.3	IWB7801-IWB58868	118.9-125.5	**C**/T	-0.2	36/143	3.0	5.3
SGW	HS	*QSGW_HS18.ubo-3A.3*	IWB7623	3A	141.6	IWB23450-IWB72058	136.5-147.1	**A**/G	-0.3	14/168	3.4	6.2
SGW	HS	*QSGW_HS18.ubo-4A*	IWB26429	4A	118.5	IWB8782-IWB22203	114.6-127.2	**A**/G	-0.2	26/156	3.9	7.4

SGW	HS	*QSGW_HS18.ubo-5B.1*	IWB44431	5B	112.3	wPt-0498-IWB73983	109.0-115.4	**A**/G	-0.3	18/160	4.0	7.9
SGW	HS	*QSGW_HS18.ubo-5B.2*	IWB68333	5B	117.1	IWB10362-IWB11813	113.9-121.7	**C**/T	0.3	162/16	4.2	8.3
SGW	HS	*QSGW_HS18.ubo-7A*	IWB7484	7A	68.7	wPt-7785-IWB70642	64.4-74.4	**A**/C	0.4	173/10	4.7	8.9
SGW	HS	*QSGW_HS18.ubo-7B*	IWB72979	7B	97.4	IWB73892-IWB5830	94.2-102.6	**C**/T	-0.3	14/164	3.8	7.0
GLE	HS	*QGLE_HS18.ubo-4B*	IWB73600	4B	15.6	IWB4336-IWB73117	12.1-18.7	**A**/G	0.15	99/77	3.2	6.3
GWI	HS	*QGWI_HS18.ubo-2A*	wPt-9277	2A	198.7	IWB72339-IWB41520	194.8-201.1	**A**/T	-0.08	43/135	3.1	5.8
GWI	HS	*QGWI_HS18.ubo-3A.1*	IWB6655	3A	115.75	wPt-8362-IWB65658	112.7-119.5	**A**/G	0.13	163/15	3.3	6.3
GWI	HS	*QGWI_HS18.ubo-3A.2*	IWB71615	3A	122.7	IWB65658-IWB58868	119.5-125.5	**A**/G	-0.13	15/163	3.3	6.3
GWI	HS	*QGWI_HS18.ubo-3B*	IWB73813	3B	23.4	IWB8426-IWB68984	19.4-26.6	**A**/C	-0.08	121/58	3.9	7.6
GWI	HS	*QGWI_HS18.ubo-4A.1*	IWB53675	4A	162.8	IWB7370-IWB23688	159.5-167.0	**A**/G	0.08	138/40	3.5	6.7
GWI	HS	*QGWI_HS18.ubo-4A.2*	IWB26246	4A	171.4	IWB72285-IWB18740	168.6-175.8	**G**/T	-0.08	59/116	3.1	5.9
GWI	HS	*QGWI_HS18.ubo-5A*	IWB55779	5A	136.3	IWB8003-IWB3132	132.3-140.1	**A**/G	0.08	75/102	3.5	7.0
GWI	HS	*QGWI_HS18.ubo-5B*	IWA8031	5B	165.2	IWB8583-IWB68167	160.6-167.6	**C**/T	-0.11	146/29	5.1	10.8
GWI	HS	*QGWI_HS18.ubo-6A*	IWB73616	6A	40.9	IWB3978-IWB24955	37.3-44.1	**C**/T	-0.11	148/31	4.0	7.8
GWI	HS	*QGWI_HS18.ubo-7A*	IWB66726	7A	53.1	IWB24920-IWB59818	49.9-56.6	**A**/C	0.08	48/130	3.2	6.0
GWI	HS	*QGWI_HS18.ubo-7B.1*	IWB60028	7B	0.1	IWB22624-IWB20228	0.1-3.3	**C**/T	-0.07	59/120	3.1	5.8
GWI	HS	*QGWI_HS18.ubo-7B.2*	IWB74056	7B	15.8	IWB6455-wPt-7318	10.2-19.2	**C**/T	-0.06	92/87	3.3	6.2

[1] Treat.: treatment. [2] marker position of the peak marker based on the tetraploid wheat consensus map (Maccaferri et al., 2015a). [3] confidence intervals based on LD of the UNIBO-Durum Panel. [4] the allele effect is referred to the allele highlighted in bold. [5] -log (p-value) refers to p-value < 0.001.

Table A3.6. List of GWAS-QTLs for reaction norm index (Δ) significantly associated with the traits days to heading (HD), days to maturity (DTM), plant height (PH), grain yield (GY), thousand kernel weight (TKW), test weight (TWT), number of spikes per linear meter (SPM), number of spikelets per spike (SKT), grain number per spike (GNO), grain weight per spike (SGW), grain length (GLE), and grain width (GWI) in the crop season of 2018.

Trait	Treat. [1]	QTL ID	Peak marker	Chr	Marker position (cM) [2]	Flanking Markers	Confidence interval (cM) [3]	Alleles [4]	Effect	Allele Frequency	-log(p-value) [5]	R^2 (%)
HD	Δ	*QHD_Δ18.ubo-1B*	IWB4238	1B	65.2	IWB46080-IWB9661	60.2-68.3	**C**/T	-2.65	14/165	3.01	5.2
HD	Δ	*QHD_Δ18.ubo-3B*	IWB73357	3B	92.1	IWB66265-IWA6720	88.9-96.3	**A**/G	-2.02	33/142	3.3	5.9
HD	Δ	*QHD_Δ18.ubo-4B*	IWB61575	4B	91.2	IWB71667-IWB73620	87.8-95.1	**A**/G	3.65	172/10	4.3	7.8
HD	Δ	*QHD_Δ18.ubo-6B*	IWB14044	6B	116.8	IWB71618-IWB12455	113.2-120.7	**C**/T	-2.1	34/147	3.5	6.3
HD	Δ	*QHD_Δ18.ubo-7A*	IWB11441	7A	75.9	IWB9080-IWB8251	70.7-78	**A**/G	2.69	156/22	3	5.5
DTM	Δ	*QDTM_Δ18.ubo-3A*	wPt-7992	3A	9.6	IWB65712-IWA851	5.9-16.5	**A**/T	-1.88	37/139	4.1	8
DTM	Δ	*QDTM_Δ18.ubo-4B*	IWB8197	4B	2.8	IWB33242-IWA1768	0.1-7.4	**A**/G	1.58	136/46	3.6	6.5
DTM	Δ	*QDTM_Δ18.ubo-5A.1*	IWB55564	5A	136.3	IWB8003-IWB3132	132.3-140.1	**A**/G	-1.62	79/86	4	7.8
DTM	Δ	*QDTM_Δ18.ubo-5A.2*	IWB58257	5A	141.4	IWB66717-IWA2350	138.3-146.5	**A**/G	1.81	88/89	4.5	8.9
DTM	Δ	*QDTM_Δ18.ubo-6A*	IWB8946	6A	15.2	IWB75264-IWA1283	11.6-21.4	**A**/G	1.26	102/80	3.1	5.5
DTM	Δ	*QDTM_Δ18.ubo-7A*	IWB59995	7A	32.6	IWB73683-IWB3124	28.6-39.8	**C**/T	-1.78	28/153	3.4	6.1
PH	Δ	*QPH_Δ18.ubo-1B*	IWB7459	1B	136.1	IWB8004-IWB67910	130.2-139.2	**A**/G	4.2	120/53	3.3	6.2
PH	Δ	*QPH_Δ18.ubo-2A*	IWB66088	2A	118.4	IWB7707-IWB71282	114.8-123.9	**A**/G	8.9	11/170	4.1	7.6
PH	Δ	*QPH_Δ18.ubo-2B*	IWB22852	2B	74.5	IWB6607-IWA3924	71-77.9	**C**/T	9.37	14/166	3.1	5.6
PH	Δ	*QPH_Δ18.ubo-3A*	IWB47601	3A	65.9	IWB72751-IWB71028	59.1-72.2	**C**/T	6.56	165/14	3.2	5.7
PH	Δ	*QPH_Δ18.ubo-4B*	IWA103	4B	27.6	IWB59588-IWB12149	23.5-30.8	**C**/T	9.36	18/164	3.1	5.3
PH	Δ	*QPH_Δ18.ubo-5A.1*	IWB54064	5A	43.8	IWB66553-IWB47433	40.6-47.3	**A**/G	9.36	10/169	4.2	8
PH	Δ	*QPH_Δ18.ubo-5A.2*	IWB55564	5A	136.3	IWB8003-IWB3132	132.3-140.1	**A**/G	-3.85	79/97	3	5.4
PH	Δ	*QPH_Δ18.ubo-5B.1*	IWB5398	5B	2.7	wPt-1302-IWA4790	0.1-6.5	**A**/G	9.47	11/172	4.6	8.6
PH	Δ	*QPH_Δ18.ubo-5B.2*	IWB20597	5B	10.1	IWA4313-IWA5176	6.8-13.5	**A**/G	7.74	11/170	3.2	5.9
PH	Δ	*QPH_Δ18.ubo-6B.1*	wPt-5383	6B	8	wPt-3774-wPt-2714	4.8-11.5	**A**/T	7.69	13/165	3.3	6
PH	Δ	*QPH_Δ18.ubo-6B.2*	IWB73427	6B	69.9	IWB5662-IWA7818	66.5-73.5	**A**/C	-4.64	43/131	3.1	5.7
GY	Δ	*QGY_Δ18.ubo-2A*	IWA2731	2A	67.3	IWB35896-IWA3193	63.4-74.6	**C**/T	12	166/11	3.1	6.6
GY	Δ	*QGY_Δ18.ubo-2B*	IWB1524	2B	175.7	IWB5439-wPt-3632	172.3-179.3	**C**/T	-12.8	9/169	3	6.3

GY	Δ	*QGY_Δ18.ubo-7A1*	IWB71609	7A	45.9	IWB9603-IWB67722	41.5-49.5	**A**/C	8.7	144/29	3.2	6.8
GY	Δ	*QGY_Δ18.ubo-7A.2*	IWB27289	7A	186.2	IWB29819-IWA865	182.9-189.5	**C**/T	6.93	110/61	3	6.5
GY	Δ	*QGY_Δ18.ubo-7B*	IWB72504	7B	97.4	IWB73892-IWB5830	94.2-102.6	**C**/T	-9.2	12/162	3	5.4
TKW	Δ	*QTKW_Δ18.ubo-3B*	IWB8426	3B	19.4	IWB1925-IWB72015	15.42-22.8	**A**/G	-4.76	84/90	3.1	4.9
TKW	Δ	*QTKW_Δ18.ubo-5A.1*	IWB9126	5A	106.6	IWB65371-IWA3827	102.2-110.5	**A**/C	7.7	165/13	3	4.6
TKW	Δ	*QTKW_Δ18.ubo-5A.2*	IWB72361	5A	151.8	IWB73150-IWB72381	147.4-155	**A**/G	-9.2	162/16	3.1	4.7
TKW	Δ	*QTKW_Δ18.ubo-5B*	IWB20326	5B	74.8	IWB47848-IWB33391	69.3-82	**A**/G	-8.1	23/157	3.5	5.5
TKW	Δ	*QTKW_Δ18.ubo-6B*	IWB7936	6B	27.1	IWB65635-IWA52	23.9-31.3	**C**/T	-8.7	167/12	3.1	4.8
TWT	Δ	*QTWT_Δ18.ubo-1B.1*	IWB7183	1B	62.2	IWA4556-IWB63365	59.1-65.3	**C**/T	-1.66	21/153	3.3	6.6
TWT	Δ	*QTWT_Δ18.ubo-1B.2*	IWA7560	1B	67.6	IWB8182-IWB5737	63.3-70.5	**A**/C	1	109/63	3.1	6.4
TWT	Δ	*QTWT_Δ18.ubo-2B.1*	IWB35071	2B	128.4	IWB73040-IWA3935	124.9-131.6	**A**/C	-1.33	28/147	3	6.1
TWT	Δ	*QTWT_Δ18.ubo-2B.2*	IWA8295	2B	140.3	IWB74096-IWA7652	136.7-143.9	**G**/T	-1.63	147/30	3.4	6.8
TWT	Δ	*QTWT_Δ18.ubo-2B.3*	IWA4118	2B	181.6	wPt-4892-IWB6614	177.5-185.7	**A**/G	-1.9	160/17	3.2	6.4
TWT	Δ	*QTWT_Δ18.ubo-4B*	IWB7100	4B	97.5	IWB57170-IWA1861	94-101.3	**C**/T	-1.36	150/27	3.1	6
TWT	Δ	*QTWT_Δ18.ubo-5A.1*	IWB52461	5A	106.6	IWB1680-IWA3827	102.2-110.5	**A**/G	-2.25	170/11	3.5	7
TWT	Δ	*QTWT_Δ18.ubo-5A.2*	IWB72361	5A	151.8	IWB73150-IWB72381	147.4-155	**A**/G	-2.59	162/16	3.6	7.4
TWT	Δ	*QTWT_Δ18.ubo-5B.1*	IWB25204	5B	34.2	IWB72021-IWA1965	30.3-38.1	**A**/G	1.15	87/86	3.4	7.8
TWT	Δ	*QTWT_Δ18.ubo-5B.2*	IWB70387	5B	120.1	IWB6202-IWB36002	116.9-125.75	**A**/G	-1.29	101/71	3.7	7.9
TWT	Δ	*QTWT_Δ18.ubo-6B*	IWB10612	6B	4.6	wPt-0351-IWA6759	2.2-8	**A**/G	1.88	14/163	3.2	6.4
TWT	Δ	*QTWT_Δ18.ubo-7A.1*	IWB11441	7A	75.9	IWB9080-IWA8161	70.7-79.9	**A**/G	-1.92	155/21	3.4	7.7
TWT	Δ	*QTWT_Δ18.ubo-7A.2*	IWB27700	7A	82.4	IWB36370-IWA3673	78.9-87.7	**C**/T	2.62	14/165	3.7	7.5
SPM	Δ	*QSPM_Δ18.ubo-1B*	IWB23021	1B	143.6	IWB72561-IWB18553	140.1-149.7	**C**/T	-11.8	164/16	3.1	6.1
SPM	Δ	*QSPM_Δ18.ubo-2A.1*	IWB48587	2A	97.3	IWB9395-IWB48756	93.2-101.5	**C**/T	10.3	39/141	3.8	7.8
SPM	Δ	*QSPM_Δ18.ubo-2A.2*	IWB71845	2A	107.7	IWB69369-IWB10949	102-112	**C**/T	-8.93	55/123	4.5	9.6
SPM	Δ	*QSPM_Δ18.ubo-2A.3*	tPt-2163	2A	208.4	IWB4717-wPt-2696	204.7-211.5	**A**/T	-5.7	63/111	3	5.9
SPM	Δ	*QSPM_Δ18.ubo-5B*	IWB64048	5B	141.7	IWB53460-tPt-1253	138.5-145	**A**/C	8.28	36/139	3.3	6.6
SKT	Δ	*QSKT_Δ18.ubo-2A*	IWA2938	2A	176.5	IWB8707-IWB72723	169.3-179.6	**A**/C	-4.21	83/94	3.3	6.5
SKT	Δ	*QSKT_Δ18.ubo-2B*	IWB9584	2B	88.4	IWB4384-wPt-2664	84-93.2	**A**/G	-10.3	171/10	3	5.7
SKT	Δ	*QSKT_Δ18.ubo-3A*	IWB69546	3A	165.9	wPt-5133-IWB814	161.4-170	**A**/G	-4.65	115/62	3.4	6.6
SKT	Δ	*QSKT_Δ18.ubo-4A*	IWB9999	4A	134.4	IWB66725-IWB53635	130.8-139.2	**C**/T	6.38	161/20	3	5.7
SKT	Δ	*QSKT_Δ18.ubo-5A*	IWB9509	5A	106.6	IWB65371-IWA7135	102.2-111.3	**A**/G	-8.55	17/184	3.8	7.5
SKT	Δ	*QSKT_Δ18.ubo-5B*	IWB66660	5B	135.6	IWB7206-IWA4539	129.7-140.3	**G**/T	-4.74	128/49	3.4	6.8

SKT	Δ	*QSKT_Δ18.ubo-6B.1*	wPt-2479	6B	43.2	wPt-4742-IWB60177	40-51.6	**A**/T	4.6	97/73	3.6	7.4
SKT	Δ	*QSKT_Δ18.ubo-6B.2*	IWB10878	6B	68.4	IWB72416-IWB52913	65.1-71.5	**A**/G	-5.8	136/44	3.2	6.3
GNO	Δ	*QGNO_Δ18.ubo-2B*	IWB39394	2B	149.3	wPt-7305-IWB46631	146-153	**C**/T	-9.37	119/59	3.7	7.4
GNO	Δ	*QGNO_Δ18.ubo-6B*	IWB73072	6B	155.1	IWB72523-IWB73036	151-155.9	**A**/G	-12.1	142/34	3.8	7.9
GNO	Δ	*QGNO_Δ18.ubo-7B*	IWB72504	7B	97.4	IWB73892-IWB5830	94.2-102.6	**C**/T	-13	14/164	3.2	6.1
SGW	Δ	*QSGW_Δ18.ubo-2B*	IWB39394	2B	149.3	wPt-7305-IWB46631	146-153	**C**/T	-7.98	119/59	3.5	7.7
SGW	Δ	*QSGW_Δ18.ubo-7B*	IWB72504	7B	97.4	IWB73892-IWB5830	94.2-102.6	**C**/T	-11.1	14/164	3.1	6.4
GLE	Δ	*QGLE_Δ18.ubo-1B*	IWB461	1B	45.3	IWB34334-IWB10897	42.2-48.7	**C**/T	-2.63	167/9	3.8	8.4
GLE	Δ	*QGLE_Δ18.ubo-2B*	IWB66493	2B	130.1	IWB71648-IWA7850	126.9-133.3	**A**/G	1.59	29/147	3.2	7.0
GLE	Δ	*QGLE_Δ18.ubo-3A*	IWB22387	3A	89.1	IWB11027-IWB1051	84.9-92.8	**A**/G	-1.32	107/71	3.4	7.3
GLE	Δ	*QGLE_Δ18.ubo-4B*	IWB73855	4B	74.7	IWB27710-IWA1382	70.3-77	**C**/T	1.44	68/103	4.5	10.7
GLE	Δ	*QGLE_Δ18.ubo-7A.1*	IWB4723	7A	90.1	IWA3673-IWB34298	87.7-99.5	**G**/T	1.92	22/155	3.3	7.2
GLE	Δ	*QGLE_Δ18.ubo-7A.2*	IWB72581	7A	102.4	IWB34651-IWB72148	99.5-106.4	**C**/T	1.65	24/153	3.5	7.5
GWI	Δ	*QGWI_Δ18.ubo-1A*	IWB59083	1A	115.9	IWB74445-IWB51933	112.4-119.8	**A**/G	-2.11	23/156	3.1	4.6
GWI	Δ	*QGWI_Δ18.ubo-5B*	IWB41039	5B	48.9	IWB7509-IWA7227	45-52.6	**C**/T	-5.17	11/168	3.9	6.1
GWI	Δ	*QGWI_Δ18.ubo-6B*	IWB46089	6B	20.4	IWA3316-IWB60219	17.6-23.9	**G**/T	-3.77	166/12	3.3	5.1

[1] Treat.: treatment. [2] marker position of the peak marker based on the tetraploid wheat consensus map (Maccaferri et al., 2015a). [3] confidence intervals based on LD of the UNIBO-Durum Panel. [4] the allele effect is referred to the allele highlighted in bold. [5] -log (p-value) refers to p-value < 0.001.

Table A3.7. List of GWAS-QTLs significantly associated with the traits days to heading (HD), days to maturity (DTM), plant height (PH), grain yield (GY), thousand kernel weight (TKW), test weight (TWT), number of spikes per linear meter (SPM), number of spikelets per spike (SKT), grain number per spike (GNO), grain weight per spike (SGW), grain length (GLE), and grain width (GWI) under control condition considering both crop season (2018, 2019) in the joint analysis.

Trait	Treat. [1]	QTL ID	Peak marker	Chr	Marker position (cM) [2]	Flanking Markers	Confidence interval (cM) [3]	Alleles [4]	Effect	Allele Frequency	-log(p-value) [5]	R^2 (%)
HD	NS	*QHD_NSJA.ubo-1B.1*	IWB69041	1B	43.6	IWB7810-IWA44	39.9-46.9	**A**/G	-4.83	167/13	3.7	4.2
HD	NS	*QHD_NSJA.ubo-1B.2*	IWB69550	1B	50.2	IWA107-IWA1109	47.1-53.9	**A**/C	-5.85	170/12	4.4	5.2
HD	NS	*QHD_NSJA.ubo-1B.3*	IWB59930	1B	108.1	IWB3634-IWB72580	103.0-111.2	**A**/G	5.18	11/172	3.2	3.5
HD	NS	*QHD_NSJA.ubo-2A.1*	IWB67305	2A	46.6	IWB1280-IWB146	36.8-50.5	**C**/T	-7.10	99/81	3.3	3.6
HD	NS	*QHD_NSJA.ubo-2A.2*	IWB65286	2A	117.6	IWB32024-IWB46634	114.5-121.0	**C**/T	3.77	34/148	3.2	3.5
HD	NS	*QHD_NSJA.ubo-2B*	wPt-8404	2B	31.4	IWB8893-IWB73192	27.7-37.2	**A**/T	-3.10	47/136	3.3	3.7
HD	NS	*QHD_NSJA.ubo-3B*	wPt-9432	3B	74.3	IWB8392-IWB71959	70.1-77.1	**A**/T	-3.19	37/146	3.1	3.4
HD	NS	*QHD_NSJA.ubo-4A*	IWB71865	4A	36.2	IWA1137-IWB32882	25.8-41.3	**C**/T	4.89	14/169	3.7	4.1
HD	NS	*QHD_NSJA.ubo-4B.1*	IWB32911	4B	12.0	IWB73905-IWB28772	7.4-15.5	**C**/T	-3.66	35/148	3.4	3.7
HD	NS	*QHD_NSJA.ubo-4B.2*	IWB52318	4B	53.0	IWB80-IWB72279	48.5-56.1	**A**/G	3.83	22/161	3.2	3.5
HD	NS	*QHD_NSJA.ubo-5A*	IWB10692	5A	150.3	IWB71757-IWB72381	147.1-155.0	**C**/T	-8.20	164/16	4.4	5.2
HD	NS	*QHD_NSJA.ubo-7A*	IWB60067	7A	89.6	IWB66777-IWB65337	84.6-92.9	**C**/T	3.43	44/132	3.2	3.6
HD	NS	*QHD_NSJA.ubo-7B*	IWB60292	7B	120.4	IWB74053-IWA1345	114.9-127.0	**C**/T	4.59	16/167	3.2	3.4
DTM	NS	*QDTM_NSJA.ubo-1B.1*	IWB69041	1B	43.6	IWB7810-IWA44	39.9-46.9	**A**/G	-3.15	167/13	3.0	3.0
DTM	NS	*QDTM_NSJA.ubo-1B.2*	IWB69550	1B	50.2	IWA107-IWA1109	47.1-53.9	**A**/C	-3.53	170/12	3.1	3.1
DTM	NS	*QDTM_NSJA.ubo-2A.1*	IWB67305	2A	46.6	IWB1280-IWB146	36.8-50.5	**C**/T	-5.89	99/81	4.0	4.1
DTM	NS	*QDTM_NSJA.ubo-2A.2*	IWB65286	2A	117.6	IWB32024-IWB46634	114.5-121.0	**C**/T	2.87	34/148	3.4	3.5
DTM	NS	*QDTM_NSJA.ubo-2B*	IWB67650	2B	171.7	IWB59226-IWB7819	167.1-174.8	**A**/G	2.16	44/138	3.0	2.9
DTM	NS	*QDTM_NSJA.ubo-4A.1*	IWB71865	4A	36.2	IWA1137-IWB32882	25.8-41.3	**C**/T	3.75	14/169	3.9	4.0
DTM	NS	*QDTM_NSJA.ubo-4A.2*	wPt-8443	4A	91.6	IWA7058-IWA4425	88.5-97.7	**A**/T	-3.27	164/19	4.1	4.2
DTM	NS	*QDTM_NSJA.ubo-5B*	IWB5705	5B	48.9	IWB7509-IWA6526	45.0-52.2	**C**/T	5.00	169/14	4.3	4.5
DTM	NS	*QDTM_NSJA.ubo-7A*	IWB60067	7A	89.6	IWB66777-IWB65337	84.6-92.9	**C**/T	2.78	44/132	3.8	4.0
DTM	NS	*QDTM_NSJA.ubo-7B*	IWB60292	7B	120.4	IWB74053-IWB73011	114.9-123.2	**C**/T	3.74	16/167	3.7	3.8

PH	NS	*QPH_NSJA.ubo-1A*	IWB72726	1A	1.7	wPt-4676-wPt-0196	0.1-5.2	**A**/G	-4.95	112/71	4.8	4.4
PH	NS	*QPH_NSJA.ubo-1B*	IWB58936	1B	35.8	wPt-2694-IWA4706	31.4-39.1	**A**/G	4.55	142/40	3.1	2.6
PH	NS	*QPH_NSJA.ubo-2A*	IWA3940	2A	162.3	IWB57860-IWA1960	159.1-169.3	**A**/G	-5.67	158/22	3.4	2.9
PH	NS	*QPH_NSJA.ubo-3A*	IWB24367	3A	50.5	IWB9559-IWB74013	43.7-53.7	**C**/T	7.94	167/15	3.4	2.9
PH	NS	*QPH_NSJA.ubo-4A*	wPt-5172	4A	172.0	IWB72285-IWB18740	168.6-175.8	**A**/T	-7.74	167/16	3.8	3.3
PH	NS	*QPH_NSJA.ubo-4B*	IWA103	4B	27.6	IWB59588-IWB12149	23.5-30.8	**C**/T	12.12	18/164	4.4	3.9
PH	NS	*QPH_NSJA.ubo-5A*	IWB10692	5A	150.3	IWB63075-IWB72381	146.5-155.0	**C**/T	-10.89	164/16	3.9	3.4
PH	NS	*QPH_NSJA.ubo-5B*	IWB42376	5B	143.7	IWB7406-IWB8086	140.5-146.8	**C**/T	5.01	147/33	3.4	3.0
PH	NS	*QPH_NSJA.ubo-6A*	IWB113	6A	125.9	IWB16528-IWA1866	122.8-129.4	**A**/C	-5.43	32/150	3.3	2.8
GY	NS	*QGY_NSJA.ubo-1A*	IWB17894	1A	10.6	IWA8622-IWB63712	5.7-15.3	**C**/T	0.66	145/38	3.3	6.4
GY	NS	*QGY_NSJA.ubo-2B*	IWB40126	2B	130.1	IWB71648-IWB28479	126.9-133.9	**C**/T	-0.76	173/10	3.1	5.9
GY	NS	*QGY_NSJA.ubo-6A*	IWB44860	6A	88.2	IWB25454-IWB26292	84.2-91.5	**C**/T	-0.74	10/173	3.2	6.1
GY	NS	*QGY_NSJA.ubo-7A.1*	IWB35137	7A	187.1	IWB29819-IWB20258	182.9-190.5	**A**/C	0.40	73/106	3.1	6.0
GY	NS	*QGY_NSJA.ubo-7A.2*	IWA179	7A	197.6	IWB73864-IWA501	193.9-200.8	**C**/T	0.43	127/54	3.2	6.1
TKW	NS	*QTKW_NSJA.ubo-2A.1*	IWB49366	2A	100.1	IWB43447-IWB8815	96.9-109.0	**A**/G	4.16	149/34	3.4	5.6
TKW	NS	*QTKW_NSJA.ubo-2A.2*	IWB72263	2A	197.6	IWB12196-IWB72876	193.4-201.1	**A**/G	-4.00	39/138	4.5	7.8
TKW	NS	*QTKW_NSJA.ubo-2B*	IWB62322	2B	7.9	IWB22939-wPt-9958	3.5-11.3	**C**/T	-4.17	160/22	3.5	5.7
TKW	NS	*QTKW_NSJA.ubo-6A*	IWB64047	6A	120.5	IWB70454-IWB45558	117.1-123.6	**A**/G	3.17	138/43	3.2	5.2
TKW	NS	*QTKW_NSJA.ubo-7B*	wPt-4843	7B	0.1	IWB22624-wPt-7975	0.1-3.7	**A**/T	3.17	138/45	3.2	5.1
TWT	NS	*QTWT_NSJA.ubo-1B.1*	IWB59930	1B	108.1	IWB3634-IWB72580	103.0-111.2	**A**/G	-1.29	11/172	3.1	4.8
TWT	NS	*QTWT_NSJA.ubo-1B.2*	IWB11265	1B	162.5	IWB71657-wPt-6142	158.0-165.6	**A**/G	0.75	131/48	3.5	5.7
TWT	NS	*QTWT_NSJA.ubo-2A.1*	IWB71223	2A	32.3	wPt-9624-IWA5410	24.9-36.6	**C**/T	0.94	35/148	3.1	5.0
TWT	NS	*QTWT_NSJA.ubo-2A.2*	IWB65286	2A	117.6	IWB32024-IWB46634	114.5-121.0	**C**/T	-1.01	34/148	3.2	5.1
TWT	NS	*QTWT_NSJA.ubo-2B.1*	IWB34613	2B	73.7	IWB56915-IWB39220	70.1-76.8	**A**/G	-1.87	167/15	4.0	6.8
TWT	NS	*QTWT_NSJA.ubo-2B.2*	IWB66226	2B	103.5	IWA326-IWB71922	100.7-107.0	**G**/T	1.24	170/13	3.0	4.7
TWT	NS	*QTWT_NSJA.ubo-2B.3*	IWB49567	2B	122.2	IWA6559-IWA3973	118.7-126.6	**A**/C	-0.75	70/109	3.2	5.4
TWT	NS	*QTWT_NSJA.ubo-2B.4*	IWB68982	2B	130.5	IWB2008-IWB28479	127.6-133.9	**A**/C	0.89	39/142	3.4	5.5
TWT	NS	*QTWT_NSJA.ubo-3B.1*	IWB32274	3B	127.5	IWB9408-IWB20294	122.5-131.4	**A**/G	-0.92	21/162	3.0	4.8
TWT	NS	*QTWT_NSJA.ubo-3B.2*	IWB68475	3B	159.5	IWB32656-IWA1094	155.5-163.2	**A**/C	-0.69	91/92	3.2	5.1
TWT	NS	*QTWT_NSJA.ubo-4A.1*	IWA4321	4A	37.8	IWA2533-IWB32882	35.1-41.3	**C**/T	-1.15	15/168	3.1	4.9
TWT	NS	*QTWT_NSJA.ubo-4A.2*	IWB44783	4A	113.9	IWB28717-IWB48435	110.7-118.3	**A**/G	1.07	161/22	3.8	6.4
TWT	NS	*QTWT_NSJA.ubo-4A.3*	IWB53393	4A	171.2	IWB71811-IWB18740	167.6-175.8	**A**/G	-1.28	164/19	3.6	5.9

TWT	NS	*QTWT_NSJA.ubo-4B*	IWB72399	4B	55.6	IWB72287-IWB72211	51.8-58.7	**A**/G	-0.68	88/93	3.0	4.8
TWT	NS	*QTWT_NSJA.ubo-5A*	IWB10054	5A	70.8	IWB72382-IWB35865	67.7-74.8	**C**/T	-0.97	139/43	3.2	5.2
TWT	NS	*QTWT_NSJA.ubo-6A.1*	IWB30932	6A	11.2	IWB36803-IWB71874	6.8-14.3	**A**/G	-1.39	169/14	4.2	7.1
TWT	NS	*QTWT_NSJA.ubo-6A.2*	IWA6288	6A	67.3	IWB74244-IWA1194	62.8-71.8	**A**/C	-1.34	9/174	3.1	4.9
TWT	NS	*QTWT_NSJA.ubo-6B*	IWB29457	6B	20.4	IWB72988-IWB60219	15.2-23.9	**C**/T	-0.77	69/114	3.8	6.4
TWT	NS	*QTWT_NSJA.ubo-7B.1*	IWB60292	7B	120.4	IWB74053-IWA1345	114.9-127.0	**C**/T	-1.45	16/167	4.4	7.5
TWT	NS	*QTWT_NSJA.ubo-7B.2*	IWB68678	7B	164.4	wPt-7191-IWB71622	159.7-167.4	**A**/C	-0.77	137/45	3.1	4.9
SPM	NS	*QSPM_NSJA.ubo-4A*	wPt-5172	4A	172.0	IWB72285-IWB74069	168.6-173.8	**A**/T	-12.54	167/16	3.3	5.9
SPM	NS	*QSPM_NSJA.ubo-4B.1*	IWA4662	4B	21.7	IWB73227-IWB73001	18.4-26.4	**G**/T	-9.42	42/138	3.3	5.9
SPM	NS	*QSPM_NSJA.ubo-4B.2*	IWB73473	4B	77.8	IWB27260-IWA2823	74.7-81.28	**G**/T	-8.58	151/32	3.2	5.6
SPM	NS	*QSPM_NSJA.ubo-5A.1*	IWA480	5A	9.7	IWB55024-IWB10603	3.0-12.9	**A**/G	-17.10	12/170	4.3	8.0
SPM	NS	*QSPM_NSJA.ubo-5A.2*	IWA1630	5A	58.1	IWB9412-IWB28350	54.9-63.4	**G**/T	11.62	167/15	3.2	5.7
SPM	NS	*QSPM_NSJA.ubo-6A*	IWB39866	6A	127.1	IWB29924-IWB73095	124.0-131.2	**A**/G	8.66	63/117	3.9	7.2
SPM	NS	*QSPM_NSJA.ubo-6B.1*	IWB71380	6B	52.6	wPt-8783-IWB69518	45.4-55.8	**A**/G	15.53	10/173	4.0	7.4
SPM	NS	*QSPM_NSJA.ubo-6B.2*	IWB71917	6B	95.9	IWB72356-IWA670	92.6-100.2	**A**/G	-13.67	170/11	4.1	7.5
SKT	NS	*QSKT_NSJA.ubo-2A*	IWB67306	2A	46.6	IWB1280-IWB146	36.8-50.5	**C**/T	-2.36	99/81	4.1	5.6
SKT	NS	*QSKT_NSJA.ubo-2B*	IWB25860	2B	115.5	IWB73809-IWA6559	112.3-118.7	**A**/G	1.27	23/160	3.6	4.9
SKT	NS	*QSKT_NSJA.ubo-3B*	IWB34730	3B	126.2	IWB9408-IWB20294	122.5-131.4	**A**/G	1.08	19/164	3.0	3.9
SKT	NS	*QSKT_NSJA.ubo-5A.1*	IWA3827	5A	110.5	IWB9509-IWB72977	106.6-113.7	**C**/T	1.75	9/174	3.5	4.6
SKT	NS	*QSKT_NSJA.ubo-5A.2*	IWB21632	5A	186.9	IWB54225-IWB11221	183.7-192.1	**A**/G	-0.92	45/138	3.2	4.3
SKT	NS	*QSKT_NSJA.ubo-5B*	IWB41039	5B	48.9	IWB7509-IWA6526	45.0-52.2	**C**/T	-2.09	11/172	3.2	4.2
SKT	NS	*QSKT_NSJA.ubo-6B*	IWB43133	6B	148.2	IWA5204-IWB9295	145.3-152.2	**A**/G	2.09	14/168	4.1	5.7
GNO	NS	*QGNO_NSJA.ubo-1B*	IWB6730	1B	83.2	IWB71349-IWB34907	79.6-87.1	**A**/G	-4.22	132/49	3.1	5.9
GNO	NS	*QGNO_NSJA.ubo-2A.1*	IWA1562	2A	7.8	IWB7398-IWB17231	2.3-11.2	**C**/T	-5.30	22/161	3.1	5.9
GNO	NS	*QGNO_NSJA.ubo-2A.2*	IWB68412	2A	16.7	IWB73487-IWB69599	13.2-20.5	**A**/G	-3.89	73/109	3.2	6.1
GNO	NS	*QGNO_NSJA.ubo-2A.3*	IWB49366	2A	100.1	IWB26960-IWB66497	95.0-106.5	**A**/G	-7.24	149/34	4.7	9.7
GNO	NS	*QGNO_NSJA.ubo-2A.4*	IWB8665	2A	114.5	IWB7897-IWB72123	109.0-117.6	**C**/T	9.49	14/169	6.2	13.6
GNO	NS	*QGNO_NSJA.ubo-2B.1*	IWA1665	2B	69.9	wPt-6477-IWB12041	65.8-73.2	**A**/G	-4.22	84/95	3.1	5.9
GNO	NS	*QGNO_NSJA.ubo-2B.2*	IWB33109	2B	76.6	IWB62870-IWA50	73.2-80.6	**C**/T	-5.44	80/100	5.4	11.5
GNO	NS	*QGNO_NSJA.ubo-3B*	IWB56459	3B	7.7	IWB8756-IWB14117	4.2-12.3	**C**/T	8.39	9/174	3.3	6.5
GNO	NS	*QGNO_NSJA.ubo-4B*	IWA1861	4B	101.3	IWB29648-IWA2031	98.2-105.5	**C**/T	-4.21	95/88	3.3	6.4
SGW	NS	*QSGW_NSJA.ubo-1B*	IWB9781	1B	93.4	IWB8066-IWB69337	90.1-96.8	**A**/G	0.24	140/42	3.7	7.3

SGW	NS	*QSGW_NSJA.ubo-2A.1*	IWA1562	2A	7.8	IWB7398-IWB17231	2.3-11.2	**C**/T	-0.26	22/161	3.2	6.0
SGW	NS	*QSGW_NSJA.ubo-2A.2*	IWB58322	2A	17.5	IWB66737-IWB35771	13.7-21.9	**A**/G	-0.25	26/157	3.2	6.1
SGW	NS	*QSGW_NSJA.ubo-2B.1*	IWB59946	2B	3.1	IWB12069-IWB7407	0.1-6.6	**C**/T	-0.32	166/16	3.0	5.6
SGW	NS	*QSGW_NSJA.ubo-2B.2*	IWB50438	2B	67.2	IWB69461-IWB41111	60.1-70.7	**C**/T	-0.22	113/66	3.5	6.7
SGW	NS	*QSGW_NSJA.ubo-2B.3*	IWB41367	2B	77.2	IWB56098-IWB8031	73.7-80.6	**G**/T	0.30	56/126	4.6	9.3
SGW	NS	*QSGW_NSJA.ubo-2B.4*	wPt-1140	2B	121.9	IWB62622-IWB21467	114.4-126.6	**A**/T	-0.23	80/102	3.7	7.1
SGW	NS	*QSGW_NSJA.ubo-3A.1*	IWB20642	3A	66.3	IWB71206-IWB68422	64.2-74.1	**A**/G	0.26	126/56	3.4	6.4
SGW	NS	*QSGW_NSJA.ubo-3A.2*	IWA7970	3A	83.5	IWB72653-IWB72035	80.3-86.9	**G**/T	-0.25	38/143	3.1	5.8
SGW	NS	*QSGW_NSJA.ubo-3A.3*	IWB71661	3A	122.1	IWB7801-IWB58868	118.9-125.5	**A**/G	-0.25	38/144	3.2	6.0
SGW	NS	*QSGW_NSJA.ubo-3A.4*	IWB11134	3A	140.5	IWB23450-IWB72058	136.5-147.1	**C**/T	-0.35	12/171	3.0	5.6
SGW	NS	*QSGW_NSJA.ubo-3A.5*	IWB1494	3A	174.4	IWB8784-IWB72043	170.6-177.9	**C**/T	0.18	62/118	3.1	5.7
SGW	NS	*QSGW_NSJA.ubo-6B*	IWB1948	6B	90.3	wPt-6889-IWB74068	86.7-93.4	**A**/G	0.24	149/32	3.0	5.7
GLE	NS	*QGLE_NSJA.ubo-3A.1*	IWB72751	3A	59.1	IWB71974-IWB67595	55.3-64.2	**G**/T	-0.18	135/47	3.2	6.0
GLE	NS	*QGLE_NSJA.ubo-3A.2*	IWB72223	3A	82.6	IWA1019-IWB72035	79.5-86.9	**A**/G	0.15	113/69	3.1	5.8
GLE	NS	*QGLE_NSJA.ubo-4A*	IWA2383	4A	91.3	wPt-7355-IWB72783	87.8-94.3	**C**/T	-0.20	25/158	3.1	5.9
GLE	NS	*QGLE_NSJA.ubo-4B.1*	IWB25162	4B	15.6	IWB4336-IWB73117	12.1-18.7	**C**/T	-0.15	97/84	3.6	7.0
GLE	NS	*QGLE_NSJA.ubo-4B.2*	IWB27331	4B	48.5	wPt-0872-IWB21302	46.6-56.1	**A**/C	-0.15	127/53	3.5	6.8
GLE	NS	*QGLE_NSJA.ubo-4B.3*	IWB72537	4B	114.0	IWB27735-IWB67498	110.4-118.8	**A**/G	0.15	129/52	3.3	6.5
GLE	NS	*QGLE_NSJA.ubo-6A*	IWB9318	6A	67.3	IWB74244-IWA1194	62.8-71.8	**C**/T	-0.17	50/113	3.2	6.1
GLE	NS	*QGLE_NSJA.ubo-6B*	IWB64219	6B	18.3	IWA8314-wPt-6916	15.2-21.4	**A**/G	0.22	19/164	3.0	5.7
GLE	NS	*QGLE_NSJA.ubo-7A*	IWB61471	7A	82.6	IWA8161-IWB25357	79.9-89.6	**A**/G	-0.23	37/145	3.2	6.1
GWI	NS	*QGWI_NSJA.ubo-2A*	IWB72263	2A	197.6	IWB12196-IWB72126	193.4-201.1	**A**/G	-0.12	39/138	5.3	11.1
GWI	NS	*QGWI_NSJA.ubo-2B*	IWB62322	2B	7.9	IWB22939-wPt-9958	3.5-11.3	**C**/T	-0.10	160/22	3.2	5.9
GWI	NS	*QGWI_NSJA.ubo-6A*	IWB70138	6A	122.1	IWA7572-IWB69444	119.0-125.2	**A**/C	0.11	32/151	3.1	5.8
GWI	NS	*QGWI_NSJA.ubo-7A*	IWB65530	7A	96.2	IWB71389-IWB34651	92.9-99.5	**C**/T	0.12	165/12	3.2	6.0
GWI	NS	*QGWI_NSJA.ubo-7B*	IWB25855	7B	0.1	IWB22624-IWB10879	0.1-3.8	**A**/G	0.09	130/53	4.0	7.7

[1] Treat.: treatment. [2] marker position of the peak marker based on the tetraploid wheat consensus map (Maccaferri et al., 2015a). [3] confidence intervals based on LD of the UNIBO-Durum Panel. [4] the allele effect is referred to the allele highlighted in bold. [5] -log (p-value) refers to p-value < 0.001.

Table A3.8. List of GWAS-QTLs significantly associated with the traits days to heading (HD), days to maturity (DTM), plant height (PH), grain yield (GY), thousand kernel weight (TKW), test weight (TWT), number of spikes per linear meter (SPM), number of spikelets per spike (SKT), grain number per spike (GNO), grain weight per spike (SGW), grain length (GLE), and grain width (GWI) under heat stress condition considering both crop season (2018, 2019) in the joint analysis.

Trait	Treat. [1]	QTL ID	Peak marker	Chr	Marker position (cM) [2]	Flanking Markers	Confidence interval (cM) [3]	Alleles [4]	Effect	Allele Frequency	-log(p-value) [5]	R^2 (%)
HD	HS	*QHD_HSJA.ubo-1A*	IWB31959	1A	147.7	IWB9141-IWB7910	144.3-150.2	**A**/C	1.9	27/147	3.1	5.2
HD	HS	*QHD_HSJA.ubo-1B*	IWB69041	1B	43.6	IWB7810-IWA44	39.9-46.9	**A**/G	-2.54	160/12	3.2	5.6
HD	HS	*QHD_HSJA.ubo-2B.1*	IWB32315	2B	5.9	wPt-8737-wPt-9958	0.9-11.3	**A**/G	-3.85	168/7	4.0	7.1
HD	HS	*QHD_HSJA.ubo-2B.2*	IWB59983	2B	165.9	IWB64535-IWB21324	161.8-169.5	**C**/T	-2.2	141/34	4.1	7.3
HD	HS	*QHD_HSJA.ubo-4A*	IWB19834	4A	157.4	IWB9122-wPt-3506	154.0-161.2	**C**/T	2.76	154/21	3.7	6.4
HD	HS	*QHD_HSJA.ubo-4B.1*	IWB32911	4B	12.0	IWA1768-IWB65475	7.4-16.0	**C**/T	-2.05	31/144	3.3	5.7
HD	HS	*QHD_HSJA.ubo-4B.2*	IWB12150	4B	30.8	IWA103-IWB73919	27.6-33.9	**A**/G	-6.41	158/16	4.7	8.6
HD	HS	*QHD_HSJA.ubo-5A*	IWB34418	5A	142.5	IWB72992-IWA2350	138.6-146.5	**A**/G	1.6	82/90	3.3	5.6
HD	HS	*QHD_HSJA.ubo-5B*	IWB39017	5B	190.9	IWB8500-IWB73352	187.5-194.7	**C**/T	-1.45	78/97	3.1	5.2
HD	HS	*QHD_HSJA.ubo-6A*	IWB39623	6A	72.4	IWA6724-IWB9445	68.3-83.7	**A**/C	2.95	14/159	3.8	6.7
HD	HS	*QHD_HSJA.ubo-6B*	IWB2097	6B	152.2	IWB44252-IWB10420	147.7-155.9	**A**/G	-3.72	155/19	5.2	9.8
HD	HS	*QHD_HSJA.ubo-7B*	IWB60292	7B	120.4	IWB74053-IWB73011	114.9-123.2	**C**/T	3.16	14/161	4.3	7.7
DTM	HS	*QDTM_HSJA.ubo-1A*	IWA4351	1A	10.6	wPt-3870-IWB63712	6.7-15.3	**A**/G	-3.56	143/32	3.1	5.2
DTM	HS	*QDTM_HSJA.ubo-4B.1*	IWB12274	4B	3.9	IWB73506-IWB73905	0.3-7.4	**A**/C	-2.59	29/144	3.5	6.4
DTM	HS	*QDTM_HSJA.ubo-4B.2*	IWB36375	4B	69.3	IWB44068-IWA2218	65.5-72.4	**A**/G	2.56	135/35	4.5	8.4
DTM	HS	*QDTM_HSJA.ubo-4B.3*	IWB1606	4B	81.5	wPt-2214-wPt-0230	77.8-84.6	**C**/T	3.72	16/158	3.2	5.6
DTM	HS	*QDTM_HSJA.ubo-5A*	IWB29981	5A	142.5	IWB72992-IWA2350	138.6-146.5	**C**/T	-2.24	90/82	4.2	7.9
DTM	HS	*QDTM_HSJA.ubo-5B.1*	IWB23813	5B	166.1	IWB8583-IWB9424	160.6-171.2	**A**/G	2.31	24/149	3.2	5.6
DTM	HS	*QDTM_HSJA.ubo-5B.2*	IWB39017	5B	190.9	IWB8500-IWB73352	187.5-194.7	**C**/T	-1.95	78/97	3.6	6.5
DTM	HS	*QDTM_HSJA.ubo-6A*	IWA1671	6A	72.4	IWA6247-IWB9445	66.9-83.7	**G**/T	3.34	15/158	3.4	5.9
DTM	HS	*QDTM_HSJA.ubo-7A*	IWB9769	7A	150.9	IWB56095-IWB70696	147.4-154.4	**A**/G	1.92	86/89	3.6	6.4
PH	HS	*QPH_HSJA.ubo-1A*	IWB60784	1A	94.9	IWB58119-IWB26708	89.0-98.2	**A**/G	-12.28	161/13	3.1	6.1
PH	HS	*QPH_HSJA.ubo-2A*	IWB66088	2A	118.4	IWB7707-IWB71282	114.8-123.9	**A**/G	9.43	11/164	4.2	8.7
PH	HS	*QPH_HSJA.ubo-2B.1*	IWB22852	2B	74.5	IWB6607-IWA3924	71.0-77.9	**C**/T	10.18	15/160	3.5	7.0

PH	HS	*QPH_HSJA.ubo-2B.2*	IWB56633	2B	132.2	IWB70548-IWB22281	128.7-135.6	**A**/G	8.83	11/164	3.5	7.0
PH	HS	*QPH_HSJA.ubo-2B.3*	IWA7909	2B	149.0	IWB2073-IWB46631	145.8-153.0	**A**/G	-6.64	13/161	3.1	6.1
PH	HS	*QPH_HSJA.ubo-4A*	wPt-5172	4A	172.0	IWB72285-IWB18740	168.6-175.8	**A**/T	-7.7	160/15	3.9	7.8
PH	HS	*QPH_HSJA.ubo-4B*	IWB19555	4B	30.8	IWA103-IWB73919	27.6-33.9	**A**/G	-22.19	161/14	6.5	14.5
PH	HS	*QPH_HSJA.ubo-5A*	IWB27060	5A	149.7	IWA2350-IWB72381	146.5-155	**A**/G	-12.76	162/12	3.5	6.8
PH	HS	*QPH_HSJA.ubo-5B.1*	IWB30992	5B	2.7	wPt-1302-IWA4790	0.1-6.5	**C**/T	9.83	10/165	4.6	9.5
PH	HS	*QPH_HSJA.ubo-5B.2*	IWA3606	5B	10.3	IWA2915-wPt-8157	7.2-13.5	**A**/C	-9.45	165/10	4.2	8.7
PH	HS	*QPH_HSJA.ubo-5B.3*	IWB56221	5B	145.9	IWB8035-IWB6823	142.6-149.0	**A**/G	-7.82	166/9	3.3	6.4
PH	HS	*QPH_HSJA.ubo-6B*	IWB8960	6B	10.3	IWA1494-IWB65148	7.2-13.3	**A**/G	7.56	12/163	3.2	6.3
GY	HS	*QGY_HSJA.ubo-1A*	IWB34341	1A	68.9	IWB51724-IWB6733	61.2-72.2	**G**/T	0.64	154/20	3.3	6.6
GY	HS	*QGY_HSJA.ubo-1B*	IWB65272	1B	156.1	IWB965-IWA4525	152.5-160.5	**A**/G	0.38	107/66	3.1	6.1
GY	HS	*QGY_HSJA.ubo-2A.1*	IWB67517	2A	50.5	IWB70473-IWB35347	47.2-54.6	**A**/C	-0.82	146/29	3.0	6.0
GY	HS	*QGY_HSJA.ubo-2A.2*	IWA2730	2A	67.3	IWB35896-IWA3193	63.4-74.6	**C**/T	-0.74	12/163	3.4	6.9
GY	HS	*QGY_HSJA.ubo-3B.1*	wPt-9012	3B	5.0	IWB41429-IWB4344	2.9-8.2	**A**/T	-0.78	156/19	3.6	7.3
GY	HS	*QGY_HSJA.ubo-3B.2*	IWB8751	3B	17.6	wPt-3536-IWB34803	13.6-21.7	**A**/G	0.75	20/154	3.0	6.0
GY	HS	*QGY_HSJA.ubo-4A.1*	IWB9431	4A	160.2	wPt-9162-IWA2123	156.9-163.4	**A**/G	-0.59	149/26	3.2	6.5
GY	HS	*QGY_HSJA.ubo-4A.2*	IWB70192	4A	173.8	IWB73467-IWB46967	170.6-175.8	**C**/T	-0.58	148/27	3.1	6.3
GY	HS	*QGY_HSJA.ubo-7A.1*	IWB74166	7A	49.7	IWB71609-IWB15959	45.9-53.0	**C**/T	0.44	117/58	3.3	6.7
GY	HS	*QGY_HSJA.ubo-7A.2*	IWB20735	7A	75.2	IWB9080-IWB74061	70.7-78.6	**C**/T	-0.52	129/44	3.7	7.8
GY	HS	*QGY_HSJA.ubo-7A.3*	IWB9633	7A	103.8	IWB72165-IWB2862	100.6-107.0	**A**/G	-0.79	11/164	3.8	7.8
GY	HS	*QGY_HSJA.ubo-7A.4*	IWA3961	7A	113.2	IWB65077-IWA3941	109.1-118.0	**A**/G	0.43	77/95	3.1	6.2
TKW	HS	*QTKW_HSJA.ubo-2A.*	wPt-9277	2A	198.7	IWB72339-IWB41520	194.8-201.1	**A**/T	-2.75	42/132	3.0	5.5
TKW	HS	*QTKW_HSJA.ubo-2B.1*	IWA3407	2B	8.3	IWB22939-IWB11421	3.5-11.6	**A**/G	3.54	23/152	3.3	6.2
TKW	HS	*QTKW_HSJA.ubo-2B.2*	IWB27823	2B	90.8	IWA4605-wPt-2664	87.7-93.2	**C**/T	3.89	24/148	3.5	6.7
TKW	HS	*QTKW_HSJA.ubo-2B.3*	IWB41739	2B	127.6	IWB20453-IWB41461	124.5-130.9	**C**/T	-2.25	100/74	3.1	5.7
TKW	HS	*QTKW_HSJA.ubo-3B.1*	IWB66970	3B	4.2	IWB13576-IWB35536	1.1-7.4	**A**/G	3.11	37/138	3.2	5.9
TKW	HS	*QTKW_HSJA.ubo-3B.2*	IWB73013	3B	19.4	IWB1925-IWB72015	15.4-22.8	**C**/T	-2.58	116/59	3.1	5.6
TKW	HS	*QTKW_HSJA.ubo-5A*	IWB73200	5A	136.3	IWB8003-IWB3132	132.3-140.1	**A**/G	-2.93	100/73	3.4	6.5
TKW	HS	*QTKW_HSJA.ubo-5B*	IWB36006	5B	166.1	IWB8583-IWB9424	160.6-171.2	**C**/T	3.32	24/148	3.6	7.0
TKW	HS	*QTKW_HSJA.ubo-6A*	IWB72637	6A	62.0	IWB61420-IWA6033	58.9-66.8	**C**/T	2.95	137/38	3.0	5.5
TKW	HS	*QTKW_HSJA.ubo-6B*	IWB24238	6B	85.9	IWA4484-IWB71758	82.5-89.1	**G**/T	-2.4	56/116	3.0	5.7
TKW	HS	*QTKW_HSJA.ubo-7A*	IWB74033	7A	106.4	IWB73952-IWB10205	102.4-111.0	**A**/C	-2.79	114/56	3.5	7.2

TWT	HS	*QTWT_HSJA.ubo-1B*	IWB8612	1B	43.6	IWB7810-IWA44	39.9-46.9	**G**/T	-1.33	13/158	3.1	6.0
TWT	HS	*QTWT_HSJA.ubo-2B.1*	wPt-6643	2B	176.0	IWB5439-wPt-3632	172.3-179.3	**A**/T	1.32	37/137	3.7	7.3
TWT	HS	*QTWT_HSJA.ubo-2B.2*	IWB6614	2B	185.7	IWB1354-IWB10003	181.6-188.6	**C**/T	-1.2	145/27	3.3	6.5
TWT	HS	*QTWT_HSJA.ubo-2B.3*	wPt-0891	2B	191.5	wPt-8284-IWB31342	188.2-191.9	**A**/T	1.24	43/132	4.2	8.4
TWT	HS	*QTWT_HSJA.ubo-6A*	IWB9600	6A	67.3	IWB74244-IWA1194	62.8-71.8	**A**/G	0.95	139/36	3.0	5.7
TWT	HS	*QTWT_HSJA.ubo-7A*	IWB27700	7A	82.4	IWB36370-IWA3673	78.9-87.7	**C**/T	1.95	12/163	3.1	6.0
SPM	HS	*QSPM_HSJA.ubo-2B.1*	IWB6031	2B	132.3	IWB70548-IWB22281	128.7-135.6	**C**/T	13.35	11/164	3.3	7.0
SPM	HS	*QSPM_HSJA.ubo-2B.2*	IWB10623	2B	181.6	wPt-4892-IWB6614	177.5-185.7	**A**/G	-9.61	151/21	3.4	7.4
SPM	HS	*QSPM_HSJA.ubo-3B*	IWB67388	3B	4.2	IWB13576-IWB19201	1.1-8.8	**A**/G	6.81	52/122	3.4	7.2
SPM	HS	*QSPM_HSJA.ubo-4A.1*	wPt-5749	4A	144.6	IWB66212-IWB67551	140.7-147.9	**A**/T	-12.51	163/12	3.8	8.4
SPM	HS	*QSPM_HSJA.ubo-4A.2*	IWB19834	4A	157.4	IWB9122-IWB34028	154.0-161.7	**C**/T	-11.2	154/21	3.9	8.5
SPM	HS	*QSPM_HSJA.ubo-4A.3*	IWB67739	4A	173.8	IWB73201-IWB46967	170.6-175.8	**G**/T	-9.92	147/28	4.1	9.0
SPM	HS	*QSPM_HSJA.ubo-7A*	IWB25155	7A	176.0	wPt-0961-IWB70291	172.9-180.2	**G**/T	7.12	149/26	3.1	6.6
SKT	HS	*QSKT_HSJA.ubo-1B*	IWB901	1B	72.9	IWB9661-IWB36064	68.3-77.3	**A**/G	-0.67	45/127	3.2	6.2
SKT	HS	*QSKT_HSJA.ubo-2A*	IWA2938	2A	176.5	IWB7563-IWB72723	171.0-179.6	**A**/C	-0.58	82/93	3.3	6.4
SKT	HS	*QSKT_HSJA.ubo-2B.1*	IWB70087	2B	51.8	IWB82-IWA6739	48.4-55.3	**C**/T	-1.3	158/16	3.5	7.1
SKT	HS	*QSKT_HSJA.ubo-2B.2*	IWB60830	2B	59.3	wPt-6199-IWB72685	55.7-62.4	**A**/G	1.27	15/160	3.6	7.1
SKT	HS	*QSKT_HSJA.ubo-4A*	IWB72314	4A	17.0	IWB72665-IWB35445	11.7-20.9	**A**/G	-0.63	114/60	3.2	6.4
SKT	HS	*QSKT_HSJA.ubo-5A*	IWB25138	5A	146.5	IWB73503-IWB27060	142.8-149.7	**A**/G	-1.53	164/11	3.6	7.1
SKT	HS	*QSKT_HSJA.ubo-5B*	IWB9424	5B	171.2	IWB73833-IWB35477	167.6-176.4	**C**/T	-0.68	120/53	3.5	7.0
SKT	HS	*QSKT_HSJA.ubo-7A*	IWB11337	7A	10.3	IWB624-IWA1735	7.2-14.1	**C**/T	-0.65	77/94	3.5	7.0
SKT	HS	*QSKT_HSJA.ubo-7B*	IWB4830	7B	177.4	wPt-2356-IWB10793	173.7-181.1	**A**/C	1.05	13/162	3.1	5.9
GNO	HS	*QGNO_HSJA.ubo-2A.1*	IWB50267	2A	78.0	IWA3193-IWA3194	74.6-90.2	**A**/G	-4.79	17/158	3.1	5.2
GNO	HS	*QGNO_HSJA.ubo-2A.2*	IWB75196	2A	97.3	IWB26960-IWB49366	95.0-100.1	**C**/T	4.41	38/135	3.0	5.0
GNO	HS	*QGNO_HSJA.ubo-2A.3*	IWA3368	2A	109.5	IWB66497-IWB7665	106.5-114.7	**A**/C	-5.41	155/19	4.6	8.5
GNO	HS	*QGNO_HSJA.ubo-2A.4*	IWA2938	2A	176.5	IWB7563-IWA3919	171.0-179.6	**A**/C	-2.62	82/93	3.1	5.2
GNO	HS	*QGNO_HSJA.ubo-2B.1*	IWB61884	2B	7.9	IWB22939-wPt-9958	3.5-11.3	**A**/G	3.09	99/73	3.5	6.0
GNO	HS	*QGNO_HSJA.ubo-2B.2*	IWB33109	2B	76.6	IWB62870-IWA50	73.2-80.6	**C**/T	-3.73	77/95	4.9	9.1
GNO	HS	*QGNO_HSJA.ubo-3A*	wPt-1092	3A	131.4	IWB72172-IWB26085	127.7-135.1	**A**/T	-3	73/101	3.4	5.9
GNO	HS	*QGNO_HSJA.ubo-3B*	IWB10783	3B	51.9	IWB6460-wPt-1159	48.8-55.0	**C**/T	3.34	91/84	4.1	7.2
GNO	HS	*QGNO_HSJA.ubo-4B.1*	IWB4336	4B	12.1	IWB73905-IWA2125	7.4-15.5	**A**/C	-0.52	18/157	3.5	6.0
GNO	HS	*QGNO_HSJA.ubo-4B.2*	IWB69708	4B	21.0	IWB34526-IWB73001	17.8-26.4	**A**/G	-2.65	92/81	3.0	5.0

GNO	HS	*QGNO_HSJA.ubo-4B.3*	IWB71883	4B	92.9	IWB71667-IWB75109	87.8-96.7	**C**/T	-6.78	11/164	3.5	5.9
GNO	HS	*QGNO_HSJA.ubo-4B.4*	IWB71806	4B	99.9	IWB75109-IWA3654	96.7-103.3	**G**/T	-3.24	76/98	3.4	5.9
GNO	HS	*QGNO_HSJA.ubo-5A*	IWB14134	5A	128.5	IWB26707-IWA6706	125.0-132.3	**C**/T	4.19	156/18	3.1	5.1
GNO	HS	*QGNO_HSJA.ubo-5B*	IWB34822	5B	57.8	IWB25678-IWA6992	54.6-61.2	**C**/T	-7.4	14/161	3.1	5.1
GNO	HS	*QGNO_HSJA.ubo-7A*	IWB67722	7A	49.5	IWB72301-IWB15959	44.9-53.0	**A**/G	3.34	117/57	3.3	5.7
GNO	HS	*QGNO_HSJA.ubo-7B*	wPt-3533	7B	142.7	IWB71474-IWB41485	139.2-146.2	**A**/T	-3.16	53/122	3.6	6.1
SGW	HS	*QSGW_HSJA.ubo-1B.1*	IWB2667	1B	109.0	IWB3634-IWB35712	103.0-113.4	**A**/G	-0.27	10/165	3.0	5.0
SGW	HS	*QSGW_HSJA.ubo-1B.2*	rPt-2940	1B	124.7	wPt-0097-IWA696	121.4-128.8	**A**/T	0.17	51/124	3.7	6.4
SGW	HS	*QSGW_HSJA.ubo-2A.1*	IWA3368	2A	109.5	IWB66497-IWB11039	106.5-113.0	**A**/C	-0.2	155/19	3.0	5.1
SGW	HS	*QSGW_HSJA.ubo-2A.2*	IWA2938	2A	176.5	IWB7563-IWA3919	171.0-179.6	**A**/C	-0.14	82/93	3.6	6.3
SGW	HS	*QSGW_HSJA.ubo-2B.1*	IWB12041	2B	73.2	IWA2556-IWB39220	70.1-76.8	**C**/T	0.26	20/155	4.0	7.0
SGW	HS	*QSGW_HSJA.ubo-2B.2*	IWB4384	2B	84.0	IWB8031-IWB59913	80.6-87.4	**C**/T	0.22	21/153	3.7	6.4
SGW	HS	*QSGW_HSJA.ubo-2B.3*	IWB1275	2B	132.6	IWA5413-IWB102	129.5-135.8	**A**/G	0.16	128/44	3.3	5.5
SGW	HS	*QSGW_HSJA.ubo-3A*	wPt-1092	3A	131.4	IWB7486-IWB7623	128.7-141.6	**A**/T	-0.15	73/101	3.7	6.4
SGW	HS	*QSGW_HSJA.ubo-3B*	IWB48996	3B	41.3	wPt-8686-IWA747	36.8-45.3	**C**/T	-0.15	74/101	3.9	6.8
SGW	HS	*QSGW_HSJA.ubo-4B.1*	IWB66537	4B	87.0	IWB32903-IWB17020	83.4-90.3	**A**/G	0.19	154/21	3.1	5.2
SGW	HS	*QSGW_HSJA.ubo-4B.2*	IWB71883	4B	92.9	IWB71667-IWB75109	87.8-96.7	**C**/T	-0.39	11/164	4.7	8.7
SGW	HS	*QSGW_HSJA.ubo-5B*	IWB68333	5B	117.1	IWB72093-IWA2255	112.1-120.1	**C**/T	0.32	159/15	5.2	9.8
SGW	HS	*QSGW_HSJA.ubo-6A*	IWB6825	6A	109.3	IWB73803-IWB12203	106.0-112.9	**A**/G	-0.24	162/13	3.3	5.5
SGW	HS	*QSGW_HSJA.ubo-7B*	wPt-3533	7B	142.7	IWB71474-IWB41479	139.2-146.2	**A**/T	-0.15	53/122	3.6	6.3
GLE	HS	*QGLE_HSJA.ubo-1A*	IWB65373	1A	4.6	IWB72690-IWB29039	1.7-8.4	**C**/T	-0.25	14/161	3.2	6.2
GLE	HS	*QGLE_HSJA.ubo-1B*	IWB71657	1B	158.0	tPt-6091-IWB62169	154.6-161.5	**C**/T	-0.22	14/161	3.2	6.2
GLE	HS	*QGLE_HSJA.ubo-4B.1*	IWB44459	4B	16.0	IWB8084-IWB72973	12.8-20.8	**C**/T	0.17	100/73	4.2	8.8
GLE	HS	*QGLE_HSJA.ubo-4B.2*	IWA3654	4B	103.3	IWB71805-IWA2595	99.9-106	**C**/T	0.22	152/22	4.1	8.3
GLE	HS	*QGLE_HSJA.ubo-5A*	IWB10273	5A	54.6	IWB70873-IWB12830	50.5-57.67	**C**/T	-0.17	58/111	3.6	7.2
GLE	HS	*QGLE_HSJA.ubo-6A*	IWB71326	6A	130.0	IWB50034-IWB73847	126.8-131.2	**C**/T	0.15	57/115	3.1	6.1
GLE	HS	*QGLE_HSJA.ubo-6B*	IWB49257	6B	92.9	IWB51061-IWB35607	89.7-96	**A**/G	0.18	26/144	3.1	6.1
GWI	HS	*QGWI_HSJA.ubo-1B*	IWB73390	1B	153.7	IWB18553-wPt-5915	149.7-157.8	**A**/G	-0.07	91/84	3.1	6.1
GWI	HS	*QGWI_HSJA.ubo-2B*	IWA3407	2B	8.3	IWB22939-IWB11421	3.5-11.6	**A**/G	0.11	23/152	3.4	6.9
GWI	HS	*QGWI_HSJA.ubo-3A*	IWB32537	3A	119.5	IWB10607-IWB71615	114.9-122.7	**C**/T	0.14	162/12	3.1	6.3
GWI	HS	*QGWI_HSJA.ubo-4B.1*	IWB36446	4B	60.0	wPt-3101-IWB36397	56.3-64.3	**A**/G	-0.09	45/130	3.1	6.1
GWI	HS	*QGWI_HSJA.ubo-4B.2*	IWB43353	4B	68.4	IWB73007-IWA3287	64.4-71.8	**A**/G	-0.09	48/126	3.6	7.5

GWI	HS	*QGWI_HSJA.ubo-5A.1*	IWB73092	5A	59.2	IWB1011-IWB28350	56.1-63.4	**A**/C	0.07	73/101	3.1	6.2
GWI	HS	*QGWI_HSJA.ubo-5A.2*	IWB73200	5A	136.3	IWB8003-IWB3132	132.3-140.1	**A**/G	-0.09	100/73	3.6	7.7
GWI	HS	*QGWI_HSJA.ubo-5B.1*	IWB71938	5B	158.3	wPt-8125-IWB11985	154.5-160.6	**G**/T	-0.08	116/55	3.2	6.5
GWI	HS	*QGWI_HSJA.ubo-5B.2*	IWA8031	5B	165.2	IWB8583-IWB11579	160.6-167.6	**C**/T	-0.11	142/29	4.6	10.1
GWI	HS	*QGWI_HSJA.ubo-6A*	IWB73616	6A	40.9	IWB3978-IWB24955	37.3-44.1	**C**/T	-0.11	147/28	3.6	7.5
GWI	HS	*QGWI_HSJA.ubo-7A*	IWB72889	7A	53.3	IWB24920-IWB59818	49.9-56.6	**C**/T	-0.09	132/42	3.4	6.9
GWI	HS	*QGWI_HSJA.ubo-7B.1*	IWB60028	7B	0.1	IWB22624-IWB67086	0.1-3.3	**C**/T	-0.09	56/119	4.2	8.7
GWI	HS	*QGWI_HSJA.ubo-7B.2*	IWB74056	7B	15.8	IWB6455-wPt-7318	10.2-19.2	**C**/T	-0.08	89/86	3.9	8.1

[1] Treat.: treatment. [2] marker position of the peak marker based on the tetraploid wheat consensus map (Maccaferri et al., 2015a). [3] confidence intervals based on LD of the UNIBO-Durum Panel. [4] the allele effect is referred to the allele highlighted in bold. [5] -log (p-value) refers to p-value < 0.001.

Table A3.9. List of GWAS-QTLs for reaction norm index (Δ) significantly associated with the traits days to heading (HD), days to maturity (DTM), plant height (PH), grain yield (GY), thousand kernel weight (TKW), test weight (TWT), number of spikes per linear meter (SPM), number of spikelets per spike (SKT), grain number spike (GNO), grain weight per spike (SGW), grain length (GLE), and grain width (GWI) considering both crop season (2018, 2019) in the joint analysis.

Trait	Treat. [1]	QTL ID	Peak marker	Chr	Marker position (cM) [2]	Flanking Markers	Confidence interval (cM) [3]	Alleles [4]	Effect	Allele Frequency	-log(p-value) [5]	R^2 (%)
HD	Δ	*QHD_ΔJA.ubo-4B*	IWB68585	4B	90.3	IWB73113-wPt-7412	87.0-93.78	**G**/T	2.48	164/11	3.0	3.7
HD	Δ	*QHD_ΔJA.ubo-5A*	IWB10692	5A	150.3	IWB72051-IWB72381	147.1-155.0	**C**/T	4.11	157/15	3.8	5.0
HD	Δ	*QHD_ΔJA.ubo-7A*	IWB26796	7A	14.1	IWB62296-IWB60043	10.6-17.8	**C**/T	1.62	78/94	3.5	4.5
DTM	Δ	*QDTM_ΔJA.ubo-1A*	IWB57961	1A	71.3	IWB8994-IWB35039	67.8-75.1	**A**/G	-1.75	19/156	3.1	5.6
DTM	Δ	*QDTM_ΔJA.ubo-4B*	IWB27710	4B	70.3	IWB72368-IWB69695	66.8-73.4	**A**/C	1.12	96/75	3.1	5.8
DTM	Δ	*QDTM_ΔJA.ubo-5A.1*	IWB10985	5A	56.5	IWB72038-IWB68691	53.0-60.75	**G**/T	-1.65	36/139	3.1	5.6
DTM	Δ	*QDTM_ΔJA.ubo-5A.2*	IWB38719	5A	140.6	IWA1486-IWA2350	136.3-146.5	**C**/T	1.83	87/84	5.7	12.1
DTM	Δ	*QDTM_ΔJA.ubo-5A.3*	IWA1670	5A	188.9	IWB51362-IWB11221	185.7-192.1	**A**/G	-1.9	148/26	3.2	5.8
DTM	Δ	*QDTM_ΔJA.ubo-5B*	IWB23813	5B	166.1	IWB8583-IWB69060	160.6-172.2	**A**/G	1.44	24/149	3.2	5.8
DTM	Δ	*QDTM_ΔJA.ubo-6A*	IWB73616	6A	40.9	IWB3978-IWB24955	37.3-44.1	**C**/T	-1.52	147/28	3.1	5.7
DTM	Δ	*QDTM_ΔJA.ubo-7A*	IWB59995	7A	32.6	IWB73683-IWB3124	28.6-39.8	**C**/T	-1.5	27/148	3.3	6.2
DTM	Δ	*QDTM_ΔJA.ubo-7B*	IWB73917	7B	13.8	IWB6455-IWB3369	10.2-17.3	**A**/C	1.23	72/102	3.6	6.7
PH	Δ	*QPH_ΔJA.ubo-1A*	IWB40833	1A	67.8	IWB51724-IWA3934	61.2-71.6	**C**/T	6.02	159/16	3.7	6.8
PH	Δ	*QPH_ΔJA.ubo-2A*	IWB66088	2A	118.4	IWB7707-IWB71282	114.8-123.9	**A**/G	8.07	11/164	3.9	7.3
PH	Δ	*QPH_ΔJA.ubo-2B*	IWB22852	2B	74.5	IWB6607-IWA3924	71.0-77.9	**C**/T	9.13	15/160	3.5	6.4
PH	Δ	*QPH_ΔJA.ubo-3A*	IWB47601	3A	65.9	IWB72751-IWB71028	59.1-72.2	**C**/T	6.14	165/10	3.1	5.4
PH	Δ	*QPH_ΔJA.ubo-4B*	IWA103	4B	27.6	IWB59588-IWB12149	23.5-30.8	**C**/T	8.25	17/157	3.0	5.4
PH	Δ	*QPH_ΔJA.ubo-5A*	IWB54064	5A	43.8	IWB66553-IWB47433	40.6-47.3	**A**/G	7.63	11/164	3.6	6.7
PH	Δ	*QPH_ΔJA.ubo-5B.1*	IWB30992	5B	2.7	wPt-1302-IWA4790	0.1-6.5	**C**/T	8.97	10/165	4.7	9.1
PH	Δ	*QPH_ΔJA.ubo-5B.2*	IWA3607	5B	10.3	IWA2915-IWA5176	7.2-13.5	**A**/G	-9.13	165/10	4.8	9.4
GY	Δ	*QGY_ΔJA.ubo-2B.1*	IWB59623	2B	48.2	IWA3868-IWB21394	45.1-51.8	**C**/T	10.3	155/19	3.0	6.4
GY	Δ	*QGY_ΔJA.ubo-2B.2*	IWB28826	2B	181.6	wPt-4892-IWB6614	177.5-185.7	**C**/T	-9.44	153/21	3.0	6.4
GY	Δ	*QGY_ΔJA.ubo-3B.1*	IWB68173	3B	8.2	wPt-8079-IWB14117	5.0-12.3	**C**/T	-8.41	132/41	3.2	6.9

GY	Δ	*QGY_ΔJA.ubo-3B.2*	IWB52160	3B	17.6	wPt-3536-IWB34803	13.6-21.7	**A**/C	11.65	20/154	3.1	6.6
GY	Δ	*QGY_ΔJA.ubo-4A.1*	IWB9431	4A	160.2	wPt-9162-IWA2123	156.9-163.4	**A**/G	-9.36	149/26	3.3	7.2
GY	Δ	*QGY_ΔJA.ubo-4A.2*	IWB44829	4A	173.8	IWB73467-IWB46967	170.6-175.8	**G**/T	-8.97	148/27	3.2	6.8
GY	Δ	*QGY_ΔJA.ubo-5B*	IWB24957	5B	49.2	IWB7509-IWA7227	45.0-52.6	**C**/T	15.68	163/12	3.3	7.0
GY	Δ	*QGY_ΔJA.ubo-7A.1*	IWB74166	7A	49.7	wPt-1163-IWB15959	44.9-53.0	**C**/T	7.21	117/58	3.7	8.1
GY	Δ	*QGY_ΔJA.ubo-7A.2*	IWB9633	7A	103.8	IWB72165-IWB2862	100.6-107.0	**A**/G	-11.09	11/164	3.3	7.0
TKW	Δ	*QTKW_ΔJA.ubo-2A*	IWB75255	2A	186.1	IWB7444-IWA5840	182.3-189.8	**C**/T	-4.65	26/149	3.5	5.9
TKW	Δ	*QTKW_ΔJA.ubo-3B.1*	IWB50787	3B	19.4	IWB1925-IWB72015	15.4-22.8	**A**/C	3.96	87/85	3.1	5.2
TKW	Δ	*QTKW_ΔJA.ubo-3B.2*	IWB5515	3B	100.9	IWB49370-IWA6221	97.2-104.6	**C**/T	-5.13	37/138	3.2	5.3
TKW	Δ	*QTKW_ΔJA.ubo-6B.1*	IWB72496	6B	60.7	IWB56050-IWB1248	57.1-64.1	**C**/T	3.89	43/131	3.5	5.9
TKW	Δ	*QTKW_ΔJA.ubo-6B.2*	IWB4259	6B	94.8	IWB70007-IWB46951	91.5-98.4	**A**/G	-5.35	151/23	3.8	6.5
TKW	Δ	*QTKW_ΔJA.ubo-7A.1*	IWB33972	7A	14.1	IWB62296-IWB60043	10.6-17.8	**A**/G	-4.25	136/39	3.4	5.6
TKW	Δ	*QTKW_ΔJA.ubo-7A.2*	IWB67852	7A	102.4	IWB7752-IWB72148	98.3-106.4	**C**/T	-6.14	159/15	3.6	6.1
TWT	Δ	*QTWT_ΔJA.ubo-2B.1*	wPt-8583	2B	59.0	wPt-6199-IWB72685	55.7-62.4	**A**/T	-0.94	73/100	3.2	7.0
TWT	Δ	*QTWT_ΔJA.ubo-2B.2*	IWB9088	2B	170.9	IWB59226-IWB30420	167.1-174.3	**C**/T	-1.13	29/146	3.4	7.4
TWT	Δ	*QTWT_ΔJA.ubo-2B.3*	IWB27000	2B	185.8	IWB12117-IWB63909	182.7-189.1	**A**/G	1.3	27/146	3.1	6.8
TWT	Δ	*QTWT_ΔJA.ubo-4B.1*	IWB33116	4B	45.9	IWB68116-IWB54727	42.7-51.1	**A**/G	-1.72	163/12	3.5	7.7
TWT	Δ	*QTWT_ΔJA.ubo-4B.2*	IWB7100	4B	97.5	IWB57170-IWB32544	94.0-103.3	**C**/T	-1.21	149/26	3.5	7.7
TWT	Δ	*QTWT_ΔJA.ubo-7A*	IWB60146	7A	76.0	IWB9080-IWA8161	70.7-79.9	**A**/G	-1.61	152/21	3.5	7.8
TWT	Δ	*QTWT_ΔJA.ubo-7B*	IWA1220	7B	25.2	wPt-2883-IWA5390	20.7-28.5	**C**/T	-1.56	156/18	3.0	6.4
SPM	Δ	*QSPM_ΔJA.ubo-1B*	IWA4680	1B	74.7	IWB6215-IWA6945	71.4-78.0	**A**/G	5.35	106/62	3.4	6.2
SPM	Δ	*QSPM_ΔJA.ubo-4A*	IWB60336	4A	46.5	IWB67877-IWA3344	42.7-51.3	**A**/G	-6.27	145/30	3.1	5.3
SKT	Δ	*QSKT_ΔJA.ubo-2A*	IWA2938	2A	176.5	IWB7563-IWB72723	171.0-179.6	**A**/C	-3.32	82/93	3.5	6.0
SKT	Δ	*QSKT_ΔJA.ubo-5A*	IWB58257	5A	141.4	IWB66717-IWA2350	138.3-146.5	**A**/G	4.06	86/85	3.5	6.0
SKT	Δ	*QSKT_ΔJA.ubo-7A*	IWB59995	7A	32.6	IWB73683-IWB3124	28.6-39.8	**C**/T	-4.63	27/148	3.5	5.9
GNO	Δ	*QGNO_ΔJA.ubo-1B.1*	IWB68093	1B	158.0	tPt-6091-IWB62169	154.6-161.5	**A**/G	6.1	130/44	3.9	8.5
GNO	Δ	*QGNO_ΔJA.ubo-1B.2*	IWB280	1B	162.3	IWB71657-wPt-6142	158.0-165.6	**C**/T	6.06	129/45	4.0	8.6
GNO	Δ	*QGNO_ΔJA.ubo-3B*	IWB41105	3B	25.4	IWB64404-IWB64361	22.3-29.27	**C**/T	7.41	158/17	3.1	6.3
GNO	Δ	*QGNO_ΔJA.ubo-4B*	IWB71883	4B	92.9	IWB71667-IWB75109	87.8-96.7	**C**/T	-12.05	11/164	4.1	8.9
GNO	Δ	*QGNO_ΔJA.ubo-5B.1*	wPt-5604	5B	117.9	IWB10362-IWB11813	113.9-121.7	**A**/T	-9.17	16/158	4.1	9.0
GNO	Δ	*QGNO_ΔJA.ubo-5B.2*	IWB52826	5B	140.3	IWB51456-IWA584	135.8-143.7	**C**/T	4.8	73/101	3.4	7.3
GNO	Δ	*QGNO_ΔJA.ubo-6A*	IWA1497	6A	97.4	IWB73260-IWB199	93.4-102.0	**C**/T	-4.75	95/80	3.0	6.1

GNO	Δ	*QGNO_ΔJA.ubo-7A*	IWB9633	7A	103.8	IWB72165-IWB2862	100.6-107.0	**A**/G	-8.37	11/164	3.0	6.1
SGW	Δ	*QSGW_ΔJA.ubo-1A*	IWB5406	1A	70.8	IWA2995-IWB35039	67.7-75.1	**C**/T	-7.11	23/151	3.7	8.6
SGW	Δ	*QSGW_ΔJA.ubo-2A.1*	IWB4625	2A	67.5	IWB35896-IWB73849	63.4-68.6	**A**/G	-5.49	27/148	3.0	6.8
SGW	Δ	*QSGW_ΔJA.ubo-2A.2*	IWB72480	2A	78.0	IWA3193-IWA3194	74.6-90.2	**A**/C	-7.22	17/158	3.2	7.3
SGW	Δ	*QSGW_ΔJA.ubo-2B.1*	IWB3996	2B	84.0	IWB8031-IWB60612	80.6-87.3	**C**/T	-6.35	153/21	3.0	6.8
SGW	Δ	*QSGW_ΔJA.ubo-2B.2*	IWB8157	2B	180.1	wPt-2724-IWA2094	176.2-183.6	**A**/G	-8.17	11/164	3.1	6.8
SGW	Δ	*QSGW_ΔJA.ubo-4B*	IWB7389	4B	92.3	IWB71667-IWB73625	87.8-95.3	**A**/G	-2.04	147/27	4.3	10.1
SGW	Δ	*QSGW_ΔJA.ubo-5B.1*	IWB68333	5B	117.1	IWB10362-IWB11813	113.9-121.7	**C**/T	8.71	159/15	4.3	10.2
SGW	Δ	*QSGW_ΔJA.ubo-5B.2*	IWB22567	5B	140.3	IWB51456-IWA584	135.8-143.7	**C**/T	4.64	77/98	3.9	9.0
SGW	Δ	*QSGW_ΔJA.ubo-7A*	IWB9633	7A	103.8	IWB72165-IWB2862	100.6-107.0	**A**/G	-7.93	11/164	3.4	7.7
GLE	Δ	*QGLE_ΔJA.ubo-4B*	IWB73855	4B	74.7	IWA3287-wPt-2214	71.8-77.8	**C**/T	1.03	67/103	3.3	7.1
GLE	Δ	*QGLE_ΔJA.ubo-5A*	IWB40699	5A	208.8	IWA7880-IWB35997	206.0-213.8	**C**/T	2.48	21/153	4.5	10.0
GLE	Δ	*QGLE_ΔJA.ubo-6A*	IWB29913	6A	120.5	IWB70454-IWB45558	117.1-123.6	**A**/G	1.18	42/132	3.2	6.7
GLE	Δ	*QGLE_ΔJA.ubo-6B*	IWB23748	6B	89.9	wPt-6889-IWA6599	86.7-93.0	**G**/T	-1.63	155/20	3.0	6.2
GLE	Δ	*QGLE_ΔJA.ubo-7A.1*	IWB46130	7A	91.2	IWB8142-IWB11840	87.7-94.7	**A**/G	-1.67	153/20	3.0	6.2
GLE	Δ	*QGLE_ΔJA.ubo-7A.2*	IWB34651	7A	99.5	IWB65530-IWB73952	96.2-102.4	**C**/T	1.71	18/156	3.6	7.6
GLE	Δ	*QGLE_ΔJA.ubo-7A.3*	IWB11124	7A	123.1	IWA3941-IWB46770	118.0-128.1	**G**/T	1.07	64/111	3.1	6.3
GLE	Δ	*QGLE_ΔJA.ubo-7A.4*	IWB9749	7A	130.7	IWB8935-IWB45289	126.0-134.6	**A**/G	-1.33	65/109	4.5	10.0
GLE	Δ	*QGLE_ΔJA.ubo-7A.5*	IWB28062	7A	181.8	wPt-7281-IWB29243	177.1-184.9	**A**/G	-1.82	164/11	3.1	6.3
GWI	Δ	*QGWI_ΔJA.ubo-2A*	IWB75255	2A	186.1	IWB7444-IWA5840	182.3-189.8	**C**/T	-2.12	26/149	3.8	6.7
GWI	Δ	*QGWI_ΔJA.ubo-4B*	IWB17754	4B	68.3	IWB73007-IWA3287	64.4-71.8	**A**/G	-1.79	48/124	3.6	6.4
GWI	Δ	*QGWI_ΔJA.ubo-6B.1*	IWB72496	6B	60.7	IWB56050-IWB190	57.1-64.3	**C**/T	1.85	43/131	4.2	7.6
GWI	Δ	*QGWI_ΔJA.ubo-6B.2*	IWB26174	6B	95.6	IWB72452-IWB73225	92.3-98.4	**C**/T	-2.35	151/21	3.6	6.6
GWI	Δ	*QGWI_ΔJA.ubo-7A.1*	IWB67909	7A	7.0	IWB35207-IWB62296	2.4-10.6	**C**/T	-2.32	23/152	3.7	6.5
GWI	Δ	*QGWI_ΔJA.ubo-7A.2*	IWB53116	7A	15.8	IWB9788-IWB73940	11.5-21.9	**A**/G	-2.3	20/155	3.0	5.2

[1] Treat.: treatment. [2] marker position of the peak marker based on the tetraploid wheat consensus map (Maccaferri et al., 2015a). [3] confidence intervals based on LD of the UNIBO-Durum Panel. [4] the allele effect is referred to the allele highlighted in bold. [5] -log (p-value) refers to p-value < 0.001.

Acknowledgments

I would like to sincerely thank my supervisor, Professor Roberto Tuberosa and my co-supervisor, Marco Maccaferri for their support, encouragement, advices and help during the period of my PhD studies.

I would like to thank the Prof. Silvio Salvi, Prof. Elisabetta Frascaroli and Prof. Maria Corina Sanguinetti for their advices and support throughout my PhD.

I would like to thank my co-supervisor Karim Ammar and all his group from the International Maize and Wheat Improvement Center at Ciudad Obregon (Mexico), for their support and help during the evaluation of the experiments under field condition.

I would like to thank Dr. Onno Muller, Dr. Christoph Jedmowski and Lars Zimmermann from the Institute of Bio- and Geosciences at Jülich (Germany), for their support during the evaluation of the experiment under greenhouse condition.

I would like to thank Dr. Ed Runge and his wife, Mrs. Pat, for their kindness and competence as Head of the Monsanto's Beachell-Borlaug International Scholars Program (MBBISP). I would also to thank all directors and the judge panel of the MBBISP for sponsor my PhD research.

I would like to extend my thanks to all my colleagues and friends from the Department of Agricultural and Food Science (DISTAL), Alberto, Danara, Giuseppe Condorelli, Giuseppe Sciara, Kai, Martina, Matteo, Sandra, Simona and Serena, who have shared with me very kind moments during my PhD.

Finally, I would like to thank my family, specially my parents (Valdir and Ivone) and my siblings (Cleber, Everton, Gilvan and Andrieli) for their wholehearted support and kindliness during all moments of my live.